



THE UNIVERSITY *of* EDINBURGH

This thesis has been submitted in fulfilment of the requirements for a postgraduate degree (e.g. PhD, MPhil, DClinPsychol) at the University of Edinburgh. Please note the following terms and conditions of use:

This work is protected by copyright and other intellectual property rights, which are retained by the thesis author, unless otherwise stated.

A copy can be downloaded for personal non-commercial research or study, without prior permission or charge.

This thesis cannot be reproduced or quoted extensively from without first obtaining permission in writing from the author.

The content must not be changed in any way or sold commercially in any format or medium without the formal permission of the author.

When referring to this work, full bibliographic details including the author, title, awarding institution and date of the thesis must be given.

Molecular and cellular mechanisms of microglia-mediated neuroprotection

Chiara Maria Stella Herzog



Doctor of Philosophy
University of Edinburgh
2019

Abstract

Traumatic brain injury (TBI) is a major cause of death and long-term disability worldwide. It is elicited by an external force injuring the brain, and leads to two phases of neuronal cell death: primary cell death, resulting from direct mechanical disruption of the tissue, and secondary cell death, caused by delayed cytotoxic cascades. While primary cell death can only be prevented by avoiding physical injury, secondary cell death occurs within hours to weeks following the initial injury and therefore lies within a therapeutic window during which pharmacological agents targeting the pathomechanisms of TBI could be applied. Pre-clinical models of brain injury in rodents have identified several neuroprotective compounds, but not a single drug has shown improved patient outcome over placebo in multi-centre phase III clinical trials. Intriguingly, the largest randomised controlled trial for TBI to date reported a higher mortality in patients treated with an immunosuppressive drug compared to patients treated with placebo, suggesting that the immune system may play a neuroprotective role following brain injuries.

To investigate the role of the immune system in more detail, I developed a model of brain injury in larval zebrafish. Larval zebrafish are amenable to genetic and pharmacological manipulation, and their optical transparency in combination with the availability of a multitude of transgenic reporter lines allows for efficient *in vivo* (timelapse) microscopy. This allowed me to visualise the cellular and molecular reactions to brain injury in real-time in a living vertebrate organism, which provided an advantage compared to the majority of studies so far, which had been done either in rodents with static end points, or *in vitro*.

Characterisation of cell death dynamics revealed that larval zebrafish reproducibly exhibit primary and secondary cell death following brain injury. In line with mammalian TBI models, I demonstrated that excitotoxicity contributes to secondary cell death. Furthermore, I described early calcium waves in response to injury that may instruct repair mechanisms; using pharmacological agents, I identified the release of glutamate, acting on neurons surrounding the injury site, and ATP, acting predominantly on glial cells, as the upstream mechanisms of calcium waves. In contrast to observations in rodent models and human TBI patients, I observed little infiltration of peripheral macrophages or neutrophils. Microglia, the resident immune cells of the brain, were rapidly

recruited to the injury site and significantly increased their phagocytic activity upon injury. Inhibition of microglial phagocytosis by targeting phosphatidyl serine receptors either pharmacologically or genetically via CRISPR/Cas9-mediated gene editing resulted in a significant increase in the rate of secondary cell death. This result demonstrated a role for rapid phagocytosis of debris in limiting the extent of secondary cell death, and suggested an overall neuroprotective role for microglial phagocytosis. Probing into the transcriptome of microglia/macrophages following injury using RNA sequencing of sorted cells revealed profound transcriptomic changes within two hours of injury, and will aid the future investigation of the role of microglia in neuroprotection.

To summarise, this body of work provides evidence for a neuroprotective role of microglia in a new larval zebrafish model of brain injury, and the transcriptomic analysis will form the basis of a more in-depth study of microglia-derived neuroprotective molecules. Using CRISPR/Cas9-guided mutation of genes of interest in larval zebrafish, we will be able to investigate the role of these genes following injury in microglia-mediated neuroprotection. Following further validation, these findings could potentially be exploited for prevention of secondary cell death after human TBI.

Lay summary

Traumatic brain injury (TBI), defined as injury to the brain caused by external force, is a major cause of death and disability worldwide. TBI can lead to a significant loss of nerve cells, or neurons, which occurs in two phases following injury: primary cell death, caused directly by physical damage, and secondary cell death, which happens in a delayed manner in the minutes to weeks following injury and is caused by cellular processes that are harmful to neuronal survival. It is thought that targeting delayed cellular processes could potentially prevent secondary neuronal cell death, and research in rodents has been aimed at understanding these harmful mechanisms and how to inhibit them. However, no pharmacological compound was able to improve the outcome of patients following TBI in clinical trials compared to placebo so far, indicating that further research is required in order to understand and treat secondary cell death. Recently, cells of the immune system are of particular interest, as they have been implicated in protecting neurons following stroke, and the largest clinical TBI trial to date showed that more patients died after receiving a drug inhibiting the immune system. In my thesis, I aimed to investigate the role of immune cells, in particular microglia, which are specialised immune cells in the brain, after brain injury.

For this purpose, I developed a new model of brain injury in larval zebrafish. Zebrafish are native to Nepal, but have been used in laboratories all over the world for several decades. Despite sharing 80% of disease-related genes with humans, zebrafish - unlike humans - have the remarkable capacity to restore function following injury in many organs, including the heart, brain, and spinal cord. Zebrafish develop rapidly and have a functional nervous system within three to four days after being born. At this time, called the larval stage, they are transparent. Researchers have established several fish lines to label distinct cell types or molecules in these fish with fluorescent markers that emit light when activated with a certain laser; in combination with the transparency of the larval zebrafish, we are therefore able to visualise cellular and molecular processes in these fish under the microscope in real-time. This provides a significant advantage over the use of rodents, where real-time microscopy in living animals proves significantly more challenging and invasive.

With my experiments, I could show that zebrafish, similar to humans, experience both primary (direct) and secondary (indirect) cell death in response to injury. Using real-time microscopy, I found

that microglia - the resident immune cells of the brain - are rapidly recruited to the site of injury and remove cells damaged by the injury. As damaged or dead cells can release toxic substances to their neighbouring cells and thereby harm them, I hypothesised that their clearance by microglia could reduce the occurrence of secondary cell death following brain injury. I tested this by inhibiting the clearance process either by application of a pharmacological compound, or genetic modification of the larvae, and found clearance of debris indeed limited the rate at which cells die following an injury, suggesting a neuroprotective role for this process. Furthermore, I performed an in-depth analysis of changes in the genetic profile of microglia following brain injury, which revealed that the injury induced the production of certain molecules which have been previously implicated in promoting neuronal survival.

Taken together, this body of work provides an insight into the dynamic function of microglia following brain injury, and will form the foundation of further investigations of microglia-derived neuroprotective molecules that could be used as therapeutic approaches for patients with TBI.

Declaration

I declare that this thesis was composed by myself and that the work contained therein is my own, except where explicitly stated otherwise in the text, and that this work has not been submitted for any other degree or professional qualification.

(Chiara Maria Stella Herzog)

Acknowledgements

First and foremost, I would like to thank my principal supervisor, Dr. Leah Herrgen, for taking me on as her first PhD student and providing me with the exciting opportunity to work on CNS repair - something I wanted to investigate since I was fifteen years old and discovered axolotls can repair their CNS. I would like to thank her for her guidance and support throughout the years - pushing me to ask the right questions while allowing me to become an independent researcher, develop my own ideas, and giving me the opportunity to present my work at several conferences.

Thanks to my thesis committee, Prof. Catherina Becker, Dr. Veronique Miron, and Prof. David Lyons, for hugely improving my work with their critical input. A special thanks to Prof. David Lyons for being an excellent chair of the thesis committee, and being there when I needed to talk.

Thanks to the Herrgen laboratory and all its new and former members. David, for being there since the very first day, for keeping the lab running smoothly without me having to worry about things, for providing scientific expertise and general life advice, and the best coffee breaks and banter anyone could hope for. Marcus, for teaching me the joys of HAGs, and your scientific support and break room chats. Juan, for being the an excellent student and taking over my work to validate the RNA sequencing. Laura, for carrying out some of the excitotoxicity experiments.

Thanks to the research community of the CDBS and the Little France Campus for being so supportive and sharing both knowledge and reagents, with a particular thanks to the Sieger laboratory and Becker laboratory without whom many of my experiments would not have happened. To the employees of the fish facility for keeping my fish happy, with particular thanks to John and Angus for keeping me happy while being over there. Thanks also to the great staff at the Flow Cytometry facility, which made everything run so smoothly during my FACS experiments.

Thanks to my friends for being patient with me when I was busy and stressed throughout these past years, or did not have the time to talk. Thanks for always being there to lend an ear when I had to vent about a failed experiment or share the happiness of a successful one - particularly Nina and Rebekka.

Finally, thanks to my family for supporting me - emotionally and financially - throughout my years of studying. I would not be where I am today without your support and belief in me. Thank you, mum, for inspiring the love of languages and travel in me that have led me to Edinburgh in the first place. Thank you, dad, for passing on your curiosity for all things *science*. Thank you, granddad, for allowing me to study in Edinburgh with your financial support. Thank you, grandma, for so many things - but especially for inspiring me to *think* since I was four years old.

This is for all of the people who believed in me and supported me with their presence in my life to make this thesis possible - *thank you*.

Abbreviations

AD	Alzheimer's disease
ATP	adenosine triphosphate
bp	base pairs
Ca²⁺	calcium
CCL2	C-C motif chemokine ligand 2
CCR2	C-C chemokine receptor type 2
CDC	Center for Disease Control and Prevention
DAMP	damage-associated molecular pattern
DC	decompressive craniectomy
dpf	days post fertilisation
ECM	extracellular matrix
GCS	Glasgow Coma Scale
hpi	hours post injury
ICP	intracranial pressure
IFNγ	interferon gamma
IL	interleukin
IL-1ra	interleukin 1 receptor antagonist
L-SOP	<i>O</i> -phospho- <i>L</i> -serine
MDD	major depressive disorder
MerTK	Mer tyrosine kinase
MFG-E8	milk fat globulin-EGF factor 8
mTBI	mild traumatic brain injury
OT	optic tectum
PAM	protospacer adjacent motif
PAMP	pathogen-associated molecular pattern
PEG-SOD	polyethylene glycol-conjugated superoxide dismutase
PS	phosphatidyl serine
RNS	reactive nitrogen species
ROS	reactive oxygen species

RTA	road traffic accident
SCI	spinal cord injury
sTBI	severe traumatic brain injury
SOD	superoxide dismutase
TBI	traumatic brain injury
TNFα	tumor necrosis factor alpha
TUNEL	terminal deoxynucleotidyl transferase dUTP nick end labeling

Contents

Abstract	II
1 Introduction	1
1.1 Traumatic brain injuries and their socio-economic burden	1
1.1.1 Neurological disorders	3
1.1.2 Psychiatric disorders	4
1.1.3 Neurodegenerative diseases	4
1.2 Wound healing and regeneration: phases and contribution of macrophages	5
1.2.1 Phases of wound healing	6
1.2.2 Wound repair in the CNS: differences to other tissues	8
1.2.3 The role of microglia/macrophages in repair and regeneration	10
1.3 Pathophysiology of secondary cell death	12
1.3.1 Excitotoxicity	13
1.3.2 Oxidative stress	15
1.3.3 Blood flow dysregulation	17
1.3.4 Neuroinflammation	17
1.4 The quest for a magic bullet: past and present clinical trials	22
1.4.1 Therapeutic strategies	24
1.4.2 Neuroprotective agents	26
1.5 The zebrafish as a model of successful (CNS) regeneration	31
1.5.1 Comparison of injury reactions between zebrafish and mammals	31
1.5.2 CNS regeneration in zebrafish	32
2 Hypothesis & Aims	37
3 Materials & Methods	39
3.1 Fish maintenance	39
3.2 Transgenic fish lines	39
3.2.1 Generation of <i>β-actin:GCaMP6f</i> transgenic fish line	40
3.3 Mosaic labelling of individual tectal neurons	40

3.4	Induction of brain injury	40
3.5	Whole-mount immunostaining of zebrafish larvae	41
3.6	Image acquisition	41
3.7	Image processing and analysis	42
3.8	Supplementary movies	43
3.9	Drug treatments	43
3.9.1	Statistical analysis of drug treatments on calcium wave parameters	44
3.10	Generation of <i>adgrb1a/b</i> crispants using CRISPR/Cas9-targeted gene editing	45
3.10.1	Guide design and injection	45
3.10.2	DNA extraction and test of guide efficiency via restriction fragment length polymorphism (RFLP)	45
3.10.3	Mutation analysis of <i>adgrb1a/b</i> crispants by sequencing	45
3.11	Quantitative real-time PCR	46
3.11.1	RNA extraction and cDNA synthesis for qRT-PCR	46
3.11.2	qRT-PCR primer design & validation	47
3.11.3	Quantitative reverse-transcription PCR (qRT-PCR)	48
3.11.4	qPCR analysis	49
3.12	RNA sequencing	49
3.12.1	Isolation of transgenically labelled fluorescent cells from larval heads via FACS	49
3.12.2	RNA extraction from FACS sorted cells	50
3.12.3	cDNA synthesis and isothermal amplification for RNA sequencing	50
3.12.4	Library preparation, sequencing and bioinformatical analysis of amplified cDNA	51
3.12.5	Generation of expression heatmaps	53
3.12.6	Gene ontology enrichment analysis	53
3.13	Statistical methods	53
4	Mechanical injury induces primary and secondary cell death in a larval zebrafish model of brain injury	55
4.1	Introduction	55
4.2	Description of injury	57
4.3	Dynamics of cell death: primary necrotic and secondary apoptotic cell death	59
4.4	Discussion	69
5	Description of calcium signalling following mechanical brain injury in larval zebrafish	75
5.1	Introduction	75
5.2	Early calcium signalling	77
5.2.1	Description of calcium waves immediately following injury	77
5.2.2	Signalling leading to early calcium waves following brain injury	80

5.2.3	Downstream effects of early calcium signalling	84
5.3	Excitotoxicity following mechanical brain injury in larval zebrafish	87
5.4	Discussion	92
5.4.1	Early calcium signalling	93
5.4.2	Sustained calcium transients	96
6	Rapid clearance of debris by microglia limits secondary neuronal cell death	99
6.1	Introduction	99
6.2	Recruitment of microglia/macrophages	100
6.3	Microglia, but not peripheral macrophages, are present within injured brain	103
6.4	Comparison of wild type and <i>irf8</i> ^{-/-} larvae	105
6.4.1	Cell death	106
6.4.2	Neutrophil recruitment	107
6.4.3	Caveats of using <i>irf8</i> ^{-/-} mutants to discern microglia/macrophage effects on cell death	108
6.4.4	Profile of cytokines and neurotrophic factors	109
6.5	Inhibition of pro-inflammatory cytokine <i>Tnfa</i> results in a reduction of secondary cell death	113
6.6	Microglia/macrophages increase rate of phagocytosis following injury	114
6.7	Inhibition of phagocytosis leads to an increase of secondary cell death	116
6.7.1	Pharmacological inhibition of phagocytosis via bath application of L-SOP	116
6.7.2	Genetic manipulation of phagocytosis using CRISPR/Cas9 targeted mutation of <i>adgrb1a/b</i>	120
6.8	Discussion	124
6.8.1	Alterations in the whole head transcription levels of cytokines and trophic factors	124
6.8.2	Microglial phagocytosis mediates neuroprotection	127
7	Microglia/macrophage transcriptomic alterations in response to injury	131
7.1	Introduction	131
7.2	Sample preparation: cell yield, RNA quantity/quality and cDNA amplification results	132
7.3	RNA sequencing results and exploratory analysis	137
7.4	Comparison of RNA sequencing results to qRT-PCR results from whole heads	141
7.5	Selected findings of interest from RNA sequencing	142
7.5.1	MAP kinase pathway inactivation (<i>dusp</i> gene upregulation)	142
7.5.2	Cytokines and cytokine receptors	142
7.5.3	Neurotrophic factors	145
7.6	Discussion	145

7.6.1	Comparison to whole head qRT-PCR	145
7.6.2	MAP kinase inactivation	146
7.6.3	Cytokine & cytokine receptors	147
7.6.4	Neurotrophic factors	150
7.6.5	Limitations of the current dataset	151
7.6.6	Future outlook	152
8	Discussion	155
8.1	A simple, new zebrafish assay to investigate secondary cell death	155
8.2	Conserved pathophysiology between rodent TBI and zebrafish mechanical brain injury	157
8.3	Early calcium signalling: friend or foe?	158
8.4	A critical role for microglial phagocytosis of debris in neuroprotection	159
8.5	Conclusion & future outlook	161
	References	161

List of Figures


1.1	Schematic of some of the pathophysiological molecular and cellular mechanisms occurring following traumatic brain injury. Not to scale; schematic created by me.	23
1.2	Clinical trials in TBI since 1980. Multi-centre phase III RCTs for traumatic brain injury plotted for initiation and success (defined as benefit over placebo). Modified from Maas et al. (2010). * 1 RCT initiated in 2014 has not reported results yet.	24
4.1	Description of the injury assay. (A) Schematic of the dorsal view of the larval zebrafish outlining forebrain (FB), optic tectum (OT), and hindbrain (HB). The site of injury is indicated by a drawing of the needle. (B) Representative brightfield images of a larva before and during injury. (C) Quantification of fractions of normal larvae, larvae with haemorrhage, and dead larvae following injury in 6 different biological replicates with a total n of 1075.	58
4.2	Mechanical injury leads to rapid cell death as monitored by of PI uptake. (A) Mechanical injury results in a prompt uptake of PI. Scale bar, 50 μm . (B) Quantification of PI ⁺ cells after mechanical injury. Dashed line indicates time of injury. n \geq 6 animals per experimental group.	60
4.3	PI⁺ cells display morphological characteristics of necrosis immediately after injury, and of apoptosis hours later. (A, B) The diameter of PI ⁺ cells (arrowheads) is not significantly different from viable cell nuclei (<i>H2A:GFP</i>) at 0 hpi. Scale bar, 10 μm . Values are the average of at least 10 PI ⁺ and <i>H2A:GFP</i> ⁺ cells in one optical section per animal. n = 5; p > 0.999 in Mann-Whitney Test. (C, D) At 6 hpi, the diameter of PI ⁺ cells (arrowheads) is significantly smaller than that of viable cell nuclei. Scale bar, 10 μm . Values are the average of at least 10 PI ⁺ and <i>H2A:GFP</i> ⁺ cells in one optical section per animal. n \geq 5; p \leq 0.005 in Mann-Whitney Test.	61

4.4	<p>Mechanical brain injury leads to delayed nuclear condensation peaking at 6 hpi. (A) Overview and close-ups of tectum in H2A:GFP transgenic animals before, and at 0, 6, and 24 hpi. Scale bar, 50 or 5 μm, respectively. (B) Close-up of a pyknotic nucleus with the Fire LUT (ImageJ), showing the distinct difference in size and intensity of pyknotic nuclei compared with surrounding normal nuclei. Scale bar, 5 μm. (C) Quantification of pyknotic nuclei present in entire tectum following injury. Dotted vertical line indicates time of injury. $n \geq 6$ animals per timepoint. (D) Heat map illustrating the spread of secondary cell death throughout the tectum in the hours following injury. XY coordinates of pyknotic nuclei from representative animals at varying timepoints following injury were plotted in 2D using the Matlab Scattercloud function.</p>	62
4.5	<p>Cells with radial glial and microglial morphology take up PI, but survive long after the injury. (A) Cells with radial glial morphology at 6 hpi and 48 hpi do not appear condensed, but have PI in their cytoplasm. Arrowheads are pointing towards cell bodies of radial glia. Scale bar, 15 μm. (B) At 6 hpi, large aggregations of PI⁺ debris were often present. Based on the size of these aggregates (larger than normal neurons), these are likely microglia that have taken up PI⁺ cells but not yet degraded them. At 48 hpi, some microglia and their processes appear PI⁺. Arrowheads are pointing to microglial cell bodies. Scale bar, 15 μm. (C) Ventricular injection of P2X subtype receptor inhibitor iso-PPADS ablates radial glial uptake of PI (6/6 animals). Images shown taken at 6 hpi in either vehicle (Calcium-free Ringer solution) or iso-PPADS injected larvae bathed in propidium iodide. Scale bar, 15 μm.</p>	64
4.6	<p>Occurrence of apoptosis following brain injury is confirmed in an apoptosis reporter line and through Caspase-3 immunostaining. (A) Apoptotic cell death takes place in the hours after mechanical injury as shown by an increase in the number of cells externalising phosphatidylserine. Scale bar, 50 μm. (B) Immunostaining for cleaved Caspase-3 shows a delayed increase in apoptosis after injury. 50 μm. (C) Quantification of Annexin 5⁺ cells. $n = 12$ animals per experimental group. *, $p < 0.05$ in two-way ANOVA. (D) Quantification of cleaved Caspase-3⁺ cells. $n = 6$ animals per experimental group. *, $p < 0.05$ in two-way ANOVA.</p>	65
4.7	<p>In vivo imaging of individual tectal neurons shows that both primary and secondary cell death occur after brain injury. (A, C, E) Confocal images of the optic tectum of H2A:GFP transgenic animals. A small number of tectal neurons in the ipsilateral (A) or contralateral (C, E) hemisphere were mosaically labelled through injection of <i>elavl3:memTdTomato</i> plasmid DNA. Scale bars, 50 μm (B, D, F) Close-up of neurons indicated in (A), (C) and (E). White arrow indicates pyknotic nucleus. Scale bars, 10 μm. Data obtained and analysed by Dr. Leah Herrgen. . . .</p>	67



4.8	<p>The majority of apoptotic cells are neurons. (A, B) Most apoptotic cells in control animals (A) and in injured animals at 6 hpi (B) colocalise with a neuronal marker NBT (arrowheads). Scale bars, 10 μm. (C, D) Most apoptotic cells in control animals (C) and in injured animals at 6 hpi (D) colocalise with a neuronal marker elavl3 (arrowheads). Scale bars, 10 μm. (E) Quantification of Annexin 5-BFP⁺ and dsRed⁺/Annexin 5-BFP⁺ cells in control and injured animals. n = 6 animals per experimental group. (F) Quantification of Annexin 5⁺ and kaede⁺/Annexin 5⁺ cells in control and injured animals. n = 6 animals per experimental group.</p>	68
5.1	<p>Injury, but not compression of the brain leads to long-range calcium waves. (A, B) Representative images taken -10s, 6s, or 20s after compression (A) or mechanical injury (B) of the optic tectum in <i>β-actin:GCaMP6f</i> transgenic larvae. Magenta arrowhead in (A) shows site of compression. Arrowheads in (A) (+ 6 s) show sites of calcium activation in the skin. Magenta circle in (B) highlights cell body activation surrounding injury site (+6 s), arrowheads show potential activation of radial glial cells (+ 20 s). ■ Figures correspond to supplementary movies S1 (compression, A), and S2 (injury, B).</p>	78
5.2	<p>Calcium waves occur in cells expressing neuronal and radial glial markers. Crossbreeding of <i>β-actin:GCaMP6s</i> animals with neuronal and radial glial marker animals revealed that calcium waves occur in NBT⁺ cells expressing dsRed (A, arrowheads), and her4.3⁺ cells expressing mCherry lining the ventricle (B, arrowheads). These waves are spatially and temporally overlapping, but radial glial waves occur slightly later than neuronal waves. Scale bar, 20 μm.</p>	79
5.3	<p>Pharmacological inhibitors reveal a key role for NMDA receptors in the neuronal calcium wave in response to injury, while ATP receptors are crucial for the glial wave. (A-H) Representative images for each treatment (Vehicle, MK801+AP5, DNQX, PPADS, iso-PPADS, Ononetin, CBX, and FFA) at 10s following injury. Scale bar, 50 μm. (I) Quantification of neuronal wave intensity as percentage of vehicle-injected controls on the same day. (J) Quantification of neuronal wave area as percentage of vehicle-injected controls on the same day. (K) Quantification of radial glial wave intensity as percentage of vehicle-injected controls on the same day. (L) Quantification of radial glial wave area as percentage of vehicle-injected controls on the same day. (M) Quantification of calcium wave velocity as percentage of vehicle-injected controls on the same day. **, p \leq 0.01; *, p \leq 0.05 in Student's <i>t</i> Test. MK-801/AP5, n = 6; DNQX, n = 14; PPADS, n = 6; iso-PPADS, n = 5; Ononetin, n = 11; CBX, n = 6; FFA, n = 6. ■ Figure corresponds to supplementary movie S3.</p>	82

5.4	Injection of ATP or Glutamate leads to calcium waves similar to observed after injury. Pregnenolone sulfate, an activator of TRPM3 channels, lead to no changes in calcium activity. Images taken 6 s after injection of calcium-free Ringer solution (vehicle), 5 mM ATP, 10 mM L-Glutamate, 0.45 mM Pregnenolone Sulfate in <i>β-actin:GCaMP6f</i> larvae.	83
5.5	MK801+AP5 inhibition of calcium signalling lasts for at least 1 h, while PPADS lasts for less than 40 min and reduces recruitment of mpeg1⁺ cells to the injury site. (A) Treatment with MK801+AP5 (ventricular injection) significantly reduces neuronal wave intensity for at least 60 min following injury. *, $p \leq 0.05$ in Kruskal-Wallis Test with Dunn's post-test. $n \geq 3$ animals / group. (B) Treatment with PPADS (ventricular injection) inhibits radial glial wave area for less than 40 min. **, $p \leq 0.01$ in Kruskal-Wallis Test with Dunn's post-test. $n \geq 4$ animals / group. (C) Injection of PPADS leads to a significant reduction in the number of mpeg1 ⁺ cells at the site of brain injury at 2 hpi, but did not lead to a decrease in the overall number of mpeg1 ⁺ cells in tectum and skin (D) (i.e., does not cause microglia/macrophage cell death).	85
5.6	Ventricular injection of BAPTA-AM 2 h prior to injury leads to significant reduction of neuronal and glial waves but solvent causes microglia/macrophage changes. (A) Quantification of calcium wave parameters as % of control values. **, $p \leq 0.01$ in Student's <i>t</i> -Test or Mann-Whitney Test, respectively. $n \geq 6$ animals / group. (B) Representative images of mpeg1:GFP transgenic larvae 2 h post injection of Ca ²⁺ -free Ringer's, Pluronic/DMSO, and BAPTA-AM (in Pluronic/DMSO), including zoom on mpeg1 ⁺ cells on the right hand side. BAPTA-AM appears to cause a reduction in number of mpeg1 ⁺ cells (not quantified) and more amoeboid morphology. Scale bars, 50 μm (left), 15 μm (right).	86
5.7	Ventricular injection of BAPTA tetrasodium salt leads to significant reduction to neuronal and radial glial wave area but not intensity. Quantification of neuronal and radial glial wave intensity and area relative to control values. **, $p \leq 0.01$ in Student's <i>t</i> -Test. $n \geq 5$ animals / group.	87

- 5.8 **Calcium transients are significantly increased for at least 6 hpi, and are increased in both neurons and microglia/macrophages. (A, B)** Live imaging of calcium dynamics in the optic tectum of *β-actin:GCaMP6f* larvae in a sham animal **(A)** and an injured animal at 0 hpi **(B)**. White arrows indicate individual tectal cells. Scale bars, 20 μm. **(C, D)** Calcium traces from the individual tectal cells highlighted in (A) and (B). **(E)** Quantification of calcium transients in the whole tectum over 30 min from indicated time. **, $p < 0.01$ in Two-Way ANOVA. $n = 6$ / group. **(F)** Quantification of calcium transients in sham or injured animals (0 hpi) in *NBT:dsRed* or *mpeg1:mCherry⁺* cells. **, $p < 0.01$ in One-Way ANOVA. $n \geq 6$ / group. Data in (E) and (F) collected and analysed by Laura Pons. 88
- 5.9 **Pyknotic cell death occurs in regions of high calcium activity.** Heatmaps of calcium transients and pyknotic nuclei in 6 larvae. Calcium transients were quantified between 2-3 h post injury, while pyknotic nuclei were quantified at 3 h post injury. 89
- 5.10 **Treatment with NMDA receptor antagonists MK801 and AP5 abolishes injury-induced sustained increase in calcium signalling and reduces secondary cell death at 6 hpi.** Treatment with NMDA receptor inhibitor mix MK801 and AP5 significantly reduced calcium transients both immediately **(A)**, and at 6 hpi **(B)** while not affecting transients in sham animals. **, $p \leq 0.01$ in Two-Way ANOVA. $n \geq 6$ animals / group. **(C)** Representative close-up images of vehicle- or MK801+AP5-treated *H2A:GFP* larvae at 6 hpi. Arrowheads are pointing at pyknotic nuclei. Scale bar, 25 μm. Experiment performed and images acquired by Laura Pons. **(D)** Representative close-up images of vehicle- or MK801+AP5-treated larvae stained with PI at 0 hpi. Arrowheads are pointing at PI⁺ cells. Scale bar, 20 μm. **(E)** Quantification of pyknotic nuclei in whole tectum of vehicle- or MK801+AP5-treated *H2A:GFP* larvae (sham or 6 hpi). **, $p \leq 0.01$ in Two-Way ANOVA. $n = 6$ animals / group. **(F)** Quantification of PI⁺ cells in whole tectum of vehicle- or MK801+AP5-treated animals (sham or 0 hpi). ns in Two-Way ANOVA. $n \geq 6$ animals / group. 91
- 5.11 **Treatment with NMDA receptor agonist L-glutamate causes a significant increase of secondary cell death at 6 hpi. (A)** Representative close-up images of vehicle- or L-Glutamate-treated *H2A:GFP* larvae at 6 hpi. Arrows are pointing at pyknotic nuclei. Scale bar, 25 μm. **(B)** Quantification of pyknotic nuclei in whole tectum of vehicle- or L-glutamate-treated *H2A:GFP* larvae (sham or 6 hpi). **, $p \leq 0.01$ in Two-Way ANOVA. $n = 6$ animals / group. 92
- 5.12 **Schematic of factors eliciting early and sustained calcium signalling following mechanic injury.** Magenta and green ellipses depict dead or healthy neurons, respectively, and mechanisms inducing early and sustained calcium signalling following injury are illustrated. 97

6.1	<p>Cells expressing the microglia/macrophage marker <i>mpeg1</i> migrate to the site of injury. Images taken before, 1, and 2 hours post injury from the same animal. PI is indicating presence of dead cells. Scale bar, 50 μm In the lower right panel: quantification of <i>mpeg1</i>⁺ cells at site of brain injury, excluding cells on the skin. n = 6 animals.</p>	101
6.2	<p><i>mpeg1</i>⁺ cells change their behaviour from sedentary surveillance to responsive migration in the first two hours following injury. (A) Traces visualizing <i>mpeg1</i>⁺ cell body movement before and 2 hpi. (B) Quantification of average <i>mpeg1</i>⁺ cell body migration speed. **, p = 0.0011 in paired <i>t</i> test; n = 8 animals. (C) Quantification of average <i>mpeg1</i>⁺ cell net displacement before and after injury. **, p = 0.0001 in paired <i>t</i> test; n = 8 animals.  Figure corresponds to movies S4 (A, before) and S5 (B, injured).</p>	102
6.3	<p>Virtually all macrophages recruited to the injury site express microglial markers P2Y₁₂ or 4C4. (A) Representative images of <i>mpeg1:mCherry;p2y12:P2Y₁₂-GFP</i> transgenic larvae at 6 hpi. Yellow arrows indicate microglia (P2Y₁₂⁺/<i>mpeg1</i>⁺ or <i>mpeg1</i>⁻), blue arrows indicate immune cells on skin (P2Y₁₂⁺ or P2Y₁₂⁻/<i>mpeg1</i>⁺). Scale bar, 40 μm. (B) Images of the brain injury site acquired at 6 hpi. Orange arrows point to microglia (4C4⁺/GFP⁺ or GFP⁻), blue arrow points to macrophages (4C4⁻/GFP⁺). Scale bar, 25 μm. (C) Images acquired from the spinal cord showing microglial cell (orange arrow; 4C4⁺/GFP⁺) in spinal cord region and macrophages (blue arrow; 4C4⁻/GFP⁺) in rest of the trunk. Scale bar, 25 μm. (D) Quantification of microglia and macrophages at the injury site in <i>mpeg1:mCherry;p2y12:P2Y₁₂-GFP</i> transgenic larvae. n = 6 animals per experimental group. (E) Quantification of microglia and macrophages at the injury site using immunohistochemistry against 4C4. n = 9.</p>	104
6.4	<p>Traces visualising past cell body displacement of skin macrophages which do not enter the brain. Traces showing past cell body displacement of <i>mpeg1:GFP</i>⁺ cell within 2 hpi. Quantification of immune cell transitions during 2 h after injury. n = 7 animals per experimental group.</p>	105
6.5	<p>Very few neutrophils are recruited to the brain injury. Representative images of <i>mpo:GFP</i> transgenic larvae before, 1, 2, or 6 hpi. Magenta arrow indicates injury site. Scale bar, 50 μm. Adjacent: quantification of <i>mpo</i>⁺ cells at the site of injury (skin or brain).</p>	105

- 6.6 ***irf8*^{-/-} mutants lacking microglia and macrophages exhibit increased numbers of (secondary) cell death following brain injury.** (A) Representative images of a wild type and *irf8*^{-/-} animal at 6 hpi labelled with PI bath application. Scale bar, 50 μm. (B) Quantification of PI⁺ cells following injury. Significance relates to wild type animals of respective treatment. **, $p \leq 0.01$ in Two-Way ANOVA. (C) Representative images of pyknotic nuclei in a wild type and *irf8*^{-/-} animal at 6 hpi. Scale bar, 50 μm. (D) Quantification of pyknotic nuclei following injury. Significance relates to sham animals of respective genotype. **, $p \leq 0.01$ in Two-Way ANOVA. (E) Representative images of cleaved Caspase-3 immunostaining in a wild type and *irf8*^{-/-} animal at 6 hpi. Scale bar, 50 μm. (F) Quantification of cleaved Caspase-3⁺ cells following injury. Significance relates to wild type animals of respective treatment. *, $p \leq 0.05$; **, $p \leq 0.01$ in Two-Way ANOVA. 107
- 6.7 **Myeloid peroxidase (*mpo*) immunoreactive cells in are found in the tectum of *irf8*^{-/-}, but not wild type animals, and are increased at 6 hours post injury.** Scale bar, 50 μm. Quantification of *mpo*⁺ cells at site of injury (brain and skin) before, 6, 24, and 48 hpi. Significance relates to wild type sham animals. **, $p \leq 0.01$ in Two-Way ANOVA with Bonferroni Post-Test. $n \geq 5$ animals / timepoint. . . 108
- 6.8 **Changes in cytokine and neurotrophic factor transcript levels elicited by injury are altered in *irf8*^{-/-} mutants.** Relative quantification of mRNA transcript levels via qRT-PCR. Significance was determined via Two-Way ANOVA and relates to sham values of respective genotype. *, $p \leq 0.05$; **, $p \leq 0.01$. Per replicate, the heads of 50 animals were pooled. $n \geq 3$ per timepoint. 111
- 6.9 **Cells with microglia and macrophage morphology express *il1b* and *tnfa*.** (A) Images taken from *il1b*:GFP transgenic larvae either in control animals, or 2 or 6 hpi. (B) Close-ups of images in (A); location in tectum indicated by dashed boxes in (A). Notice the change of morphology of cells expressing *il1b* at 6 hpi (C) Representative images acquired using the *tnfa*:eGFP-F transgenic line. 112
- 6.10 ***tnfa* crispants exhibit a reduction in secondary cell death following brain injury.** (A) Representative close-up images of injury site in uninjected or *tnfa* crispant transgenic *H2A*:GFP larvae at 6 hpi. Arrowheads point to pyknotic nuclei. Scale bar, 25 μm. (B) Quantification of pyknotic nuclei in uninjected or *tnfa* crispant animals either uninjured (sham) or 6 hpi. *, $p \leq 0.05$ in Two-Way ANOVA; $n \geq 9$ per group. 113
- 6.11 **Orthogonal view of neurons (magenta) in *mpeg1*⁺ cell (green) at 2 hours post injury.** Scale bar, 10 μm 114

6.12	Phagocytosis is significantly increased upon injury. (A, B) Representative images of timelapses of <i>mpeg1</i> :GFP animals stained with PI either before or 0.5 h after injury. Scale bar, 15 μ m. (C) Quantification of average phagocytic events of PI ⁺ cells per <i>mpeg1</i> ⁺ cell per 48 minutes. **, $p \leq 0.01$ in Mann-Whitney Test. $n \geq 8$ animals / group. (D, E) Representative images phagocytosis in <i>mpeg1</i> :GFP animals either before (D) or 0.5 h after injury (E). Representative <i>mpeg1</i> :GFP ⁺ cell in (D) is engulfing PI ⁻ cargo, while <i>mpeg1</i> :GFP ⁺ cell in (E) has already engulfed PI ⁺ cargo and is currently engulfing PI ⁻ cargo. Scale bar, 15 μ m. (F) Quantification of average phagocytic events per <i>mpeg1</i> ⁺ cell per 48 minutes. **, $p \leq 0.01$ in Mann-Whitney Test. $n = 8$ animals / group.  Figure corresponds to movies S6 (A, before) and S7 (B, 0.5 hpi).	115
6.13	No internalised PI⁺ cells or debris can be seen in her4.3⁺ radial glia in sham or injured animals. Scale bar, 25 μ m. ns in Mann-Whitney test; $n = 6$ animals / group	116
6.14	Phagocytosis of PI⁺ cells is significantly decreased after treatment with L-SOP. Representative images of timelapses of vehicle- (A) or L-SOP-treated (B) animals following injury. Scale bar, 15 μ m. (C) Quantification of average PI ⁺ phagocytic events per <i>mpeg1</i> ⁺ cell per 48 minutes. **, $p \leq 0.01$ in Student's <i>t</i> -Test. $n \geq 6$ animals / group.  Subfigure (B) corresponds to supplementary movie S8	117
6.15	Effect of L-SOP treatment on recruitment of <i>mpeg1</i>:GFP⁺ cells towards the site of brain injury (A), and effect on calcium transients in uninjured and injured β-actin:GCaMP6f larvae (B). L-SOP had no significant effect on either of these two parameters. (A) ns for all timepoints in Two-Way ANOVA. (B) ns in Two-Way ANOVA.	118
6.16	Microglial phagocytosis limits secondary cell death. (A) Representative images of vehicle- or L-SOP-treated animals at 6 hpi. Scale bar, 25 μ m. (B) Representative images of two timepoints of timelapse of vehicle- or L-SOP-treated animals between 4.5 and 5 hpi. Scale bar, 25 μ m. (C) Quantification of pyknotic nuclei in sham or injured animals treated with vehicle or L-SOP. **, $p \leq 0.01$ in Two-Way ANOVA. $n \geq 6$ animals / group. (D) Quantification of newly appearing pyknotic nuclei in sham or injured animals treated with vehicle or L-SOP. **, $p \leq 0.01$ in Two-Way ANOVA. $n \geq 6$ animals / group.	119
6.17	CRISPR-guided mutation of <i>adgrb1a</i> and <i>adgrb1b</i> causes loss of endonuclease restriction site and reduction of transcript levels. (A) Representative gel image following PCR product digestion with <i>Bsll</i> in uninjected controls and crispants. (B) qRT-PCR analysis of relative expression of <i>adgrb1a</i> and <i>adgrb1b</i> transcript levels in whole larval bodies at 4 dpf. **, $p \leq 0.01$ in One-Way ANOVA compared to uninjected controls; 10 animals pooled per sample; $n = 4$	120

6.18	Mutations in <i>adgrb1a</i> transcripts revealed by sequencing. First line shows wild type sequence, with guide RNA target sequence underlined and highlighted proto-spacer adjacent motive (PAM) site. Insertions are highlighted with purple, while deletions are represented by -. Total number of inserted or deleted bases and frequency of each mutation shown next to each sequence.	121
6.19	Mutations in <i>adgrb1b</i> transcripts revealed by sequencing. First line shows wild type sequence, with guide RNA target sequence underlined and highlighted PAM site. Insertions are highlighted, with purple while deletions are represented by -. Total number of inserted or deleted bases and frequency of each mutation shown next to each sequence.	121
6.20	Phagocytosis of PI⁺ cells is significantly decreased after CRISPR/Cas9 targeted mutation of zebrafish paralogues of PS receptor BAI1. Representative images of timelapses of uninjected (A) or crisprant animals (B) following injury. Scale bar, 15 μm. (C) Quantification of PI ⁺ cells being engulfed per <i>mpeg1</i> ⁺ cell in 48 minutes. **, $p \leq 0.01$ in Two-Way ANOVA. $n \geq 6$ animals / group. (D) Quantification of <i>mpeg1</i> :GFP ⁺ cells at the site of brain injury before, 0, 1, 2, and 6 hpi. ns for all timepoints in Two-Way ANOVA. $n \geq 9$ animals / group. 🎬 Subfigure (B) corresponds to supplementary movie S8.	122
6.21	Inhibition of microglial phagocytosis through genetic manipulation of <i>adgrb1a</i> and <i>adgrb1b</i> significantly increases number of pyknotic nuclei at 6 hpi, and increases the rate of secondary cell death. (A) Representative images of uninjected or <i>adgrb1a/b</i> crisprant animals at 6 hpi. Scale bar, 25 μm. (B) Representative images of two timepoints of timelapse of uninjected or <i>adgrb1a/b</i> crisprant animals between 4.5 and 5 hpi. Scale bar, 25 μm. (C) Quantification of pyknotic nuclei in sham or injured uninjected or crisprant animals. **, $p \leq 0.01$ in Two-Way ANOVA. $n \geq 6$ animals / group. (D) Quantification of pyknotic nuclei in sham or injured uninjected or crisprant animals. **, $p \leq 0.01$ in Two-Way ANOVA. $n \geq 6$ animals / group.	123
7.1	Representative plots of side scatter (SSC) to GFP intensity from FACS reports sorting for 4C4 or <i>mpeg1</i>:GFP. (A) SSC against GFP intensity for 4C4 ⁺ cell sorting. White asterisk indicates population of cells unspecifically stained by the secondary antibody (as determined by no secondary control). (B) Population report. Only 0.9% of live cells are GFP ⁺ . (C) SSC against GFP intensity for <i>mpeg1</i> :GFP sorting. (D) Population report. 2.1% of live cells are GFP ⁺	134
7.2	Quantification of <i>mpeg1</i>⁺ and 4C4⁺ cells in the whole larval head. Acquired from dorsal or ventral imaging of the whole head in <i>mpeg1</i> :GFP transgenic larvae and anti-4C4 immunostained larvae.	135

7.3	Quality control gel of cDNA following Amplification using NuGEN® Ovation RNA-Seq System V2. A1, Ladder. B1, Sham 1. C1, Sham 2. D1, Sham 3. E1, Sham 4. F1, Sham 5. G1, Sham 6. H1, 2 hpi 1. A2, 2 hpi 2. B2, 2 hpi 3. C2, 2 hpi 4. D2, 2 hpi 5. E2, 2 hpi 6. F2, Empty lane.	135
7.4	Excerpt of significantly upregulated genes and their respective expression in individual samples. FDR \leq 0.05, fold change \geq 1.2.	138
7.5	Excerpt of significantly downregulated genes and their respective expression in individual samples. FDR \leq 0.05, fold change \leq 1.2.	138
7.6	Visual representation of enriched GO terms in list of upregulated genes from RNA sequencing dataset. Genes were filtered by an FDR \leq 0.05, and a fold change of \geq 1.2	139
7.7	Expression of genes previously analysed in whole head qRT-PCR in RNA sequencing from sorted microglia/macrophages.	142
7.8	Heatmaps of relative transcript levels of selected genes in RNA sequencing dataset, normalised per row (assigned z-Score). (A) Relative transcript levels for genes in the GO term MAP kinase inactivation. (B) Relative transcript levels for cytokine and cytokine receptors that were upregulated in RNA sequencing dataset. (C) Relative transcript levels for genes implicated in neurotrophic functions.	144

List of Tables

1.1	Glasgow Coma Scale. Developed by Teasdale and Jennett (1974).	2
1.2	Therapeutic approaches to treat TBI. Compounds that have been used in the clinic, their respective targeted pathomechanism, and reported outcomes in clinical trials.	30
3.1	Zebrafish lines. Transgenic and mutant zebrafish lines used over the course of my research.	39
3.3	Drugs used for pharmacological manipulation. Drug name, concentration, and mode of delivery.	44
3.5	Primers used for qRT-PCR. Gene RefSeq numbers, primer sequence, length, melting temperature (T_m), and GC content.	47
3.6	Primer efficiency following optimisation. Gene target, optimal concentration, slope on cDNA concentration curve including r^2 , and Efficiency (E/%) are included in this table.	48
3.7	Contrasts specified for differential analysis. Any variable specified under blocking was used as part of an additive model, and accounted for in differential analysis of that contrast.	52
7.1	Cell and RNA yields using different markers for fluorescence activated cell sorting. Values for antibody-dependent sorting of 4C4 ⁺ microglial cells, or sorting using the <i>mpeg1</i> :GFP) transgenic line. RNA amounts were determined on the the LabChip GX24.	134
7.2	Cell yields, RNA quantity/quality and cDNA quantity. Cell number obtained following FACS of <i>mpeg1</i> :GFP ⁺ cells. RNA quantity and quality obtained following RNA extraction by analysis on the LabChip GX24. cDNA quantity obtained by analysis on the NanoDrop One following amplification reaction.	136
7.3	Gene ontology analysis of upregulated genes in RNA sequencing dataset. Analysis shows mapped genes in background, and how many of these are represented in the upregulated list. Fold enrichment is then performed based on expected values in a random dataset.	140

7.4	Counts per million (CPM) values for genes previously analysed using qRT-PCR from whole heads in wild type and <i>irf8</i>^{-/-} mutant animals. n.d. = not detected; n.a. = not applicable.	141
7.5	Counts per million (CPM) values for <i>dusp</i> genes. Notice the FDR for <i>dusp6</i> and <i>dusp1</i> is > 0.05.	143
7.6	Counts per million (CPM) values for cytokine and cytokine receptor genes.	143
7.7	Counts per million (CPM) values for genes encoding neurotrophic factors.	143

Chapter 1

Introduction

1.1 Traumatic brain injuries and their socio-economic burden

Traumatic brain injury (TBI) is defined as alteration of brain function, or other evidence of brain pathology, caused by an external force (Menon et al., 2010). TBI is a critical problem in public health and poses a significant socio-economic burden worldwide: direct medical and indirect costs, such as lost productivity, have been reported to amount to an annual economic burden of £5.7 billion in the UK (Fineberg et al., 2013). Internationally, TBI has been estimated to pose a socio-economic burden of \$400 billion, reflecting 0.5% of the global economic output (Maas et al., 2017). TBI is one of the leading causes of death, particularly in adults under the age of 45, and life-long disabilities are common in those who survive (Faul and Coronado, 2015; Maas et al., 2008).

TBIs are prevalent in both high- and low-income countries. Fifty million people experience TBI worldwide per year, and it is estimated that about half of the population will have one or more TBIs in their lifetime (Maas et al., 2017). It can affect people from all ages and genders, but is more common in males than females across all ages (Peeters et al., 2015; Taylor et al., 2017; Thurman, 2016). Male to female ratios in Europe have been reported to range from 1.2:1 (Numminen, 2011) to 4.6:1 (Mauritz et al., 2008). In terms of age distribution, TBIs are most common children or adolescents and the elderly (below 25 and above 75, respectively) (Peeters et al., 2015; Taylor et al., 2017). Falls are the most frequent cause of TBI in high-income countries both above the age of 75 and below the age of 15, as road traffic accidents (RTAs) have been significantly reduced by implementation of safety regulations (Faul et al., 2010; Peeters et al., 2015; Taylor et al., 2017). Between the ages of 15 to 25, RTAs remain the most prevalent cause of TBI (Faul et al., 2010; Peeters et al., 2015; Taylor et al., 2017; Thurman, 2016). Furthermore, sports accidents are a common and increasing cause of TBI in adolescents (Centers for Disease Control and Prevention (CDC), 2011; Hootman et al., 2007; Ilie et al., 2013; Lincoln et al., 2011). Conversely, in low- and middle income countries, where 90% of all TBIs occur, the incidence of TBI is steadily increasing

Table 1.1: **Glasgow Coma Scale**. Developed by Teasdale and Jennett (1974).

Domain	Response	Score
Eye opening	Spontaneous	4
	To speech	3
	To pain	2
	None	1
Verbal response	Oriented to time, person, and place	5
	Confused	4
	Inappropriate words	3
	Incomprehensible sounds	2
	None	1
Motor response	Obeys command	6
	Moves to localised pain	5
	Flex to withdraw from pain	4
	Abnormal flexion	3
	Abnormal extension	2
	None	1

due to the enhanced use of motorised vehicles (Johnson and Griswold, 2017; Maas et al., 2008, 2017), and one TBI-related fatality occurs every three minutes in India (Maas et al., 2017).

TBI is classified according to severity. The most commonly used scale for this is the Glasgow Coma Scale (GCS) (Teasdale and Jennett, 1974). The GCS assesses the eye opening, verbal, and motor response of patients with impaired consciousness and assigns them scores from 3 to a maximum of 15 (Table 1.1). Scores from 15-13 are associated with mild TBI (mTBI), 12-9 with moderate TBI, and 3-8 with severe TBI (sTBI) (Rimel et al., 1982). Based on this classification, approximately 80% of all TBI patients admitted to hospital have been classified as mTBIs, while the remaining 20% are split evenly between moderate and severe TBI (Rimel et al., 1982; Saatman et al., 2008). It is difficult to estimate the total number of patients experiencing TBI, however, as many patients with mTBI do not seek medical attention, but roughly 42 million people worldwide are thought to experience mTBI per year (Gardner and Yaffe, 2015).

TBIs can be furthermore classified according to underlying mechanism: these include closed head injury caused by rotational forces or acceleration/deceleration, and open brain injury caused by penetration of the brain (Maas et al., 2008).

As seen in Table 1.1, the acute signs of TBI can vary considerably (Teasdale and Jennett,

1974); symptoms range from disorientation, vomiting, nausea, dizziness, and headache to loss of consciousness, coma, and even death (Bryan, 2013; Center for Disease Control and Prevention (CDC) and National Center for Injury Prevention and Control, 2003; Faul and Coronado, 2015). Long-term consequences depend on magnitude and location of the initial injury, but 43% of TBI survivors have been reported to develop long-term disabilities, increasingly so with age (Rutland-Brown et al., 2003; Selassie et al., 2008). TBI can result in poor concentration, attention deficits, and personality changes reflecting alterations in emotional and behavioural regulation such as irritability, mood changes, aggressiveness, and self-centred behaviour (Belanger et al., 2010; Tramontana et al., 2014). These changes in personality have been shown to affect interpersonal relationships and contribute to poorer social and vocational integration following brain injuries (Roozenbeek et al., 2013). Consistent with this, people with a history of TBI have been reported to experience social isolation, have a lower quality of life and general health, and attempt suicide more frequently than the general population (Hawthorne et al., 2009; Silver et al., 2001). Rimel et al. (1982) previously showed that that 66% of TBI patients do not return to work. This has been confirmed to occur for patients with moderate and severe TBI (Hawthorne et al., 2009; Rimel et al., 1982), where cognitive impairment persists in as many as 65% of patients (Rabinowitz and Levin, 2014). Following mTBI, return to work is not affected, but these patients often exhibit ongoing cognitive and memory deficits interfering with everyday tasks (Cancelliere et al., 2014; Ponsford et al., 2011).

In addition to social, behavioural, and emotional consequences, TBI can result in a variety of neurological, psychiatric, and neurodegenerative diseases which I have summarised below.

1.1.1 Neurological disorders

Traumatic brain injury is a significant risk factor for the development of epilepsy and sleep disorders. Patients with a history of TBI were found to be eleven times more likely to develop epilepsy (one and a half times more likely after mTBI, up to seventeen times more likely after sTBI) (Annegers et al., 1998). This finding was recently also replicated in a population-based cohort study of children and young adults in Denmark, where TBI increased the risk of epilepsy even after ten years (Christensen et al., 2009).

Seventy percent of TBI outpatients self-reported sleep problems (McLean et al., 1984), and a study employing polysomnography confirmed sleep disturbances in 45% of patients in a group of 71 patients on average three years following traumatic brain injury (Masel et al., 2001). A history of TBI was additionally associated with an increased risk of obstructive sleep apnea, which occurred in 23% of patients (Castriotta et al., 2007), and TBI patients with obstructive sleep apnea performed significantly worse in measures of cognitive function than TBI patients without obstructive sleep apnea (Wilde et al., 2007).

1.1.2 Psychiatric disorders

In a small 2004 case-controlled study, 33% of 91 patients with TBI developed major depressive disorder (MDD) and exhibited a higher risk for depression than a control group of 27 patients with other traumas but lacking damage to the brain (Jorge et al., 2004). TBI patients with MDD were more likely to develop other comorbidities such as anxiety and aggressive behaviour, and had reduced executive function and poorer social functioning. These findings were also correlated with reduced gray matter volume in CT or MRI.

Two larger studies (559 and 722 patients, respectively) report similar values of MDD occurrence following TBI (53.1% and 42%, respectively), but lack control subjects (Bombardier et al., 2010; Kreutzer et al., 2001).

For mTBI, mood disorders are the most common long-term consequence. Anxiety, MDD, and post-traumatic stress disorder are frequently encountered in patients who suffered mTBI (as often as in patients who suffered moderate or severe TBI), even if no gross brain scan abnormalities are visible (Bombardier et al., 2010).

1.1.3 Neurodegenerative diseases

A particularly worrying perspective for the long-term consequences of traumatic brain injuries is that they have been shown to significantly increase the risk of developing neurodegenerative diseases. Several studies and meta-analyses have found an association of a history of TBI with increased risk for several forms of dementia, such as Alzheimer's disease (AD) (Barnes et al., 2014; Fleminger et al., 2003; Gardner et al., 2014; Lee et al., 2013; Mortimer et al., 1991), young-onset dementia (Nordström et al., 2014), and fronto-temporal dementia (Barnes et al., 2014; Kalkonde et al., 2012; Rosso et al., 2003).

More recently, doubts have been cast on the link between TBI and AD, mainly because most of the studies utilised retrospective self-reporting of TBI (which may be biased at a time when cognitive impairment from dementia is already apparent) and the clinical diagnosis of AD, which lacks specificity, rather than newly-developed biomarkers (Weiner et al., 2017). A 2016 neuropathological study found no increased risk of AD in TBI patients (Crane et al., 2016), although the authors did observe an increased risk for accumulation of Lewy Bodies and Parkinson's disease. This suggested that while the risk for AD was not increased, TBI may increase the risk for other forms of dementia such as dementia with Lewy Bodies or Parkinson's-associated dementia. On the other hand, the study by Barnes et al. (2014) (detecting an increased link between history of TBI and AD) included only male subjects (veterans), and Fleminger et al. (2003) only found the increased risk in males, indicating there might be a gender-specific aspect to the link of TBI-AD which may in part be

responsible for the lack of reproducibility in the study by Crane et al. (2016).

In contrast to AD, the link between TBI and Parkinson's disease is much less controversial. Several studies and meta-analyses have found a significantly increased risk of developing Parkinsonism after suffering from TBI (Crane et al., 2016; Gardner et al., 2015; Jafari et al., 2013). Importantly, even mild traumatic brain injury increased the risk for Parkinson's disease (Gardner et al., 2015), although, as mentioned above, this is generally difficult to assess as many patients do not seek medical attention after experiencing mTBI.

Furthermore, TBI has been found to increase the risk of developing amyotrophic lateral sclerosis threefold; with repeated injuries this risk rises up to elevenfold compared to control patients with limb fractures and no evidence of central nervous system injuries (Chen et al., 2007).

It is unclear as to how exactly traumatic brain injuries can lead to these devastating long-term consequences, but research is currently ongoing to untangle these effects.

To summarise, there is an increasing awareness that TBI is actually a disease process rather than a single event (Masel and DeWitt, 2010). This idea is not new, and the concept that TBI can lead to neurodegeneration was first established in 1927 by Osnato and Giliberti, shortly after which *dementia pugilistica*, or punch-drunk syndrome, was described in retired boxers (Martland, 1928; Osnato and Giliberti, 1927). This form of post-traumatic neurodegenerative disease is caused by repeated blows to the head - as occur in boxing or other forms of aggressive contact sports -, and is characterised by a decline of cognitive and motor functions over time. In the last decades, clinical research has investigated many more of the pathological consequences of TBI. The cost figures mentioned above underline the fact that traumatic brain injuries not only pose a significant health issue to the individual, but the health system as a whole, and treatments are duly needed to prevent the pathological consequences of TBI, and potentially in further course, decline of brain function and neurodegenerative disease.

1.2 Wound healing and regeneration: phases and contribution of macrophages

Regardless of tissue context, complex molecular and cellular cascades must be initiated immediately following an injury if tissue integrity and homeostasis are to be restored. Cells rapidly undergo significant changes in gene expression profile and migration, proliferation, and differentiation behaviour in response to injury, including cells of the immune system (Gurtner et al., 2008). During the process of wound healing, previously functional tissue occasionally becomes a patch of

cells with disorganised extracellular matrix (ECM), commonly referred to as a scar (Gurtner et al., 2008). While scar formation helps to replace lost tissue and potentially provides a survival benefit by preventing influx of pathogens and further mechanical deformation, it significantly hampers the function of tissue, and results in loss of elasticity (skin) (Corr and Hart, 2013), reduced cardiac output or even cardiac insufficiency (heart) (Talman and Ruskoaho, 2016), inability to regrow axons (spinal cord injury, TBI) (Silver and Miller, 2004) or generate new neurons (TBI) (Moeendarbary et al., 2017), amongst other functional deficits. However, some eukaryotic organisms have the ability to completely restore original tissue architecture and function through a process called regeneration; in fact, most organisms have the ability to regenerate during development, but it is frequently lost in adulthood, particularly in mammals (Colwell et al., 2003). Conversely, some vertebrate organisms, such as salamanders and zebrafish, retain the ability to regenerate in adulthood (Becker et al., 2004; Godwin et al., 2013; Petrie et al., 2015). While is not yet known why humans lose the capacity to regenerate after development, and why some adult human tissues retain the ability to regenerate (liver) while others do not (heart, central nervous system), it is thought that the macrophages, cells of the innate immune system, may play a role in regulating a switch between scar formation and regeneration, as they are key to the orchestration of wound healing phases (Gurtner et al., 2008).

The response to injuries is remarkably similar between different mammalian tissues, including skin, heart, or central nervous system. Wound repair is divided into three (overlapping) phases: (i) inflammation, (ii) proliferation (generation of new tissue), and (iii) remodelling. Additionally, early transcription-independent signalling mechanisms can influence and modulate wound repair. Here, I have summarised phases of wound healing.

1.2.1 Phases of wound healing

Early, transcription-independent wound signals

Although the process of wound healing is often lengthy, wound repair actually starts immediately after an insult. The immediate detection of wounds is crucial for initiation and orchestration of repair programmes. To this end, conserved transcription-independent signals can both inform about a wound and initiate a repair programme (Cordeiro and Jacinto, 2013). Transcription-independent signals include calcium (Ca^+) waves (Antunes et al., 2013; Herrgen et al., 2014; Razzell et al., 2013; Sammak et al., 1997; Sieger et al., 2012; Xu and Chisholm, 2011; Yoo et al., 2012), release of adenosine triphosphate (ATP) (Davalos et al., 2005; Kotwal et al., 2015), and the establishment of a hydrogen peroxide (H_2O_2) gradient (Love et al., 2013; Niethammer et al., 2009).

Calcium has been described as one of the earliest damage signals. Calcium waves in response to injury are observed in a variety of species and tissues, including epithelia of *Drosophila melanogaster*, *Caenorhabditis elegans* and zebrafish (*Danio rerio*) (Antunes et al., 2013; Xu and Chisholm, 2011;

Yoo et al., 2012), bovine endothelial cell culture (Sammak et al., 1997), human and rat astrocytic cell culture (Ravin et al., 2016), and neural tissue of developing zebrafish and *Xenopus laevis* (Herrgen et al., 2014; Sieger et al., 2012). Calcium waves initiate repair by recruitment of immune cells (Sieger et al., 2012; Razzell et al., 2013), and can promote wound closure through actin-dependent mechanisms (Antunes et al., 2013; Herrgen et al., 2014; Xu and Chisholm, 2011). Similarly, calcium waves can amplify the wound response by activation of hydrogen peroxide-generating enzyme dual oxidase (duox) (Razzell et al., 2013; Yoo et al., 2012). Strikingly, inhibiting calcium signalling at the time of injury can significantly diminish regeneration and wound repair in otherwise regenerating systems, and therefore determines later recovery (Antunes et al., 2013; Xu and Chisholm, 2011; Yoo et al., 2012).

In addition to calcium waves, ATP is a conserved transcription-independent damage signal (Cordeiro and Jacinto, 2013). Following injury, ATP is released from injured cells (often passively due to membrane rupture), and binds P2 receptors. As a consequence, this can enhance wound closure (Takada et al., 2014; Yin et al., 2007), recruit immune cells (Davalos et al., 2005), and alter immune cell polarisation (Kotwal et al., 2015).

Importantly, interference with early transcription-independent wound signals can impair late regenerative success (Antunes et al., 2013; Love et al., 2013; Xu and Chisholm, 2011; Yoo et al., 2012). Additionally, as the phases of inflammation described below are often only initiated after a lag, transcription-independent signals have the capacity to fast-track repair and regeneration, in particular by wound closure and modulation of macrophages (Kotwal et al., 2015), which are critical regulators of wound healing. Therefore, transcription-independent signals are indispensable mediators of tissue repair.

(i) Inflammation

Inflammation is the first phase of wound repair. It is initiated either by the presence of pathogen-associated molecular patterns (PAMPs) or, in case of sterile injury, damage-associated molecular patterns (DAMPs) such as ATP. This first phase of wound repair is primarily aimed at removal of pathogens, debris, and cell corpses to pave the way for later stages of regeneration (Gurtner et al., 2008). Cells of the innate immune system, in particular neutrophils and macrophages can bind PAMPs and DAMPs via surface receptors and alter their behaviour, for example to induce production of bactericidal reactive oxygen species (ROS), or to enhance removal of debris and cellular corpses via phagocytosis.

(ii) Proliferation

Following clearance of debris in the inflammatory phase, this second phase is initiated. It is characterised by revascularisation, angiogenesis, migration, and proliferation of cells of the connective tissue (in particular fibroblasts), and deposition of extracellular matrix (ECM) to fill the damaged tissue that has been removed during the inflammatory phase. The proliferative phase is critical to regain structural integrity of tissue (Gurtner et al., 2008; Stroncek and Reichert, 2008). Importantly, macrophages are a key factor for induction of the proliferative phase; for example, they can promote angiogenesis in hypoxic tissue environments by secretion of the angiogenetic vascular endothelial growth factor (Henson, 2005).

(iii) Remodelling

The third and final phase of wound healing is the remodelling phase, which is characterised by downregulation of the previously induced wound repair processes, wound retraction, and resolution of inflammation. The aim is to reduce the amount of excessive ECM deposited during the proliferative phase in order to strengthen tissue, and align the ECM through contraction (Gurtner et al., 2008). A failure to remove or remodel ECM results in fibrosis (thickening of scar tissue by excessive ECM deposition) (Gurtner et al., 2008).

For successful wound repair to occur, all these phases have to be carefully orchestrated in a timely and organised manner. For example, a failure to remodel impairs the regenerative capacity of the liver and instead results in fibrosis. The transitions between phases are regulated by macrophages; several macrophage polarisations are required sequentially (inflammatory, tissue repair, and resolving macrophages) (Das et al., 2015; Wang et al., 2014; Wynn et al., 2016). When the transitions between wound repair are dysregulated, overhealing (hypertrophic scar and keloids), or underhealing (chronic scars associated with diabetes or radiation) can occur (Gurtner et al., 2008).

1.2.2 Wound repair in the CNS: differences to other tissues

The responses to injury are remarkably similar across adult mammalian tissues, and the general principles of wound repair apply also to the CNS. Both calcium waves and ATP have been shown to inform the surrounding tissue of a neural injury (Davalos et al., 2005; Herrgen et al., 2014; Sieger et al., 2012). While enhanced calcium levels in the brain are typically associated with mediating cell death via excitotoxicity (see Chapter 1.3), research suggests that early calcium waves following an injury can be (neuro)protective: either by inhibiting excessive apoptosis following an injury (Justet et al., 2016; Kanemaru et al., 2013), but also via other mechanisms such as actin remodelling, rapid wound closure, and expulsion of dead cells from intact tissue (Herrgen et al., 2014; Minns et al., 2016). Furthermore, calcium waves have been reported to attract microglia, the resident immune cells of the brain, to sites of injury (Davalos et al., 2005; Sieger et al., 2012).

However, there are several cellular players different from wound repair in other tissues. This includes astrocytes, which are glial cells that provide the healthy CNS with trophic support and participate in a plethora of other homeostatic functions essential to CNS function (reviewed by Allen and Lyons (2018)). Following CNS trauma, astrocytes take on a similar role that fibroblasts serve in the periphery, and proliferate to fill in the lesion site (for small CNS injuries) (Fitch et al., 1999; Li and David, 1996), or form a border surrounding the lesion site (Shechter and Schwartz, 2013). While this plug or barrier, called glial scar, is a necessary interim to contain damage and prevent it from spreading to healthy tissue (Faulkner et al., 2004), it often persists for years; therefore, it leads to a failure to remodel, and the lack of regenerative capacity of the CNS has been partially attributed to the glial scar (Shechter and Schwartz, 2013).

Furthermore, unlike other tissues, the CNS is usually isolated from peripheral cells and molecules by the blood brain barrier (BBB), consisting of endothelial cells forming tight junctions (Rubin and Staddon, 1999). Therefore, the CNS does not depend on circulating monocytes for macrophages, but has its own resident and self-renewing macrophages, called microglia. Microglia are derived from primitive myeloid precursors in mammals (Ginhoux et al., 2010), and maintenance of microglia is independent of circulating progenitors: the constant population of microglia has been shown to be regulated by coupled proliferation and apoptosis of resident cells (Askew et al., 2017). Although microglia are capable of carrying out similar functions as macrophages in the periphery and have the capacity to phagocytose and release molecules modulating repair processes, it is known that they exert additional functions critical to CNS development and homeostasis. Microglia regulate fasciculation of axons in the corpus callosum and thereby mediate proper wiring of the brain during development (Pont-Lezica et al., 2014; Squarzoni et al., 2014). They furthermore instruct positioning of newborn neurons in development (Squarzoni et al., 2014), as well as regulate neuronal numbers during development by promoting neuronal survival via release of trophic factors or phagocytosing superfluously generated neurons (Cunningham et al., 2013; Ueno et al., 2013). In the adult brain, microglia are involved in regulating hippocampal neurogenesis (Sierra et al., 2010). Furthermore, microglia are able to shape synaptic fields by synaptic pruning, an activity- and complement-dependent process regulating uptake of synapses by microglia (Paolicelli et al., 2011; Schafer et al., 2012; Stevens et al., 2007). Therefore, although microglia are named the resident macrophages of the brain, they are known to carry out a multitude of functions contributing to CNS development and homeostasis and are therefore specialised macrophages that may respond to injuries differently than other macrophages.

In contrast to some mammalian tissues (liver), the CNS is not capable of full regeneration and trauma results in a glial scar. The limited capacity of the CNS to repair has been proposed to result from a failure to remodel wounds, elicited by the lack of timely orchestration of preceding phases

of wound repair (Shechter and Schwartz, 2013), and may be the result of a dysregulated activation of immune cells. Indeed, functional magnetic resonance imaging in human patients revealed that pathological immune cell activation persisted for up to 17 years after TBI (Ramlackhansingh et al., 2011). In addition to potentially providing an explanation for the failure of CNS regeneration, dysregulation of inflammation has been associated with neurodegenerative diseases, and may therefore explain the link between TBI and Alzheimer's disease, Parkinson's disease, and other neurodegenerative diseases (reviewed by Colonna and Butovsky (2017) and Prinz et al. (2011)).

1.2.3 The role of microglia/macrophages in repair and regeneration

Macrophages, cells of the innate immune system named after the Greek word for *big eater* (Metchnikoff, 1905), play a key role in each phase of wound repair and orchestrate transitions between phases. During the acute phase of an injury, macrophages react to damage signals (DAMPs and PAMPs) and subsequently undergo changes in gene expression and phagocytosis, termed as activation. Traditionally, two types of macrophage activation have been described: M1 (pro-inflammatory), and M2 (anti-inflammatory) (Mantovani et al., 2004; Mills et al., 2000), based on the previously described polarisation of T-helper cells Th1 and Th2 (Mosmann et al., 1986). This classification is based on a subset of markers found on activated macrophages. Interferon γ (IFN γ) and lipopolysaccharide (LPS, a particle found in the cell wall of bacteria) were seen as the main factors eliciting an M1 phenotype, inducing expression of pro-inflammatory factors such as inducible nitric oxide synthase (iNOS), tumour necrosis factor α (TNF α), and interleukin-1 β (IL-1 β). In contrast, the cytokines interleukin-4 (IL-4) and interleukin-13 (IL-13) are typical inducers of the anti-inflammatory M2 polarization that is associated, amongst other factors, with expression of arginase-1 (Arg1), transforming growth factor β (TGF β), and interleukin-10 (IL-10) (Martinez and Gordon, 2014). During the inflammatory phase of wound repair, M1 macrophages are able to neutralise bacteria and other pathogens via production of nitric oxide. In contrast to that, M2 macrophages are generally seen as suppressors of inflammation, and mediators of tissue remodelling.

With the availability of high-throughput transcriptomic and epigenomic methods, in combination with the use of more dynamic *in vivo* imaging tools in rodents and zebrafish, it has become increasingly clear that rather than two specific polarisations, macrophages are able to adopt a wide variety of activation patterns not limited to these ends of the spectrum (Martinez and Gordon, 2014; Mosser and Edwards, 2008; Ransohoff, 2016a). M1 and M2 polarisations were discovered after stimulating cells *in vitro*; however, textbook M1 and M2 macrophages are rarely encountered *in vivo* (Chiu et al., 2013; Morganti et al., 2016), and M1/M2 markers have actually been shown not to predict the overall gene expression pattern (Kim et al., 2016). To this end, the simplified classification of macrophage activation into M1/M2 could actually hinder research by overlooking potential other factors, and it is argued that it is to be discarded (Ransohoff, 2016a).

Macrophages have been shown to be crucial to repair by orchestration of the phases of wound healing. For example, specific depletion of macrophages during acute liver injury (which normally results in full regeneration) resulted in a failure to regenerate due to insufficient matrix restructuring (Duffield et al., 2005). Similarly, in the neonatal rodent or adult salamander heart, the remarkable capacity of cardiac regeneration depends on the presence of macrophages to instruct matrix remodelling and other pro-regenerative processes (Aurora et al., 2014; Godwin et al., 2017). Even in adult rodents, when cardiac repair following an insult is known to be limited, depletion of macrophages following cardiac injury leads to increased mortality, decreased wound debridement, and decreased cardiac regeneration (Frantz et al., 2013; van Amerongen et al., 2007). Not only cardiac muscle, but also skeletal muscle regeneration was found to depend on macrophages, and suppression of macrophage function via anti-M-CSF-antibody injection was found to result in excessive fibrosis (Segawa et al., 2008). Successful kidney repair has been shown to depend on macrophage infiltration and production of pro-regenerative Wnt7b (Lin et al., 2010). Epimorphic skin regeneration in African spiny mice was found to depend on macrophages to stimulate regenerative processes (Simkin et al., 2017). More complex regenerative processes, such as salamander limb regeneration, or zebrafish fin regeneration, have also been found to depend on the presence of macrophages (Godwin et al., 2013; Nguyen-Chi et al., 2017; Petrie et al., 2015).

In contrast to the relatively well-established role for macrophages in the orchestration of repair and regeneration in many tissues, they have historically been classified as detrimental following CNS injuries due to activation and initiation of neuroinflammation (see Chapter 1.3.4), and this hypothesis still remains present: Gerber et al. (2018) inhibited proliferation of microglia, the resident macrophages of the brain, following spinal cord injury in mice and observed improved functional outcome and tissue morphology. However, sparse correlational hypotheses that microglia/macrophages could support CNS repair have been reported as early as the 1980s. Perry et al. (1987) observed abundant macrophage infiltration following peripheral nervous system (PNS) injury but to a lesser extent following injury in the CNS (optic nerve injury), and hypothesised that differing macrophage number and activation could potentially explain the regenerative capacity of PNS over CNS. Similarly, Prewitt et al. (1997) found that more macrophages were found in regions with a higher extent of axonal outgrowth following spinal cord injuries. These findings were highly correlative, but further studies directly investigated the capacity of microglia/macrophages to modulate axonal outgrowth; indeed, it was found that microglia- (or 'brain macrophage')-derived molecules can mediate axonal outgrowth following optic nerve injury *in vitro* (Chamak et al., 1994) and *in vivo* (Yin et al., 2003, 2006). In contrast to these findings, another study reported that microglia/macrophages can lead to axonal retraction following spinal cord injury (Horn et al., 2008). Upon closer inspection it was however discovered that the retracted axons were highly dystrophic, and microglia/macrophages in fact only removed debris via phagocytosis. Furthermore, three other recent studies found that

microglia/macrophages play a distinct role in neuroprotection following stroke (Szalay et al., 2016) and spinal cord injury in both zebrafish and mice (Brennan et al., 2018; Tsarouchas et al., 2018), where they protect from lesion expansion and improve functional recovery.

The correct polarisation of microglia/macrophages is crucial to support repair and regeneration, and polarisation can be modified in order to enhance repair. This was recently shown following cardiac injury in rats, where adult macrophages were capable of being pushed to a cardioprotective phenotype (de Couto et al., 2015). To make matters more complex, macrophages are not a homogeneous group of cells, and subsets have been reported to be beneficial. For example, in cardiac repair, resident macrophages (derived from embryonic macrophages) were found to be crucial for regeneration. However, following an injury, resident macrophages were replaced by heavily infiltrating monocyte-derived macrophages. Inhibition of this infiltration and replacement improved cardiac repair (Lavine et al., 2014). Furthermore, macrophage depletion following liver injury only hampers regeneration if it occurs during the acute phase (Duffield et al., 2005). Conversely, during continuous exposure to a liver toxin, depletion of macrophages proved beneficial, suggesting that subsets of macrophages with different functions ultimately determine the outcome of regenerative processes (Duffield et al., 2005). Furthermore, a transient pro-inflammatory response - despite being usually thought of as being detrimental - is beneficial in some injury models, including zebrafish fin and spinal cord injury (Hasegawa et al., 2017; Nguyen-Chi et al., 2017; Tsarouchas et al., 2018). Successful regeneration may ultimately be achieved by shifting microglia/macrophage polarisation to a pro-regenerative phenotype (whatever this may be in terms of tissue context) at the right time. Depletion of all microglia/macrophages therefore only provides limited information on the overall outcome, and may explain why it has been so difficult to reach a consensus on the overall role of microglia/macrophages to repair and regeneration, especially in the CNS.

Over the past decade there has been mounting evidence of tissue regenerative and potentially neuroprotective functions of microglia/macrophages. As microglia/macrophages are highly dynamic and plastic cells, thorough investigation of these cell types requires analysis methods that are capable of detecting these dynamic changes.

1.3 Pathophysiology of secondary cell death

In addition to scar formation, TBI is characterised by significant neuronal loss. TBI leads to two waves of neuronal cell death: primary and secondary cell death. The key conceptual distinction between these is their direct or indirect relation to the initial injury: while primary cell death is a direct consequence of the initial injury (i.e., physical disruption of tissue), secondary cell death is mediated by indirect, non-mechanical, biochemical alterations elicited by the injury. Secondary cell death occurs within minutes to weeks of the injury, and TBI is characterised by progressive

neuronal cell death that can spread to regions distant from the original injury site (Bayly et al., 2006; Stoica and Faden, 2010). While enhancing CNS regeneration via inhibition of glial scar (or axonal outgrowth, respectively) is an area of active research to improve outcome of TBI and SCI, the prevention of secondary cell death is a promising additional therapeutic avenue. Secondary cell death occurs with a delay, therefore presenting a potential therapeutic window, and application of drugs could improve patient outcome. This is emphasised by the fact that secondary neuronal cell death is associated with a poorer prognosis of patients following TBI (Miñambres et al., 2008; Nathoo et al., 2004). Similarly, several rodent studies have suggested that inhibition of cell death following TBI via several approaches (either general inhibition of apoptosis, or targeted inhibition of pathomechanisms outlined below) resulted in a significantly improved cognitive outcome: for example, inhibition of apoptotic cell death by administration of Caspase-3 inhibitors z-VAD-fmk or z-DEVD-fmk 15 min after experimental TBI has been shown to improve cognitive outcome in rats (Knobloch et al., 2002; Yakovlev et al., 1997). Similarly, targeting several other pathomechanisms that elicit secondary cell death mentioned below significantly improved neurological outcome in experimental TBI models (Hall et al., 1988; Faden et al., 1989).

Along with several other cascades initiated by the primary cell death, secondary cell death can contribute to the 'talk and die' syndrome that was first described in 1975: patients who were initially capable of talking and other cognitive functions following injury often progressively declined (and potentially died) (Reilly et al., 1975). Nonetheless, the delayed nature of secondary cell death allows for potential salvage of patients and prevention of further damage if applied within a given therapeutic window. In order to prevent secondary cell death, there has therefore been considerable pre-clinical research both *in vitro* and *in vivo* to elucidate mechanisms leading to neuronal cell death following TBI, and to discover neuroprotective strategies. Overall, neuronal dysfunction and death following an injury appears to stem from aberrant neurotransmitter and ion homeostasis, oxidative stress, changes in the vasculature, and energy failure (summarised below; Park et al. (2008); Werner and Engelhard (2007)).

1.3.1 Excitotoxicity

One of the key pathophysiological events eliciting secondary neuronal cell death following TBI is a phenomenon termed glutamate excitotoxicity. Glutamate is the major excitatory amino acid in the brain, and it is physiologically released for neurotransmission in a highly controlled temporal and spatial manner at the synapse (Clements et al., 1992). Following an insult to the brain, however, there is excessive release of glutamate from injured cells which can lead to death of neighbouring cells (Lipton and Rosenberg, 1994). Glutamate acts on several receptors that have been named after their specific agonists (α -amino-3-hydroxy-5-methyl-4-isoxazolepropionic acid, or AMPA, receptor; and N-methyl-D-aspartate, or NMDA, receptor). Excessive NMDA receptor activation can lead to

cell death via several pathways:

- *Cytotoxic cellular swelling.*

NMDA receptors (and other ion channels responsive to glutamate) preferentially transport Ca^{2+} ions but are also capable of transporting Na^{+} (and passively Cl^{-}) into the cell, which in turn leads to release of K^{+} into the extracellular space (Fig. 1.1) (Katayama et al., 1990). This unregulated and excessive flux of ions leads to cellular influx of water molecules, predominantly through aquaporin-4 channels (Fig. 1.1) (Manley et al., 2000), which results in cytotoxic cellular swelling, and on a tissue level, cytotoxic oedema (Liang et al., 2007). Cytotoxic oedema is frequently observed following traumatic brain injury and thought to be a main cause of brain swelling and elevated intracranial pressure (ICP) (Unterberg et al., 2004). In severe cases, this increased pressure may lead to compression of respiratory centres in the brain stem and result in death. In addition to cell swelling, the disrupted ionic balance interferes with physiological function of neurons; in order to fire again, ionic equilibrium must be restored. Exchange of Na^{+} with K^{+} is achieved by the $\text{Na}^{+}/\text{K}^{+}$ -ATPase, an ATP-dependent ion pump working against the chemical gradient. The disruption of ionic homeostasis following traumatic brain injury therefore drastically increases the ATP demand and alters the glucose metabolism, the predominant source of neuronal energy. Immediately following TBI, this results to a hypermetabolic state, which can be prevented by application of glutamate antagonists (Yoshino et al., 1991). This finding supported the hypothesis that the altered metabolic state was linked to glutamate excitotoxicity (Kawamata et al., 1992).

- *Mitochondrial dysfunction.*

Under physiological conditions, mitochondria can buffer large amounts of intracellular calcium (Nicholls and Saunders, 1996). However, abnormally high levels of calcium result in an altered mitochondrial membrane potential, and therefore disrupt the cellular energy supply by mitochondrial dysfunction, which is a key element of glutamate excitotoxicity (Hiebert et al., 2015; Schinder et al., 1996), and further exacerbates neuronal energy deficit in response to TBI.

- *Lipase and protease activation*

NMDA receptor-dependent Ca^{2+} influx can lead to activation of a series of phosphatases and lipases (Fig. 1.1), resulting in neuronal self-digest by protein breakdown and lipid peroxidation (Choi, 1988; Lipton and Rosenberg, 1994). Lipid peroxidation is defined as the oxidative breakdown of lipids and can lead to cell membrane instability and death. It can be initiated by NMDA receptor-dependent calcium influx activation of enzymes (such as phospholipase A2), or mediated by reactive oxygen species (Anthonymuthu et al., 2016). This pathway is convergent with other NMDA receptor-induced molecular pathomechanisms, as activation of NMDA receptors has additionally been shown to lead to synthesis of nitric oxide (NO) from

L-arginine *in vitro* (Dawson et al., 1991; Garthwaite et al., 1989; Sattler et al., 1999) and *in vivo* (Girouard et al., 2009). This occurs under physiological conditions, and NO has in fact been shown to be involved in memory formation and its cellular correlates, synaptic plasticity, whereby inhibition of NO *in vivo* has been shown to lead to learning impairments (Chapman et al., 1992), and inhibition *in vitro* leads to decreased synaptic plasticity (Schuman and Madison, 1991; Shibuki and Okada, 1991). However, under pathologically elevated conditions, NO was shown to be a key mediator of glutamate excitotoxicity: NMDA receptor-elicited NO has been shown to mediate apoptotic cell death in cell culture (Dawson et al., 1991; Leist et al., 1997; Sattler et al., 1999), while inhibition of the neuronal NO synthase was able to protect from NMDA receptor-dependent excitotoxic cell death in slice cultures (Izumi et al., 1992), and resulted in a decreased lesion volume following excitotoxic brain injury *in vivo* (Schulz et al., 1995).

While NMDA receptors have been mainly shown to be neurotoxic and their manipulation (either genetical or pharmacologically) has been implicated in neuroprotection following traumatic brain injury (Morikawa et al., 1998; Rao et al., 2001; Rothman and Olney, 1986; Simon et al., 1984), NMDA receptors also serve neuroprotective roles. Developmentally, NMDA receptors are critical for brain function, and genetic NMDA receptor knockout results in death within a few hours from birth (Forrest et al., 1994). Transient pharmacological inhibition or genetic deletion of NMDA receptors in perinatal rats caused extensive apoptosis of neurons (Adams et al., 2004; Gould et al., 1994; Ikonomidou et al., 1999; Monti and Contestabile, 2000; Zhang-Hooks et al., 2016), exacerbated neuronal loss in an adult model of neurodegeneration (Ikonomidou et al., 2000), and impaired survival of newborn neurons in the dentate gyrus of the hippocampus (Tashiro et al., 2006), one of the few regions of the adult mammalian brain with adult neurogenesis. It appears that both too much and too little NMDA receptor activation can be harmful. Indeed, Hardingham et al. (2002) found that synaptic NMDA receptors render neurons more resilient to apoptotic stimuli via activation of CREB (cAMP response element binding protein) and BDNF (brain derived neurotrophic factor), while activation of extrasynaptic NMDA receptors leads to mitochondrial dysfunction and loss of mitochondrial membrane potential. It appears that as with nitric oxide, a delicate balance is required for normal function and neuroprotection, and this may explain why several drugs targeting NMDA receptors - which initially appeared to be ideal targets for neuroprotection from glutamate excitotoxicity following brain injury - failed in clinical trials (see Chapter 1.4.2).

1.3.2 Oxidative stress

The brain is highly sensitive to oxidative stress as it consumes approximately 20% of the oxygen amount of the body, and has the highest oxygen metabolic rate of any organ (Maiese, 2002). Free radicals, including reactive oxygen species (ROS) and reactive nitrogen species (RNS), are usually scavenged by endogenous antioxidant enzymes such as superoxide dismutase (SOD) and glutathione

peroxidase (Chong et al., 2005). However, following TBI, an accumulation of both ROS and RNS is observed (Fabian et al., 1998; Kontos and Wei, 1986). This is mediated by enhanced production of ROS and RNS due to mitochondrial damage, NADPH oxidase upregulation, and enhanced inducible nitric oxide synthase (iNOS) expression (Choi et al., 2012; Gahm et al., 2000; Hiebert et al., 2015; Orihara et al., 2001; Sullivan et al., 1999; Wada et al., 1998; Zhang et al., 2012), and a concomitant suppression of antioxidant enzyme expression (Cernak et al., 2000), tipping the balance to result in oxidative stress.

The accumulation of ROS [superoxide ($\cdot\text{O}_2^-$), singlet oxygen ($^1\text{O}_2$), and hydroxyl radical ($\cdot\text{OH}$)] and RNS [nitric oxide (NO) and peroxynitrite (ONOO^-)] can result in significant neuronal injury. Unscavenged excess of free radicals was shown to result in peroxidation of cellular lipid structures, protein oxidation or nitration (depending on whether ROS or RNS are involved) (Hall et al., 2004), cleavage of DNA via endonucleases, disruption of the mitochondrial electron transport chain (Radi et al., 1994; Yamamoto et al., 2002), further exacerbating the energy dysfunction experienced following TBI. These pathological events can be partly counteracted by increasing free radical scavenger levels: overexpression of scavenging enzyme SOD resulted in reduced membrane lipid peroxidation, protein nitration, and neuronal cell death after focal cerebral ischemia *in vivo* (Keller et al., 1998). Treatments with antioxidants such as polyethylene glycol-conjugated SOD (PEG-SOD), transgenic elevation of SOD levels, application of anti-oxidant hormone melatonin, or superoxide radical scavenger OPC-14117 have been shown to improve the neurological outcome and reduce cell death in experimental models of TBI (Aoyama et al., 2002; Chan et al., 1995; Hamm et al., 1996; Mikawa et al., 1996; Mésenge et al., 1998; Xiong et al., 2005). Interestingly, levels of endogenous melatonin in the brain were found to be increased in patients with TBI, suggesting a potential rescue attempt of the brain to scavenge excess free radical levels (Seifman et al., 2008). Moreover, direct targeting of pathological events induced by ROS or RNS were shown to improve outcome following TBI: inhibition of lipid peroxidation significantly improved neurological outcome following experimental TBI in rats (Hall et al., 1988), and inhibition of endonucleases following TBI increased neuronal survival *in vitro* (Vincent and Maiese, 1999).

As previous research had shown that ROS and RNS can significantly contribute to pathology of TBI, inhibition of enzymes involved in generation of ROS and RNS was attempted to achieve neuroprotection. However, deletion of iNOS actually enhanced oxidative stress after TBI: transgenic iNOS knockout mice, and mice treated with NOS inhibitor aminoguanidine, were reported to have a poorer functional outcome following TBI, although the authors state that a variety of mechanisms could be linked to neuroprotection via (i)NOS not exclusive to oxidative stress (Sinz et al., 1999). NO can promote neuroprotection at lower (physiological) levels by modulating ion channel permeability via protein S-nitrosylation. The NMDA receptor is a target of this modulation: S-Nitrosylation alters permeability, inhibits Ca^{2+} influx, and therefore reduces subsequent NMDA receptor-dependent

neuronal cell death (Calabrese et al., 2007; Choi et al., 2000; Jaffrey et al., 2001). Furthermore, NO can be produced by both neurons and immune cells (Bayir et al., 2005; Heneka and Feinstein, 2001). Bayr et al. (2006) showed that tyrosine nitrosylation of superoxide dismutase and subsequent exacerbation of oxidative stress in response to NO is dependent on the neuronal NOS isoform nNOS. Taken together, this suggests that timing, source, and concentration of NO may decide whether neuroprotection or neurotoxicity occurs.

1.3.3 Blood flow dysregulation

Rodent models and a third of TBI patients experience a reduction of blood flow following brain injury (Chesnut et al., 1993; Yamakami and McIntosh, 1991). Most commonly, it occurs due to a disruption of cerebral autoregulation: normally, the brain tightly regulates its blood flow by energy demand. Following TBI, the brain increases its energy demand; if this cannot be met (via a decrease of blood flow, and mitochondrial dysfunction), the secondary injury will be exacerbated. Here, NO can act as a neuroprotective agent by enhancing blood flow via blood vessel relaxation or protection of cerebral autoregulation (Curvello et al., 2018; DeWitt et al., 1997; Huang et al., 1996).

1.3.4 Neuroinflammation

As with any injury, inflammation is a common consequence of TBI. Within minutes of a traumatic injury, a robust inflammatory response is elicited in the injured brain, which consists of cellular components and secreted factors.

Cellular components

◇ *Innate immune system*

The innate immune system is the first line of defense against pathogens or an injury. Microglia are the resident immune cells of the brain, and make up almost 10% of brain cells (Aguzzi et al., 2013). Microglia sense injuries via DAMPs, excessive glutamate, or calcium waves, and are among the first responders at the site of brain injury (Davalos et al., 2005; Sieger et al., 2012). Upon sensing damage, often via purinergic P2 receptors (Davalos et al., 2005; Haynes et al., 2006), microglia undergo marked changes in their morphology (changing from a resting-state ramified morphology to an activated amoeboid-like morphology) and behaviour (including a release of pro- and anti-inflammatory cytokines and phagocytosis) (Loane et al., 2014). The release of cytokines then further alters activation states of microglia, rendering them either more pro-inflammatory or pro-repair (see Chapter 1.2.3). The exact polarisation and contribution of microglia to injury progression or repair heavily depends on the cues they are exposed to (Corps et al., 2015).

A number of studies has assigned microglial responses to injury a neurotoxic function (Chao et al., 1992; Festoff et al., 2006; Neher et al., 2011, 2013; Pyo et al., 1998; Qin et al., 2004; Rogove and Tsirka, 1998; Tikka and Koistinaho, 2001; Yrjänheikki et al., 1998). The detrimental effect of microglia on neuronal survival after TBI has been concluded from studies inhibiting the immune system unspecifically, or *in vitro* studies. However, it is now clear that (a) many cells of the immune system participate in the response to CNS injuries, therefore unspecific inhibition may suppress both protective and destructive immune cell (sub)types, and (b) microglia (or any type of macrophage) are not responding homogeneously to CNS injury. Hsieh et al. (2013) showed that experimental TBI elicits distinct responses in microglial subpopulations, and the balance of microglial activation has been suggested to determine the functional outcome, as an increased pro-inflammatory microglial activation has been associated with the poorer outcome of aged animals following TBI (Kumar et al., 2013). Therefore, generalistic studies on immune suppression are potentially only of limited value for identification of the role of microglial cells following injury.

Furthermore, *in vitro* studies that have shown a neurotoxic effect of activated microglia suffered from several limitations. Microglia adapt a distinctly different morphology as soon as they are cultured, and flatten out on the surface (Giulian and Baker, 1986; Jeong et al., 2013). Adult homeostatic microglia have been found to lose their unique signature rapidly and partially de-differentiate following removal from their CNS environment (as measured by downregulation of microglia-specific signature genes such as Tmem119 or P2yr12) (Bohlen et al., 2017). Additionally, microglia in culture assume characteristics of more neuroinflammatory and early developmental microglia, and appear more pro-inflammatory than microglia *in vivo* (Bohlen et al., 2017). Cultured microglia produce large amounts of inducible nitric oxide synthase (iNOS) and lead to neuronal death in co-culture when stimulated with LPS or other inflammatory stimulators (Chao et al., 1992; Pyo et al., 1998). In contrast to that, while morphologically activated microglia positive for pro-inflammatory cytokine IL-1 are found in lesion sites *in vivo*, neurons in these regions are generally healthy, and microglia lack expression of other cytotoxic mediators (Jeong et al., 2010a,b; Min et al., 2012). Furthermore, microglia-mediated inflammation alone is not sufficient to cause cell death *in vivo* (Jeong et al., 2010a). What could potentially cause this discrepancy between microglial function *in vivo* and *in vitro*? As wound healing and inflammation are multicellular processes, it is important to see a system as a whole. Neurons have been described to express certain receptors to keep microglial activation at bay, such as CD200 (Hoek et al., 2000), or fractalkine (Cardona et al., 2006). These molecules are recognised by receptors on microglia and can dampen microglial inflammation; for example, fractalkine receptor knockout animals display significantly enhanced inflammation and neuronal loss in mouse models of Parkinson's disease or amyotrophic lateral sclerosis (Cardona et al., 2006). This highlights the fact that for disease-relevant investigation of microglia, *in vivo* investigations are critical.

The immune response is elicited immediately following CNS trauma, but has been shown to persist for years after trauma (Gentleman et al., 2004; Johnson and Griswold, 2017; Loane et al., 2014; Nagamoto-Combs et al., 2007; Nonaka et al., 1999; Ramlackhansingh et al., 2011). While microglial activation *per se* may not be neurotoxic (or is suggested to be neuroprotective), persistent and dysregulated activation of microglia (called microgliosis) has been proposed to result in an increased neuronal loss and neurodegeneration following CNS injuries (Faden et al., 2016; Ransohoff, 2016b), as responses can become maladaptive over time due to exposure to different combinations of stimuli (Zhang et al., 2014). Inhibition of microgliosis with minocycline was shown to reduce the lesion volume after spinal cord injury (Festoff et al., 2006). However, Bye et al. (2007) found that while minocycline was able to inhibit microglial activation, it did not affect acute neuronal cell death, and another study by Scott et al. (2018) found that neuronal loss was even exacerbated in the chronic phase following minocycline treatment after experimental traumatic brain injury, which highlights the fact that unspecific inhibition of the immune system may not be an appropriate tool to target secondary cell death. Additionally, selective depletion of proliferating microglia was shown to exacerbate brain injury (Lalancette-Hebert et al., 2007). The contrasting results on microglia in neuroprotection or neurotoxicity illustrate how difficult it is to investigate the role of microglia, as they exhibit tremendous functional plasticity in their responses dependent on tissue and injury context. Recent transcriptomic studies demonstrate that even within the homeostatic brain there is considerable heterogeneity of microglia transcriptomes from distinct brain regions (Böttcher et al., 2019; Grabert et al., 2016).

Although microglia are the resident immune cells and primary responders to CNS injuries, their activation results in amplification of the immune response by recruitment of peripheral cells of the innate immune system via release of chemokines and an alteration of endothelial integrin levels (Carlos et al., 1997; Kielian et al., 2002; Tang et al., 2014; Zhou et al., 2006). This is presumably aimed at preventing a saturation of the phagocytic system by recruitment of phagocytic neutrophils and macrophages (Carlos et al., 1997; Tang et al., 2014). Brain entry of neutrophils is mediated by adhesion to vasculature by enhanced expression of integrins, and extravasation (Carlos et al., 1997). Carlos et al. (1997) found that neutrophils can appear at the injury site within minutes, and peak at two hours post injury. In autopsy samples collected from patients who died within five minutes of TBI, 43% showed neutrophil presence within the injury site (Oehmichen et al., 2003). Despite this recruitment, studies suggest that microglia are the predominant phagocyte following CNS injuries (Greenhalgh and David, 2014; Lampron et al., 2015; Schilling et al., 2005) and the presence of peripheral immune cells may, instead of providing phagocytic support, cause neurotoxicity. This is supported by the fact that neutrophil depletion reduces tissue loss and apoptotic cell death following TBI in mice (Kenne et al., 2012). Neutrophils are important mediators of inflammation in peripheral lesions to prevent bacterial invasion, and while they may not be inherently neurotoxic, Allen et al. (2012) reported that transmigration through the endothelial barrier activated a neurotoxic pheno-

type and mediated the release of de-condensed DNA, called neutrophil extracellular traps (Allen et al., 2012) (Fig. 1.1), which is of paramount importance to fight infectious agents in the periphery (Brinkmann et al., 2004) but causes neuronal death following brain injury (Allen et al., 2012). Similarly, the production and release of ROS by neutrophils is critical in peripheral injuries, but in the brain contributes to their neurotoxic characteristics (Liao et al., 2013; Neumann et al., 2008; Nguyen et al., 2007). Interestingly, although microglia initially participate in recruitment, they can also counteract neutrophil neurotoxicity by rapid engulfment of neutrophils (Neumann et al., 2008).

In contrast to neutrophils, the role of peripheral macrophages in the CNS is not as clearly neurotoxic following TBI. However, unlike resident microglia, macrophages exhibit a highly inflammatory phenotype in the CNS which may confer neurotoxic effects (Yamasaki et al., 2014). Infiltration of macrophages occurs only days after injury, and is mediated by binding of C-C motif chemokine ligand 2 (CCL2) to the C-C chemokine receptor type 2 (CCR2) receptor on macrophages. Recruitment of inflammatory macrophage subpopulations via CCR2 was shown to be required for induction of angiogenesis during wound healing in the skin (Willenborg et al., 2012), and genetic knockdown of CCR2 in mice led to significantly impaired wound repair at all times, suggesting a crucial role for inflammatory control of wound repair for CCR2 (Boniakowski et al., 2018). In the injured brain, however, macrophages recruited by a CCR2-mediated mechanism appear to be neurotoxic: CCR2^{-/-} mice, or mice treated with a CCR2 antagonist, had a significantly improved functional long-term outcome (Hsieh et al., 2014; Morganti et al., 2015). Similarly, genetic knockdown of CCL2 resulted in an improved outcome after experimental brain injury (Semple et al., 2010). Interestingly, the neuroprotective effect of CCL2 knockdown was only visible with a delay, showing a reduced lesion size and functional benefit over wild type at two and four weeks after injury; this may correspond with the fact that macrophages only appear at the lesion site with a delay (24 to 48 hours) and therefore cannot mediate an effect in the acute phase (within a few hours of the injury) (Semple et al., 2010; Soares et al., 1995).

◇ *Adaptive immune system*

Several studies have addressed the role of B- and T-cells in the pathogenesis of neuroinflammation following TBI. Fee et al. (2003) reported a detrimental role for CD4⁺ T cells in the acute phase (within 24 hours) of TBI by transfer of these cells into Rag1^{-/-} animals lacking the adaptive immune system. However, T cell recruitment in wild type animals or human patients usually only occurs at later times following injury, and both in experimental and human TBI, T cell infiltration at 24 hours after injury is found to be minimal, or non-existent, respectively (Clausen et al., 2009; Holmin et al., 1998). Weckbach et al. (2012) challenged the findings by Fee et al., and found that depletion of the adaptive immune cells via knockout of the crucial immune regulator *rag1* did not confer neuroprotection following TBI. Several more recent strands of evidence point to a potential neuroprotective role of the adaptive immune cells. This can be achieved through production of neutrotrophins that

have been shown to promote neuronal survival (Barouch and Schwartz, 2002; Moalem et al., 1999, 2000), and modulation of the microglial polarisation by release of anti-inflammatory cytokines IL-4 and IL-10 (Butovsky et al., 2006).

Secreted components

Following activation of immune cells, but also injury of neurons, a plethora of secreted immune messengers can be released. These include pro- and anti-inflammatory cytokines, chemotactic cytokines, prostaglandins, and ROS/RNS. Depending on their receptors, secreted components can either initiate, propagate, or inhibit the inflammatory response. Common cytokines detected in the CNS following TBI are interleukin-1 β (IL-1 β), TNF α , and IL-6. IL-1 β and TNF α are potent pro-inflammatory cytokines that are rapidly upregulated following brain injury. In experimental models of brain injury, both IL-1 β and TNF α were upregulated as early as one hour after injury (Fan et al. (1995); Kamm et al. (2006); Kinoshita et al. (2002), and Fan et al. (1995); Knoblach et al. (1999); Shohami et al. (1994), respectively). Similarly, in postmortem tissue from human TBI patients, tissue upregulation was detected in patients who died within seventeen minutes of TBI (Frugier et al., 2010). IL-1 β levels in the serum of patients were found to correlate with GCS at six hours post injury (Taşç et al., 2003), but no correlation with outcome was observed (Winter et al., 2004), which suggests IL-1 β serum levels are only of limited predictive value. Conversely, increased levels of the immunomodulatory IL-6 were associated with a better outcome of patients (Winter et al., 2004).

TNF α is capable of both promoting neuronal survival and neuronal death, depending on receptor activation. This has been demonstrated by a number of studies and explains why previous research yielded confusing results as to whether pro-inflammatory TNF α is neurotoxic or neuroprotective. Contrary to the general belief that neuroinflammation and pro-inflammatory cytokines may cause neurotoxicity (Jara et al., 2007; Talley et al., 1995), Bruce et al. (1996) showed that genetic deletion of TNF receptors exacerbates damage following brain injury. Stahel et al. (2000) reported that mice deficient for TNF α or IL-6 both had increased mortality following TBI. Longhi et al. (2013) showed that deletion of p75 TNF α receptor results in a significant worsening of sensorimotor deficits following TBI in mice, while knockout of p55 TNF α significantly reduced lesion volume, cell death, and improvement of sensorimotor ability compared to wild types. This suggested that different receptor subtypes determine the outcome. Activation of TNF receptor 2 on microglia can promote an anti-inflammatory polarisation of microglia (Veroni et al., 2010), and can rescue neurons directly from oxidative stress (Fischer et al., 2011). Therefore, while TNF α may confer neuroprotection in many situations, this heavily depends on receptor subtype activation.

In contrast to TNF α , the role of IL-1 β appears more neurotoxic overall; IL-1 β antagonism inhibits neuronal damage after brain injury (Toulmond and Rothwell, 1995; Relton and Rothwell,

1992). Interestingly, IL-1 β has an endogenous antagonist, interleukin 1 receptor antagonist (IL-1ra), which is a secreted glycoprotein preventing the action of IL-1 β by acting as a decoy receptor (Boraschi et al., 1995). Endogenous IL-1ra provides significant neuroprotection in a variety of brain insults (Hutchinson et al., 2007; Loddick et al., 1997; Pinteaux et al., 2006), and administration of recombinant IL-1ra can provide neuroprotection and reduce seizure susceptibility following TBI (Relton and Rothwell, 1992; Semple et al., 2017; Sun et al., 2017b). A phase II human trial with recombinant human IL-1ra (Anakinra) was successful in demonstrating safety and brain penetration (Helmy et al., 2014), with a dose-range study for moderate to severe TBI being currently underway (ClinicalTrials.gov, registration number NCT02997371).

To discuss the role of additional individual cytokines in more detail would be beyond the scope of this thesis; a summary of the role of pro- and anti-inflammatory cytokines and their respective roles in TBI is provided by Ziebell and Morganti-Kossmann (2010) and Morganti-Kossmann et al. (2018).

Considerable progress has been made in elucidating molecular pathways initiating secondary neuronal cell death following TBI, yet it appears that there is an intricate interplay of multiple molecular factors that is not easily dissected. This may be additionally complicated by the fact that many of these studies rely on static snapshots of what is happening at a certain timepoint, or *in vitro* work, which may give an incomplete picture of the underlying molecular pathophysiology.

1.4 The quest for a magic bullet: past and present clinical trials

Epidemiological numbers of the incidence of TBI as well as the high percentage of long-term disability and death highlight that TBI is a prevalent and pressing medical issue. To reduce the impact and ameliorate the consequences of TBI, both preventative and curative strategies have been aimed for. Prevention of TBI can be achieved on three levels (Park et al., 2008): primary prevention aims to obviate TBI altogether, mainly by policy changes such as enforcing speed limits, helmet use, or changing culture such as reducing alcohol intake, which may lead to a decline in risk-taking behaviours. Secondary prevention entails limiting the biological impact of the injury (i.e., prevention of secondary cell death). Tertiary prevention does not include traditional prevention but entails neuro-rehabilitation and symptom management in order to restore a patient's daily functioning.

The delayed nature of secondary cell death renders this phenomenon an ideal target for meaningful medical intervention in terms of secondary prevention as outlined above. Experimental models of brain injuries in the 1970s had identified several neuroprotective candidate drugs that could potentially prevent secondary damage in humans following TBI. In combination with the establishment

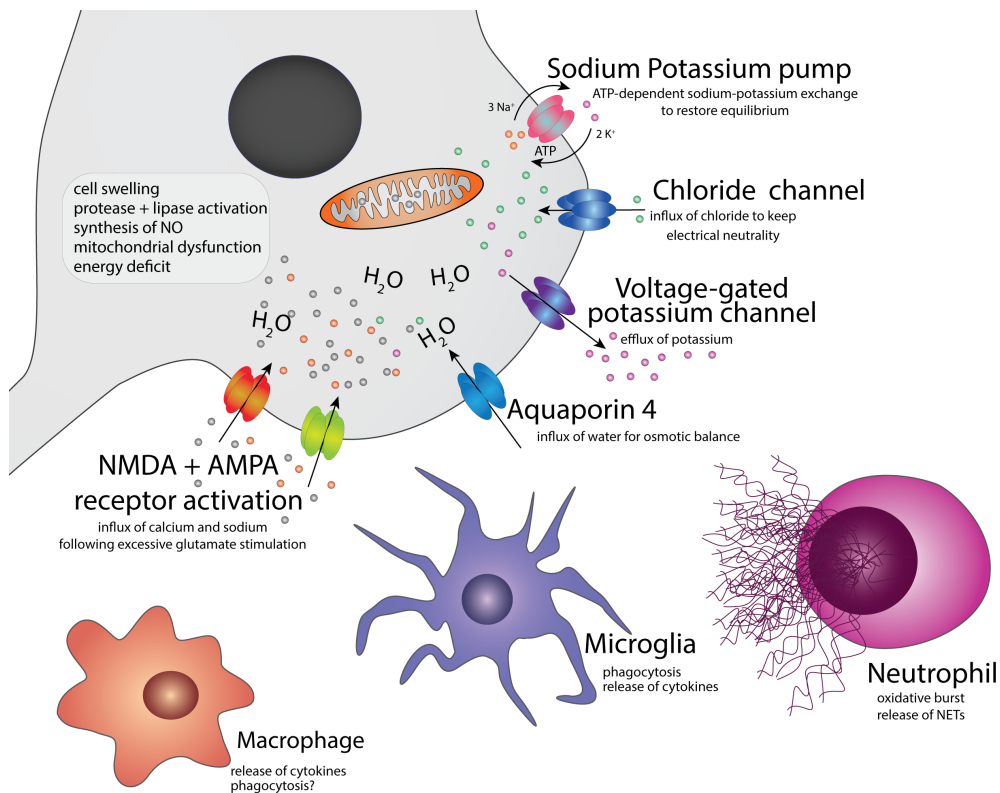


Figure 1.1: **Schematic of some of the pathophysiological molecular and cellular mechanisms occurring following traumatic brain injury.** Not to scale; schematic created by me.

of the Glasgow Coma Scale (GCS) as standard assessment of severity of brain injuries by visual, verbal and motor function in patients (Table 1.1) (Teasdale and Jennett, 1974), this fuelled the initiation of several clinical trials in the 1980s (Maas et al., 2010). Patients could be classified ranging from mild (GCS score 13-15), moderate (GCS score 9-15), to severe (GCS score <9) in an internationally standardised manner (Rimel et al., 1982), rendering clinical trials more comparable between centres. The peak of initiation of randomised controlled trials, both for neuroprotective agents and therapeutic strategies (such as hypothermia or decompressive craniectomy), was in the 1990s. Unfortunately, the interventions in these clinical trials were largely futile, which resulted in a reluctance of pharmaceutical companies or individual investigators to undertake financially burdensome clinical trials, and a decrease of study initiation in the 2000s (Fig. 1.2).

Here and in Table 1.2, I have summarised the therapeutic approaches that were investigated in phase III randomised controlled clinical trials so far.

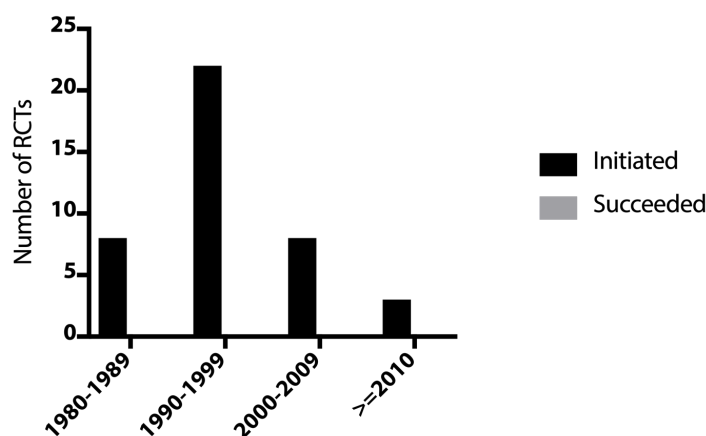


Figure 1.2: **Clinical trials in TBI since 1980.** Multi-centre phase III RCTs for traumatic brain injury plotted for initiation and success (defined as benefit over placebo). Modified from Maas et al. (2010).
* 1 RCT initiated in 2014 has not reported results yet.

1.4.1 Therapeutic strategies

Hypothermia

Mild hypothermia - the cooling of the body and brain down to 32 °C - emerged as a promising therapeutic strategy in the 1990s, targeting glutamate release and cytotoxic oedema. This was a result of several rodent studies reporting improved cognitive and sensorimotor outcome (Bramlett et al., 1995; Clifton et al., 1991; Dixon et al., 1998), reduced mortality (Clark et al., 1996), decreased glutamate release (Globus et al., 1995), and reduced neuronal cell death (Dietrich et al., 1994a) following hypothermia after acute brain injury. Similarly, two small-scale phase II clinical trials in the 1990s provided encouraging results on an improved outcome of patients treated with mild hypothermia as measured by GCS improvement (Clifton et al., 1993) or disability (Marion et al., 1993) at three months following injury. Although later results showed that hypothermia may hasten the recovery rather than provide an overall beneficial effect (as Glasgow Outcome Scale was significantly improved in patients treated with hypothermia at three months, but not at twelve months, compared to normothermic controls) (Marion et al., 1997), preliminary data from earlier studies provided enough evidence to initiate a larger scale, phase III randomised controlled trial (National Acute Brain Injury Study - NABIS). Patients were treated with hypothermia within eight hours from the initial insult. Hypothermia proved futile in ameliorating outcome, and patients treated with hypothermia had more hospital days than normothermic controls (Clifton et al., 2001). Fifty-seven per cent of patients in both groups experienced poor outcome (death, severe disability, or vegetative state), which can most likely be attributed to the fact that recruited patients were in a coma to begin with. Nonetheless, hypothermia did not cause any improvement of outcome.

A pre-clinical study published the same year as the NABIS trial investigated the therapeutic window of hypothermia following acute brain injury in rodents, and found that hypothermia was

only effective at improving the outcome if applied within 60 minutes of the insult in rats (Markgraf et al., 2001). This inspired the initiation of a second NABIS hypothermia trial (NABIS:H IIR) with very early application of hypothermia, setting a tighter therapeutic window (two and a half instead of eight hours). This trial was terminated as, even when applied within two and a half hours, hypothermia again proved futile and did not improve poor outcome of patients compared to the control group (death, severe disability, or vegetative state) (Clifton et al., 2011). Post-hoc analysis drew attention to potential effectiveness in patients under the age of 18 years. This stood in contrast to a 2008 trial assessing the effect of hypothermia following TBI in children which had shown a worsening of clinical outcome and an increase in mortality when treated with hypothermia within eight hours (Hutchison et al., 2008); however, issues with the study design and chosen endpoints raised questions about the validity of these prior findings and provided the incentive to evaluate the outcome on a larger scale (Adelson, 2009). A separate RCT was initiated evaluating the effect of hypothermia applied within six hours following injury in children and young adults (Cool Kids study). Similar to previous trials in adults, hypothermia was ineffective at reducing unfavourable outcomes and the study was prematurely terminated for futility (Adelson et al., 2013).

Decompressive craniectomy

Decompressive craniectomy (DC) following traumatic head injuries was first described by Kocher in 1901 to alleviate ICP (Kocher, 1901). Interest in the procedure waned over time due to low success rates, and particularly following a report that DC may actually increase oedema following experimental brain injury in dogs up to sevenfold (Cooper et al., 1979). In the 1990s, there was a resurgence of interest due to new technologies to monitor intracranial pressure and image the brain, resulting in a number of studies and RCTs published in the 2000s. Initially, the majority of studies were retrospective reports, which found that although DC was effective at reducing intracranial pressure, it did not have a beneficial effect on the clinical outcome (Münch et al., 2000; Pompucci et al., 2007; Williams et al., 2009). Interestingly, these studies also found that younger patients benefited more from DC, suggesting patient age may play a factor deciding the success of this intervention, which was confirmed by pilot studies reporting early DC in young patients resulted in a better outcome (Figaji et al., 2003; Taylor et al., 2001).

Later RCTs conducted in adults, or both adults and children, could not prove a beneficial effect of DC. Cooper et al. (2011) report that while intracranial pressure was significantly lowered in patients receiving DC compared to standard medical care, DC patients had longer stays in the intensive care unit and an overall worse outcome. A larger-scale study (RescueICP) published in 2016 showed that DC was effective at reducing mortality, yet increased the occurrence of severe disability and vegetative state (Hutchinson et al., 2016), which suggests that DC can prevent mortality by lowering ICP but does not prevent any other secondary damage. This was confirmed by a 2017

metanalysis reporting that DC is effective at lowering intracranial pressure and may therefore reduce mortality, but does not affect outcome (Zhang et al., 2017). Therefore, DC may be a useful therapeutic strategy in the management of derailing intracranial pressure following TBI, but has no functional benefit over standard care. DC has its own set of complications including brain herniation through the skull, and trephination, which could require further surgery to treat (Honeybul and Ho, 2011), and therefore the current recommendation for performing DC is only within strict regulations and justification.

1.4.2 Neuroprotective agents

Over the years, several clinical trials have been targeting a variety of pathomechanisms involved in secondary damage following TBI by pharmacological intervention. These neuroprotective agents had often shown great promise in rodent models of TBI, yet failed in the clinic: they either showed no therapeutic effect compared to placebo, or - in some cases - actually resulted in higher mortality and therefore these studies had to be prematurely terminated. To date, there is no pharmacological agent that has shown a superior effect than placebo in any multi-center randomised controlled trial. Here, I will provide an overview over the most historically prominent candidates for treating TBI.

Steroids

Similar to DC, the initial indication of corticosteroids in TBI in the 1980s was to alleviate intracranial pressure. RCTs describing 'high-dose', 'megadose', and 'ultrahigh' doses of the widely-used corticosteroid dexamethasone provided no evidence of any beneficial treatment effect over placebo (Braakman et al., 1983; Dearden et al., 1986; Gaab et al., 1994). Another study using the glucocorticoid triamcinolone reported that, while there was no overall treatment benefit, patients with focal lesions had made a better recovery at one year post injury (Grumme et al., 1995). Further pre-clinical research investigating neuroinflammation (summarised by Morganti-Kossmann et al. (2002)) provided the incentive for the largest clinical trial to date in TBI: the MRC CRASH trial (Corticosteroid Randomisation After Significant Head Injury), applying corticosteroid methylprednisolone. The MRC CRASH trial had to be prematurely terminated after recruiting 10,000 patients (the initial aim was 20,000) due to a significantly higher mortality and increased risk of severe disability in the treatment group compared to controls (Edwards et al., 2005).

Progesterone, a steroid hormone with many targets, was a promising candidate in treatment for TBI until 2014. Progesterone was initially discovered as a neuroprotective candidate due to the fact that females tended to recover better from TBI than males from experimental brain injury (Bramlett and Dietrich, 2001; Roof et al., 1993). Further pre-clinical research showed that progesterone attenuated oedema (in males and females) (Roof et al., 1992, 1996), decreased neuroinflammation and inflammation-associated cytokines (only tested in males) (He et al., 2004; Pettus et al., 2005),

and facilitated cognitive recovery while reducing neuronal loss and gliosis (only tested in males) (Djebaili et al., 2005; Roof et al., 1994; Shear et al., 2002). Consistent with pre-clinical results, two small-scale phase II RCTs reported improved outcomes in patients treated with progesterone (Wright et al., 2007; Xiao et al., 2008), which provided the incentive to carry out larger scale phase III studies (PROtectIII, SYNAPSE), dosing with progesterone began either within four or eight hours following injury, respectively. The SYNAPSE study reported no clinical benefit of progesterone administration over placebo within eight hours in a randomised sample of 1195 patients (Skolnick et al., 2014). The PROtectIII study was terminated before recruiting the initially planned patient sample of 1140 over futility, as it showed no improved outcome following progesterone treatment with four hours of TBI in 882 patients (Wright et al., 2014). In a secondary study assessing cognitive and motor functioning such as memory, attention, fine motor coordination, executive function and language (rather than the usual assessment of reduced mortality and improved Glasgow Outcome Scale) in the PROtectIII patient group, researchers did not find any improvement compared to placebo, again suggesting that progesterone did not provide a neuroprotective effect in the clinic (Goldstein et al., 2017).

NMDA receptor antagonists and other calcium channel inhibitors

Throughout the 1990s and 2000s, several NMDA receptor and calcium channel inhibitors were tested for neuroprotection through inhibition of excitotoxicity following TBI in a clinical setting, all of which ultimately failed to elicit an improved outcome. Several pharmaceutical companies, including Bayer, Novartis, Pfizer, and Parke Davis moved compounds that had previously shown neuroprotective effects in animal models of TBI forward to the clinic. None of these compounds managed to prove successful in the clinic. Nimodipine, a calcium channel blocker, initially showed a reduction in unfavourable outcome (death and vegetative state) at six months (Harders et al., 1996), but a later study failed to confirm this finding (Vergouwen et al., 2006). Other compounds targeting excitotoxicity and/or calcium signalling suffered an even worse fate. A RCT assessing the effect of NMDA receptor antagonist Selfotel in patients with TBI was terminated over safety concerns following a report of increased mortality in contemporary clinical trials of Selfotel in ischaemic stroke patients (Davis et al., 1997, 2000). Although post-hoc analysis revealed that there was no increased mortality following TBI compared to placebo, there was also no significant treatment benefit (Morris et al., 1999). SNX-111, a presynaptic calcium channel antagonist, showed a strong neuroprotective effect in an experimental brain injury model (Perez-Pinzon et al., 1997), but higher mortality in humans compared to placebo following TBI, leading to termination of the RCT (unpublished, mentioned by Maas et al. (2010)). Similarly, and although not terminated, treatment with magnesium sulfate (which causes NMDA receptor blockade and calcium channel inhibition, amongst other mechanisms), resulted in a poorer outcome than treatment with placebo at six months (Temkin et al., 2007) and was therefore abandoned as a therapeutic strategy. A final

trial involving a competitive NMDA receptor antagonist (Dexanabinol) failed although the compound showed a highly neuroprotective effect in pre-clinical studies (Maas et al., 2006). No more clinical trials targeting calcium channels or NMDA receptors have been initiated so far, and it is generally thought that this therapeutic strategy has failed. This could be due to several reasons, and some of it is attributed to the fact that NMDA receptors can physiologically promote neuronal survival; following initial calcium overload immediately after an injury, NMDA receptors may resume their pro-survival functions (Ikonomidou and Turski, 2002). Therefore, it seems the picture is much more complex than previously thought, and further research is required to elucidate the molecular mechanisms underlying secondary cell death.

Free radical scavengers and inhibitors of lipid peroxidation

As a reduction of oxidative stress via administration of SOD had shown promising results in experimental models of TBI (Kontos and Wei, 1986), clinical trials using a more stable, polyethylene glycol-conjugated version of SOD (PEG-SOD) were initiated in the 1990s. An initial small phase II study revealed an improvement of GCS at three and six months following injury compared to placebo in patients with severe head injury (although not statistically significant) (Muizelaar et al., 1993). This led to initiation of a phase III trial, which however was unable to demonstrate an improved outcome (Young et al., 1996), although animal studies conducted around the same time showed significant neuroprotective effects by elevation of SOD levels (Chan et al., 1995; Mikawa et al., 1996; Xiong et al., 2005) and PEG-SOD treatment (Hamm et al., 1996). It is likely that the human trials failed due to the relatively short therapeutic window; pre-clinical research suggested that ROS bursts predominantly occurred within the first hour following injury (Hall et al., 1993; Smith et al., 1994). Furthermore, PEG-SOD may have low brain permeability and only affect microvasculature but not brain parenchyma (Hall et al., 2010).

Based on these limitations, it was concluded that direct targeting of detrimental downstream effects of free radicals, such as lipid peroxidation, may be a more viable therapeutic option. Lipid peroxidation is initiated within the first hour following injury (Smith et al., 1994) but persists for several days following injury (Du et al., 2004). Experimental models of TBI in mice, rats, and cats had shown a neuroprotective effect of lipid peroxidation inhibitor tirilazad (21-aminosteroid U74006F) (Dimlich et al., 1990; Hall et al., 1988; McIntosh et al., 1992). A phase III clinical trial did not show a positive treatment effect compared to placebo (Marshall et al., 1998), although post-hoc analysis revealed a potential beneficial effect for males with subarachnoid haemorrhage (SAH), consistent with pre-clinical findings that tirilazad was highly effective for treating SAH (Hall et al., 1994).

Current status and future outlook

Following the 1990s peak of clinical trials, trial initiations have significantly decreased, and none succeeded (Fig. 1.2). The only multi-centre trial of a neuroprotective drug for TBI registered on clinicaltrials.gov as of February 21st 2019 is a nitric oxide synthase inhibitor (VAS 203, Ronopterin; NCT02794168). Ronopterin showed promising results and improved patient outcome in a phase II study (Stover et al., 2014). The phase III trial is currently still recruiting and study results are expected in June 2019.

What made so many highly promising candidates fail in clinical trials? The main argument for this is currently the large heterogeneity of patients with traumatic brain injury. No TBI is the the same as the next - depending on the type of insult, location, patient age, and comorbidities. In contrast to that, experimental models of traumatic brain injury are carried out in a tightly regulated manner (Maas et al., 2010). Additionally, endpoint measurements in human clinical trials may be insensitive to smaller changes. Nonetheless, there is a need for further investigation of neuroprotective mechanisms following TBI (and other CNS injuries), and innovative models to investigate the cellular and molecular processes *in vivo* are required to provide a more detailed picture of the pathophysiology.

Table 1.2: **Therapeutic approaches to treat TBI.** Compounds that have been used in the clinic, their respective targeted pathomechanism, and reported outcomes in clinical trials.

Therapeutic approach	Target	Outcome in Phase III RCTs
Hypothermia	Elevated ICP, glutamate release	<ul style="list-style-type: none"> · NABIS study: more hospital days (adults) (Clifton et al., 2001) · NABIS:H IIR study: terminated for futility (adults) (Clifton et al., 2011) · Cool Kids study: terminated for futility (< 18 years) (Adelson et al., 2013)
Decompressive craniectomy	Elevated ICP	<ul style="list-style-type: none"> · worse outcome and longer hospital stay (Cooper et al., 2011) · RescueICP study: reduced mortality, but increased occurrence of severe disability and vegetative state (Hutchinson et al., 2016)
Methylprednisolone	neuroinflammation	<ul style="list-style-type: none"> · MRC CRASH study: terminated due to higher mortality and increased risk of severe disability in treatment group (Edwards et al., 2005)
Progesterone	neuroinflammation, oedema	<ul style="list-style-type: none"> · SYNAPSE study: no improved outcome (Skolnick et al., 2014) · ProTECTIII study: terminated for futility (Wright et al., 2014) · assessment of cognitive functions in patients of Wright et al. (2014) no improved cognitive function (Goldstein et al., 2017)
Selfotel	excitotoxicity	<ul style="list-style-type: none"> · terminated over safety concerns (Davis et al., 1997, 2000)
SNX-111	excitotoxicity	<ul style="list-style-type: none"> · terminated and unpublished, higher mortality (Maas et al., 2010)
Magnesium sulfate	excitotoxicity	<ul style="list-style-type: none"> · poorer outcome at six months (Temkin et al., 2007)
Dexanabinol	excitotoxicity, oxidative stress	<ul style="list-style-type: none"> · no improved outcome (Maas et al., 2006)
PEG-SOD	oxidative stress	<ul style="list-style-type: none"> · no significant treatment effect (Young et al., 1996)
Tirilazad	lipid peroxidation	<ul style="list-style-type: none"> · no significant treatment effect (Marshall et al., 1998)
Ronopterin	nitric oxide synthase	<ul style="list-style-type: none"> · expected June 2019

1.5 The zebrafish as a model of successful (CNS) regeneration

The zebrafish (*Danio rerio*) gained popularity as a model organisms for developmental biology in the 1990s due to its external and rapid development. Importantly, in contrast to the classical developmental model (*Drosophila melanogaster*), the zebrafish is a vertebrate, and is able to shed light on vertebrate development. George Streisinger is considered the pioneer of zebrafish research. He hoped to use genetic tools to study vertebrate development using zebrafish, and introduced the world of molecular and developmental biology to zebrafish in the 1980s (Streisinger et al., 1981). Following his passing in 1984, the zebrafish was picked up by several other labs, including that of 1995 Nobel Prize Winner Christiane Nüsslein-Volhard. The breakthrough of zebrafish as a laboratory organism is often thought to be the 1996 special issue of the journal *Development*, containing 38 zebrafish research papers from four different groups containing the results of a large-scale screen for genes regulating development analogous to a previous one in *Drosophila*.

While zebrafish started out as a popular developmental biology model, the sequencing of the zebrafish genome revealed that the zebrafish shares 70% of genes with humans, and 84% of genes associated with human disease have a zebrafish counterpart (Howe et al., 2013). In addition to its extensive use in developmental biology, the zebrafish is capable of scarless healing and complex tissue regeneration, including regeneration of fin, heart, brain, and spinal cord (Gemberling et al., 2013). In combination with the fact that zebrafish are more economical to keep than traditional disease models such as rodents, this renders zebrafish an attractive model organism for many research areas.

1.5.1 Comparison of injury reactions between zebrafish and mammals

While mammalian wound repair is scarless in embryogenesis, scars are left behind in adulthood. Conversely, adult zebrafish are capable of repair with minimal or no scarring and complex tissue regeneration (Becker et al., 2004; Petrie et al., 2015; Richardson et al., 2013), which instigated the investigation of reactions to injury in these animals to identify potential therapeutic targets. Research showed that zebrafish wound repair recapitulates phases of mammalian wound repair (inflammation, proliferation, remodelling) (Kroehne et al., 2011; Richardson et al., 2013; Sánchez-Iranzo et al., 2018). In contrast to mammals, where skin re-epithelialisation (and therefore re-establishment of a barrier) depends on cell proliferation, skin re-epithelialisation in zebrafish is rapid, transcription- and proliferation-independent, occurs within one to three hours of wounding, and is achieved by a thin epidermal layer migrating to cover the wound (Poleo et al., 2001; Richardson et al., 2013). This suggests that transcription-independent factors as mentioned in Chapter 1.2.1 play a critical role in adult zebrafish repair and regeneration. Conversely, later steps such as the proliferation of progenitors require inflammation and potentially even scarring (Hasegawa et al., 2017; Kyritsis et al., 2012; Richardson et al., 2013; Sánchez-Iranzo et al., 2018). Sánchez-Iranzo et al. (2018) show that inhibition of fibrosis prevented cardiomyocyte proliferation during cardiac repair. Although fibrosis -

typically associated with scarring - occurs in this injury model, zebrafish are capable of switching off pro-fibrotic response to allow successful regeneration both in the heart and skin (Richardson et al., 2013; Sánchez-Iranzo et al., 2018). Research is currently investigating how successful repair and regeneration is achieved in zebrafish. It appears likely that macrophage control of wound repair is crucial to this regenerative success, as absence of this cell type has been shown to impair wound repair and regeneration in zebrafish (Lai et al., 2017; Petrie et al., 2015; Tsarouchas et al., 2018).

1.5.2 CNS regeneration in zebrafish

Much of the research investigating CNS regeneration in zebrafish has been performed in adult zebrafish as researchers aimed to identify factors that could initiate a successful and scarless regenerative response in a mature central nervous system (Becker and Becker, 2008). However, the zebrafish larva has recently also been established as an attractive model to investigate regeneration for its amenability to pharmacological and genetic manipulation as well as the ability to perform time-lapse *in vivo* imaging to visualise repair processes over time (Hasegawa et al., 2017; Morsch et al., 2015; Ohnmacht et al., 2016; Tsarouchas et al., 2018; Wehner et al., 2017). Here, I have summarised the research to date investigating regenerative neurogenesis, axonal outgrowth, and cell death following CNS trauma in zebrafish.

Absence of bona fide astrocytes: the reason for scarless CNS repair?

Zebrafish lack *bona fide* astrocytes. As astrocytes form a glial scar following CNS injuries, the absence of this cell type could potentially explain the scarless response. However, zebrafish possess radial glia. These cells have been found to directly transform into astrocytes during late mammalian development (Barry and McDermott, 2005; Voigt, 1989). It is possible that while this step does not occur in zebrafish, radial glia become specialised to serve astrocyte functions. This is supported by the fact that subsets of radial glia express reactive astrocyte marker glial fibrillary astrocyte protein (GFAP) (Lyons et al., 2003), participate in tight junctions (Corbo et al., 2012), or function as progenitors (Mahler and Driever, 2007) (astrocytes and radial glia have been shown to function as neural stem cells in the adult mammalian CNS) (Kriegstein and Alvarez-Buylla, 2009). Similar to reactive astrocytes, radial glia are present following injuries to zebrafish brain (Baumgart et al., 2012; Kishimoto et al., 2012; Kroehne et al., 2011; März et al., 2011), spinal cord (Goldshmit et al., 2012; Hui et al., 2010), and optic nerve (Neve et al., 2012), and overexpression of lipocalin-2 (a mediator of reactive astrocytosis in mammals) results in thickening of GFAP⁺ radial glia processes (Lee et al., 2009). Importantly, in contrast to scar-forming astrocytes in the mammalian CNS, radial glia promote CNS repair by neurogenesis (Baumgart et al., 2012; Kroehne et al., 2011; Kishimoto et al., 2012; März et al., 2011), guidance of newborn neurons along their processes (Kishimoto et al., 2012), and may support axon outgrowth following SCI via glial bridges (Goldshmit et al., 2012) although recent time-lapse imaging reveals that axons may find their path independently (Tsarouchas

et al., 2018).

Thus, although zebrafish lack astrocytes, they have radial glia which perform similar functions in their CNS, and it appears unlikely that the absence of scar-forming astrocytes is the main reason for their regenerative success. However, it may be possible to study radial glia behaviour following injuries and identify pathways to modify astrocytes in order to push them into a more radial glia-like phenotype, promoting repair.

Regenerative neurogenesis

While the mammalian brain is capable of adult neurogenesis, this only occurs in discrete regions of progenitor pools (dentate gyrus of the hippocampus, subventricular zone of the lateral ventricle, and olfactory bulb) (Ming and Song, 2005). Brain injury in mammals leads to an increase of neurogenesis in these proliferative zones (Dash et al., 2001; Rice et al., 2003; Sun et al., 2005; Urrea et al., 2007), but the percentage of neurons that can be replaced after brain insult is estimated to represent only 0.2% of the lost number (Arvidsson et al., 2002), and the evidence for functional integration of neurons generated in response to injury is conflicting (Arvidsson et al., 2002; Sun et al., 2007). Furthermore, injury in the mammalian brain was shown to cause aberrant migration and misplacement of newborn cells in the hippocampus (Ibrahim et al., 2016).

Conversely, zebrafish exhibit constitutive adult neurogenesis in most parts of their brain (Grandel et al., 2006; Zupanc, 2006), and the extent of proliferation is one to two orders of magnitude higher than in mammals: the number of new cells formed in proliferating zones per day in the mouse or rat brain correspond to 0.003% to 0.03% of the estimated number of total cells in the brain (Cameron and McKay, 2001; Herculano-Houzel and Lent, 2005; Lois and Alvarez-Buylla, 1993; Williams, 2000). In contrast to that, in any given two hour period, 0.2% of total estimated cells in the fish brain are dividing in proliferating zones (Zupanc and Horschke, 1995). The progenitors (radial glia) are situated along the ventricle and usually only supply new neurons within one to two cell diameters of the ventricular surface in the brain (Adolf et al., 2006). Several research groups have investigated response of neural progenitors following a mechanical brain injury to the adult zebrafish telencephalon (Baumgart et al., 2012; Kishimoto et al., 2012; Kroehne et al., 2011; März et al., 2011). This research revealed that newly generated cells can be driven out to the parenchyma to replenish lost cells in response to brain injury, survive for at least 100 days and express mature neuronal markers (Baumgart et al., 2012; Kishimoto et al., 2012; Kroehne et al., 2011; März et al., 2011). Migration of newborn neurons after zebrafish brain injury occurs in an organised manner and is guided by radial fibers (Kishimoto et al., 2012), which resembles migration of newborn neurons during of the mammalian cortex (Noctor et al., 2001). Not only the brain, but also the spinal cord of zebrafish is capable of regenerative neurogenesis. This has been demonstrated following

mechanical spinal cord injury as well as targeted genetic or pharmacological ablation of spinal cord motor neurons in zebrafish (Ohnmacht et al., 2016; Reimer et al., 2008).

Identifying pathways that potentiate neurogenesis and increase the permissiveness of newborn neuron survival following an injury could potentially prove paramount to treatment of human brain injuries, and research so far has shown that while mammalian regenerative neurogenesis is very limited to begin with, the newborn neurons that are generated do not survive well (Arvidsson et al., 2002). Kizil et al. (2012) found that chemokine receptor *cxcr5*, previously predominantly known to be involved in B-cell follicle maturation, played a role in conveying the permissiveness of adult neurogenesis. Kishimoto et al. (2012) identified the Notch pathway as a key regulator of neurogenesis in the telencephalon following an injury. Shimizu et al. (2018) showed that Wnt signalling regulates the regenerative response of the optic tectum following stab injury. Furthermore, inflammation can boost proliferation of neural progenitors in zebrafish (Kyritsis et al., 2012). Conversely, inflammation has previously been shown to be detrimental to mammalian adult neurogenesis (Ekdahl et al., 2003; Monje et al., 2003), although more recent evidence suggests that polarisation of microglia may dictate whether neurogenesis is suppressed or enhanced by inflammation (reviewed by Kohman and Rhodes (2013)).

Similar to mechanical injury, induction of excitotoxic lesion by injection of quinolonic acid into the zebrafish brain was shown to induce neurogenesis, and newly generated neurons were able to survive long-term (at least for eight weeks post quinolonic acid application) and form long-distance projections with synapses in the contralateral hemisphere of the telencephalon (Skaggs et al., 2014). Interestingly, the regenerative response to brain injury seems to decrease with age, although the molecular mechanisms underlying this are not yet clear (Edelmann et al., 2013).

Spinal cord regeneration

Zebrafish are capable of functional central nervous system repair in the spinal cord; adult zebrafish regain the ability to swim within six weeks following spinal cord transection (Becker et al., 1997). This requires axonal regrowth, and inhibition of axonal crossing of the lesion site by application of a mechanical barrier prevents functional recovery (Becker et al., 2004). Studies in the larval zebrafish have enabled *in vivo* imaging of the spinal cord repair process. Ohnmacht et al. (2016) showed that larval zebrafish functionally recover within two days post lesion after spinal cord transection. Recent studies showed that the inflammation, macrophages, and deposition of a permissive extracellular matrix by deposition of collagen XII are crucial for axonal outgrowth and functional recovery following larval zebrafish spinal cord injury (Tsarouchas et al., 2018; Wehner et al., 2017).

Cell death following CNS trauma

A number of papers have investigated cell death following CNS trauma in fish. Zupanc et al. (1998) assessed apoptotic cell death following cerebellar lesioning in fish by morphological cell analysis and terminal deoxynucleotidyl transferase dUTP nick end labeling (TUNEL) staining. The authors showed that TUNEL⁺ cells appear within five minutes, peak at thirty minutes post injury, and decrease from two days post lesion to achieve baseline levels around twenty days post lesion. The authors conclude that apoptotic cell death in the fish brain aids to limit inflammation typically associated with mammalian brain injury, leads to efficient removal of cells, and may be associated with the tremendous regenerative potential of fish following CNS injuries (Zupanc et al., 1998).

Three studies have investigated cell death following spinal cord injury. Ohnmacht et al. (2016) investigated cell death of olig2⁺ oligodendrocyte-lineage cells in the larval zebrafish spinal cord following injury, and did not detect an increased number of TUNEL⁺/olig2⁺ cells following injury. Tsarouchas et al. (2018) assessed cell death following SCI by TUNEL staining and found an increase one day post lesion, but numbers of TUNEL⁺ cells were rapidly restored to baseline levels at two days post lesion. In the adult zebrafish, Hui et al. (2010) quantified cell death by TUNEL and immunohistochemistry against a key enzyme in the apoptotic cascade (Caspase-3). Both these markers were reported to occur from six hours post lesion, peak at one day post lesion, and return to baseline within three days post lesion (Hui et al., 2010). In line with Zupanc et al. (1998), Hui et al. (2010) suggested that apoptotic cell death may help to control inflammation and promote debris clearance, key to the regenerative potential of zebrafish.

In the adult telencephalon, Kroehne et al. (2011) found that although numbers of TUNEL⁺ cells return to baseline levels rapidly (as early as three days after lesioning), cell death is not spatially confined to the lesion site, which is similar to what is observed in mammalian brain injuries (Bayly et al., 2006; Pohl et al., 1999). Skaggs et al. (2014) find that excitotoxic lesioning of the telencephalon by quinolonic acid injection leads to significant cell death. Both quinolonic acid and vehicle injection caused early cell death at four hours post lesion as monitored by TUNEL. Similar to Kroehne et al. (2011), the authors found that TUNEL⁺ cells spread from the injury site throughout the whole telencephalic hemisphere at one and two days post lesion, although significantly more so for quinolonic acid than for vehicle, suggesting a role for excitotoxicity in promoting cell death in zebrafish (Skaggs et al., 2014).

Chapter 2

Hypothesis & Aims

There is currently a lack of successful neuroprotective strategies to prevent or limit secondary neuronal cell death following acute CNS trauma, which has been emphasised by the failure of clinical trials to improve outcomes following TBI (Maas et al., 2010, 2017). In my thesis, I aimed to elucidate processes that underlie secondary cell death from a new angle: a limitation of the majority of previous studies investigating mechanisms of secondary cell death and neuroprotection was the reliance upon static snapshots of the molecular and cellular processes following sacrifice of rodents, or *in vitro* models which only provide an incomplete picture of what is happening *in vivo* (Jeong et al., 2013). To circumvent these limitations, I aimed to establish a larval zebrafish model of brain injury. Larval zebrafish offer the key advantages of optical transparency and the availability of a multitude of transgenic fluorescent reporter lines, which allow for real-time observation of cellular and molecular processes *in vivo*. Furthermore, larval zebrafish develop rapidly and by three days post fertilisation, the optokinetic response is established; by five days, larval zebrafish are able to track and capture prey, suggesting a rapid maturation of the optic tectum, the largest part of the larval zebrafish brain (Cooper et al., 2015). Finally, the larval zebrafish has previously been successfully used to investigate the molecular and cellular mechanisms of spinal cord repair *in vivo* (Ohnmacht et al., 2016; Tsarouchas et al., 2018; Wehner et al., 2017).

Although several studies have previously investigated cell death in response to CNS injury in the zebrafish (Chapter 1.5.2), there is only limited knowledge about the occurrence and dynamics of primary cell death and secondary cell death (directly caused by mechanical disruption of tissue injury, versus indirectly caused by biochemical cascades elicited by injury) in these animals. To address this gap in the literature and assess the suitability of the larval zebrafish to investigate the mechanisms underlying secondary cell death, I aimed to characterise primary and secondary (direct and indirect) cell death in response to a mechanical injury to the optic tectum, which was easily accessible for mechanical manipulation and microscopy due to its superficial position.

To investigate potentially neuroprotective mechanisms, I then aimed to study early, transcription-independent wound signalling mechanisms and the immune system. Over the past decade, there has been mounting evidence of tissue regenerative and potentially neuroprotective functions of microglia/macrophages. As microglia/macrophages are highly dynamic and plastic cells, thorough investigation of these cell types requires analysis methods that are capable of detecting these dynamic changes; the larval zebrafish model is therefore ideal to investigate the functions of these cells following injury. Furthermore, as the adaptive immune system only fully matures at four to six weeks post fertilisation in the zebrafish (Novoa and Figueras, 2012), this enabled me to specifically investigate the role of the innate immune cells in secondary cell death.

I formulated the following hypotheses for my research:

1. Secondary cell death occurs in larval zebrafish following brain injury, and is mediated by similar mechanisms as in mammals.
2. Brain injury leads to rapid calcium waves that can influence and induce repair mechanisms by suppressing excessive cell death, recruiting microglia, and stimulating neurogenesis.
3. Microglia mediate neuroprotection following brain injury.

To test the outlined hypotheses, I set out the following aims for my project:

1. to describe cell death dynamics in response to injury, including distinction between primary and secondary cell death
2. to identify and describe early signalling pathways, in particular calcium signalling, and its effect on microglia recruitment, cell death, and neurogenesis
3. to study the role of microglia/macrophages in brain injury: which cells are recruited to the injury? What is their function once at the injury site? Is their presence beneficial or harmful?
4. to identify microglia/macrophage-derived molecules that could present potential therapeutic targets for neuroprotective treatments.

Chapter 3

Materials & Methods

3.1 Fish maintenance

All animals used were maintained under standard conditions (Westerfield, 2007), and experiments were performed in accordance with the British Home Office Regulations. Fish were kept at the Queen's Medical Research Institute fish facility on a 14 h light and 10 h dark cycle. Embryos were raised in E3 at 28.5 °C (Westerfield, 2007). If necessary, larvae were raised in E3 containing 0.001% *N*-Phenylthiourea (Sigma-Aldrich, P7629) to avoid formation of pigment. AB and WIK strains were used as wild type animals.

3.2 Transgenic fish lines

The following transgenic zebrafish lines were used throughout the course of my research:

Table 3.1: **Zebrafish lines.** Transgenic and mutant zebrafish lines used over the course of my research.

Name	Reference
tg(<i>β-actin</i> :GCaMP6f)	Christian Moritz, Francesca Peri, unpublished; see below
tg(<i>mpeg1</i> :GFP)	Ellett et al. (2011)
tg(<i>mpeg1</i> :mCherry)	Ellett et al. (2011)
tg(<i>p2y12</i> :P2Y ₁₂ -GFP; <i>mpeg1</i> :mCherry)	Sieger et al. (2012), Ellett et al. (2011)
tg(<i>H2Az</i> :GFP)	Pauls et al. (2001)
tg(<i>NBT</i> ::ΔLexR-LexOP::secA5-BFP), referred to as tg(<i>NBT</i> :secA5-BFP)	Mazaheri et al. (2014)
tg(<i>NBT</i> :dsRed)	Peri and Nüsslein-Volhard (2008)

tg(<i>her4.1</i> :TetA-GBD-p2a-mCherry ^{tud6}), referred to as tg(<i>her4.1</i> :mCherry)	Knopf et al. (2010)
tg(<i>her4.3</i> :GFP)	Yeo et al. (2007)
tg(<i>elav3</i> :kaede)	Sato et al. (2006)
tg(<i>mpo</i> :GFP)	Renshaw et al. (2006)
irf8 ^{st95/st95} , referred to as irf8 ^{-/-}	Shiau et al. (2015)
tgBAC(<i>il1b</i> :GFP)SH445, referred to as <i>il1b</i> :GFP	Ogryzko et al. (2018)
tg(<i>tnfa</i> :eGFP-F)	Nguyen-Chi et al. (2015)

3.2.1 Generation of β -actin:GCaMP6f transgenic fish line

The transgenic line β -actin:GCaMP6f was generated by Dr. Christian Moritz in the laboratory of Dr. Francesca Peri. Briefly, the transgenic line was generated by in by placing the GCaMP6f sequence (Chen et al., 2013) under the zebrafish β -actin promoter, flanked by Tol2 sites (Kwan et al., 2007). The construct was injected into one-cell stage embryos together with Tol2 transposase. Larvae from F2 or subsequent generations were used for this study.

3.3 Mosaic labelling of individual tectal neurons

The plasmid was generated by Ryan Kelly and Dr. David Greenald. To generate the *elav3*:TdTTomato-CAAX plasmid, referred to as *elav3*:memTdTTomato, we combined the entry clones p5E-*elav3* (Don et al., 2017), pME-TdTTomato-CAAX (Walton et al., 2015) and p3E-polyA (Kwan et al., 2007) with the destination vector pDestTol2pA2 (Kwan et al., 2007) using Gateway LR Clonase II enzyme (Life Technologies) according to manufacturer's instructions. For mosaic labelling of tectal neurons, 1 nL of *elav3*:memTdTTomato plasmid DNA at a concentration of 25 ng/ μ L was injected into one cell stage zebrafish embryos, and animals were allowed to develop until four days post fertilisation.

3.4 Induction of brain injury

Zebrafish larvae at 4 days post fertilisation (dpf) were anaesthetised using bath application of 0.01% Ethyl 3-aminobenzoate methanesulfonate (MS-222) and mounted in 1% low-melting point agarose (Life Technologies) in E3. The optic tectum was then injured under visual guidance of a stereomicroscope using a minutien pin (Fine Science Tools) mounted on a micromanipulator (World Precision Instruments). Larvae were released from the agarose and allowed to recover for varying amounts of time depending on experimental requirements. If calcium imaging was performed during

and immediately after injuring, the injury was induced on the stage of a confocal microscope in the same manner as described above.

3.5 Whole-mount immunostaining of zebrafish larvae

All steps were carried out at room temperature and under gentle agitation unless otherwise specified. Larvae were euthanised in 0.4% MS-222 at desired timepoint and fixed in 4% paraformaldehyde (Sigma-Aldrich, 158127) in PBS with 1% DMSO for 12 to 16 h at 4 °C. After fixation, larvae were washed in PBS. If necessary, pigment was removed by incubation in bleaching solution (3% H₂O₂, 0.5X SSC, 5% formamide) for 30 to 40 min without agitation. Larvae were then permeabilised by application of 2 mg/mL collagenase in PBS for 25 min, and subsequently post-fixed in 4% paraformaldehyde with 1% DMSO for 30 min (both steps without agitation). Blocking was carried out for 2 h in blocking buffer (1% normal goat serum, 1% bovine serum albumin, 1% DMSO, 1% Triton X-100, and 0.01% sodium azide in PBS). Primary antibodies were applied in blocking buffer for 12 to 16 h at 4 °C. I used the following primary antibodies: rabbit monoclonal anti-cleaved Caspase-3 (BD Pharmingen, catalogue number 559565; 2 µg/µL); rabbit polyclonal anti-mpo (GeneTex, catalogue number GTX128379-50ul; 6.5 µg/µL); mouse polyclonal anti-4C4 (courtesy of Becker lab, 1:50 [concentration not known]); chicken polyclonal anti-GFP (Abcam, catalogue number ab13970, 25 µg/µL). Larvae were washed in PBS with 1% Triton X-100, and treated with 100 µg/mL RNase A in PBS for 30 min at 37 °C to remove RNA if nuclear counterstaining with PI was required. They were then incubated in secondary antibody and, if nuclear counterstaining was required, 1 µg/mL PI, in blocking buffer for 12 to 16 h at 4 °C. The following secondary antibodies were used (all at 4 µg/µL, i.e., 1:500): goat anti-rabbit IgG Alexa Fluor 488 (A11008); goat anti-mouse IgG Alexa Fluor 488 (A11001) (all by Life Technologies); donkey anti-chicken Alexa Fluor 488 (703-545-155); donkey anti-mouse Alexa Fluor 647 (715-605-151) (both by Jackson ImmunoResearch). Larvae were washed in PBS with 1% Triton X-100 and subsequently in PBS before mounting in 1% low melting point agarose in PBS for confocal imaging.

3.6 Image acquisition

For fixed samples, larvae were prepared as described above, mounted in 1% low melting point agarose in PBS, and imaged at the Zeiss LSM 710 or 880 laser scanning confocal microscope.

For live confocal imaging, zebrafish larvae were anaesthetised using 0.01% MS-222 and mounted in 1% low melting point agarose in E3. After a brief waiting period to allow the agarose to settle, the agarose was covered with embryo medium containing 0.01% MS-222 to prevent desiccation during imaging. For visualization of necrotic and late apoptotic cells, 1 µg/mL propidium iodide (PI) were added to the embryo medium. Imaging was conducted on Zeiss LSM 710 or 880 laser

scanning confocal microscopes. Z-stacks of the optic tectum were acquired with 3.6 to 6 μm intervals between optical planes to a depth of 100 to 120 μm in fixed or live larvae. For time-lapse imaging of calcium signalling, images were acquired every 2 s. For timelapse imaging of microglia phagocytic behaviour, z-stacks of the whole optic tectum were acquired every 6 min. For visualisation of the rate of cell death in *H2A:GFP* larvae, z-stacks of the whole optic tectum were acquired every 25 min.

3.7 Image processing and analysis

Cell quantifications were performed manually in Image J (<https://imagej.nih.gov/ij>) from stacks of confocal images. PI^+ cells, pyknotic nuclei in *H2A:GFP* animals, Annexin 5^+ cells in *NBT:secA5-BFP* animals, Annexin $\text{A5}^+/\text{NBT}^+$ in *NBT:secA5-BFP*; *NBT:dsRed* animals, and Caspase 3^+ cells were counted across both tectal hemispheres and across all consecutive images in z-stacks of the optic tectum. Double labelling was only scored if both fluorophores were detected in the same optical plane. Quantifications were carried out blinded to experimental group.

The diameter of PI^+ and PI^- at 0 hpi and 6 hpi was measured manually in Image J across both tectal hemispheres in one optical plane, in at least 10 cells per animal.

For generation of heatmaps illustrating the density of apoptotic cells, pyknotic nuclei were manually selected in Image J from confocal images of *H2A:GFP* animals. Their xy coordinates were identified, and used to generate heatmaps through a custom-written script in MATLAB using a modified scattercloud function (Eilers and Goeman, 2004). The heatmaps were then overlaid with a masked outline of the optic tectum in Adobe Illustrator CC 2017.

For quantitative analysis of calcium signalling, time series of confocal images from *β -actin:GCaMP6f* animals acquired every 2 s were registered using the StackReg plugin in ImageJ to correct for xy drift. Two hundred and fifty to 300 regions of interest at a distance of 10 μm were manually selected in ImageJ, covering the entire cellular layer of one optical slice of the optic tectum, and $\delta\text{F}/\text{F}$ traces and calcium transients for each individual region of interest were calculated using custom-written MATLAB script (Herrgen et al., 2014). Transients were defined as a $\delta\text{F}/\text{F}$ greater than $4.25 \times$ standard deviation of baseline fluorescence (F), and with a duration of longer than 2 frames. The total number of transients for each larva was calculated by summation of all transients detected in individual cells.

For generation of heatmaps illustrating the spatial distribution of calcium transients, a matrix was created based on the location and number of transients in individual tectal cells using the *accumarray* function, smoothed by 15 pixels for illustrative purposes, and plotted using the *imagesc* function. All steps were performed in MATLAB.

To quantify the number of microglia, peripheral macrophages, and neutrophils at the site of brain injury, *mpeg1*⁺, *p2y12*⁺/*mpeg1*⁺, and *mpo*⁺ cells were counted in respective transgenic lines (*mpeg1*:GFP, *p2y12*:P2Y₁₂-GFP; *mpeg1*:mCherry, or *mpo*:GFP) in a region of interest measuring 200 μm horizontally and 200 μm vertically centered on the injury site across all consecutive images in z-stacks of the optic tectum. The injury site was visualised by the presence of PI⁺ primary necrotic cells. Cells residing on the skin were excluded from quantification.

Tracking of microglial cells within the brain, or of epidermal macrophages on the skin, was carried out using IMARIS 8.2.1. For this, time-lapse movies of *mpeg1*:GFP were visualised in IMARIS, and individual cells were tracked using an autoregressive motion algorithm under manual supervision. Speed and net displacement of microglial cell bodies were obtained as outputs of the algorithm.

To determine the frequency of phagocytic events, time-lapse movies of *mpeg1*:GFP animals incubated with PI were visualised in IMARIS, individual *mpeg1*⁺ cells were followed over time, and phagocytic events were identified manually. A phagocytic event was defined as formation of a phagocytic cup around PI⁺ cellular debris followed by movement of engulfed cargo towards the cell body, or movement of the cell body towards the cargo. The same protocol was used to determine the frequency of phagocytic events in radial glial cells, except that *her4.3*:GFP transgenic larvae were used.

All figures were assembled in Adobe Illustrator CC 2017.

3.8 Supplementary movies

Movies were generated from timelapse movies, timestamped using ImageJ or IMARIS, and labelled in Adobe Photoshop CC 2015.5. Supplementary movies are referred to in the text and captions of appropriate Figures, and signposted by the video camera symbol (📹). Supplementary movies can be found on Dropbox (<https://bit.ly/2Dlpqg8> or linked by adjacent QR-code).



3.9 Drug treatments

Pharmacological agents (Table 3.3) were delivered by ventricular injection or bath application. For injection, the drugs were diluted in calcium-free Ringer's solution (116 mM NaCl, 2.9 mM KCl, 5 mM HEPES pH 7.2), placed in fine a glass electrode, and delivered to the ventricle under a stereomicroscope. 0.03% FastGreen FCF (Alfa Aesar, 2353-45-9) were added to the solution to

visualise it. For bath application, drugs were diluted in E3 medium and pre-incubated for 1 h prior to the injury unless otherwise stated. The time between injection of compounds and imaging was kept to a minimum (<5 minutes) unless otherwise stated. I used the following compounds:

Table 3.3: **Drugs used for pharmacological manipulation.** Drug name, concentration, and mode of delivery.

Drug name	Type	Concentration	Mode of delivery
<i>D</i> -AP5	NMDA receptor inhibitor	5 mM	injection
MK801		3 mM	
<i>D</i> -AP5	NMDA receptor inhibitor	10 μ M	bth application
MK801		100 μ M	
DNQX	AMPA receptor inhibitor	5 mM	injection
PPADS	pan-P2 receptor inhibitor	20 mM	injection
<i>iso</i> -PPADS	P2X receptor subtype inhibitor	20 mM	injection
BAPTA-AM	intracellular calcium chelator	up to 80 mM	injection
BAPTA tetrasodium salt	extracellular calcium chelator	177 mM	injection
ATP	ATP receptor agonist	5 mM	injection
<i>L</i> -Glutamate	NMDA and AMPA receptor agonist	9 mM	injection
<i>L</i> -Glutamate	NMDA and AMPA receptor agonist	10 μ M	bath application
<i>O</i> -Phospho- <i>L</i> -Serine	mimicks <i>L</i> -phosphatidyl serine	1 μ M	bath application

ATP and glutamate (9 mM) were injected on-stage of a confocal microscope to visualise immediate effects of receptor-binding.

3.9.1 Statistical analysis of drug treatments on calcium wave parameters

Statistical analysis was carried out using Student's *t* Test or One-Way ANOVA with Bonferroni post-hoc test (or corresponding non-parametric tests if data was not normally distributed) as appropriate, comparing animals treated with vehicle or respective drug from the same day (one drug treatment occurred per day, or two per day when assessing ATP receptor inhibitors PPADS and *iso*-PPADS) in at least two independent experimental days. Power calculations were performed after initial preliminary data collection of 5 animals to estimate required sample sizes for a power of 80%. Data is summarised in Fig. 5.3 and portrayed as percentage of vehicle-injected controls.

3.10 Generation of *adgrb1a/b* crispants using CRISPR/Cas9-targeted gene editing

3.10.1 Guide design and injection

For CRISPR/Cas9-mediated disruption of *tnfa*, I used a guide previously published by Tsarouchas et al. (2018). The target sequence was 5'-CCCAGATGATGGCATTATTTTGT-3'.

For disruption of BA11 paralogues *adgrb1a* and *agrb1b*, I designed CRISPR guide RNAs for exonic sequences of *adgrb1a* (ENSDART00000143118.4) and *adgrb1b* (ENSDART00000188431.1) to target *Bsll* restriction enzyme sites. The target sequences were 5'-CAAGGGGGGGCTGCTGGATA-3' (*adgrb1a*) and 5'-CCCTCATACGGCGGCTCCGAGTG-3' (*adgrb1b*). The injection mix contained 1 μ L of each crRNA, 1 μ L tracrRNA (all 250 ng/ μ L), from Merck KGaA, Darmstadt), 0.2 μ L Cas9 enzyme (NEB #M0386T), 0.2 μ L FastGreen FCF tracer in RNase free water to 5 μ L, and was injected at the one-cell stage.

3.10.2 DNA extraction and test of guide efficiency via restriction fragment length polymorphism (RFLP)

The effect of mutagenesis was analysed for each animal by RFLP analysis following imaging. Briefly, gDNA was extracted by boiling individual larvae for 10 min in 100 μ L of 50 mM NaOH, and DNA was subsequently precipitated by adding 10 μ L of 1 M Tris-HCL pH 8.0 and vortexing. PCR was performed using the following primers:

<i>adgrb1a</i>	fw	5'-CACTTTCTCATCGTTGTGTCTCC-3'
	rev	5'-GGCAGTGGGAGTCTTGCTC-3'
<hr/>		
<i>adgrb1b</i>	fw	5'-AGTTGATGGATTCTGGAACGACT-3'
	rev	5'-GGTGTTTAGTGTACCAGGGCA-3'

PCR products were digested for 1 h at 55 °C using *Bsll*, and fragment length was analysed on a 1.8% agarose gel containing Ethidium Bromide, and subsequently imaged at the UV GelDoc.

3.10.3 Mutation analysis of *adgrb1a/b* crispants by sequencing

Sequencing and mutation analysis was performed by Dr. Marcus Keatinge. Briefly, to identify and sequence CRISPR/Cas9-induced mutations, PCR products from eight injected embryos were pooled and sub-cloned using the Strataclone PCR cloning system (Invitrogen, Catalog #240205). The ligated plasmid was transformed and 100 colonies sequenced. Finally, sequences were compared to the respective ENSEMBL transcript IDs.

3.11 Quantitative real-time PCR

3.11.1 RNA extraction and cDNA synthesis for qRT-PCR

Larvae were euthanised in 0.4% MS-222 if whole body RNA extract was acquired. Tissue was either processed immediately, or stored in QIAGEN[®] RNeasy Lysis Buffer (QIAGEN[®], # 76104) at 4 °C until processing for a maximum of one week. If samples were stored in RNeasy Lysis Buffer, RNeasy Lysis Buffer was removed prior to RNA extraction by washing samples 3 x in sterile PBS. SV Total RNA Isolation kit (Promega, # Z3100) or RNeasy Micro kit (QIAGEN[®], # 74004) were used for RNA extraction, and RNA extraction was carried out according to protocol. For whole body RNA samples, ten larvae were pooled. For RNA samples enriched from heads, fifty heads were cut using surgical microscissors (3 mm straight blade, FST[®] 15000-00) in ice-cold E3 + 0.4% MS-222.

For RNA extraction using SV Total RNA Isolation kit, 175 µL of lysis buffer were added to the tissue, and samples were triturated using 23 G needles. 350 µL of RNA dilution buffer were added and samples were incubated at 70 °C for 3 min. Samples were centrifuged at 13,000 g for 10 min, and supernatant was carefully transferred to a new tube. 200 µL of sterile 95% ethanol were added to the cleared supernatant and mixed by pipetting three to four times. The mix was then transferred to the SV Total RNA isolation kit spin columns and centrifuged at 13,000 g for 1 min. The spin column was washed with 600 µL RNA wash buffer, and incubated with DNase I to digest genomic DNA at room temperature for 15 min. Column was washed twice (600 and 250 µL) and RNA was eluted in 25 µL nuclease-free water.

For RNA extraction using QIAGEN[®] RNeasy Micro kit, 350 µL of buffer RLT⁺ containing 1% β-mercaptoethanol were added to sample, and samples were triturated using 23 G needles. Samples were centrifuged for 2 min at full speed in Qiagen Qias shredder columns to further lyse cells. Lysate was then mixed with 350 µL 70% ethanol and placed in QIAGEN[®] RNeasy MinElute spin columns, and centrifuged for 30 s at ≥ 8000 g. Column was subsequently washed with 700 µL buffer RW1 and 500 µL buffer RPE, with 15 s spins at ≥ 8000 g in between. Five hundred µL of 80% ethanol were added to tubes, and spun for 2 min at ≥ 8000 g. Spin columns were transferred to fresh collection tubes, and the membrane was dried by centrifuging for 5 min at full speed with an open lid. RNA was eluted from the column using 14 µL nuclease-free water and centrifugation for 1 min at full speed.

Following both methods, RNA concentration was measured at the NanoDrop One, and RNA was stored at -80 °C until further use. cDNA was synthesised using the iScript[™] cDNA synthesis kit (Bio-RAD, # 1708890) according to protocol. cDNA samples were stored at -20 °C.

3.11.2 qRT-PCR primer design & validation

Primers (Table 3.5) were designed to a length of 100 to 300 base pairs (bp) using NCBI Primer Blast, avoiding targets on other annotated *Danio rerio* mRNAs (<https://www.ncbi.nlm.nih.gov/tools/primer-blast/>). Melting temperatures (T_m) were designed around 60 °C, and 3' self-complementarity value was < 2. Target size was confirmed by running PCR products on a 1.5% agarose gel.

Table 3.5: **Primers used for qRT-PCR.** Gene RefSeq numbers, primer sequence, length, melting temperature (T_m), and GC content.

Gene		5' - 3' sequence	Product length (bp)	T_m (°C)	GC Content (%)
actb2 NM_181601.4	fw	ctggcccctagcacaatgaa	199	60.03	55
	rev	gagtcggcgtgaagtggtaa		60.04	
tnfa NM_212859.2	fw	ccatgcagtgatgcgctttt	166	60.11	50
	rev	gtctgtgccagctctgtctc		60.04	
tnfb NM_001024447.1	fw	atacacagatgcggtgaggg	196	59.53	55
	rev	cccgaagaatgttttggcgt		59.40	
bdnf NM_131595.2	fw	ccaaaggatccgctcagtca	195	59.97	55
	rev	tctcgatattcgtccgctc		60.04	
ngfb NM_199210.1	fw	tcaggttacggttgctttg	224	59.06	50
	rev	cttcggtcacgtctgcctta		59.76	
tgfb1a NM_182873.1	fw	tgtacccgcaatccttgacc	169	60.04	55
	rev	ccgactgagaaatcgagcca		59.83	
il1b NM_212844.2	fw	ggcatgcgggcaatatgaag	116	60.04	55
	rev	tgtagctcattgcaagcgga		60.04	
il4 NM_001170740.1	fw	ggatcctgaatgggaaagggg	211	60.13	57.14
	rev	cattccccgaggtcgaac		60.74	
il10 NM_001020785.2	fw	gaccattctgccaacagctc	102	59.19	55
	rev	accatatcccgttgattcc		59.86	
adgrb1a NM_001020785.2	fw	tgtgtgtccagaacatgggg	259	59.89	55
	rev	ctccgaattcgctgcattg		59.97	
adgrb1b NM_001020785.2	fw	aacggagcctgggatgaatg	158	59.19	55
	rev	cacacggcaatgttcagaa		59.86	

To achieve a reaction efficiency of 100%, I optimised primers by performing qRT-PCR reactions with cDNA dilution curves (at least 5 dilution points). Different primer concentrations were tested until efficiency was within 6% of 100%. Two technical replicates were run per data point. Graphs were plotted in GraphPad Prism 7.0 and slope value was determined (shown in Table 3.6). r^2

values had to be > 0.95 for primer dilution to be considered.

Table 3.6: **Primer efficiency following optimisation.** Gene target, optimal concentration, slope on cDNA concentration curve including r^2 , and Efficiency (E/%) are included in this table.

Target	Concentration used	slope	r^2	Efficiency (E)	Efficiency (%)
actb2	0.2 μ M	-3.304	0.9971	2.0075	100.75
tnfa	0.25 μ M	-3.228	0.9929	2.036	103.6
tnfb	0.1 μ M	-3.472	0.9751	1.941	94.10
bdnf	0.25 μ M	-3.357	0.9985	1.986	98.57
ngfb	0.1 μ M	-3.21	0.9995	2.049	104.89
tgfb1a	0.2 μ M	-3.216	0.9647	2.0462	104.62
il1b	0.2 μ M	-3.419	0.9816	1.961	96.10
il4	0.1 μ M	-3.377	0.9806	1.978	97.75
il10	0.25 μ M	-3.376	0.9938	1.978	97.76
adgrb1a	1 μ M	-3.202	0.9631	2.053	105.26
adgrb1b	1 μ M	-3.234	0.9500	2.038	103.81

3.11.3 Quantitative reverse-transcription PCR (qRT-PCR)

qRT-PCRs were performed on the LightCycler[®] 96 Real-Time PCR System (Roche) using the SsoAdvanced[™] Universal SYBR[®] Green Mix (BioRad, # 1725271). Reaction mixes were prepared in LightCycler[®] 480 Multiwell Plate 96 (Roche, 04729692001) and then sealed with a foil to prevent evaporation of reagents. The samples were then spun down on an Eppendorf 5804 plate centrifuge. The following programme was run:

Step	Cycles	Temperature	Time (s)
Preincubation	1	95 °C	300
3-Step Amplification	45	95 °C	10
		55 °C	30
		72 °C	15
Melting	1	95 °C	10
		65 °C	60
		97 celsius	1
Cooling	1	40 °C	10

3.11.4 qPCR analysis

Ct values were extracted from raw data using the LightCycler® 96 Software by Roche. The ratio of gene expression compared to a reference gene between conditions was according to the Pfaffl method (Pfaffl, 2001). Briefly, the following formula was applied:

$$ratio = \frac{E_{target}^{\Delta C_{t_{target}} (control - sample)}}{E_{reference}^{\Delta C_{t_{reference}} (control - sample)}}$$

Values were calculated as mean of two technical replicates. At least four biological replicates were analysed per condition.

3.12 RNA sequencing

3.12.1 Isolation of transgenically labelled fluorescent cells from larval heads via FACS

To investigate cell-type specific changes to gene expression following injury, microglia/macrophages were sorted using Fluorescence Activated Cell Sorting at the Flow Cytometry Facility at the Queen's Medical Research Institute, Edinburgh. I used anti-4C4 antibody staining to extract microglia, the *mpeg1*:GFP transgenic line to extract both microglia and macrophages, or wild types as negative controls. Preparation of the cell suspension for cell sorting was performed as previously published (Mazzolini et al., 2018). Briefly, larvae were anaesthetised at 2 hpi with 0.4% MS-222, and transferred to a fresh petri dish containing ice cold E3 with 0.01% MS-222. Heads were cut using surgical microscissors (3 mm straight blade, FST®15000-00) and transferred into a cooled glass dounce homogeniser (1 mL) containing 1 mL medium A (15 mM HEPES, 2 mM D-Glucose in 1 X HBSS).

Once all the heads were collected, medium A was replaced with 1 mL fresh medium A. Heads were homogenised thirty times using a dounce homogeniser. Two mL of medium A were added to the cell suspension and ran through a 40 µm cell strainer (Falcon 352340). The cell suspension was then transferred into 1.5 mL Eppendorf tubes (1 mL each) and centrifuged at 300 g for 10 min at 4 °C. The supernatant was discarded using a 5 mL syringe (BD 309647) and 23 G needle (BD 300800). The cell pellet was resuspended with 1 mL of ice cold 22% Percoll and overlaid with 0.5 mL 1X DPBS to build a density gradient. The tubes were centrifuged for 30 min at 950 g at 4 °C. The supernatant containing DPBS, myelin-containing interphase and density medium was discarded and the cell pellet was washed with 0.5 mL medium A + 2% NGS (300 g for 10 min at 4 °C). The cell suspension was transferred through a 35 µm cell strainer cap into 5 mL FACS tubes (BD 352235) and sorted at FACS Aria II at the Flow Facility at the QMRI. The cell sorting gate was calibrated using wild type larvae undergoing the same protocol. Cells were

sorted directly into chilled 1.5 mL Eppendorf tubes containing 1 mL of RNAProtect Cell Reagent to stabilise cellular RNAs. Tubes were stored until RNA extraction at 4 °C for a maximum of three days.

Anti-4C4 immunolabelling of microglia was performed as described by Mazzolini et al. (2018). Unspecific interactions of the Fc receptor with the secondary antibody were prevented by incubation with 1% anti-CD16/CD32 antibody (Biolegends, # 302013, clone 3G8) prior to each antibody incubation step. Briefly, cell suspension was incubated in mouse anti-4C4 antibody (1:20) at 4 °C for 30 min following removal of myelin, and washed twice with medium A + 2% NGS. Cell suspension was then incubated with secondary anti-mouse Alexa Fluor 488 for 30 min at 4 °C, washed twice with medium A + 2% NGS, and placed in FACS tubes as described above.

3.12.2 RNA extraction from FACS sorted cells

Following FACS, cells were pelleted at 5000 × g for 5 min. The supernatant was aspirated and RNA was extracted from the cell pellet using the QIAGEN® RNeasy Plus Micro kit (QIAGEN®, # 74034) according to the manufacturer's instructions. Briefly, the cell pellet was re-suspended in 75 µL Buffer RLT Plus containing 1% β-Mercaptoethanol. The cell suspension was then transferred to gDNA eliminator columns and centrifuged for 30 s at ≥ 8000 g. The column was discarded. One volume (350 µL) of ice cold 70% ethanol were added to the flowthrough, mixed well by pipetting, and immediately transferred to MinElute columns. The samples were spun for 15 s at ≥ 8000 g. The flow-through was discarded. Seven hundred µL of buffer RW1 were added to the column, and the samples were centrifuged for 15 s at ≥ 8000 g. The flowthrough was discarded again and 500 µL of buffer RPE were added. The tubes were centrifuged for 15 s at ≥ 8000 g. Next, 500 µL of 80% ethanol were added to wash the column and the samples were centrifuged for 2 min at ≥ 8000 × g. To remove any leftover ethanol in the column and dry the membrane before elution, the column was placed in a fresh 2 mL collection tube and centrifuged for 5 min at full speed with an open lid. The column was then placed in a fresh 1.5 mL collection tube and the RNA was eluted by adding 14 µL directly to the membrane and centrifuging the tube for 15 s at full speed.

Quantification of RNA quality and quantity was then carried out at the Labchip GX24 (PerkinElmer) by Dr. Pamela Brown at the Shared University Research Facility, Queen's Medical Research Institute, University of Edinburgh.

3.12.3 cDNA synthesis and isothermal amplification for RNA sequencing

RNA was reverse transcribed and amplified using the NuGEN Ovation® RNA-Seq System V2 (# 7102-08) according to manufacturer's instructions with an input of at least 500 ng RNA in 500 µL. Amplified cDNA was then purified using the QIAGEN® MinElute® Reaction Cleanup Kit (# 28204) and quantified using the NanoDrop One.

3.12.4 Library preparation, sequencing and bioinformatical analysis of amplified cDNA

This part of the methods was carried out by Edinburgh Genomics. Libraries were prepared from each sample using a manual TruSeq DNA Nano gel free library kit (350 bp insert). The samples were sequenced on a NovaSeq instrument producing 50PE data (at least 250M + 250M reads).

Bioinformatical quality control and differential analysis

Bioinformatical analysis was carried out by Dr. Katie Emelianova (Edinburgh Genomics).

Trimming

Reads were trimmed using Cutadapt (Martin, 2011) (version cutadapt-1.9.dev2). Reads were trimmed for quality at the 3' end using a quality threshold of 30 and for adapter sequences of the TruSeq DNA Nano kit (AGATCGGAAGAGC). Reads after trimming were required to have a minimum length of 35.

Reference

The reference used for mapping was the *Danio rerio* (GRCz10) genome from Ensembl. The annotation used for counting was the standard GTF-format annotation for that reference (annotation version 84).

Alignment

Reads were aligned to the reference genome using STAR (Dobin et al., 2013) (version 2.5.2b) specifying paired-end reads and the option `--outSAMtypeBAMUnsorted`. All other parameters were left at default.

Read count by feature

Reads were assigned to features of type exon in the input annotation grouped by `gene_id` in the reference genome using `featureCounts` (Liao et al., 2014) (version 1.5.1). `featureCounts` assigns counts on a fragment basis as opposed to individual reads such that a fragment is counted where one or both of its reads are aligned and associated with the specified features. Strandness was set to reverse and a minimum alignment quality of 10 was specified.

In addition to the counts matrix used in downstream differential analysis, a matrix of Fragments Per Kilobase of transcript per Million mapped reads (FPKM) values was generated, using the `rpkm()` function of `edgeR` (Robinson et al., 2010) (version 3.20.1) and normalised effective library sizes. Gene lengths for the FPKM calculation were the number of bases in the exons of each gene (only counting bases once where they occur in multiple exon annotations). Gene names and other fields

were derived from input annotation and added to the count/expression matrices.

Count preprocessing

The raw counts table was filtered to remove genes consisting predominantly of near-zero counts, filtering on counts per million (CPM) to avoid artefacts due to library depth. Specifically, a row of the expression matrix was required to have values greater than 0.1 in at least 3 samples, corresponding to the smallest sample group as defined by Group, once any samples were removed (where applicable).

Reads were normalised using the weighted trimmed mean of M-values method (Robinson and Oshlack, 2010), passing TMM as the method to the *calcNormFactors* method of edgeR.

Exploratory analysis

A principal components analysis was undertaken on normalised and filtered expression data to explore observed patterns with respect to experimental factors. The cumulative proportion of variance associated with each factor was used to study the level of structure in the data, while associations between continuous value ranges in principal components and categorical experimental factors was assessed with an ANOVA test.

Differential analysis

Differential analysis was carried out with edgeR (Robinson et al., 2010) (version 3.20.1) with the contrasts shown in Table 3.7. Fold changes were estimated as per the default behaviour of edgeR, to avoid artefacts which occur with empirical calculation.

Table 3.7: **Contrasts specified for differential analysis.** Any variable specified under blocking was used as part of an additive model, and accounted for in differential analysis of that contrast.

Variable	Group 1	Group 2	Blocking
Group	Sham	2 hpi	None

Specifically, a small prior count is added to each observation before fitting a model, in proportion to the library size. Log fold-changes are shrunk towards 0, to a greater degree with genes of low count, and infinite fold changes are avoided. Statistical assessment of differential expression was carried out with the quasi-likelihood (QL) F-test using the contrasts shown in Table 3.7. Where specified in this table, confounding covariates (for example sample pairing, batch effects) were adjusted for by incorporating them as a blocking factor in an additive model.

3.12.5 Generation of expression heatmaps

For generation of expression heatmaps, raw counts (fragments per kilobase million, FPKM) were extracted from the RNA sequencing data for genes of interest using MATLAB. I created expression matrices containing gene name and counts per million for each sample submitted to RNA sequencing. Expression heatmaps were then created using the *gplots* package in R, normalising expression per gene row. Color scheme was provided by the *viridis* package.

3.12.6 Gene ontology enrichment analysis

Gene ontology enrichment analysis was carried out using an online tool (<https://www.panther.db>) based on the PANTHER Classification system (Mi et al., 2013). The list of genes of interest was uploaded to the website, alongside with a reference gene list of all detected genes in the RNA sequencing (i.e., background list). Gene lists were analysed for 'GO Biological process complete'. Test type performed was Fisher's exact test with Bonferroni correction for multiple comparisons.

3.13 Statistical methods

All population data are presented as mean \pm SEM. Statistical analysis was performed using Prism 7.0 (GraphPad). Briefly, data sets were assessed for normality, and appropriate statistical tests were carried out as stated in the figure legends.

Analysis was performed blinded to treatment and the power was calculated for significant values. Randomisation of larvae to treatment was carried out manually by selecting random larvae under anaesthesia from of petri dishes of 50 larvae. If the power was below 80%, required sample sizes were calculated and added accordingly.

Chapter 4

Mechanical injury induces primary and secondary cell death in a larval zebrafish model of brain injury

4.1 Introduction

Traumatic brain injury is a prevalent and pressing global medical issue (Maas et al., 2010, 2017). It can affect patients of all genders, ages, and backgrounds, and there are no targeted treatments available to alleviate the consequences. TBI is a major cause of death in young adults, and lifelong disabilities are common in survivors - it is estimated that 5.3 million people in the US and 7.7 million people in the EU are living with TBI-related disabilities (Langlois and Sattin, 2005; Tagliaferri et al., 2006), and over half the population will have one or more TBIs in their lifetime (Maas et al., 2017).

TBI leads to significant neuronal loss via primary cell death (directly caused by mechanical injury) and secondary cell death (elicited by biochemical cascades initiated by the injury). Secondary (or delayed) cell death occurs both in experimental models of TBI (Beer et al., 2000; Clark et al., 2000; Keane et al., 2001) and in human patients (Clark et al., 1999), and is related to a poorer cognitive status after brain injuries (Miñambres et al., 2008; Nathoo et al., 2004; Yakovlev et al., 1997). Despite intensive research efforts to elucidate the molecular mechanisms of TBI and identify neuroprotective strategies, there are no therapeutic approaches or neuroprotective drugs that have shown benefit over placebo in multi-centre clinical trials so far (Maas et al., 2010, 2017). While this may be a reflection of poor study design and insensitive end point measurements (Maas et al., 2010), it also highlights the fact that potentially more dynamic models of brain injury may be needed to capture and understand the molecular processes underlying secondary cell death following brain injury *in vivo*.

The first aim of my thesis was to establish such a model in order to investigate neuroprotective strategies following TBI. For this purpose, I developed a robust and simple assay to reliably induce cell death in larval zebrafish by lesioning the brain with a fine metal pin. I introduced the injury in the optic tectum (OT), the largest subdivision of the larval zebrafish brain (Cooper et al., 2015). The OT is easily accessible to micromanipulation and microscopy due to its superficial positioning in the brain and already has a clearly defined and highly structured architecture at 4 days post fertilisation (Scott and Baier, 2009), which is the timepoint I aimed to carry out my analysis at. In comparison with rodent and larger animal experimental models, the larval zebrafish had several advantages: more economic husbandry, the ability to easily perform *in vivo* timelapse imaging facilitated by a multitude of transgenic fluorescent reporter lines, and the ease of pharmacological and genetic manipulation to tease apart molecular and cellular mechanisms contributing to secondary cell death.

Initially, I needed to describe the dynamics of cell death following TBI, and more specifically, how they relate to what is observed in human patients and other experimental models. I employed several tools to analyse cell death following brain injury:

- propidium iodide (PI):
PI is a nuclei acid dye that can only enter cells with a compromised membrane (Kroemer et al., 2009), therefore it can be used in bath application to visualise necrotic (and late apoptotic) cell death.
- nuclear condensation (in *H2A:GFP* transgenic larvae):
Nuclear condensation (pyknosis) is a hallmark of late apoptosis (Kroemer et al., 2009; Oberhammer et al., 1994; Toné et al., 2007), therefore I employed a green fluorescent protein (GFP)-tagged histone to visualise apoptotic cells.
- Annexin 5 (in *NBT:secA5-BFP* transgenic larvae):
Annexin 5 can bind phosphatidyl serine (PS) exposed on early apoptotic cells (Balasubramanian and Schroit, 2003; Segawa and Nagata, 2015). I used a transgenic line in which a blue fluorescent protein (BFP)-tagged version of Annexin 5 is secreted by neurons and therefore apoptotic cells (both neurons and other cells exposing PS) appear BFP⁺.
- cleaved Caspase-3 (via immunostaining):
To quantify activation of Caspase-3, a key enzyme in the execution of apoptosis (Porter and Jänicke, 1999; Wyllie, 1997), I performed an immunostaining against cleaved Caspase-3 in fixed larvae.

In this chapter, I will lay out the description of the mechanical injury assay developed at the start of my project. As I later aimed to investigate calcium waves occurring immediately following injury, it

was of advantage that the assay could both be carried out on a stereomicroscope and on a confocal microscope. I investigated primary and secondary cell death dynamics, and performed repeated *in vivo* imaging to further describe this novel assay. The work described in this chapter will lay the foundation for further experiments and the selection of timepoints for endpoint analyses described in later chapters of this thesis.

4.2 Description of injury

I induced a mechanical brain injury by penetrating the optic tectum of 4 dpf larval zebrafish using a minutien pin under visual guidance under a microscope. The minutien pin was mounted on a micromanipulator for precise and reproducible delivery of the injury. For induction of the injury, the larvae were immobilized in a dorsal orientation in 1% low melting point agarose. The optic tectum is the largest part of the larval zebrafish brain and lies superficially on the dorsal side of the zebrafish brain, therefore making it easily accessible to mechanical injury and microscopy. A schematic and brightfield images of this are shown in Fig. 4.1 A and B.

The larvae recovered well from the injury once released of the agarose and placed in fresh medium, and showed little mortality over 24 h (<1%). Occasionally, blood vessels were ruptured during the injury leading to ventricular haemorrhage (< 2%). Larvae exhibiting ventricular haemorrhage after injury were excluded from later quantifications of cell death to exclude any potential confounding effects of haemorrhage on cell death. A quantification of adverse effects over 1075 larvae in 6 biological replicates is shown in Fig. 4.1 C.

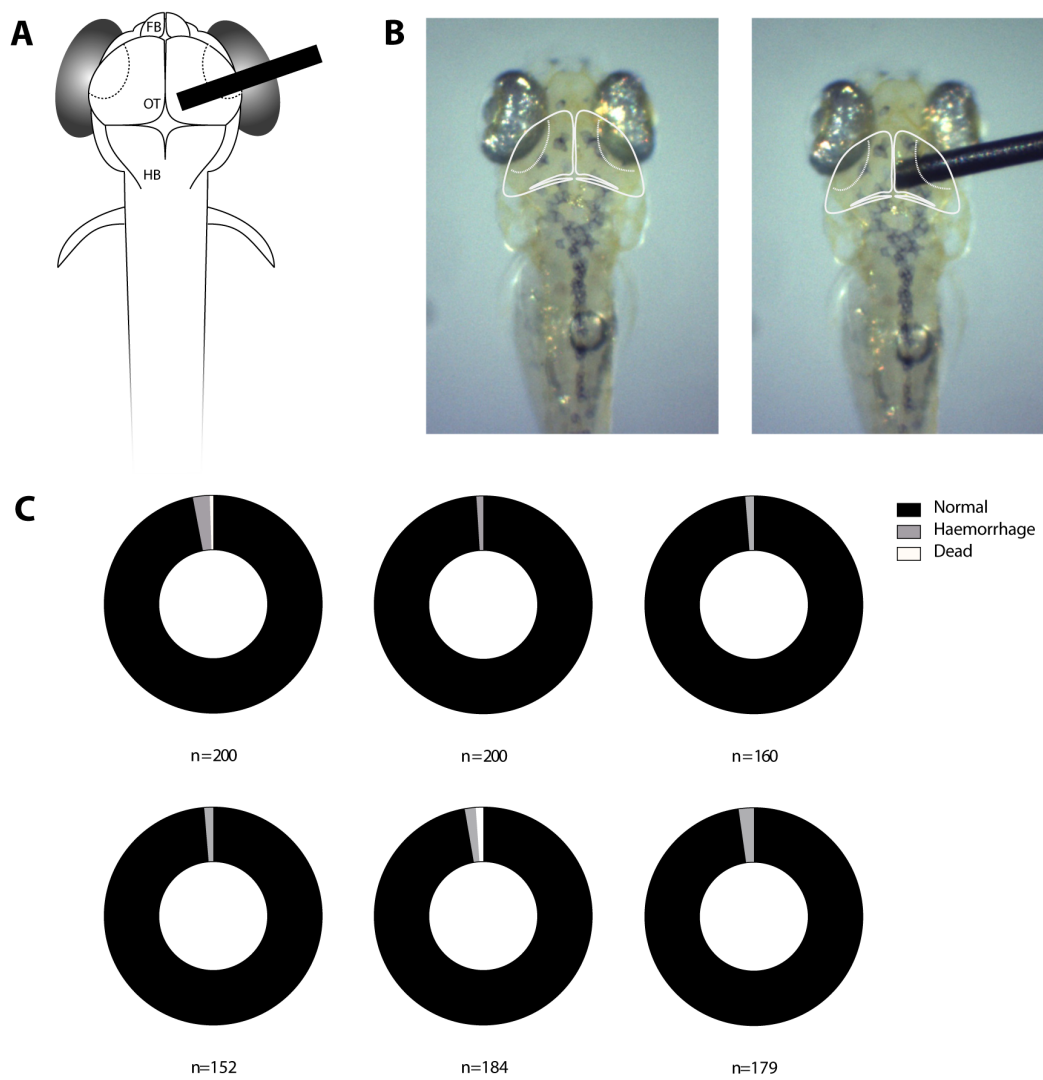


Figure 4.1: **Description of the injury assay.** (A) Schematic of the dorsal view of the larval zebrafish outlining forebrain (FB), optic tectum (OT), and hindbrain (HB). The site of injury is indicated by a drawing of the needle. (B) Representative brightfield images of a larva before and during injury. (C) Quantification of fractions of normal larvae, larvae with haemorrhage, and dead larvae following injury in 6 different biological replicates with a total n of 1075.

4.3 Dynamics of cell death: primary necrotic and secondary apoptotic cell death

I aimed to assess the dynamics of cell death following mechanical injury. Using *H2A:GFP* transgenic animals (Pauls et al., 2001) allowed me to visualise pyknotic nuclei of apoptotic cells (Kroemer et al., 2009). In combination with the presence of PI, labelling necrotic and late apoptotic cells (Kroemer et al., 2009), this enabled me to visualise injury-induced necrosis and apoptosis in real-time.

Mechanical injury resulted in a sharp increase of PI⁺ cells at 0 hpi (Fig. 4.2). The lack of pyknosis (Fig. 4.3; diameter of PI⁺ cells at 0 hpi: $4.7 \pm 0.3 \mu\text{m}$; diameter of PI⁻ cells at 0 hpi: $4.9 \pm 0.1 \mu\text{m}$; $n = 5$ animals; $p > 0.999$ in Mann-Whitney test), as well as their rapid appearance identified these PI⁺ cells as necrotic cells. Quantification of PI⁺ cells over time revealed that these necrotic cells were rapidly removed from the tissue (Fig. 4.2), with a significant drop evident as early as one hour post injury (1 hpi). Conversely, *in vivo* imaging with *H2A:GFP* larvae showed that pyknotic nuclei were not present immediately after the injury, but appeared around 1 hpi, where they originated at the injury site, and peaked at 6 hpi, where they spread to both hemispheres (Fig. 4.4 D). This occurrence of delayed apoptotic cell death in regions distant from the original injury site was reminiscent of findings following mammalian brain injury, where cell death is observed at regions remote from the original injury site (Rink et al., 1995). The peak of pyknotic nuclei at 6 hpi was accompanied by a small secondary peak of PI⁺ cells. However, PI⁺ cells at 6 hpi had a significantly smaller diameter than healthy nuclei (Fig. 4.3; diameter of PI⁺ at 6 hpi: $2.2 \pm 0.1 \mu\text{m}$; diameter of PI⁻ healthy nuclei at 6 hpi: $4.8 \pm 0.2 \mu\text{m}$; $n \geq 5$ animals; $p \leq 0.005$ in Mann-Whitney test), which suggested these PI⁺ cells were late apoptotic cells.

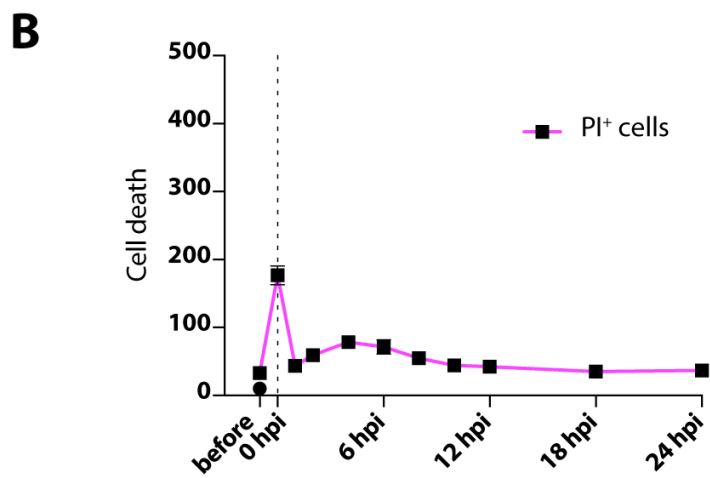
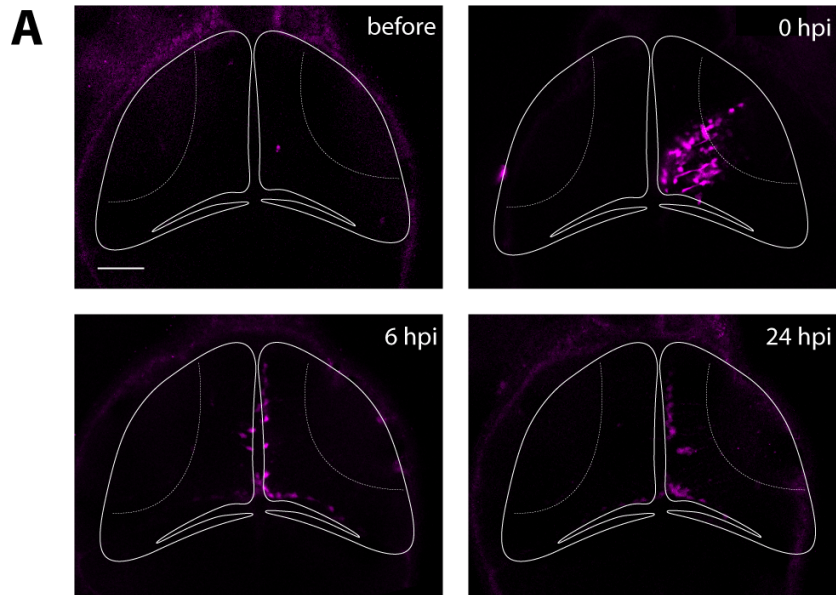


Figure 4.2: **Mechanical injury leads to rapid cell death as monitored by of PI uptake. (A)** Mechanical injury results in a prompt uptake of PI. Scale bar, 50 μm . **(B)** Quantification of PI⁺ cells after mechanical injury. Dashed line indicates time of injury. $n \geq 6$ animals per experimental group.

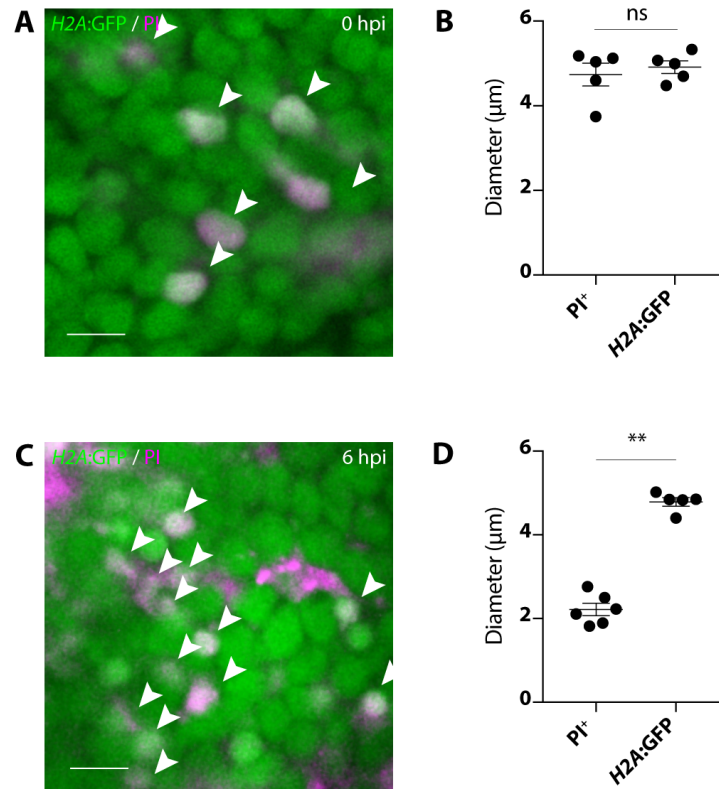


Figure 4.3: PI^+ cells display morphological characteristics of necrosis immediately after injury, and of apoptosis hours later. **(A, B)** The diameter of PI^+ cells (arrowheads) is not significantly different from viable cell nuclei ($H2A:GFP$) at 0 hpi. Scale bar, $10\ \mu m$. Values are the average of at least 10 PI^+ and $H2A:GFP^+$ cells in one optical section per animal. $n = 5$; $p > 0.999$ in Mann-Whitney Test. **(C, D)** At 6 hpi, the diameter of PI^+ cells (arrowheads) is significantly smaller than that of viable cell nuclei. Scale bar, $10\ \mu m$. Values are the average of at least 10 PI^+ and $H2A:GFP^+$ cells in one optical section per animal. $n \geq 5$; $p \leq 0.005$ in Mann-Whitney Test.

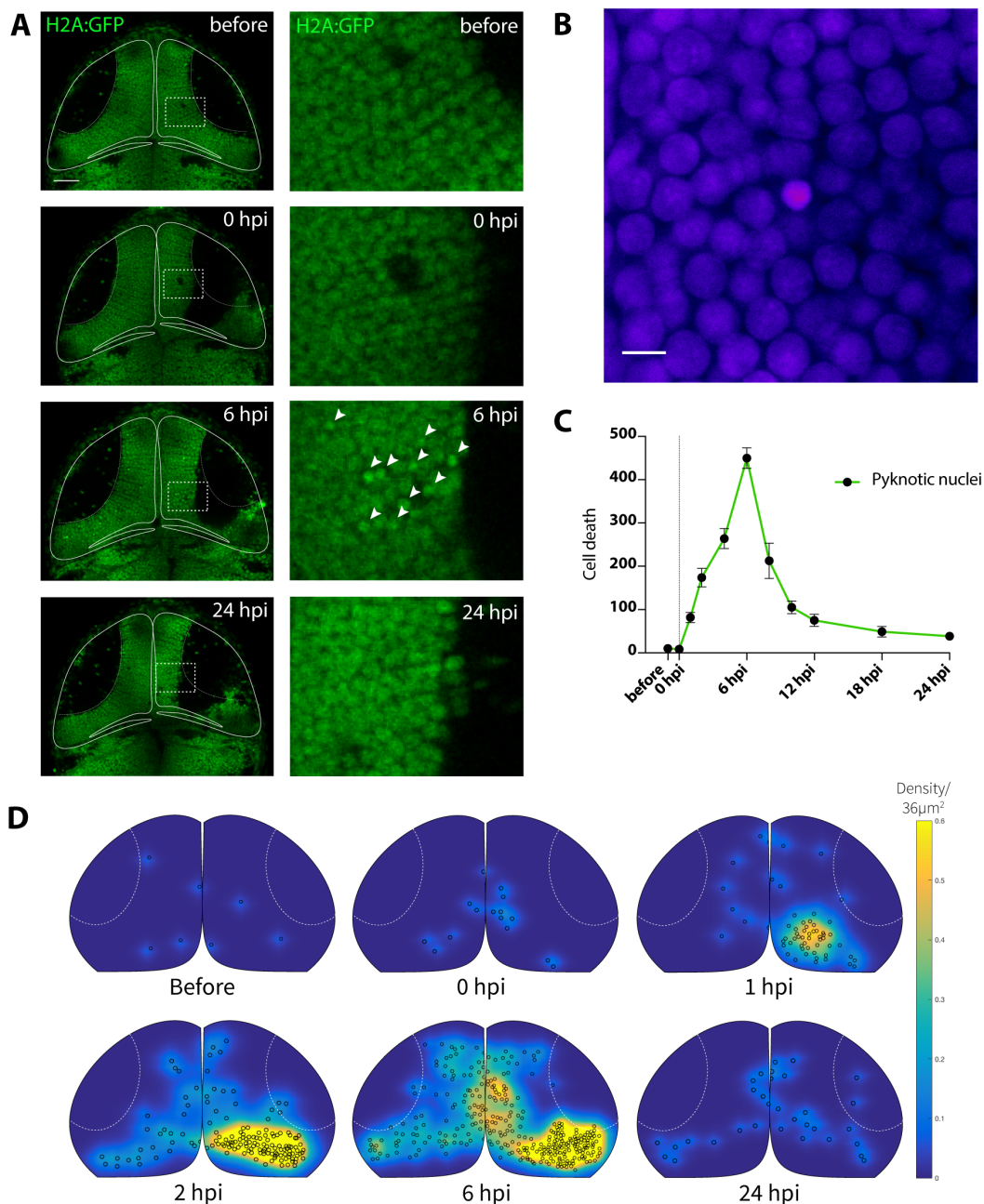


Figure 4.4: Mechanical brain injury leads to delayed nuclear condensation peaking at 6 hpi. (A) Overview and close-ups of tectum in H2A:GFP transgenic animals before, and at 0, 6, and 24 hpi. Scale bar, 50 or 5 μm , respectively. (B) Close-up of a pyknotic nucleus with the Fire LUT (ImageJ), showing the distinct difference in size and intensity of pyknotic nuclei compared with surrounding normal nuclei. Scale bar, 5 μm . (C) Quantification of pyknotic nuclei present in entire tectum following injury. Dotted vertical line indicates time of injury. $n \geq 6$ animals per timepoint. (D) Heat map illustrating the spread of secondary cell death throughout the tectum in the hours following injury. XY coordinates of pyknotic nuclei from representative animals at varying timepoints following injury were plotted in 2D using the Matlab Scattercloud function.

Interestingly, I also observed PI uptake in the cell bodies of radial glia and microglia/macrophages following injury (Fig. 4.5). The continued presence of PI⁺ radial glia and microglia/macrophages for up to 48 hpi suggested these cells were neither necrotic nor apoptotic, and PI may have entered via a mechanism other than disrupted membrane integrity due to cell death. In the case of macrophages/microglia (Fig. 4.5 B), it was likely that PI inside these cells originated from necrotic cells they had previously engulfed. In radial glia (Fig. 4.5 A), I hypothesised that the emergence of PI⁺ cells was the result of opening of pore-forming ion channels. ATP-dependent P2X subtype receptors have previously been shown form large ion channel pores in glial cells following CNS injury (James and Butt, 2002). To investigate whether this was the case in radial glia following brain injury, I injected pan-P2X receptor inhibitor iso-PPADS or vehicle into the ventricle of larvae prior to injury. Using iso-PPADS, I was able to completely abolish PI labelling of radial glia in all animals (n = 6 per group, Fig. 4.5C) at 6 hpi, suggesting P2X receptors play a crucial role in dye uptake, potentially through P2X receptor-dependent pore formation. Conversely, I did not observe a significant effect on PI labelling of microglia/macrophages using iso-PPADS.

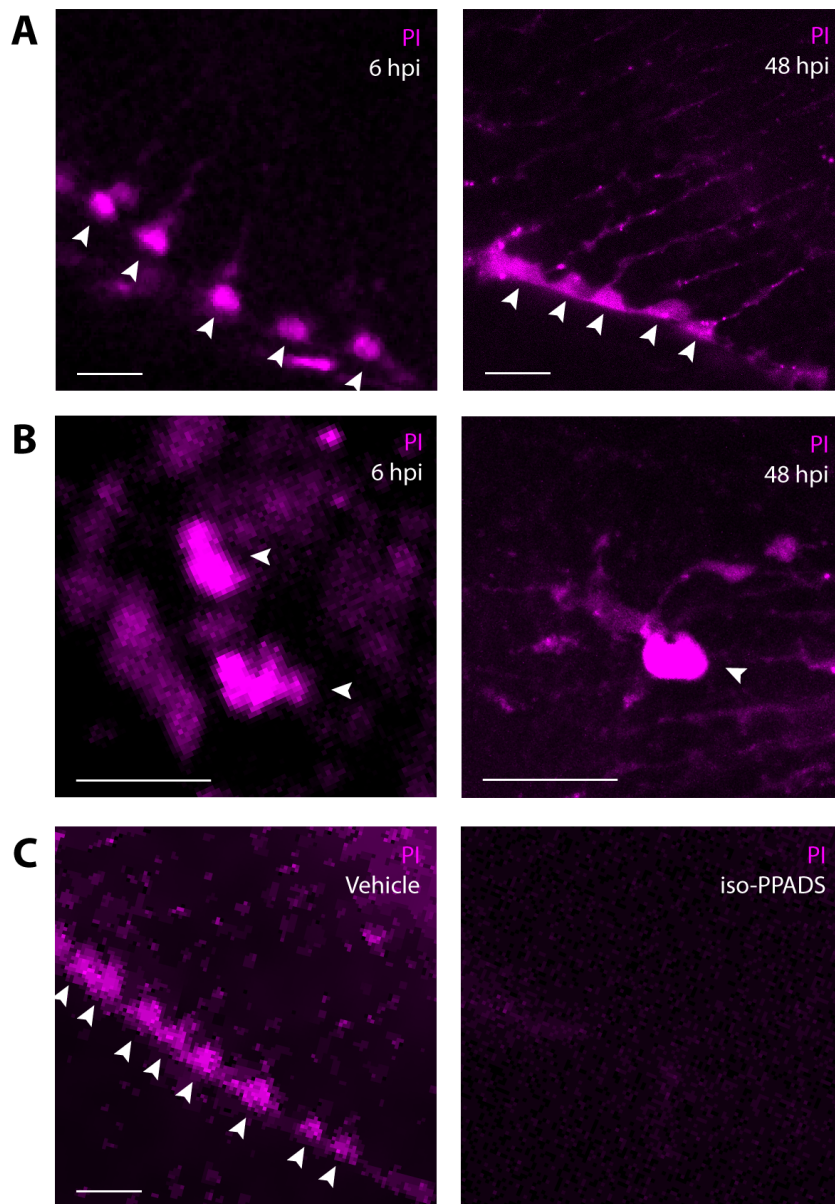


Figure 4.5: **Cells with radial glial and microglial morphology take up PI, but survive long after the injury.** **(A)** Cells with radial glial morphology at 6 hpi and 48 hpi do not appear condensed, but have PI in their cytoplasm. Arrowheads are pointing towards cell bodies of radial glia. Scale bar, 15 μ m. **(B)** At 6 hpi, large aggregations of PI⁺ debris were often present. Based on the size of these aggregates (larger than normal neurons), these are likely microglia that have taken up PI⁺ cells but not yet degraded them. At 48 hpi, some microglia and their processes appear PI⁺. Arrowheads are pointing to microglial cell bodies. Scale bar, 15 μ m. **(C)** Ventricular injection of P2X subtype receptor inhibitor iso-PPADS ablates radial glial uptake of PI (6/6 animals). Images shown taken at 6 hpi in either vehicle (Calcium-free Ringer solution) or iso-PPADS injected larvae bathed in propidium iodide. Scale bar, 15 μ m.

In vivo imaging in *H2A:GFP* transgenic animals in the presence of PI had suggested that both necrosis and apoptosis occurred following mechanical brain injury in larval zebrafish with distinct temporal patterns (Fig. 4.2, Fig. 4.4). To strengthen this evidence, I employed two additional approaches for the detection of apoptosis in the brain: *in vivo* imaging of the transgenic line *NBT:secA5-BFP* (Mazaheri et al., 2014), and immunohistochemistry against cleaved Caspase-3, a key enzyme in the apoptotic caspase cascade (Wyllie, 1997). Both markers of apoptosis exhibited a peak of positive cells at 6 hpi (Fig. 4.6), whereas levels were similar to baseline at 0 hpi and 24 hpi, recapitulating data from *H2A:GFP* transgenic larvae.

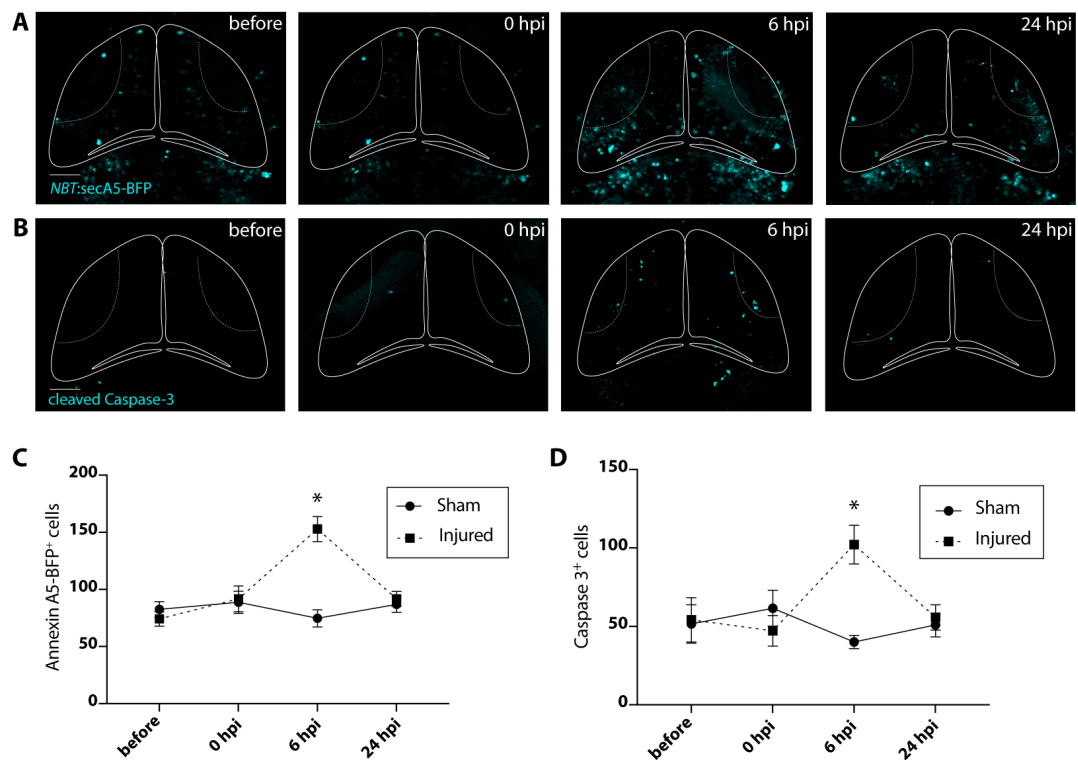


Figure 4.6: Occurrence of apoptosis following brain injury is confirmed in an apoptosis reporter line and through Caspase-3 immunostaining. (A) Apoptotic cell death takes place in the hours after mechanical injury as shown by an increase in the number of cells externalising phosphatidylserine. Scale bar, 50 μ m. (B) Immunostaining for cleaved Caspase-3 shows a delayed increase in apoptosis after injury. 50 μ m. (C) Quantification of Annexin 5⁺ cells. n 12 animals per experimental group. *, p < 0.05 in two-way ANOVA. (D) Quantification of cleaved Caspase-3⁺ cells. n 6 animals per experimental group. *, p < 0.05 in two-way ANOVA.

The data presented so far suggested that both (early) necrosis and (delayed) apoptosis occur in response to mechanical injury. However, it did not provide any insight on whether cells were dying due to primary cell death (direct mechanical disruption) or secondary cell death (indirect biochemical changes). I hypothesised that PI⁺ cells appearing at the injury site promptly died due to direct structural damage; to test this, we followed individual neurons after injury. We generated a construct to express a membrane-tagged TdTomato under the neuronal promoter

elav3. Injection of the *elav3:memTdTomato* construct into one cell stage *H2A:GFP* embryos resulted in mosaic expression at 4 dpf. We followed both cells at the prospective injury site as well as in the contralateral hemisphere, and identified whether they were structurally damaged by the injury. We observed direct structural damage at 0 hpi, and subsequent removal until 6 hpi, in 28 neurons residing at the injury site (Fig. 4.7 A, B; n = 15 animals). This finding suggested that these cells die through primary cell death.

Conversely, the delayed appearance of pyknotic nuclei (and other markers of apoptosis) (Fig. 4.4, Fig. 4.6) raised the question whether these cells were structurally injured, but not enough to kill them immediately, and underwent delayed primary cell death; or whether they escaped mechanical damage and were killed by an indirect mechanism such as excitotoxicity or oxidative stress, which would be considered secondary cell death. We followed 56 neurons in 15 animals at least 50 μm from the injury site (both ipsi- and contra-lateral), and found that they did not exhibit structural damage. Most of these cells survive until 6 hpi (Fig. 4.7 C, D), but we detected cell death at 6 hpi in a small proportion (Fig. 4.7 E, F; n = 5 cells in 15 animals), characterised by nuclear pyknosis and disrupted dendritic morphology. The absence of structural damage at 0 hpi followed by cell death at 6 hpi strongly suggested that these cells underwent secondary cell death.

Finally, as I was predominantly interested in neuronal protection and survival, I aimed to confirm that the cells dying from the injury were, as in mammalian models of brain injury, predominantly neurons. To elucidate whether this was the case and to further characterise my injury model, I cross-bred the transgenic line *NBT:secA5-BFP* labelling apoptotic cells using neuronal reporter lines *NBT:dsRed* (Fig. 4.8 A-C) or *elav3:kaede* (Fig. 4.8 D-F). I imaged the same animals before injury and at 6 hpi, and quantified double positive cells (Annexin 5-BFP⁺/dsRed⁺, or Annexin 5-BFP⁺/kaede⁺). This revealed that most cells both before and at 6 hpi were double positive for Annexin 5-BFP and dsRed or Annexin 5-BFP and kaede, although the total number of double positive increased following injury (Fig. 4.8). This data confirmed that, as in mammalian models, the majority of dying cells in the zebrafish brain following injury were neurons.

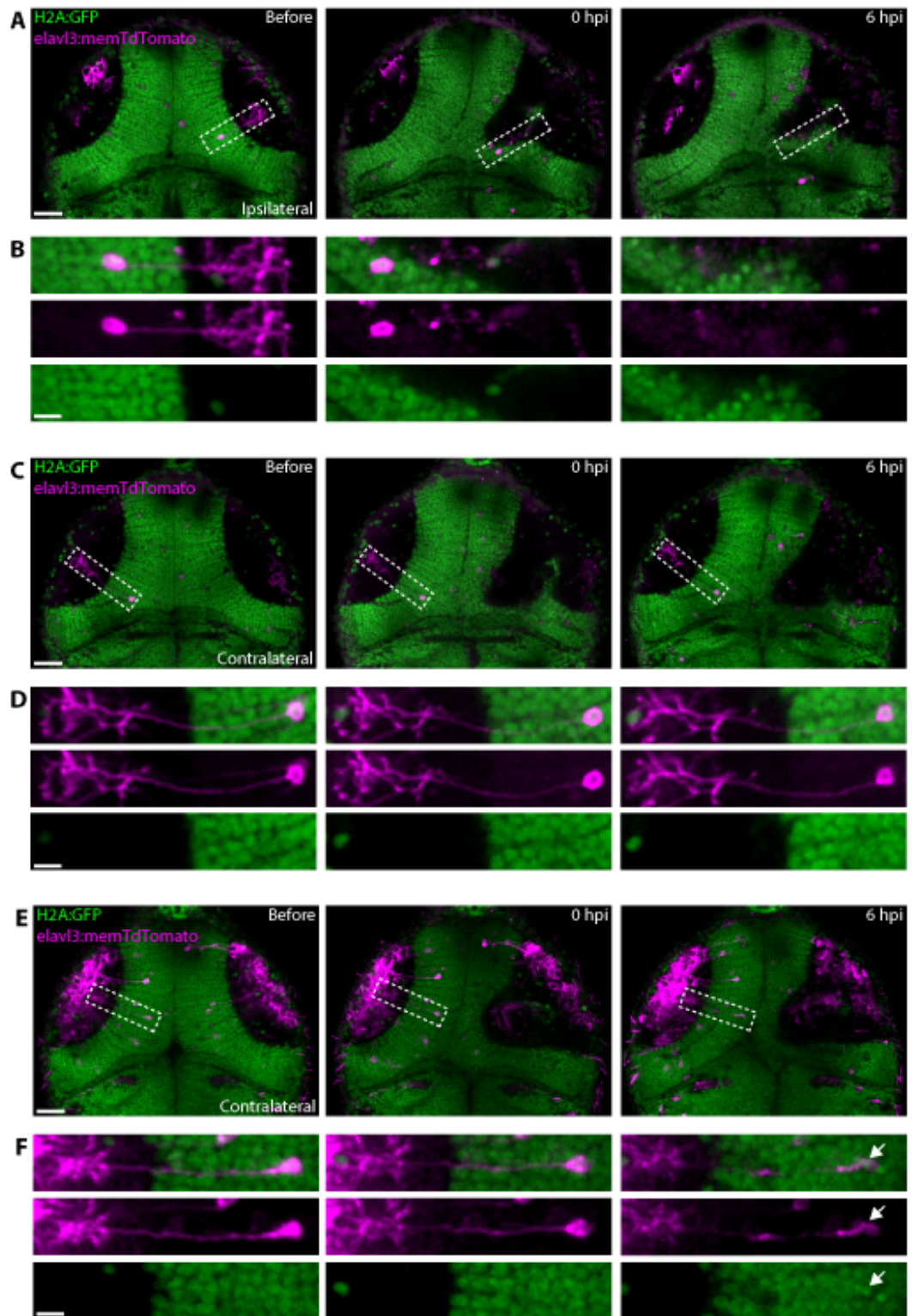


Figure 4.7: **In vivo imaging of individual tectal neurons shows that both primary and secondary cell death occur after brain injury.** (A, C, E) Confocal images of the optic tectum of *H2A:GFP* transgenic animals. A small number of tectal neurons in the ipsilateral (A) or contralateral (C, E) hemisphere were mosaically labelled through injection of *elav3:memTdTomato* plasmid DNA. Scale bars, 50 μm (B, D, F) Close-up of neurons indicated in (A), (C) and (E). White arrow indicates pyknotic nucleus. Scale bars, 10 μm .

Data obtained and analysed by Dr. Leah Herrgen.

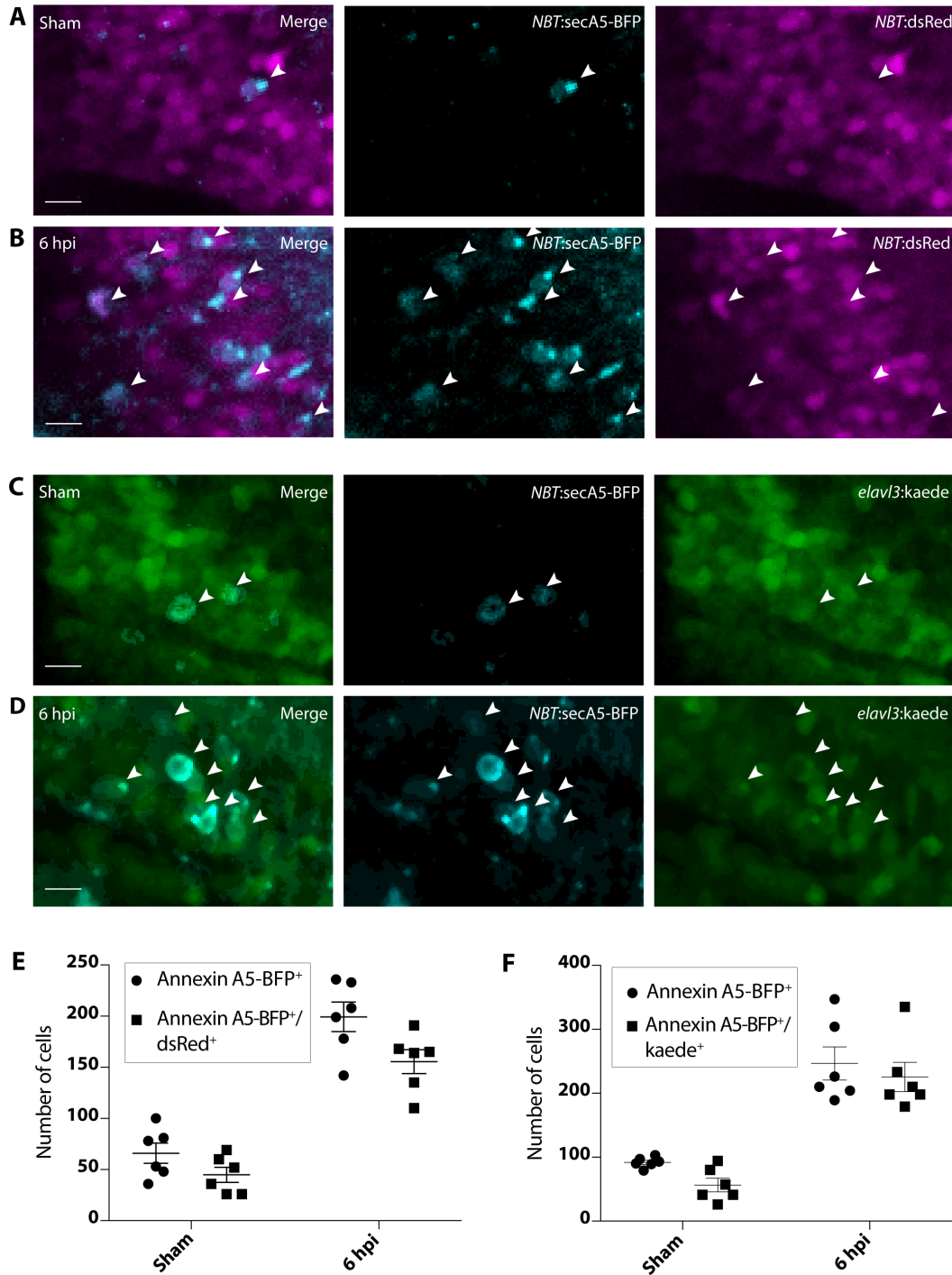


Figure 4.8: **The majority of apoptotic cells are neurons.** (A, B) Most apoptotic cells in control animals (A) and in injured animals at 6 hpi (B) colocalise with a neuronal marker NBT (arrowheads). Scale bars, 10 μ m. (C, D) Most apoptotic cells in control animals (C) and in injured animals at 6 hpi (D) colocalise with a neuronal marker *elavl3* (arrowheads). Scale bars, 10 μ m. (E) Quantification of Annexin 5-BFP⁺ and dsRed⁺/Annexin 5-BFP⁺ cells in control and injured animals. $n = 6$ animals per experimental group. (F) Quantification of Annexin 5⁺ and kaede⁺/Annexin 5⁺ cells in control and injured animals. $n = 6$ animals per experimental group.

4.4 Discussion

Secondary cell death is a phenomenon following CNS insults such as TBI widely studied in experimental rodent models. Although some zebrafish models of CNS injuries have investigated cell death (Morsch et al., 2015; Ohnmacht et al., 2016; Skaggs et al., 2014; Tsarouchas et al., 2018; Zupanc et al., 1998), no study enquired whether cells die through primary or secondary cell death. The data presented in this chapter are therefore, to my knowledge, the first to describe the cell death dynamics, including distinction between primary and secondary cell death, following a mechanical brain injury in larval zebrafish *in vivo*.

Using *in vivo* imaging of zebrafish larvae with several markers of necrotic and apoptotic cell death allowed me to monitor and quantify cell death in real-time, and to distinguish between primary necrotic and secondary apoptotic cell death. To thoroughly investigate necrosis and apoptosis following brain injury, I used four different markers: propidium iodide uptake (necrosis/secondary necrosis), nuclear pyknosis, phosphatidyl serine exposure and activation of Caspase-3 via cleavage (all apoptosis). With respect to the apoptosis markers, the processes that are being detected occur during different phases of apoptotic cell death and therefore do not share the same absolute numbers of apoptotic cells. Apoptosis usually is initiated by effector caspases, frequently caspase-3, which can activate multiple different downstream processes to orchestrate cell suicide (Porter and Jänicke, 1999; Wyllie, 1997). Caspase-3 is therefore one of the earliest markers of a subset of cells undergoing apoptosis, which I was able to detect via immunostaining (Fig. 4.6 A, C). There is also a parallel, caspase-independent apoptosis-inducing pathway by release of apoptosis-inducing factor (AIF) following mitochondrial membrane potential depolarisation (Susin et al., 1999), which identifies a subset of apoptotic cells that would not be labelled by Caspase-3. Zebrafish are known to express homologues of AIF, and although I did not specifically investigate this mode of cell death following my injury assay, it is possible that cells undergoing apoptosis via the AIF pathway were present following injury in larval zebrafish. Downstream of Caspase-3, cells rapidly externalise phosphatidyl serine (PS) as an '*eat me*' signal for phagocytes in an energy-dependent manner (Balasubramanian and Schroit, 2003; Segawa and Nagata, 2015), which I was able to visualise using a BFP-tagged Annexin 5 (Fig. 4.6 B, D). Later in the process of apoptosis, both caspase-dependent and -independent, chromatin is tightly packed and nuclear pyknosis is observed (Oberhammer et al., 1994; Toné et al., 2007), which I could trace using a GFP-tagged histone variant to assess nuclear morphology (Fig. 4.4).

The fact that these markers label cells during different stages of apoptosis explains the differences in absolute (baseline) numbers. There is a high amount of developmental apoptosis in the 4 dpf zebrafish brain. As cleaved Caspase-3 and Annexin 5 label early apoptotic cells, cells positive for either of these have not had a chance yet to be phagocytosed, resulting in a higher steady-state

number (Fig. 4.6). There is, however, a low baseline level of cells with condensed nuclei or PI⁺ cells, as these cells are in the late stages of apoptosis (or necrotic) and have usually already been removed and digested by microglia before they reach this stage.

Why is it of interest to distinguish between different modes of cell death? Cells undergoing necrotic or apoptotic cell death create different milieus for their surrounding cells, and elicit different immune responses upon phagocytic clearance (Green et al., 2016). Necrosis is cell death mediated by cell membrane rupture, energy failure, or other ways that noxious stimuli - such as mechanical injury - can damage cells. Intracellular contents are passively released and spill over in the environment (Peter et al., 2010), potentially exacerbating cell death in the surroundings. In terms of phagocytic clearance, this poses a challenge as not only the necrotic cell corpses have to be cleared, but also the toxic intracellular contents that have been spilled (Peter et al., 2010). Finally, necrosis generally leads to an inflammatory response, for example through release of chromatin protein HMGB1 (Scaffidi et al., 2002), and the release of pro-inflammatory cytokines by phagocytes.

Conversely, apoptotic cell death results in an anti-inflammatory environment for the surviving neighbouring cells. To explain why apoptosis and necrosis are so different, one can take a look at development: apoptosis is a crucial cellular process during development and morphogenesis (reviewed by Meier et al. (2000)), and occurs frequently. Even in adulthood, it is estimated that one million adult human cells undergo apoptosis every second (Ravichandran, 2010). Yet, it is rare to observe an apoptotic cell in healthy tissue (Hochreiter-Hufford and Ravichandran, 2013), which demonstrates the efficiency of the phagocytic system in detecting and clearing apoptotic cells. However, it also highlights the fact that the apoptotic cell response is immunologically silent, otherwise chronic inflammation would reign in our bodies. Apoptotic cells release a number of '*find me*' signals to attract phagocytes and organise their own clearance, such as the nucleotides ATP and UTP (Elliott et al., 2009) and certain lipids (Gude et al., 2008; Lauber et al., 2003), amongst other factors (reviewed by Ravichandran (2011)). The advertisement of cell death may occur even before apoptosis is completed (Hoepfner et al., 2001), and the release of ATP to alert immune cells during apoptosis was found to be energy-dependent (Elliott et al., 2009), illustrating that it cannot occur once the cell is fully dead. A distinction between necrotic and apoptotic cell death appears to be the amount of '*find me*' signals released: while in apoptotic cells only roughly 0.01% of ATP are released in an energy-dependent manner (Elliott et al., 2009), necrotic cells release large amounts of it (as mentioned above, intracellular contents are passively spilled due to membrane disruption). While apoptosis is carefully orchestrated and involves a series of cellular cascades aimed at neatly packing intracellular substances into apoptotic bodies, necrosis was generally seen as a descent into chaos although it is now appreciated that organised forms of necrosis do exist (Bournazou et al., 2009; Festjens et al., 2006; Golstein and Kroemer, 2007). Furthermore, in contrast to engulfment of necrotic material which induces inflammation, engulfment of apoptotic material (also called

efferoctosis) dampens the immune response (Elliott and Ravichandran, 2010; Henson, 2005), and was shown to suppress the release of pro-inflammatory cytokines by monocytes *in vitro* (Kim et al., 2004a; Voll et al., 1997). Finally, apoptotic cells can also modulate the phagocyte recruitment via release of 'keep out' factors: apoptotic cells were found to release lactoferrin, which repels neutrophils from an injury site (Bournazou et al., 2009).

Mechanical forces induce a wave of primary necrotic cell death in many injuries including TBI (Lenzlinger et al., 2001; Liou et al., 2003; Lou et al., 1998; Stoica and Faden, 2010). Consistent with previous findings, I observed the occurrence of primary necrotic cell death in my zebrafish model of mechanical brain injury (Fig. 4.2, Fig. 4.7). To my surprise, the majority of these necrotic PI⁺ cells disappeared within one hour as observed by repeated *in vivo* imaging in the hours following injury (Fig. 4.2), although there was a slight increase of PI⁺ cells at 6 hpi. This secondary peak in PI⁺ cells was most likely linked to the increased presence of late apoptotic cells, which is supported by the fact that PI⁺ cells at 6 hpi often have pyknotic nuclei and hence a significantly decreased diameter compared to healthy surrounding nuclei (Fig. 4.3).

In addition to PI⁺ late apoptotic cells, I also observed PI⁺ cells with microglial and radial glial morphology (Fig. 4.5). These cells did not appear to be necrotic and were present in the tectum for up to 48 hpi during repeated live imaging, arguing against the fact that they were undergoing cell death. It had previously been shown that CNS injury can lead to large pore formation in glial cells following ATP-dependent stimulation of P2X receptors (James and Butt, 2002), and these P2X receptors can allow diffusion of molecules of up to 900 Da (Steinberg et al., 1987; Virginio et al., 1999; Yan et al., 2008). PI has a molecular weight of 668 Da, therefore could potentially enter cells via P2X-dependent pores. To investigate whether pore formation occurred in radial glia following injury, I applied iso-PPADS, a P2X receptor subtype specific inhibitor. This treatment completely abolished PI uptake in radial glia (Fig. 4.5), suggesting the formation of a P2X receptor-dependent large pore following brain injury. Previous research has shown that P2X receptors are involved in a variety of pathways: inducing cell death or proliferation (Adinolfi et al., 2005), including proliferation of neural progenitors (Pearson et al., 2005), or driving inflammation in a variety of cells, including glial cells (Albalawi et al., 2017; Monif et al., 2009). Whether any of these occur in the larval zebrafish remains to be elucidated.

Necrosis and apoptosis can modulate repair mechanisms by either enhancing or suppressing inflammation, therefore the decision of a cell whether to undergo necrosis or apoptosis may be a crucial factor for the functional outcome following brain injuries. Zupanc et al. (1998) and Hui et al. (2010) showed that apoptosis is the predominant mode of cell death in zebrafish following brain or spinal cord injury, respectively. Conversely, my data reveal the occurrence of both necrotic and apoptotic cell death. Importantly, these occur as distinct waves, and primary necrotic cell

death is elicited by structural damage and PI⁺ cells are only found at the injury site (Fig. 4.2, Fig. 4.7), while secondary apoptotic cell death is elicited by indirect mechanisms and occurs both at the injury site and remotely (Fig. 4.4, Fig. 4.7). In mammals, necrotic cell death is observed as early as 10 minutes following experimental TBI in rodents (Cortez et al., 1989; Dietrich et al., 1994b; Hicks et al., 1996; Sutton et al., 1993), and is the predominant mode of cell death during acute TBI in humans (Graham et al., 1989). However, unlike in zebrafish, where primary necrotic cells are only found at the injury site and are furthermore rapidly removed (Fig. 4.2), necrosis after TBI in mammals is found in regions distant from the original injury site and can be detected for several weeks following injury (Cortez et al., 1989; Sato et al., 2001; Zhou et al., 2012). Similarly, although neuronal apoptosis is initiated early after injury - with first cells being detected around 12 to 72 hours post injury in mammalian models (Rink et al., 1995) -, and peaks around 24 hours in mammalian models (Conti et al., 1998) or 25 to 48 hours human patients (Smith et al., 2000), apoptotic cells persist for weeks to months in the brain (Clark et al., 1999; Williams et al., 2001). This suggests that while zebrafish recapitulate typical characteristics of primary and secondary cell death detected in mammals, they are able to limit both necrotic and apoptotic cell death, and can return to baseline numbers of dead cells in the brain rapidly. Since clearance of debris (including corpses of dead cells) is a crucial step for the further repair process (Neumann et al., 2009), the rapid clearance of both primary and secondary cell death may explain enhanced regenerative success of zebrafish compared to mammals. Swift removal of dead cells could potentially be fast-tracked by transcription-independent mechanisms (Kotwal et al., 2015); in the next chapters, I will therefore investigate the early reactions to injury, including transcription-independent mechanisms, such as calcium waves, and microglial responses, to investigate how a rapid clearance of dead cells is achieved in the zebrafish.

To summarise, the data presented in this chapter demonstrate that zebrafish experience two waves of neuronal cell death following mechanical brain injury, and exhibit the same markers of necrotic and apoptotic cell death as previously found in experimental models of brain injury and TBI patients. Although primary necrotic cells following mechanical brain injury are cleared within an hour, I could still observe the occurrence of secondary cell death. The mechanisms underlying secondary cell death are only incompletely understood, but could include the release of toxic intracellular substances by primary necrotic cells and a progressive network dysfunction resulting in excessive synaptic glutamate release, amongst other pathological processes. I observed secondary apoptotic cell death as early as 1 hpi, with a progressive increase until 6 hpi. As previously observed in other experimental models of TBI and TBI patients (Bayly et al., 2006; Liou et al., 2003; Mukhin et al., 1998; Stoica and Faden, 2010), secondary cell death occurs both at the injury site and at a distance from the original injury site (Fig. 4.4, Fig. 4.7), providing another layer of evidence of the suitability of the larval zebrafish model to investigate the cellular and molecular processes following mechanical brain injury.

Although zebrafish appear to be much more efficient at removing both primary and secondary dead cells than mammals following CNS injury, the fact that they replicated the occurrence of secondary cell death encouraged me to use the larval zebrafish for the investigation of potential neuroprotective strategies decreasing or inhibiting secondary cell death. I was interested in two particular strands of investigation:

- immediate, transcription-independent signalling mechanisms, and their role in suppression of excessive cell death, immune cell recruitment, and neurogenesis
- the role of microglia/macrophage functions, such as phagocytosis and secretion of cytokines and other factors, in secondary cell death

In my upcoming chapters, I will therefore focus on these two topics.

Chapter 5

Description of calcium signalling following mechanical brain injury in larval zebrafish

5.1 Introduction

In any organism, uni- or multicellular, rapid detection of wounds is crucial for survival. Early detection of wounds via transcription-independent damage signals such as calcium, reactive oxygen species, or ATP is often not only a key part of initiating the wound repair response, but can be a deciding step for the later regenerative success (Love et al., 2013; Yoo et al., 2012). One of the most prominent and conserved damage signals in nature, ranging from plants to mammals, is calcium signalling. Calcium is a key messenger molecule for conveying a multitude of intra- and intercellular signals, including wounding. Calcium waves are a conserved wounding signal and have been described in a variety of different organisms, including *Drosophila melanogaster* (Antunes et al., 2013), *Xenopus laevis* (Clark et al., 2009; Herrgen et al., 2014), *Caenorhabditis elegans* (Xu and Chisholm, 2011), cow (cell culture) (Chifflet et al., 2012; Klepeis et al., 2001), human (cell culture) (Shabir and Southgate, 2008), and zebrafish (Sieger et al., 2012; Yoo et al., 2012). Calcium waves occur within seconds from injury. They inform surrounding cells about the injury and can fast-track wound healing by initiating repair mechanisms such as wound closure (Antunes et al., 2013; Xu and Chisholm, 2011), expulsion of dead cells (Herrgen et al., 2014), or rapid leukocyte recruitment (Sieger et al., 2012; Razzell et al., 2013). Therefore, calcium waves are a critical first step of the wound healing process. I had three distinct hypotheses regarding the effects of calcium waves following injury in the larval zebrafish, and how they could confer neuroprotection or contribute to repair:

1. PI⁺ primary necrotic cells following mechanical injury to the larval zebrafish brain are largely

cleared away within one to two hours post injury (Fig. 4.2). Sieger et al. (2012) had previously shown that calcium waves recruit microglia following laser injury of the larval zebrafish optic tectum. Therefore, I hypothesised that mechanical injury elicits calcium waves that recruit microglia. Microglia then aid in the repair process by phagocytosis of necrotic cells, and may therefore play a neuroprotective role by preventing spillage of toxic intracellular substances by necrotic cells.

2. Justet et al. (2016) had shown previously that calcium waves can suppress excessive apoptosis following injury, which suggested early calcium waves following an injury could therefore confer neuroprotection; I aimed to assess whether this was the case by inhibiting early calcium waves and assessing the extent of cell death at later timepoints (particularly 6 hpi, as this was the peak of secondary cell death in my injury assay).
3. Finally, calcium waves have been described as a signal preceding neurogenesis in neural progenitors (Weissman et al., 2004); therefore, they could instruct regenerative neurogenesis in response to injury.

I aimed to investigate these hypotheses using the genetically encoded reporter GCaMP6f in the *β -actin:GCaMP6f* transgenic line. First, I intended to describe calcium waves occurring after mechanical injury. For interference with calcium waves, I aimed to identify upstream mechanisms by injection of pharmacological inhibitors of mechanisms previously shown to elicit calcium waves (ATP, glutamate, mechanosensitive channels, gap junctions) and subsequent assessment of calcium waves (Antunes et al., 2013; Herrgen et al., 2014; Razzell et al., 2013; Sieger et al., 2012). As a readout of the downstream mechanisms, I aimed to assess microglial recruitment to the injury using the transgenic line *mpeg1:GFP*, quantify pyknotic nuclei during the peak of secondary cell death at 6 hpi in *H2A:GFP* larvae, and investigate proliferation of radial glia in response to injury following inhibition of early calcium waves.

In the context of brain injury, sustained calcium signalling has furthermore been linked to glutamate excitotoxicity and neuronal death (Choi, 1985, 1988; Lipton and Rosenberg, 1994). Therefore, in addition to investigating calcium waves within seconds of injury, I aimed to study calcium signalling dynamics in the minutes to hours following injury, and how this relates to cell death. Therefore, I performed time-lapse imaging of the *β -actin:GCaMP6f* reporter line, and aimed to interfere with NMDA receptors, which have previously been implicated in excitotoxicity and secondary cell death (Faden et al., 1989), to assess the effect on NMDA receptor mediated calcium signalling and death following injury.

5.2 Early calcium signalling

5.2.1 Description of calcium waves immediately following injury

I first assessed whether calcium waves occurred in the first seconds after mechanical brain injury of the larval zebrafish. I induced a mechanical injury in transgenic *β-actin:GCaMP6f* larvae on stage of a confocal microscope while acquiring images every 2s. Injuring of the brain lead to a rapid increase of GCaMP6f fluorescence (5.1 B, Movie S2), indicating an increase of intracellular calcium occurred. Ensuring that calcium waves were specific to neuronal injury (which results in presence of PI⁺) and could not be elicited by compression of the brain which did not cause neuronal necrosis (data not shown), I performed the same assay without eliciting neuronal cell death (i.e., compression of one hemisphere instead of penetration of the tissue). Compression of one tectal hemisphere for 5s did not cause an increase in GCaMP6f fluorescence in the brain (5.1 A, Movie S1, 5/5 animals) while eliciting calcium waves in the skin (white arrowheads, Fig. 5.1 A). This was consistent with cell death-related injury-induced signalling eliciting the observed calcium waves in the brain.

Next, I assessed the spatial dynamics of calcium waves. Directly surrounding the initial injury site, I observed a strong and rapid increase of GCaMP6f fluorescence in cell bodies immediately surrounding the injury site (pointed out by magenta circle in 5.1 B, 6s). The predominant cell type in the optic tectum are neurons (Scott and Baier, 2009), therefore I hypothesised that these cells were neurons. I also observed a distinct pattern of activation in cells lining the ventricle and spreading throughout most of these cells in the optic tectum (arrows in 5.1 B, 20s). This activation pattern resembled progenitors lining the ventricle of the tectum, so I hypothesised these cells could be radial glia. To confirm this hypothesis, I cross-bred the calcium reporter line with animals expressing fluorescent reporters in neurons (*NBT:dsRed*) or radial glia (*her4.3:mCherry*) and repeated the experiment. Using double transgenic larvae, I was able to confirm that these initial waves indeed occurred in cells expressing neuronal and radial glial markers (Fig. 5.2). Interestingly, the calcium wave in radial glia appeared with a slight delay - four seconds on average - compared to the neuronal wave, suggesting potentially different mechanisms of calcium release underlying these two waves.

I had so far described two distinct immediate calcium waves following injury:

- Neuronal wave surrounding the immediate injury site
- Radial glial wave spanning the progenitors both close and remote to the injury site

It was unclear what elicited these early calcium waves, and whether or how these waves could play a role in instructing repair mechanisms. Therefore, I next aimed to dissect the pharmacology of how these calcium waves were elicited, in order to later potentially perturb them. For this purpose, I next performed quantitative analysis of wave areas and intensities for both neuronal and radial

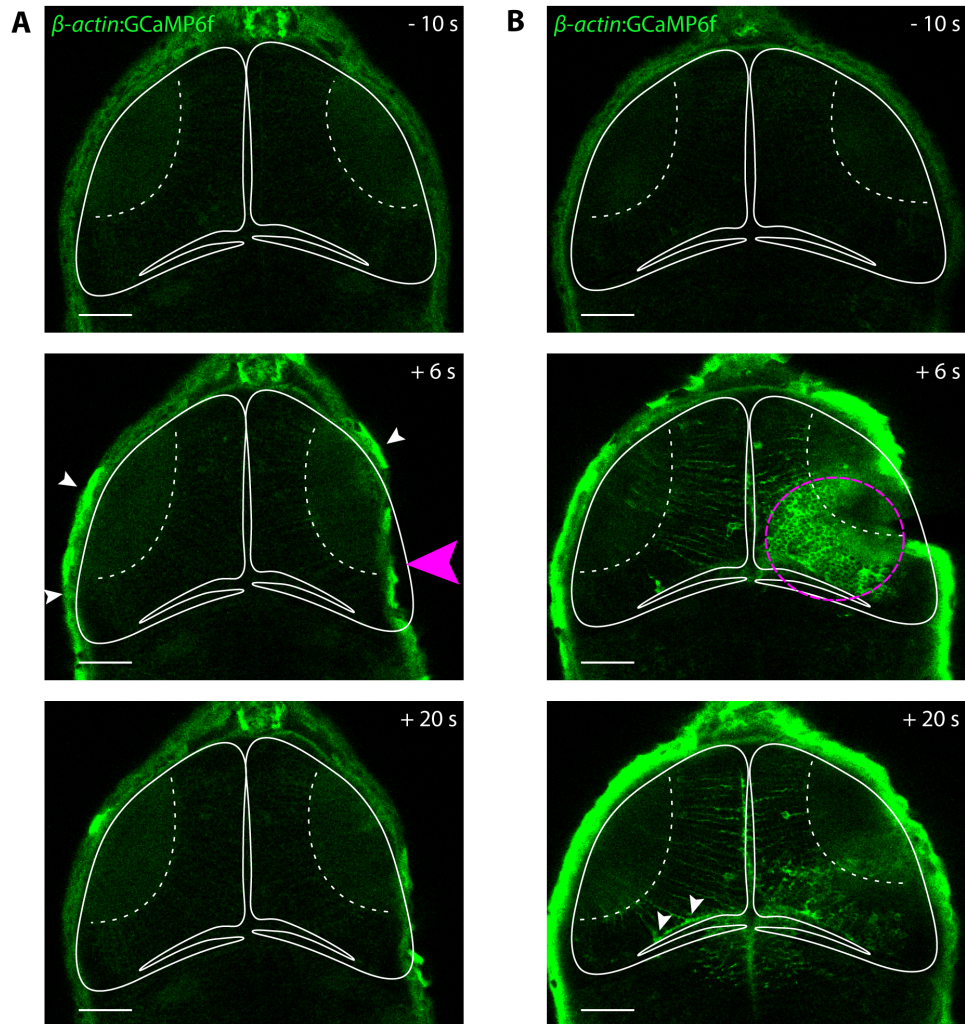


Figure 5.1: **Injury, but not compression of the brain leads to long-range calcium waves.** (A, B) Representative images taken -10 s, 6 s, or 20 s after compression (A) or mechanical injury (B) of the optic tectum in β -actin:GCaMP6f transgenic larvae. Magenta arrowhead in (A) shows site of compression. Arrowheads in (A) ($+6$ s) show sites of calcium activation in the skin. Magenta circle in (B) highlights cell body activation surrounding injury site ($+6$ s), arrowheads show potential activation of radial glial cells ($+20$ s).

■ Figures correspond to supplementary **movies S1** (compression, A), and **S2** (injury, B).

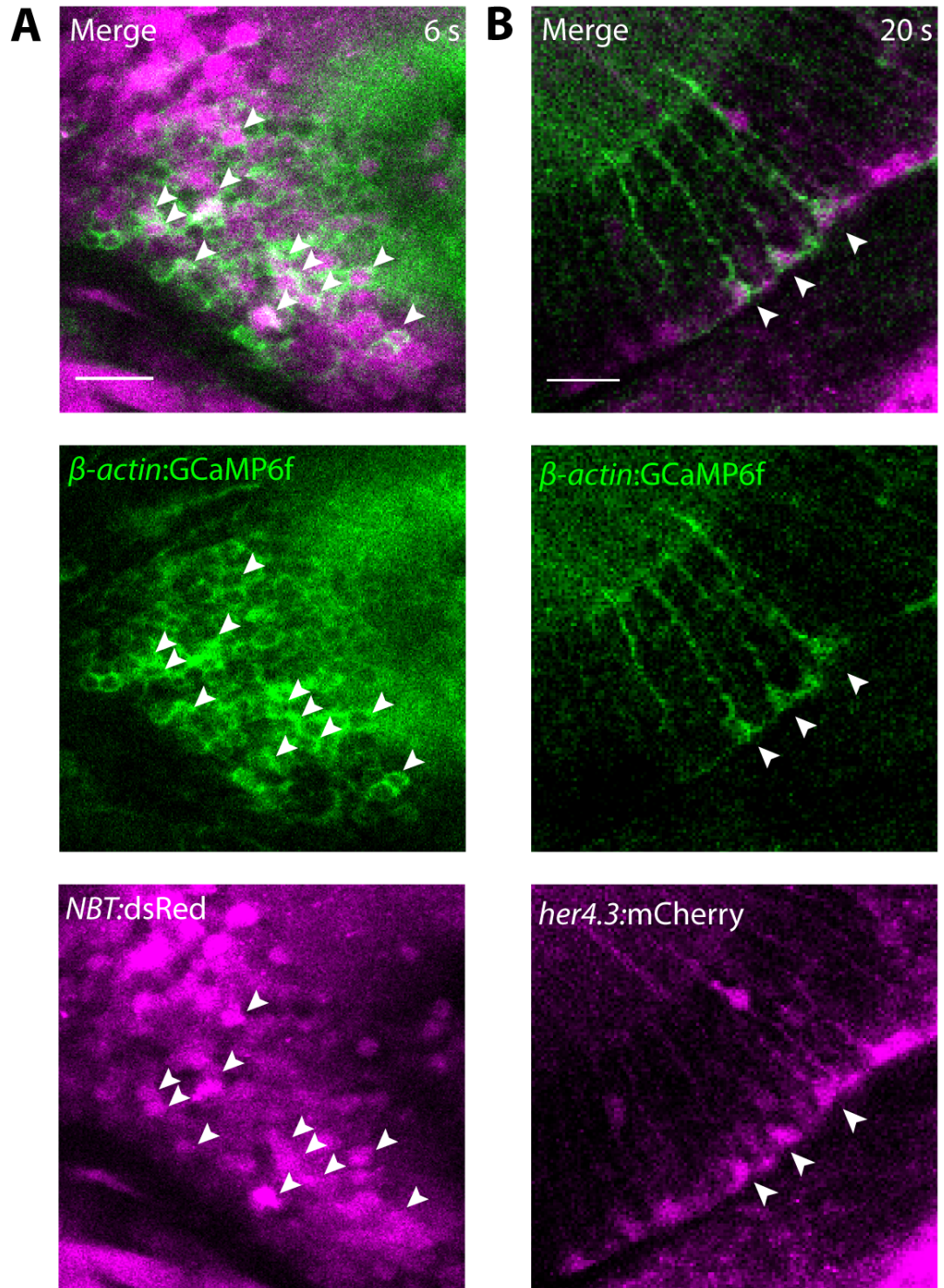


Figure 5.2: **Calcium waves occur in cells expressing neuronal and radial glial markers.** Crossbreeding of β -actin:GCaMP6s animals with neuronal and radial glial marker animals revealed that calcium waves occur in NBT⁺ cells expressing dsRed (A, arrowheads), and her4.3⁺ cells expressing mCherry lining the ventricle (B, arrowheads). These waves are spatially and temporally overlapping, but radial glial waves occur slightly later than neuronal waves. Scale bar, 20 μ m.

glial waves using a MATLAB script (modified version of script used by Herrgen et al. (2014)) in combination with pharmacological perturbation of signalling. This enabled me to use the calcium wave as a readout of which receptors are activated following injury and result in calcium waves.

5.2.2 Signalling leading to early calcium waves following brain injury

Previous studies in *Xenopus laevis* and zebrafish identified ATP and *L*-glutamate among the earliest factors released following brain injuries, and were both shown to elicit calcium waves (Herrgen et al., 2014; Sieger et al., 2012). Mechanosensitive TRPM3 channels and gap junctions had been shown to mediate either initiation or propagation of calcium waves in response to injury (Antunes et al., 2013; Herrgen et al., 2014; Liu et al., 2010; Weissman et al., 2004). To identify which of these pathways are active following mechanical brain injury in larval zebrafish, I injected pharmacological inhibitors of NMDA receptors, AMPA receptors, P2 receptors, TRPM3 receptors, and gap junctions into the ventricle of the fish 10 minutes before injury and then quantified the area and intensity of neuronal and radial glial calcium wave, as well as the velocity of the calcium wave.

NMDA receptors

After injection of the NMDA receptor mix MK801 and AP5 (previously used by Sieger et al. (2012)), the neuronal wave was undetectable (Fig. 5.3 B, I, Movie S3), and the radial glial wave area was slightly reduced (Fig. 5.3 B, J, Movie S3; $n = 6$ animals; *, $p = 0.0363$ in Student's *t* test). The radial glial wave intensity remained unchanged. This data suggests a crucial role for the NMDA receptor signalling in the initiation of the early neuronal wave surrounding the injury site, and a minor role in the propagation of the radial glia wave. The velocity of the overall calcium wave remained unchanged.

AMPA receptors

Injection of DNQX, an AMPA receptor inhibitor, resulted in a 40% reduction of the neuronal wave area and intensity (Fig. 5.3 C, I, J, Movie S3; $n = 14$ animals; **, $p = 0.0035$ in Mann-Whitney, and 0.0065 in Student's *t* test, respectively). All other factors were not significantly altered (ns for radial glia wave intensity, area, and wave velocity). This data suggested that AMPA receptors play a role in neuronal wave propagation.

ATP signalling

To investigate the role of P2 receptor-mediated ATP signalling on the initiation or propagation of calcium waves following injury, I injected PPADS (pan-P2 receptor inhibitor) (Charlton et al., 1996; Connolly, 1995) and iso-PPADS (P2X receptor subtype inhibitor) (Connolly, 1995) in the ventricle prior to injury. I was presented with the opposite effect of glutamate receptor inhibitors: following ventricular injection of either PPADS or iso-PPADS, the radial glial calcium wave was absent (Fig.

5.3 C, D, K, L, Movie S3; $n = 6$ or 5 animals, respectively; **, $p \leq 0.01$ in Kruskal-Wallis-Test with Dunn's Post-Test). Treatment with PPADS but not iso-PPADS led to a significant decrease of the neuronal wave intensity compared to vehicle (Fig. 5.3 C, I; **, $p = 0.0038$ in One-Way ANOVA with Bonferroni Post-Test), however, neuronal wave area or wave velocity remained unchanged (Fig. 5.3 J, M). This suggested that P2 receptors were crucial for radial glia wave initiation. P2Y receptors may contribute to calcium release in neurons following injury.

Stretch-activated calcium channels

Injection of Ononetin, a TRPM3 antagonist, into the ventricle prior to injury caused a significant decrease of the neuronal wave intensity compared to vehicle (36%; Fig. 5.3 F, I, Movie S3; $n = 11$ animals; **, $p = 0.0038$ in Student's t test). All other factors remained unchanged (Fig. 5.3 J-M). TRPM3 channels may therefore play a role in the neuronal calcium wave initiation or propagation.

Gap junctions

To decrease gap junction permeability, I used two different inhibitors: carbenoxolone (CBX) and flufenamic acid (FFA). Injection of CBX did not affect any parameters I measured compared to vehicle (Fig. 5.3 G, I-M, Movie S3; $n = 6$; all parameters ns compared to vehicle in Student's t test). Injection of FFA significantly decreased the area of the neuronal wave compared to vehicle (65% reduction; Fig. 5.3 H, J; **, $p = 0.001$ in Student's t test), while leaving other parameters unaffected (Fig. 5.3 J-M). This suggested a role for a subset of gap junctions in propagation of the neuronal calcium wave immediately after injury. Alternatively, this could be due to non-gap junction-mediated effects of FFA; although FFA is commonly used as a gap junction inhibitor (Harks et al., 2001; Herrgen et al., 2014; Srinivas and Spray, 2003), it can also modulate ATP release and a wide variety of other ion channels (Braet et al., 2003; Guinamard et al., 2013; Stout et al., 2002).

Activation of calcium signalling via injection of ATP and *L*-Glutamate

Using pharmacological inhibitors, I had shown that several signalling pathways played a role in eliciting calcium waves following injury, in particular glutamate and ATP. To confirm that these molecules are sufficient to induce calcium waves as the data in Fig. 5.3 suggested, I injected ATP and *L*-glutamate into the brain ventricle of β -*actin*:GCaMP6f larvae on the stage of a microscope while imaging at a temporal resolution of 2s (Fig. 5.4). Injection of vehicle (calcium-free Ringer's solution) did not cause a change in GCaMP6f fluorescence. ATP injection resulted an increase in calcium in radial glia close to the ventricle (6/6 animals). *L*-glutamate injection elicited calcium release mainly in neuronal cell bodies and axons in the neuropil (6/6 animals), but it cannot be excluded that also radial glia are amongst the cells that show calcium signalling upon glutamate. My data does not suggest so, however, as no cells in proximity of the ventricle were reactive. Injection of pregnenolone sulfate, a TRPM3 agonist, did not lead to any change in calcium signalling.

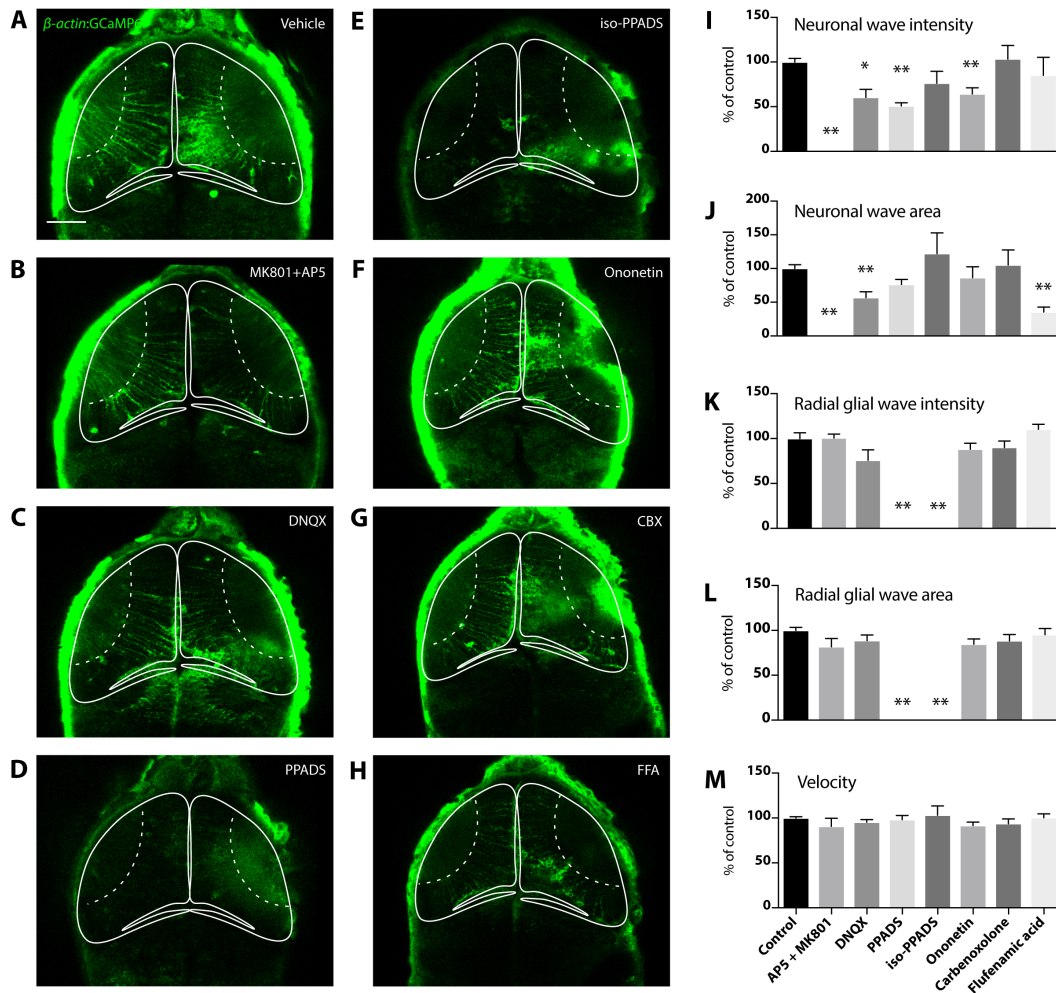


Figure 5.3: **Pharmacological inhibitors reveal a key role for NMDA receptors in the neuronal calcium wave in response to injury, while ATP receptors are crucial for the glial wave.** (A-H) Representative images for each treatment (Vehicle, MK801+AP5, DNQX, PPADS, iso-PPADS, Ononetin, CBX, and FFA) at 10s following injury. Scale bar, 50 μ m. (I) Quantification of neuronal wave intensity as percentage of vehicle-injected controls on the same day. (J) Quantification of neuronal wave area as percentage of vehicle-injected controls on the same day. (K) Quantification of radial glial wave intensity as percentage of vehicle-injected controls on the same day. (L) Quantification of radial glial wave area as percentage of vehicle-injected controls on the same day. (M) Quantification of calcium wave velocity as percentage of vehicle-injected controls on the same day. **, $p \leq 0.01$; *, $p \leq 0.05$ in Student's *t* Test. MK-801/AP5, $n = 6$; DNQX, $n = 14$; PPADS, $n = 6$; iso-PPADS, $n = 5$; Ononetin, $n = 11$; CBX, $n = 6$; FFA, $n = 6$.

Figure corresponds to supplementary movie S3.

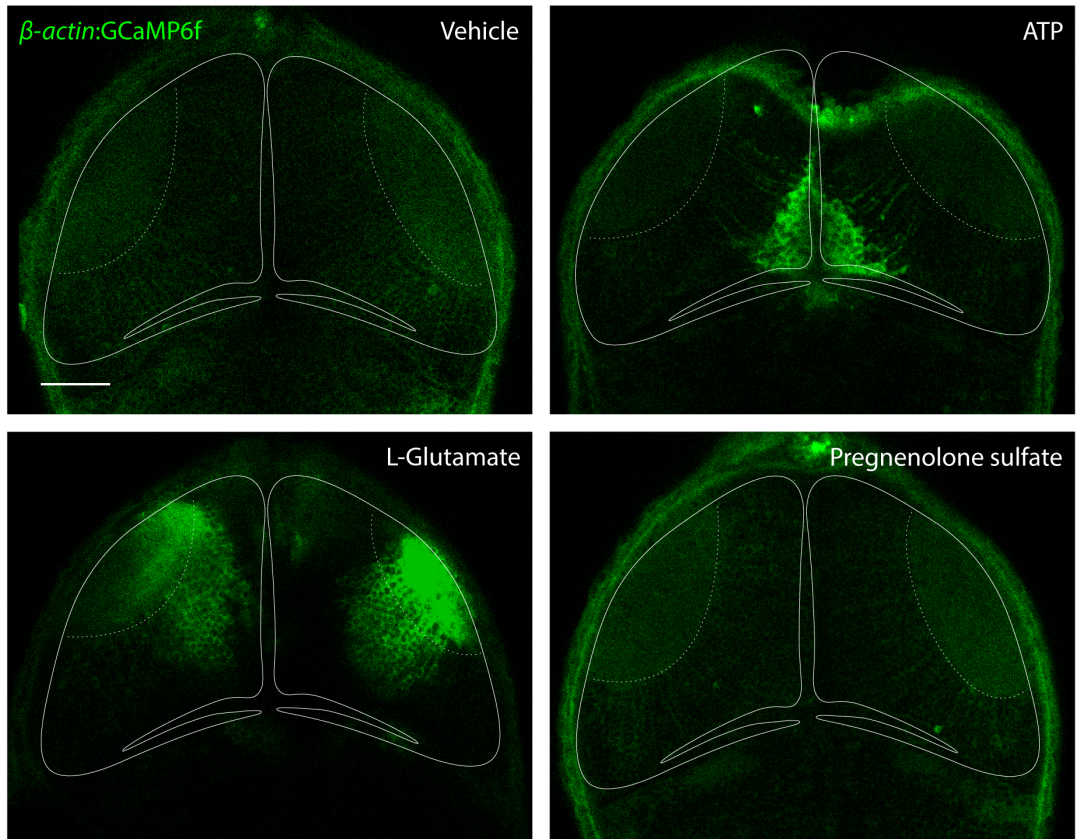


Figure 5.4: **Injection of ATP or Glutamate leads to calcium waves similar to observed after injury. Pregnenolone sulfate, an activator of TRPM3 channels, lead to no changes in calcium activity.** Images taken 6 s after injection of calcium-free Ringer solution (vehicle), 5 mM ATP, 10 mM L-Glutamate, 0.45 mM Pregnenolone Sulfate in β -actin:GCaMP6f larvae.

5.2.3 Downstream effects of early calcium signalling

Next, I aimed to elucidate the downstream effects of early calcium signalling. As Sieger et al. (2012) had previously shown that calcium waves can recruit microglia following laser injury in the zebrafish brain, I was interested in microglia recruitment. Furthermore, Justet et al. (2016) had shown that early calcium waves can inhibit excessive apoptosis following an injury, and I aimed to assess cell death at 6 hpi injury. I attempted to inhibit calcium waves using pharmacological inhibitors I had previously identified (Fig. 5.3), and I tested how long the inhibiting effects of MK801 + AP5 and PPADS lasted. To do so, I injected the drugs into the ventricle and performed injuries after varying amounts of time to see whether inhibition of the calcium waves subsided over time. Using this approach, I found that MK801 + AP5 inhibited a neuronal calcium wave for at least 1 hpi (Fig. 5.5 A), therefore suggesting that this treatment was not temporally specific enough for this purpose, although *n* numbers in this experiment were low. As preliminary experiments did not appear promising, I decided to abandon this potential strategy of inhibiting early calcium waves. Additionally, inhibition of NMDA receptors could result in neuronal survival or death potentially unrelated to early calcium waves (see Chapter 5.3). PPADS inhibited the radial glial wave significantly between 10 and 40 min (Fig. 5.5 B). However, blocking ATP receptors could result in downstream effects other than inhibition of the radial glial calcium wave following injury: in particular, microglia/macrophages have previously been shown to use ATP-P2 receptor signalling to as a chemotactic cue. Using *mpeg1*:GFP transgenic larvae labelling macrophage-lineage cells including macrophages and microglia cells with GFP, I found that using PPADS significantly decreased the number of *mpeg1*⁺ cells at the site of brain injury at 2 hpi, but it was unclear whether this was directly mediated by calcium waves, or by ATP receptors on microglia sensing damaged cells, or whether there was some cross-talk between the two signalling mechanisms. With the tools I had at hand, I was unable to tease these effects apart. However, I was able to confirm that PPADS treatment did not cause cell death of *mpeg1*:GFP⁺ cells, as the number was unaltered between control (vehicle) and PPADS-treated larvae (Fig. 5.5 D).

I then attempted to use the intracellular calcium chelator BAPTA-AM to inhibit both neuronal and glial early calcium signalling following injury. While BAPTA-AM injection resulted in a significant reduction of calcium waves following injury (Fig. 5.6 A), the low solubility of BAPTA-AM in water required that it was dissolved in Pluronic F-127 (20% solution in DMSO, referred to as Pluronic / DMSO), which led to alteration of microglia/macrophage morphology and number at 2 h post injection (Fig. 5.6 B), although this was not quantified. Furthermore, BAPTA-AM has been shown to cause delayed neuronal necrosis in cortical cultures (Wie et al., 2001). It was likely that injection of BAPTA-AM, as well as Pluronic / DMSO without BAPTA-AM, led to toxicity and I therefore decided not to follow up on this strategy.

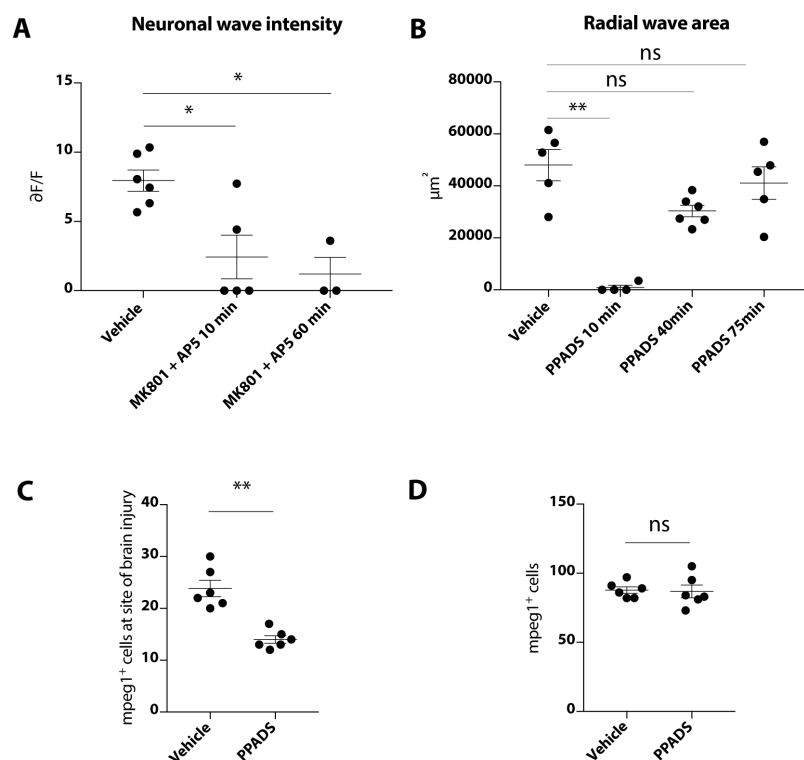


Figure 5.5: **MK801+AP5 inhibition of calcium signalling lasts for at least 1 h, while PPADS lasts for less than 40 min and reduces recruitment of mpeg1⁺ cells to the injury site.** (A) Treatment with MK801+AP5 (ventricular injection) significantly reduces neuronal wave intensity for at least 60 min following injury. *, $p \leq 0.05$ in Kruskal-Wallis Test with Dunn's post-test. $n \geq 3$ animals / group. (B) Treatment with PPADS (ventricular injection) inhibits radial glial wave area for less than 40 min. **, $p \leq 0.01$ in Kruskal-Wallis Test with Dunn's post-test. $n \geq 4$ animals / group. (C) Injection of PPADS leads to a significant reduction in the number of mpeg1⁺ cells at the site of brain injury at 2 hpi, but did not lead to a decrease in the overall number of mpeg1⁺ cells in tectum and skin (D) (i.e., does not cause microglia/macrophage cell death).

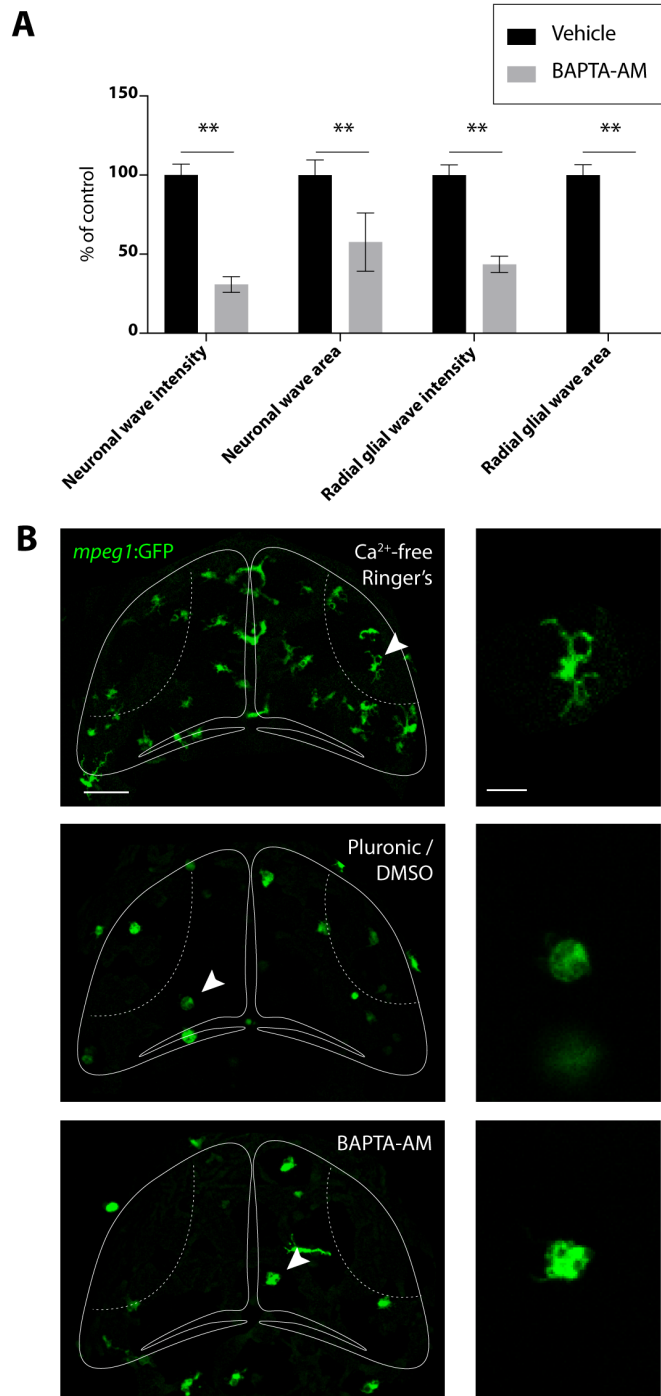


Figure 5.6: Ventricular injection of BAPTA-AM 2 h prior to injury leads to significant reduction of neuronal and glial waves but solvent causes microglia/macrophage changes. **(A)** Quantification of calcium wave parameters as % of control values. **, $p \leq 0.01$ in Student's *t*-Test or Mann-Whitney Test, respectively. $n \geq 6$ animals / group. **(B)** Representative images of *mpeg1:GFP* transgenic larvae 2 h post injection of Ca^{2+} -free Ringer's, Pluronic/DMSO, and BAPTA-AM (in Pluronic/DMSO), including zoom on *mpeg1*⁺ cells on the right hand side. BAPTA-AM appears to cause a reduction in number of *mpeg1*⁺ cells (not quantified) and more amoeboid morphology. Scale bars, 50 μm (left), 15 μm (right).

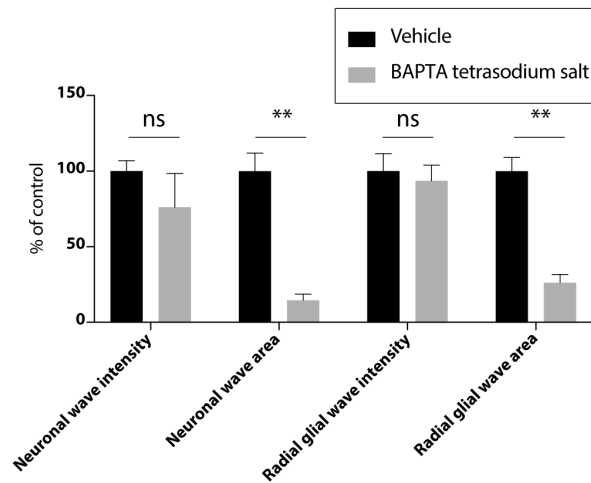


Figure 5.7: **Ventricular injection of BAPTA tetrasodium salt leads to significant reduction to neuronal and radial glial wave area but not intensity.** Quantification of neuronal and radial glial wave intensity and area relative to control values. **, $p \leq 0.01$ in Student's *t*-Test. $n \geq 5$ animals / group.

Finally, I attempted the use of BAPTA tetrasodium salt, an extracellular calcium chelator, to inhibit calcium signalling in the immediate phase following injury. BAPTA tetrasodium salt did cause a significant decrease in the area of the neuronal and glial wave, but not the intensity (Fig. 5.7). I did not follow up on this approach and decided to instead focus on the role of persistent calcium signalling and microglia/macrophages on secondary cell death.

5.3 Excitotoxicity following mechanical brain injury in larval zebrafish

Following initial calcium waves in response to a mechanical injury of the optic tectum, we were able to quantify a sustained increase in single-cell calcium transients for at least 6 hpi (Fig. 5.8 A-F). We were interested whether neurons, or microglia/macrophages, or both increased their calcium activity; increased neuronal calcium transients have been linked to excitotoxicity (Randall and Thayer, 1992), while increased microglia/macrophage transients are a sign of their activation (Bader et al., 1994; Eichhoff et al., 2011; Pozner et al., 2015). To investigate whether neurons and microglia/macrophages increased their calcium activity, we cross-bred the *β -actin:GCaMP6f* reporter line with *NBT:dsRed* animals, or *mpeg1:mCherry* animals, and quantified the number of transients in double positive cells. Both neurons and microglia/macrophages exhibited significantly increased calcium transients following injury over at least a 30 min window of observation (Fig. 5.8 F); we did not assess radial glial calcium transients, although it is possible that these cells also significantly increased their calcium transient activity.

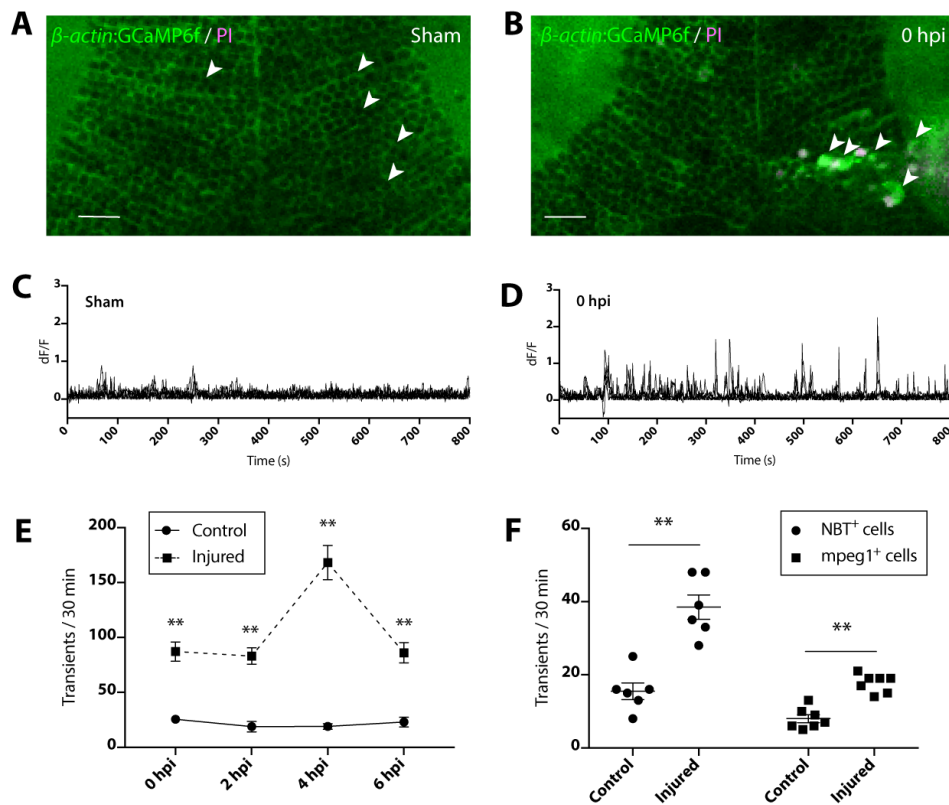


Figure 5.8: Calcium transients are significantly increased for at least 6 hpi, and are increased in both neurons and microglia/macrophages. (A, B) Live imaging of calcium dynamics in the optic tectum of β -actin:GCaMP6f larvae in a sham animal (A) and an injured animal at 0 hpi (B). White arrows indicate individual tectal cells. Scale bars, 20 μ m. (C, D) Calcium traces from the individual tectal cells highlighted in (A) and (B). (E) Quantification of calcium transients in the whole tectum over 30 min from indicated time. **, $p < 0.01$ in Two-Way ANOVA. $n = 6$ / group. (F) Quantification of calcium transients in sham or injured animals (0 hpi) in *NBT:dsRed* or *mpeg1:mCherry*⁺ cells. **, $p < 0.01$ in One-Way ANOVA. $n \geq 6$ / group. Data in (E) and (F) collected and analysed by Laura Pons.

Using *in vivo* timelapse imaging in β -actin:GCaMP6f larvae for 1 h (between 2 and 3 hpi) followed by fixation, nuclear staining, and imaging of nuclei in the same optical plane as previous calcium imaging, I identified a high density of pyknotic nuclei in regions of high calcium activity as reflected by single-cell transients (Fig. 5.9). Therefore, I demonstrated a spatiotemporal correlation of calcium activity and cell death; this was interesting, as previous studies in rodents had linked increased calcium activity with excitotoxic cell death (Randall and Thayer, 1992; Young, 1992). However, calcium activity could also be found in regions with low densities of pyknotic nuclei. This could be caused by a number of factors. First, cell death could occur in a delayed manner relative to calcium transients and we had not studied the timescale of the calcium transient-cell death axis. Second, a certain threshold of calcium may be required to induce cell death. Third, calcium signalling could also reflect the occurrence of other cellular pathways, as calcium has not exclusively been linked to cell death but also a variety of other processes, such as migration or gene expression (reviewed by Berridge et al. (2003)).

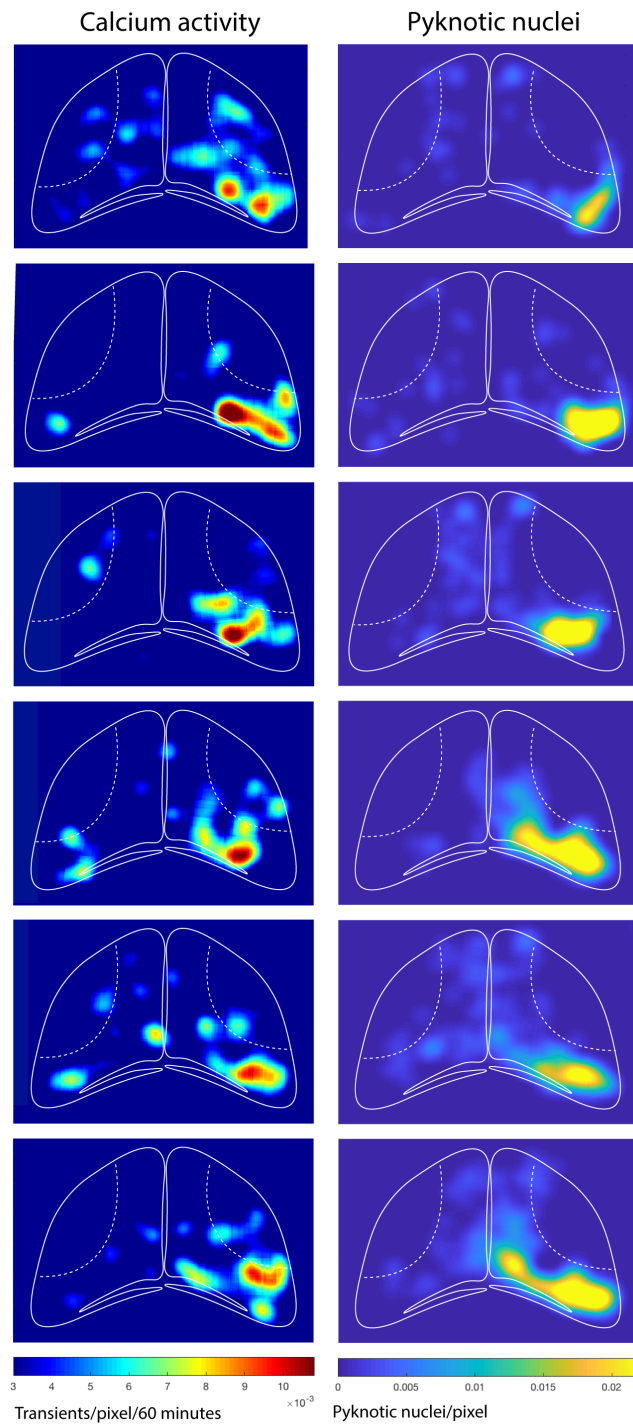


Figure 5.9: **Pyknotic cell death occurs in regions of high calcium activity.** Heatmaps of calcium transients and pyknotic nuclei in 6 larvae. Calcium transients were quantified between 2-3 h post injury, while pyknotic nuclei were quantified at 3 h post injury.

To investigate whether the sustained calcium activity we observed following injury was elicited by glutamate and mediated by NMDA receptors and could therefore represent excitotoxicity as previously described in mammalian models of central nervous system injuries (Faden et al., 1989; Randall and Thayer, 1992), I bathed larvae in the NMDA receptor inhibitor mix MK801 + AP5 and quantified the number of calcium transients following injury. Application of MK801 + AP5 abolished the significant increase of calcium transients following injury that was observed in untreated larvae both at 0 and 6 hpi (Fig. 5.10 A, B). Furthermore, treatment with MK801 and AP5 significantly decreased the number of pyknotic nuclei in *H2A:GFP* larvae 6 h post injury (Fig. 5.10 C, D), while not affecting the number of PI⁺ cells at 0 hpi (Fig. 5.10 E, F). This provided further evidence that PI⁺ cells at 0 hpi die through primary cell death, while pyknotic nuclei at 6 hpi die through secondary cell death, and suggested that NMDA receptor-mediated calcium signalling could play a role in secondary cell death. The fact that NMDA receptor application only partially inhibited secondary cell death suggested that, as in mammals, other mechanisms may play a role in mediating secondary cell death, such as oxidative stress.

Finally, I assessed whether glutamate could be used to exacerbate secondary cell death. Therefore, I increased glutamate levels via bath application of *L*-glutamate as previously used by McCutcheon et al. (2016) and quantified number of pyknotic nuclei at 6 hpi. Treatment with *L*-glutamate following injury led to a significant increase of pyknotic nuclei, therefore providing further evidence that excitotoxicity is - at least in part - responsible for secondary cell death in our brain injury model.

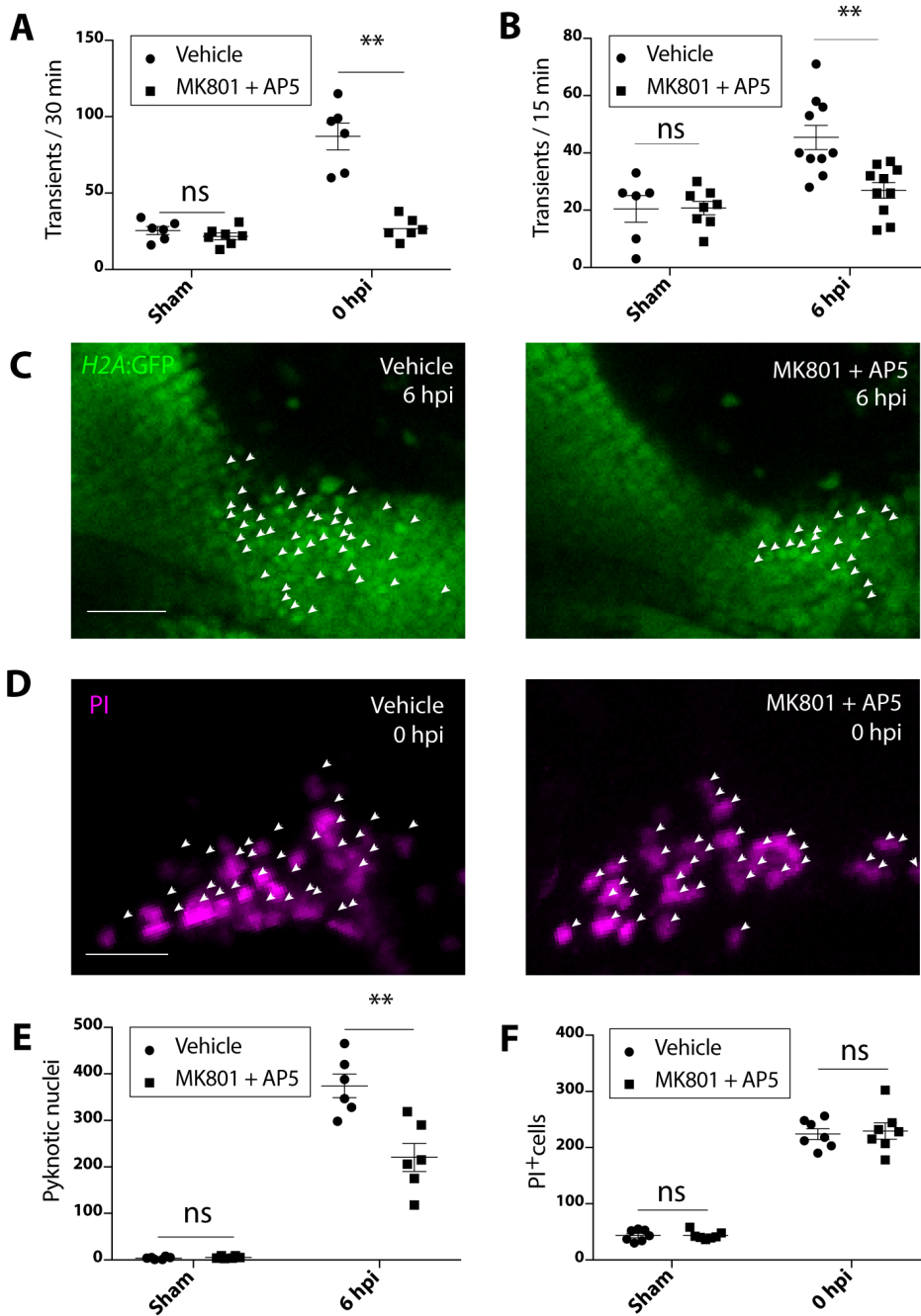


Figure 5.10: **Treatment with NMDA receptor antagonists MK801 and AP5 abolishes injury-induced sustained increase in calcium signalling and reduces secondary cell death at 6 hpi.** Treatment with NMDA receptor inhibitor mix MK801 and AP5 significantly reduced calcium transients both immediately (A), and at 6 hpi (B) while not affecting transients in sham animals. **, $p \leq 0.01$ in Two-Way ANOVA. $n \geq 6$ animals / group. (C) Representative close-up images of vehicle- or MK801+AP5-treated *H2A:GFP* larvae at 6 hpi. Arrowheads are pointing at pyknotic nuclei. Scale bar, 25 μm . Experiment performed and images acquired by Laura Pons. (D) Representative close-up images of vehicle- or MK801+AP5-treated larvae stained with PI at 0 hpi. Arrowheads are pointing at PI⁺ cells. Scale bar, 20 μm . (E) Quantification of pyknotic nuclei in whole tectum of vehicle- or MK801+AP5-treated *H2A:GFP* larvae (sham or 6 hpi). **, $p \leq 0.01$ in Two-Way ANOVA. $n = 6$ animals / group. (F) Quantification of PI⁺ cells in whole tectum of vehicle- or MK801+AP5-treated animals (sham or 0 hpi). ns in Two-Way ANOVA. $n \geq 6$ animals / group.

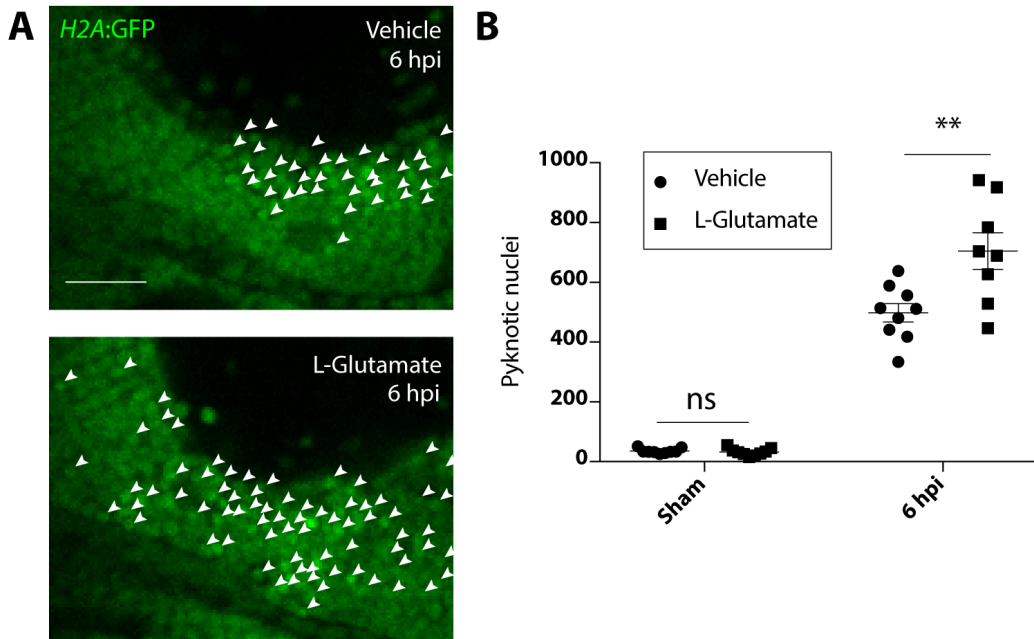


Figure 5.11: **Treatment with NMDA receptor agonist *L*-glutamate causes a significant increase of secondary cell death at 6 hpi.** (A) Representative close-up images of vehicle- or L-Glutamate-treated *H2A:GFP* larvae at 6 hpi. Arrows are pointing at pyknotic nuclei. Scale bar, 25 μ m. (B) Quantification of pyknotic nuclei in whole tectum of vehicle- or *L*-glutamate-treated *H2A:GFP* larvae (sham or 6 hpi). **, $p \leq 0.01$ in Two-Way ANOVA. $n = 6$ animals / group.

5.4 Discussion

The idea that an early calcium signal plays a crucial role in injury repair is not new. One of the first observations that wound healing is inhibited in the absence of calcium signalling was made by Stanisstreet in the *Xenopus* embryo ectoderm in 1982 (Stanisstreet, 1982). Since then, injury-induced calcium waves have been studied in a variety of organisms and tissue contexts. Similarly, sustained increases in calcium signalling, called glutamate excitotoxicity, following CNS injuries have been studied for several decades (Faden et al., 1989; Katayama et al., 1990).

In this chapter, I have described the investigation of calcium signalling following larval zebrafish brain injury both within seconds (early), and within minutes to hours (sustained responses). Working with larval zebrafish equipped me with tools to visualise injury-induced calcium signalling. Although pharmacological perturbation of early calcium waves was complicated by a lack of specific (particularly temporal) inhibitors without toxicity, this platform potentially allows for easy perturbation of signalling mechanisms upstream of calcium waves and the effects on downstream readouts such as microglial recruitment or cell death in real-time.

5.4.1 Early calcium signalling

I was able to provide evidence for distinct pathways eliciting calcium signalling after acute mechanical brain injury in larval zebrafish. Several receptors were activated by injury of neural tissue, leading to calcium waves in specific cell types: the first cells to increase intracellular calcium surrounding the injury site were neurons (starting within zero to two seconds of injury and lasting until fourteen seconds post injury on average) upon glutamate receptor activation (both NMDA and AMPA receptors, although NMDA receptors appear to be the predominant type; NMDA receptor inhibition was able to completely abolish the neuronal calcium wave, and may therefore act upstream of AMPA receptors) (Fig. 5.3 B, C, I, J). Similarly, I was able to increase calcium in neurons by ventricular injection of *L*-glutamate (Fig. 5.4). Increases of calcium in neuronal cell bodies immediately following injury were aided by activation of P2Y subtype ATP receptors (Fig. 5.3 D, E, K, L, Movie S3), as well as TRPM3 mechanosensitive channels (Fig. 5.3 F, I, J, Movie S3). However, injection of P2 receptor agonist ATP or TRMP3 agonist ononetin were unable to elicit a significant calcium increase in cells with neuronal morphology (Fig. 5.4). Finally, gap junctions may in part play a role in propagation of the neuronal calcium wave. Inhibition of connexin 43 channels via carbenoxolone (CBX) did not cause any effect on the parameters I measured, whereas application of a different type of gap junction inhibitor, flufenamic acid (FFA), significantly decreased neuronal wave area (Fig. 5.3 J, Movie S3). This finding needs to be interpreted with caution: although FFA has previously been used as a reversible gap junction inhibitor (Harks et al., 2001; Herrgen et al., 2014; Srinivas and Spray, 2003), it is now known that FFA can also modulate the release of ATP and glutamate via connexin 43 gap junctions (Braet et al., 2003; Stout et al., 2002), and is a promiscuous modulator of calcium, chloride, sodium, and TRPM3 mechanosensitive ion channels (reviewed by Guinamard et al. (2013)). Therefore, it could be the case that FFA modulates the neuronal calcium wave propagation via modulation of ion channels and ATP or glutamate release.

Activation of neuronal cells following injury was closely followed by an intracellular increase of calcium in radial glia (starting from four seconds and lasting up to thirty seconds post injury) elicited by ATP signalling via the P2X receptor subtype (Fig. 5.2, Fig. 5.3 D, E, K, L, Movie S3). Application of pan-P2 receptor inhibitor PPADS, or P2X receptor subtype-specific inhibitor iso-PPADS, completely abolished radial glial calcium signalling following injury (Fig. 5.3, Movie S3); I did not assess the effect of P2Y subtype receptor inhibitors, although these have previously been used in the investigation of calcium waves (Kulick and von Kügelgen, 2002; Suplat et al., 2007; Tovell and Sanderson, 2008). In line with the finding that P2 receptors were able to inhibit radial glial calcium waves following injury, ventricular injection of ATP (a P2 receptor agonist) led to a rapid increase of GCaMP6f fluorescence in radial glia (Fig. 5.4). No other pharmacological inhibitor I tested, including glutamate receptor inhibitors, mechanosensitive channel inhibitors, or gap junction inhibitors, had an effect on the radial glial calcium wave (Fig. 5.3 J). This was

surprising, as previous research had shown that calcium waves in radial glia can be inhibited by application of carbenoxolone *in vitro*, targeting connexin 43 channels (Weissman et al., 2004). Nonetheless, the data suggested that ATP is the predominant signalling mode for glial cells following brain injury in the larval zebrafish.

The findings described in this chapter are consistent with previous observations that injuring of neural tissue leads to calcium waves (Herrgen et al., 2014; Kanemaru et al., 2013; Kraft et al., 2017; Sieger et al., 2012; Vargas et al., 2015). However, it was unclear whether these calcium wave were a passive reaction to release of ATP and glutamate from dying neurons, or whether they could instruct reparative and regenerative downstream processes in the immediate phase following brain injury (or both). Previous research has shown that calcium waves can exert (neuro)protective functions, for example by inhibiting excessive apoptosis following an injury (Justet et al., 2016; Kanemaru et al., 2013), but also via other cellular mechanisms such as actin remodelling, rapid wound closure, and expulsion of dead cells from intact tissue (Herrgen et al., 2014; Minns et al., 2016). Furthermore, calcium waves have been reported to attract microglia to sites of brain injury (Sieger et al., 2012). Sieger et al. (2012) showed that calcium waves and ATP are required to recruit microglia to a site of neuronal injury in the 3 dpf zebrafish tectum, which I confirmed with my experiments in the 4 dpf zebrafish tectum. I was furthermore able to reproduce the prior finding that ATP is required for microglia recruitment to an injury site (Fig. 5.5 C) (Davalos et al., 2005; Honda et al., 2001; Ohsawa et al., 2007), although the effect was small using the P2 receptor inhibitor PPADS, which is most likely attributed to the fact that PPADS inhibition of P2 receptors is only temporary (Fig. 5.5 B), and other factors may contribute to the recruitment of microglia.

My attempts to employ calcium chelators to specifically block immediate calcium signalling following injury were not successful (Fig. 5.6 and 5.7). However, there appears to be a consensus in the literature that an early calcium wave following (neuronal) injury is benign rather than cytotoxic (Herrgen et al., 2014; Justet et al., 2016; Kanemaru et al., 2013; Vargas et al., 2015), although further research into this is required to understand the exact role of it in this mechanical injury assay. This will hopefully be enabled by more precise tools to spatially and temporally inhibit calcium signalling in the future.

In addition to recruitment of leukocytes and potential inhibition of excessive apoptosis, calcium waves in radial glia may play a role in regulating regenerative neurogenesis in response to injury. In the optic tectum of the larval zebrafish, radial glia lining the ventricle are progenitor cells. Although developmental neurogenesis in the optic tectum decreases after two to three days post fertilisation (Wullmann and Knipp, 2000), these cells retain the capacity to produce new neurons throughout the whole life of the zebrafish and can therefore be reactivated by injury - a calcium wave could be one of these signals to prime radial glia for proliferation. My finding that ATP acts on radial glia

to produce calcium waves following injury is particularly exciting as a previous study has reported that ATP can induce calcium waves which then increase proliferation of rat radial glia *in vitro* (Weissman et al., 2004). ATP has also been shown to be a positive regulator of neural stem cell proliferation in rodents *in vivo* (Cao et al., 2013; Gampe et al., 2015), while calcium waves have been shown to be an effector of proliferation (Justet et al., 2016; Kraft et al., 2017) although a link through ATP was not addressed in these studies.

The detailed investigation into the link between ATP, calcium, and radial glial proliferation was hampered by technical issues: I was unable to specifically inhibit calcium signalling only in radial glia immediately following the injury. Although PPADS and iso-PPADS were able to completely inhibit the radial glial calcium wave, these drugs are not specific inhibitors for P2 receptors on radial glia and also inhibited recruitment of microglia (Fig. 5.5 D), which have previously been shown to play a role in modulating progenitor proliferation in a brain injury model of adult zebrafish (Kyritsis et al., 2012). I could therefore not discern whether reactivation following injury was a direct or indirect effect of calcium waves, mediated by radial glial calcium waves or mediated by microglia, respectively. There are, however, two other approaches I propose to investigate a link between radial glial proliferation and calcium signalling:

- Use of BACCS (blue light-activated calcium channels):
Rather than specifically inhibiting calcium in radial glia following an injury, with BACCS I could elicit calcium signalling specifically in radial glia using blue light. There are several different versions of BACCS with different response dynamics (i.e., rapid or slow calcium response, slow or fast recovery) that could be employed (described by Ishii et al. (2015)). A proposed experiment could be to inject BACCS constructs under a radial glial promoter such as *her4.3* into β -*actin*:GCaMP6f larvae to create mosaic expression in single radial glia, and expose these cells to light to elicit a calcium response. At certain timepoints (e.g. 1 day post blue light), proliferation could be assessed using a BrdU pulse experiment and compared to non-activated cells. This experiment would require thorough planning and trouble-shooting, but could provide more causal information on the link of radial glial calcium activity and proliferation.
- Use of the CaMPARI (Calcium Modulated Photoactivatable Ratiometric Integrator) system:
Although initial calcium waves may initiate neurogenesis (Weissman et al., 2004), persistent or rhythmic calcium bursts may play a role in further execution of proliferation as previously shown (Johansen et al., 2017; Owens and Kriegstein, 1998; Pearson et al., 2005; Resende et al., 2010a,b; Somasundaram et al., 2014). It would prove challenging to continuously image the activity pattern of radial glia in order to detect calcium oscillations, and then assess proliferation, which occurs a few days later (2 days post injury in the larval zebrafish spinal cord

(Ohnmacht et al., 2016); 2 to 3 days post injury in our injury model, unpublished data, Leah Herrgen). Employing CaMPARI (developed by Fosque et al. (2015)) could provide a solution to this problem. This genetically encoded calcium indicator undergoes irreversible green-to-red photoconversion when calcium is active and the cell is irradiated with UV light of a wavelength of 400 nm, therefore providing a snapshot of activity. This system has previously been shown to elicit efficient photoconversion, and has been employed in freely-moving zebrafish and flies (Fosque et al., 2015). CaMPARI could be expressed under a radial glial promoter in larval zebrafish, and the larvae could be exposed to photoconverting light at certain times following the injury while freely moving, and proliferation could be assessed with a BrdU pulse experiment in the same larvae. This would require some trouble-shooting and timepoints would need to be carefully chosen. Although this experiment would not provide causal information, it could provide a correlative insight between radial glial calcium activity at a given timepoint and later proliferation.

5.4.2 Sustained calcium transients

Following initial calcium waves, the optic tectum showed an increased calcium transient frequency compared to controls for at least 6 hours post injury (Fig. 5.8 A). Our data of cross-breeding of *β-actin:GCaMP6f* and *NBT:dsRed* fish showed that neurons increase their transients following injury (Fig. 5.8 B). Similarly, calcium activity was increased in microglia/macrophages as timelapse imaging of double transgenic *β-actin:GCaMP6f; mpeg1:mCherry* larvae revealed (Fig. 5.8 B). Previous work has shown that microglia display an increase of calcium transients when activated (Bader et al., 1994; Eichhoff et al., 2011; Pozner et al., 2015). Future work could involve studying double transgenic *β-actin:GCaMP6f; mpeg1:mCherry* larvae in more detail to investigate how calcium transients in microglia/macrophages are temporally related to cellular functions in response to zebrafish brain injury *in vivo* (such as migration or phagocytosis), as previous work has shown calcium transients in microglia induce migration *in vitro* (Bader et al., 1994) and phagocytosis *in vivo* (Koizumi et al., 2007).

Investigating neuronal calcium activity following injury, I observed that secondary cell death predominantly occurred in regions that had previously also shown a high number of calcium transients (Fig. 5.9). This suggested that these regions potentially experienced a cytotoxic calcium overload. This phenomenon following CNS injuries is commonly referred to as excitotoxicity and has been extensively studied in experimental models of CNS injuries. Previous research had shown that the glutamate-NMDA receptor pathway is responsible for increased calcium activity following brain injury (Faden et al., 1989; Randall and Thayer, 1992); I employed NMDA receptor antagonist mix MK801 and AP5 to decrease calcium signalling following injury (Fig. 5.10), which lead to a significant reduction of pyknotic nuclei at 6 hpi but not PI⁺ cells at 0 hpi (Fig. 5.10), showing

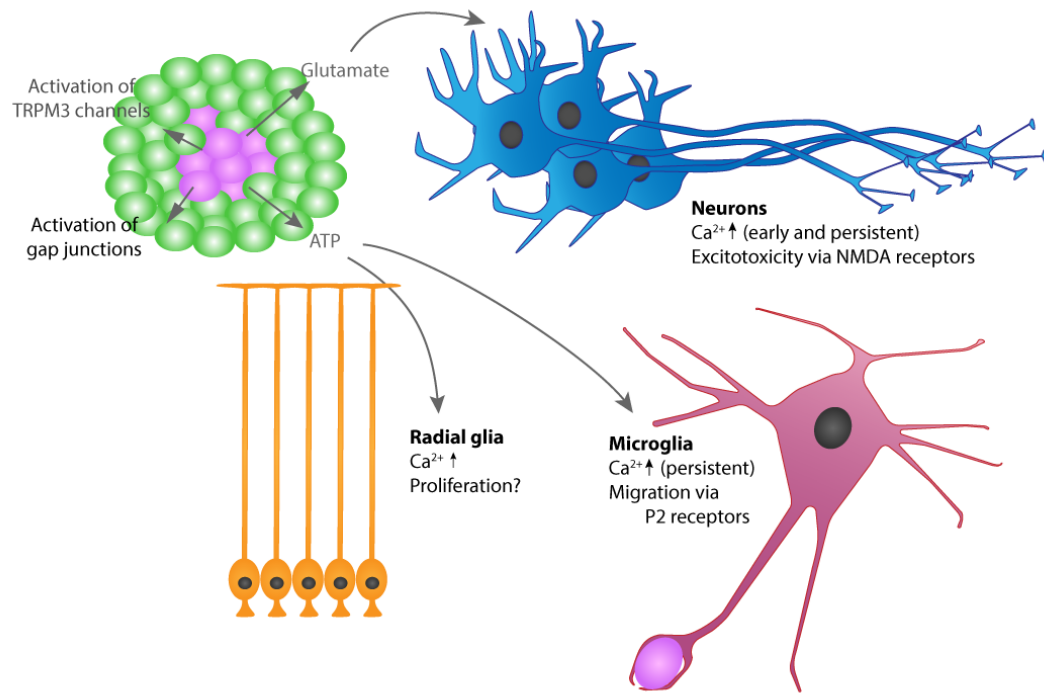


Figure 5.12: **Schematic of factors eliciting early and sustained calcium signalling following mechanical injury.** Magenta and green ellipses depict dead or healthy neurons, respectively, and mechanisms inducing early and sustained calcium signalling following injury are illustrated.

that, as in rodent models, the NMDA receptor pathway mediated secondary cell death in larval zebrafish. Similarly, supplying external *L*-glutamate via bath application following the injury (which was previously shown to cause apoptotic cell death after 24 hours in a larval zebrafish model of excitotoxicity by McCutcheon et al. (2016)), led to a significant increase of pyknotic at 6 hpi in injured but not sham animals (Fig. 5.11). The discrepancy between my results (a lack of cell death in sham animals following *L*-glutamate treatment) and what McCutcheon et al. (2016) published (apoptotic cell death in what would be 'sham' animals in my assay) can be explained by the different timescales; I only applied *L*-glutamate for 6 hours, while McCutcheon et al. (2016) left the larvae in *L*-glutamate for 24 hours. In combination, my dataset strongly suggests that sustained neuronal calcium transients following injury in larval zebrafish are excitotoxic, and that the occurrence of glutamate excitotoxicity eliciting secondary cell death appears to be conserved between zebrafish and rodents following brain injury .

To summarise, this dataset provides novel information on calcium signalling events following mechanical brain injury in the larval zebrafish, and is useful for several reasons:

1. It confirms and expands data on early calcium waves and their upstream signalling mechanisms following injury (summarised in Fig. 5.12).

2. It shows that excitotoxicity is a conserved neurotoxic mechanism following brain injury in larval zebrafish.
3. It could provide the basis to a novel study investigating calcium signalling in relation to radial glia behaviour, including physiological and injury-induced (regenerative) neurogenesis.

Chapter 6

Rapid clearance of debris by microglia limits secondary neuronal cell death

6.1 Introduction

Microglia are the resident macrophages of the brain. They are involved in brain development and responsible for surveillance of the brain, protection from pathogen invasion, and removal of cellular debris and apoptotic cells (Cunningham et al., 2013; Paolicelli et al., 2011; Pont-Lezica et al., 2014; Schafer et al., 2012; Sierra et al., 2010; Stevens et al., 2007; Squarzoni et al., 2014; Ueno et al., 2013). In the context of injury, the role of microglia and peripheral macrophages has been ambiguous: initially, many studies found a detrimental role of neuroinflammation mediated by microglia and macrophages in neuronal survival following brain injuries (Festoff et al., 2006; Li et al., 2013; Wirenfeldt et al., 2005). Conversely, other studies suggest that, depending on their polarisation, microglia/macrophages can be critical for tissue repair and mediate neuroprotection (Chamak et al., 1994; Szalay et al., 2016; Tsarouchas et al., 2018; Yin et al., 2003, 2006).

Microglia are made aware of injuries by ATP released in the environment as a DAMP (Davalos et al., 2005) and calcium waves (Sieger et al., 2012). Sieger et al. (2012) demonstrated that microglia are rapidly recruited to brain injuries in larval zebrafish and engulf debris. Whether phagocytosis is beneficial or detrimental is subject of an ongoing debate (Sierra et al., 2013). Several previous studies suggest a neurotoxic role for microglial phagocytosis following neuronal injuries due to phagocytosis of stressed-but-viable neurons, exacerbating tissue loss (Fricker et al., 2012a,b; Neher et al., 2011, 2013). Furthermore, phagocytosis can result in generation of superoxide anions, also known as respiratory burst (Minakami and Sumimotoa, 2006), which may exacerbate oxidative

stress in response to injury. Consistent with this, microglial phagocytosis has previously been shown to cause ROS production and neuronal death *in vitro* (Claude et al., 2013; Wilms et al., 2003). On the other hand, phagocytosis removes debris that may otherwise spill toxic intracellular factors (Green et al., 2016; Wolf et al., 2017), and can promote a more anti-inflammatory polarisation of microglia (Fadok et al., 1998; Wolf et al., 2017).

Here, I aimed to assess microglial recruitment and phagocytosis in the larval zebrafish. Although previous studies in rodents had used 2-photon imaging of microglia/macrophages to assess microglial behaviour in response to injury or disease *in vivo* (Davalos et al., 2005; Locatelli et al., 2018; Pozner et al., 2015; Roth et al., 2014), this is much more challenging than in larval zebrafish which are easily amenable to live imaging. Using *in vivo* imaging in larval zebrafish enabled me to easily assess dynamic changes in microglial behaviour in response to injury. Furthermore, in contrast to mammals, zebrafish are able to rapidly decrease both primary and secondary cell death (Fig. 4.2, Fig. 4.4), and therefore microglial responses may differ from mammalian models; identification of the mechanisms that render zebrafish microglia neuroprotective could provide a valuable tool for treatment of brain injuries.

In the upcoming chapter, I will describe the work I undertook to investigate microglia/macrophages in my injury assay. As I hypothesised that microglia/macrophages could act neuroprotective, in particular through rapid phagocytosis of debris, I first assessed microglia/macrophage recruitment and phagocytosis in response to injury using timelapse *in vivo* imaging, and then aimed to inhibit phagocytosis using pharmacological and genetic perturbation of phagocytic receptors. I also employed the *irf8*^{-/-} mutant line lacking microglia and macrophages (Shiau et al., 2015) to investigate the effect of complete absence of these cells on secondary cell death, and compared cytokine levels in these mutants with wild type animals using quantitative reverse-transcription PCR (qRT-PCR).

6.2 Recruitment of microglia/macrophages

I started off my investigation into immune cell function by assessing recruitment of microglia and macrophages. For this purpose, I employed the *mpeg1*:GFP transgenic line, labelling all macrophages including microglia. I performed *in vivo* imaging before, 0, 1, and 2 hpi in the same animals. *mpeg1*⁺ cells within the brain rapidly migrated to the brain injury site (Fig. 6.1), suggesting a recruitment via transcription-independent mechanisms as previously shown (Fig. 5.5 C, Sieger et al. (2012)). Additionally, *mpeg1*⁺ cells present on the skin were rapidly recruited to the site of skin injury. The adjacent quantification only shows *mpeg1*⁺ cells inside brain, as the exact number of cells at the site of skin injury was often difficult to determine due to the dense positioning of the cells and interaction of processes, and moreover my primary interest was neuronal repair.

I performed timelapse imaging before and within the first two hours after injury to gain a more

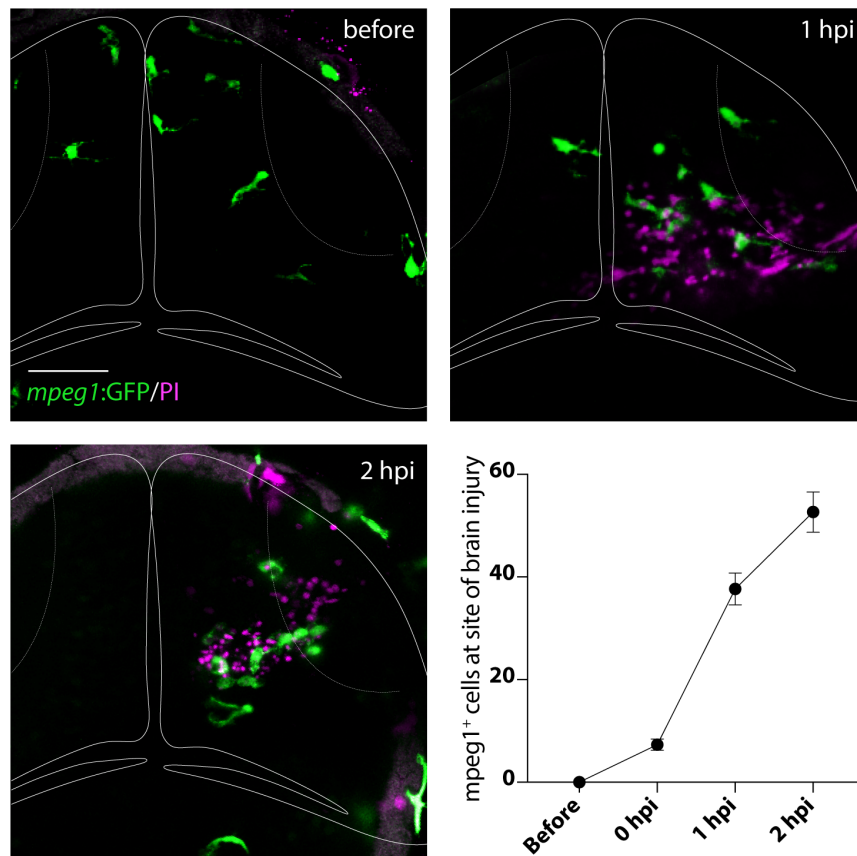


Figure 6.1: Cells expressing the microglia/macrophage marker *mpeg1* migrate to the site of injury. Images taken before, 1, and 2 hours post injury from the same animal. PI is indicating presence of dead cells. Scale bar, 50 μ m In the lower right panel: quantification of *mpeg1*⁺ cells at site of brain injury, excluding cells on the skin. $n = 6$ animals.

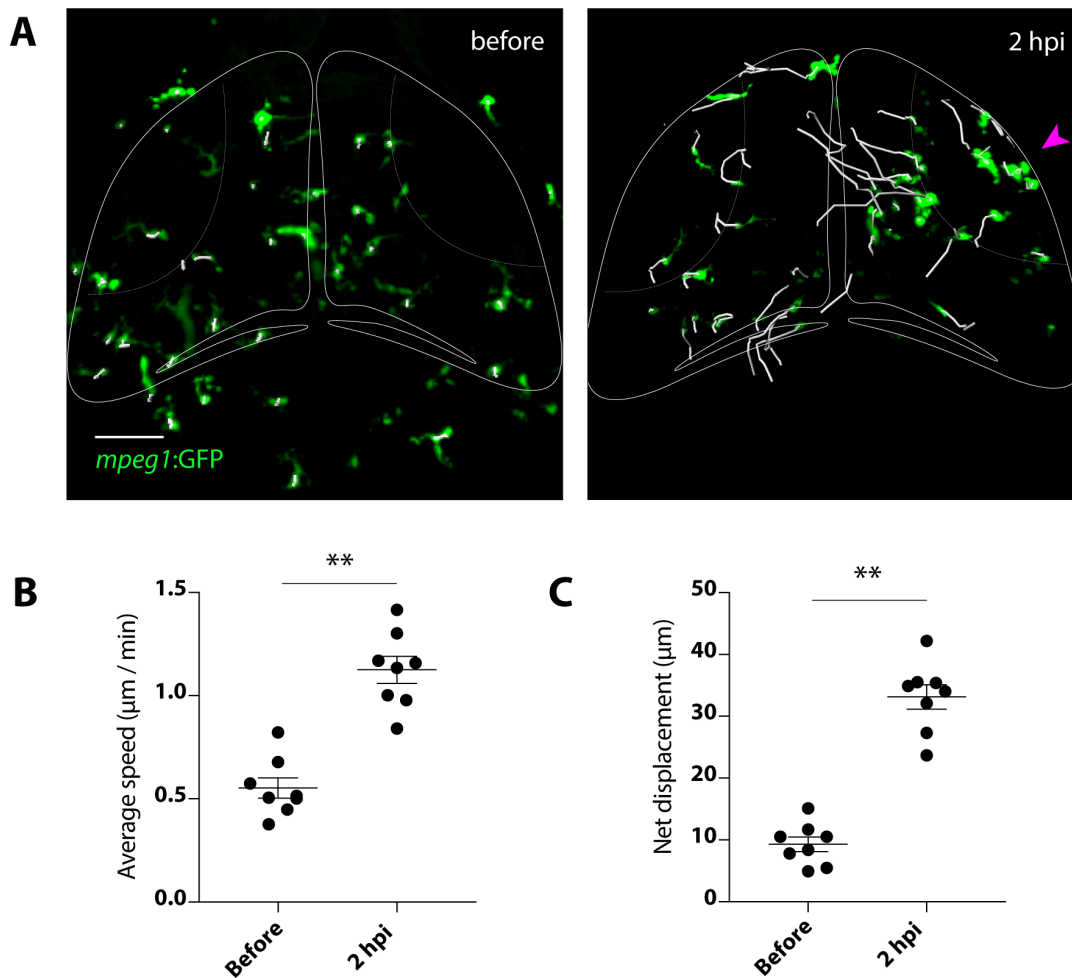


Figure 6.2: **mpeg1⁺ cells change their behaviour from sedentary surveillance to responsive migration in the first two hours following injury.** (A) Traces visualizing mpeg1⁺ cell body movement before and 2 hpi. (B) Quantification of average mpeg1⁺ cell body migration speed. **, $p = 0.0011$ in paired t test; $n = 8$ animals. (C) Quantification of average mpeg1⁺ cell net displacement before and after injury. **, $p = 0.0001$ in paired t test; $n = 8$ animals.

■ Figure corresponds to **movies S4** (A, before) and **S5** (B, injured).

dynamic understanding of mpeg1⁺ cell recruitment. The first mpeg1⁺ cells migrated to the injury site within five minutes of injury. Using the 3D-rendering software IMARIS, I was able to trace microglia/macrophages, and measure the migration speed and net displacement before and after injury. Traces are visualised in Fig. 6.2 and in supplementary movies S4 and S5. mpeg1⁺ cells significantly increased their average migration speed following injury, from $0.55 \mu\text{m}/\text{min}$ to $1.125 \mu\text{m}/\text{min}$ (**, $p = 0.0011$ in paired t test before - after injury; $n = 8$ animals). Similarly, net displacement of mpeg1⁺ cells was significantly increased from $9.30 \mu\text{m}$ to $33 \mu\text{m}$ following injury (**, $p = 0.0001$ in paired t test before - after injury; $n = 8$). This data therefore revealed a significant behavioural response of mpeg1⁺ cells within two hours of injury from (resting) surveillance to migration to the injury site.

6.3 Microglia, but not peripheral macrophages, are present within injured brain

I had so far used the number of *mpeg1*⁺ cells at the site of brain injury to quantify microglia/macrophage recruitment. However, this transgenic line does not reveal whether these cells were brain-resident microglia or peripheral 'invading' macrophages from the skin or other regions of the body following injury. As it had previously been described that microglia and macrophages can have very distinct injury-induced signatures and inflammatory responses, I wanted to assess if there was a predominant cell type at the site of brain injury, or if there was heterogeneous recruitment of both microglia and peripheral macrophages.

To address this question, I followed two approaches: first, I performed repeated *in vivo* imaging of the double transgenic line *Tg(p2y12:P2Y₁₂-GFP; mpeg1:mCherry)*, in which all macrophages are labelled red with mCherry and microglia additionally express GFP, allowing me to distinguish between the two cell types. Imaging these animals before, 0, 1, 2 and 6 hpi revealed that virtually all *mpeg1*⁺ cells at the site of brain injury expressed the well-established microglial marker P2Y₁₂ (Bennett et al., 2016; Butovsky et al., 2014; Mildner et al., 2017), and were therefore probably microglia (Fig. 6.3 A, D). The second approach I used was to perform a double immunostaining against the microglial marker 4C4 (Becker et al., 2004) and GFP on the transgenic *mpeg1*:GFP background at 6 hpi. This showed that most cells present at the brain injury site were immunoreactive for 4C4 (Fig. 6.3 B, E), while they were predominantly 4C4⁻ in the trunk of the fish apart from in the spinal cord (Fig. 6.3 C).

I was intrigued by the fact that macrophages did not appear to enter the brain in our injury model, seeing as they were the predominant type of immune cell present in spinal cord lesions of larval zebrafish (Tsarouchas et al., 2018), and infiltration of monocyte-derived macrophages (MDMs) is frequently observed following mammalian brain injuries (Gyoneva et al., 2015). To explore whether microglia/macrophages ever transition between skin to brain or brain to skin following injury in our model, I re-investigated the timelapses I acquired for Fig. 6.2. As the skin is autofluorescent in zebrafish, this allowed me to easily observe if any cells were transitioning between skin and brain in the 2 hours following injury. I observed very few occasions where macrophages or microglia were 'trespassing' into each other's territories within this two hour period. Fig. 6.4 shows a representative image of a skin macrophage being recruited to the site of injury, but stopping at the skin injury and not entering the brain within the window of observation. This is reflected by the quantification in Fig. 6.4.

Finally, I aimed to assess recruitment of neutrophils; in mammals, neutrophils are some of the earliest immune cells to arrive at the injury site, and are additionally recruited by activated microglia

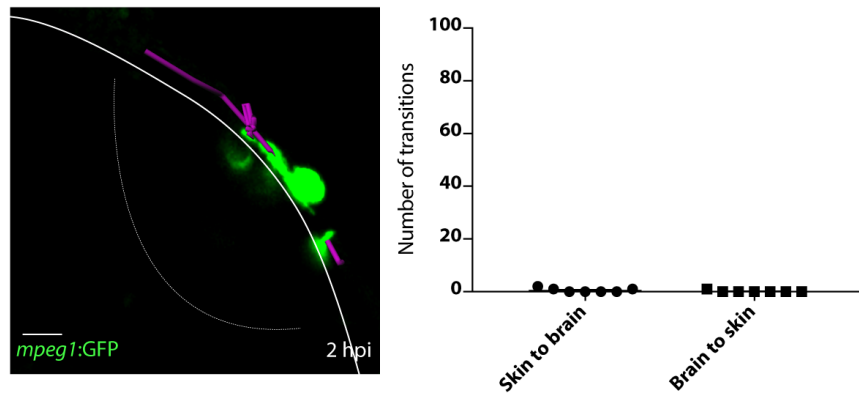


Figure 6.4: **Traces visualising past cell body displacement of skin macrophages which do not enter the brain.** Traces showing past cell body displacement of *mpeg1:GFP*⁺ cell within 2 hpi. Quantification of immune cell transitions during 2 h after injury. n = 7 animals per experimental group.

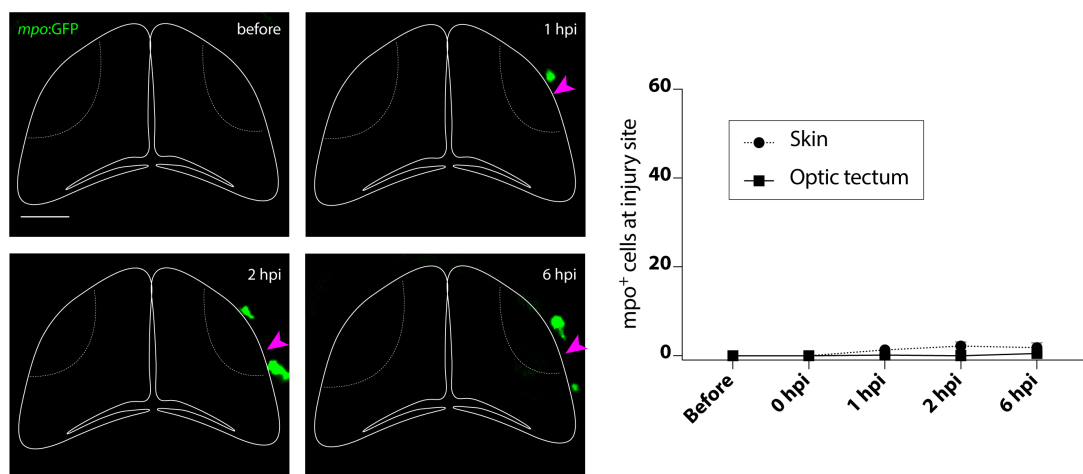


Figure 6.5: **Very few neutrophils are recruited to the brain injury.** Representative images of *mpo:GFP* transgenic larvae before, 1, 2, or 6 hpi. Magenta arrow indicates injury site. Scale bar, 50 μ m. Adjacent: quantification of *mpo*⁺ cells at the site of injury (skin or brain).

(Carlos et al., 1997; Oehmichen et al., 2003). In the larval zebrafish spinal cord, neutrophils are abundantly recruited to the injury site within a few hours (Tsarouchas et al., 2018). To investigate neutrophil recruitment in our brain injury model, I performed repeated *in vivo* imaging using a transgenic neutrophil reporter line (*mpo:GFP*). This showed that neutrophils were present in much lower numbers than microglia or macrophages in the head, and only few cells were recruited to the skin injury site. Moreover, very few cells (and at most times none at all) were present inside the brain, suggesting that in the larval zebrafish brain, neutrophils play only a minor role in wound repair.

6.4 Comparison of wild type and *irf8*^{-/-} larvae

Given that microglia were highly reactive to the injury, I wanted to investigate the role of these cells following injury, particularly their contribution to cell death. I employed a comparison between wild

type animals and *irf8*^{-/-} mutants (Shiau et al., 2015), lacking all microglia (and macrophages) until at least 6 days post fertilisation. These animals survive until fertile adulthood and have no gross morphological defects, although they have an increased number of neutrophils (Shiau et al., 2015).

6.4.1 Cell death

Using PI bath application for *in vivo* imaging, I assessed the extent of cell death in these animals following injury. I observed a significant increase of PI⁺ cells at 6 hours post injury compared to wild type animals, which usually have managed to decrease necrotic PI⁺ cell levels significantly at this point (Fig. 6.6 A, B).

To assess apoptosis in response to injury, I quantified the number of pyknotic nuclei and cleaved Caspase-3⁺ cells comparing wild type animals with *irf8*^{-/-} mutants. Both of these cell death markers were already significantly increased in uninjured *irf8*^{-/-} mutants at 4 dpf (Fig. 6.6 C-E), which is most likely due to a lack of clearance of developmentally apoptotic cells in the absence of microglia (Casano et al., 2016; Xu et al., 2016). Although the baseline levels of pyknotic nuclei and Caspase-3⁺ cells were higher than in wild type animals, the difference between baseline numbers and numbers at 6 hpi was higher in *irf8*^{-/-} mutants than in wild types. Therefore, the number of dead cells was enhanced following injury in microglia- and macrophage-less animals compared to wild type animals. However, the data in Fig. 6.6 represent a steady state; the numbers provide no information on whether the enhanced number of cells positive for cell death markers in *irf8*^{-/-} larvae at 6 hpi was due to a lack of collection and degradation of dead cells in the hours leading up to 6 hpi (and therefore increased accumulation of dead cells compared to wild type animals), or due to an exacerbation of secondary cell death elicited by enhanced neurotoxicity in the absence of microglia/macrophages.

Interestingly, the numbers of Caspase-3⁺ cells were not significantly different from uninjured animals at 24 hpi (Fig. 6.6 F), while pyknotic nuclei were (Fig. 6.6 D). As these two markers label different phases of apoptotic cell death (early for Caspase-3, late for nuclear pyknosis), this could indicate that Caspase-3⁺ cells present at 6 hpi stay around to become pyknotic (and Caspase-3⁻) later instead of being removed. Conversely, nuclear pyknosis - a marker for late apoptosis - remained high at 24 hpi, which can potentially be explained by a lack of clearance, and the progression of early apoptotic (Caspase-3⁺) cells to later stages of apoptosis. Nonetheless, the number of pyknotic nuclei also did not increase. Likewise, the number of PI⁺ cells reached baseline levels at 24 hpi, which suggested there may be a capacity, although limited, to remove dead cells even in *irf8*^{-/-} larvae. This is likely achieved by phagocytosis through neutrophils (Esmann et al., 2010), or could be mediated by other mechanisms mediated by neighbouring cells such as macropinocytosis (Henson, 2005), and expulsion of dead cells via tissue contractions (Herrgen et al., 2014). It is somewhat curious that

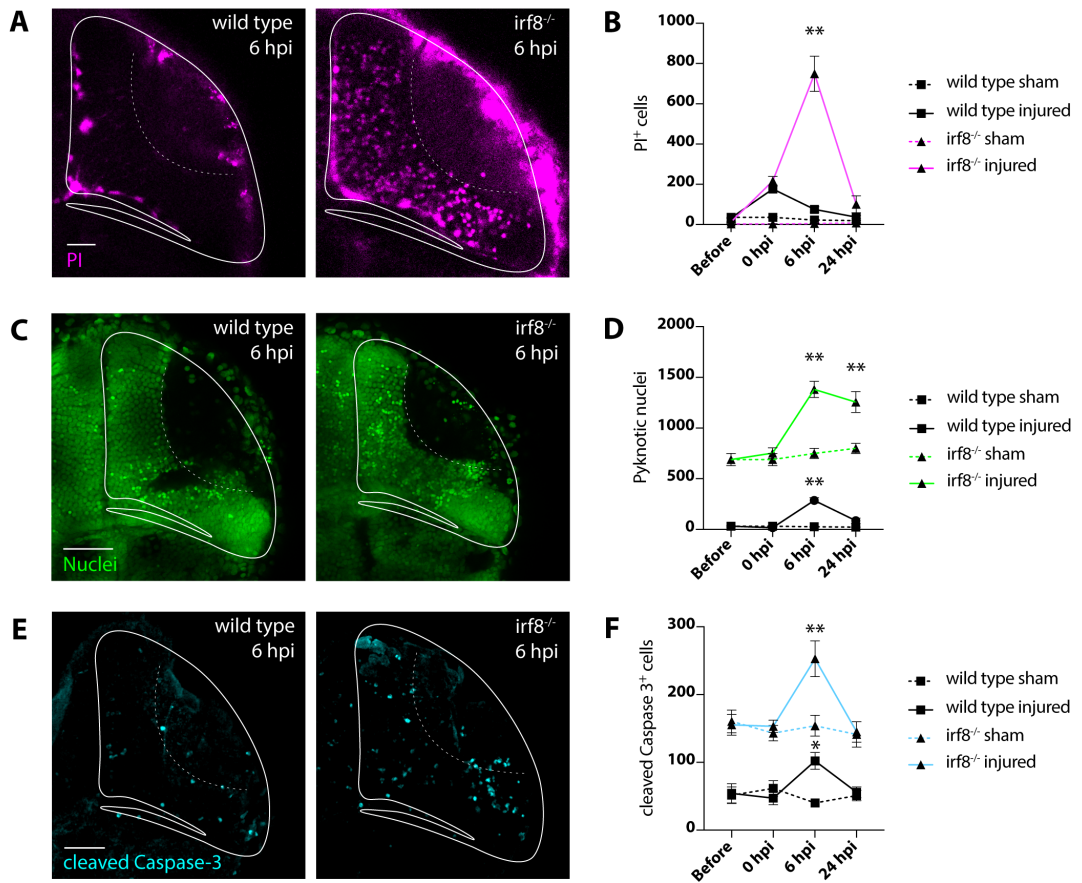


Figure 6.6: *irf8*^{-/-} mutants lacking microglia and macrophages exhibit increased numbers of (secondary) cell death following brain injury. (A) Representative images of a wild type and *irf8*^{-/-} animal at 6 hpi labelled with PI bath application. Scale bar, 50 μ m. (B) Quantification of PI⁺ cells following injury. Significance relates to wild type animals of respective treatment. **, $p \leq 0.01$ in Two-Way ANOVA. (C) Representative images of pyknotic nuclei in a wild type and *irf8*^{-/-} animal at 6 hpi. Scale bar, 50 μ m. (D) Quantification of pyknotic nuclei following injury. Significance relates to sham animals of respective genotype. **, $p \leq 0.01$ in Two-Way ANOVA. (E) Representative images of cleaved Caspase-3 immunostaining in a wild type and *irf8*^{-/-} animal at 6 hpi. Scale bar, 50 μ m. (F) Quantification of cleaved Caspase-3⁺ cells following injury. Significance relates to wild type animals of respective treatment. *, $p \leq 0.05$; **, $p \leq 0.01$ in Two-Way ANOVA.

PI⁺ cells return to baseline levels between 6 and 24 hpi while pyknotic nuclei do not; this may be explained by the fact that the abovementioned factors (phagocytosis by neutrophils, expulsion via tissue remodeling, etc.) may be sufficient to remove PI⁺ cells present at 6 hpi, but cannot keep up efficient clearance, and cannot prevent cells that are in early apoptotic stages (Caspase-3⁺) at 6 hpi to progress to later stages characterised by nuclear pyknosis, which results in accumulation of pyknotic nuclei at 24 hpi.

6.4.2 Neutrophil recruitment

irf8 is a key transcription factor regulating macrophage versus neutrophil fate in development, and *irf8*^{-/-} mutants have excess neutrophils during embryogenesis (Shiau et al., 2015). Neutrophils are a major source of reactive oxygen species, and can create inflammatory environments detrimental

to neuronal survival. To assess neutrophil recruitment and to test whether *irf8*^{-/-} mutants have an increased presence of neutrophils in the brain upon injury, I performed an immunostaining against myeloid peroxidase (mpo). This showed that there was an increased presence of neutrophils in the brain of *irf8*^{-/-} animals compared to wild types. In uninjured wild type animals, I rarely observed neutrophils in the brain, whereas I observed an average of 3.3 ± 0.6 neutrophils in uninjured *irf8*^{-/-} larvae. Upon injury, the number of neutrophils in the brain significantly increased in *irf8*^{-/-} larvae (51 ± 6.5 neutrophils at 6 hpi; 30 ± 1.5 at 24 hpi; **, $p \leq 0.01$ compared to sham for both timepoints in two-way ANOVA with Bonferroni Post-Test), but not in wild type animals (1.3 ± 0.4 at 6 hpi; 0.75 ± 0.25 at 24 hpi; ns compared to sham for both timepoints in Two-Way ANOVA with Bonferroni Post-test). This showed that in the absence of microglia, neutrophil presence is increased in the uninjured brain, and is further enhanced upon injuring.

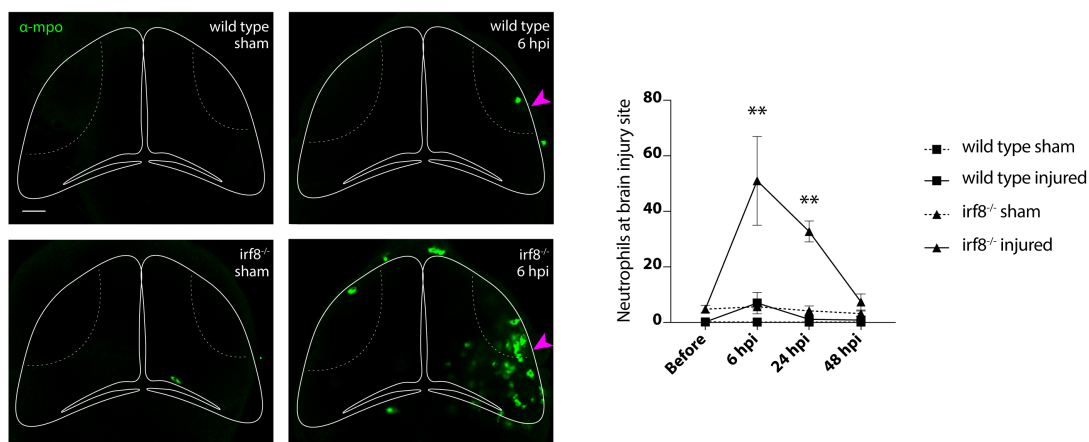


Figure 6.7: Myeloid peroxidase (mpo) immunoreactive cells are found in the tectum of *irf8*^{-/-}, but not wild type animals, and are increased at 6 hours post injury. Scale bar, 50 μ m. Quantification of mpo⁺ cells at site of injury (brain and skin) before, 6, 24, and 48 hpi. Significance relates to wild type sham animals. **, $p \leq 0.01$ in Two-Way ANOVA with Bonferroni Post-Test. $n \geq 5$ animals / timepoint.

As previous research has shown that neutrophils can play a neurotoxic role following TBI in mammals (Allen et al., 2012), it is possible that the enhanced neutrophil number played a role in exacerbation of secondary cell death in *irf8*^{-/-} animals, for example by generation of ROS.

6.4.3 Caveats of using *irf8*^{-/-} mutants to discern microglia/macrophage effects on cell death

I attempted to gain an initial insight in the role of microglia in secondary cell death using the *irf8*^{-/-} mutant lacking this cell population. A major caveat of this mutant line is that *irf8*^{-/-} animals had higher baseline levels of pyknotic nuclei and Caspase-3⁺ cells than wild type animals even before injury; this is presumably caused by a failure to clear developmental apoptosis due to the lack of microglia in these animals (Casano et al., 2016; Xu et al., 2016). However, *irf8*^{-/-} mutants

did not exhibit higher number of PI⁺ cells than wild types prior to injury. As PI can label both necrotic and late apoptotic cells (both having lost their membrane integrity), this suggested that although high numbers of apoptotic cells were present in uninjured *irf8*^{-/-} brains, these were able to contain their membrane integrity under normal conditions. Timelapse imaging using *irf8*^{-/-} larvae revealed that within minutes of the injury, many of these cells lose their membrane integrity and become PI⁺ (data not shown). Although developmental apoptosis is a physiological process that occurs to control for a surplus of generated neurons in the brain (Yamaguchi and Miura, 2015), the loss of membrane integrity of these cells results in the spillage of toxic intracellular factors and could have a considerable impact on secondary cell death. Mechanical injury may have caused the large number of already present apoptotic cells in *irf8*^{-/-} larvae to rapidly experience energy deficiency, for example via mitochondrial dysfunction which is well-documented following brain injuries (Hiebert et al., 2015), and lose their membrane integrity to undergo secondary necrosis.

Furthermore, the number of neutrophils in the brain of *irf8*^{-/-} mutants was significantly increased compared to wild types in response to injury (Fig. 6.7). Although *irf8*^{-/-} mutants are known to have an expanded neutrophil population, there were only approximately 3 neutrophils in the brain of uninjured mutants. Conversely, in response to injury, there was a substantial recruitment of neutrophils (Fig. 6.7). Microglia may therefore, as previously suggested, be required to prevent neutrophil infiltration to the brain in response to an injury (Neumann et al., 2008). Whether this has any influence on cell death - for example via increased reactive oxygen species production - is not clear from my experimental data. However, the fact that wild type animals exhibit considerable amounts of secondary cell death despite the absence of neutrophil infiltration suggests that other mechanisms, such as excitotoxicity (Fig. 5.3, Fig. 5.10, Fig. 5.11), play a prominent role in mediating secondary cell death in our model.

For the purpose of investigating the role of microglia on cell death following injury, *irf8*^{-/-} mutants exhibited the major caveat of a high baseline number of apoptotic cells as outline above. In combination with excess neutrophils, this made it difficult to discern whether the increased cell death at 6 hpi was the result of the loss of membrane integrity in apoptotic cells in *irf8*^{-/-} mutants, the lack of microglia, or the expanded neutrophil populations (or a combination of all three, or other factors). I therefore went on to investigate microglial functions in response to injury, such as production of cytokines or phagocytosis.

6.4.4 Profile of cytokines and neurotrophic factors

To discern the contribution of microglia/macrophages to the inflammatory - or trophic - environment following injury, I then assessed the profiles of cytokines and neurotrophic factors following brain injury in wild type and *irf8*^{-/-} animals. I chose to assess levels of several pro- and anti-inflammatory

cytokines as well as trophic factors that had previously been studied in CNS trauma and could potentially modulate secondary cell death and CNS repair (Fan et al., 1995; Kamm et al., 2006; Kinoshita et al., 2002; Knobloch et al., 1999; Shohami et al., 1994; Tsarouchas et al., 2018). qRT-PCR from larval heads at distinct points following injury (1, 2, and 6 hpi) revealed that a lack of microglia/macrophages significantly altered levels of several cytokines. In wild type animals, *tnfa*, *il1b*, *il10*, *bdnf*, and *ngfb* were quickly and significantly upregulated following injury (within 1-2 hpi) (Fig. 6.8). This failed to happen in *irf8*^{-/-} mutants, where levels remained unaltered. Conversely, *irf8*^{-/-} mutants exhibited increased transcript levels of *tgfb1a* and *il4* (though not significantly for the latter one).

As I performed qRT-PCR on cDNA extracted from whole heads, I could not determine the cellular source of transcripts. While many of the studied transcripts are probably of microglial origin following brain injury, they can also be produced by other cells such as neurons or neutrophils (Ziebell and Morganti-Kossmann, 2010), and the increase of *tgfb1a* and *il4* in *irf8*^{-/-} animals indicates that also in the larval zebrafish, cells other than microglia/macrophages are capable of cytokine upregulation following brain injury. Therefore, I aimed to investigate the cellular sources of some of the studied transcripts; this was enabled by transgenic reporter lines for *il1b* and *tnfa*. To investigate the cellular sources of *il1b* and *tnfa*, I performed *in vivo* imaging with the transgenic lines *il1b*:GFP and *tnfa*:eGFP-F. This revealed that *il1b* and *tnfa* were present in cells with microglial/macrophage morphology in the brain or on the skin, respectively (Fig. 6.9), and explained the lack of *il1b* or *tnfa* expression in *irf8*^{-/-} mutants following injury. Due to a lack of time, I did not cross these lines to the *mpeg1*:mCherry reporter line to confirm this finding, but based on morphology I was confident that these cells were indeed microglia/macrophages. Ramified cells with microglial morphology appeared to express high levels of *il1b* already at baseline, and GFP fluorescence under the *il1b* promoter remained high until 6 hpi, although the cellular morphology changed: cells became more amoeboid or rounded, which has been linked to more activated and phagocytic polarisations (Fig. 6.9 B) (Loane and Kumar, 2016; Nimmerjahn et al., 2005). For *tnfa*:eGFP-F, expression was interestingly detected within the brain at 2 hpi but on the skin at 6 hpi (Fig. 6.9 C, labelled with arrowheads). Based on my data that microglia and macrophages do not usually cross between brain and skin (Fig. 6.4), this indicates there may be a different temporal regulation of *tnfa* expression following injury between microglia and macrophages.

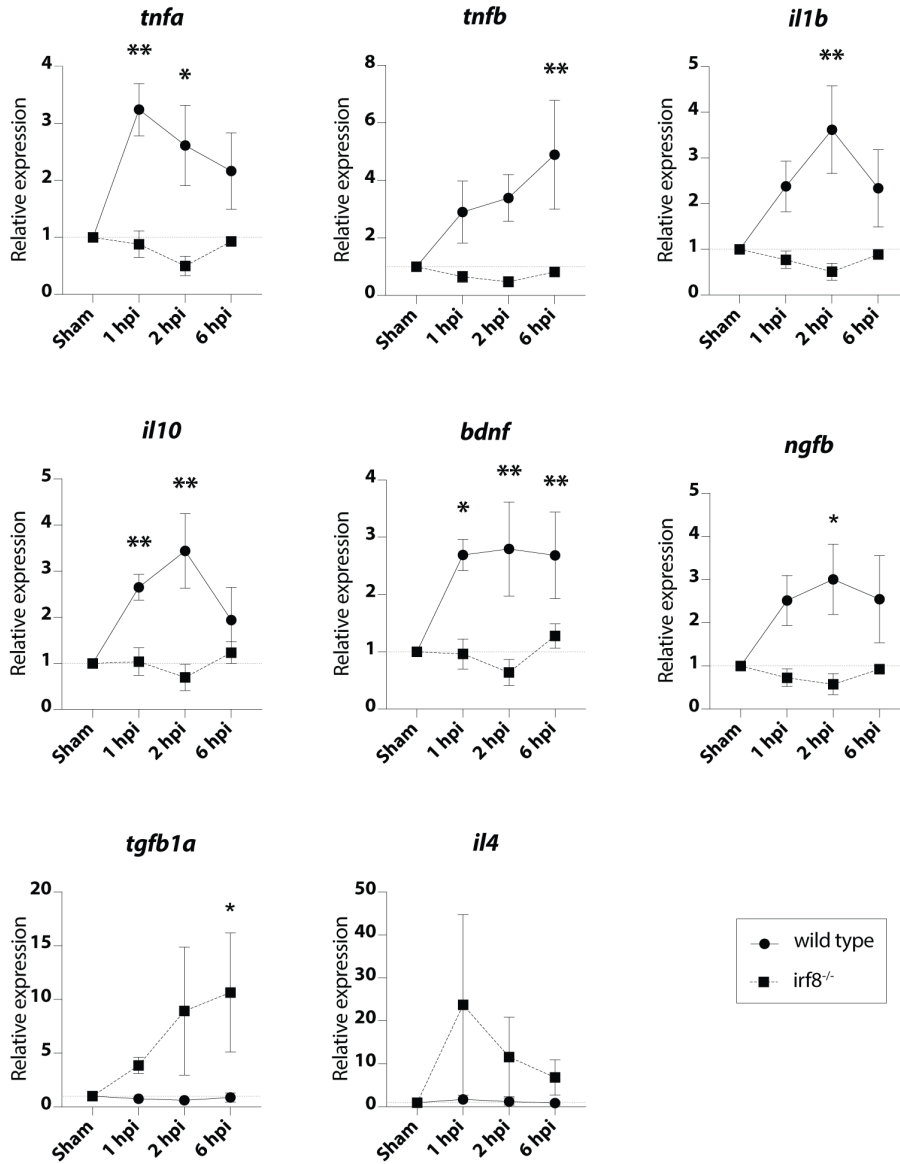


Figure 6.8: Changes in cytokine and neurotrophic factor transcript levels elicited by injury are altered in *irf8*^{-/-} mutants. Relative quantification of mRNA transcript levels via qRT-PCR. Significance was determined via Two-Way ANOVA and relates to sham values of respective genotype. *, $p \leq 0.05$; **, $p \leq 0.01$. Per replicate, the heads of 50 animals were pooled. $n \geq 3$ per timepoint.

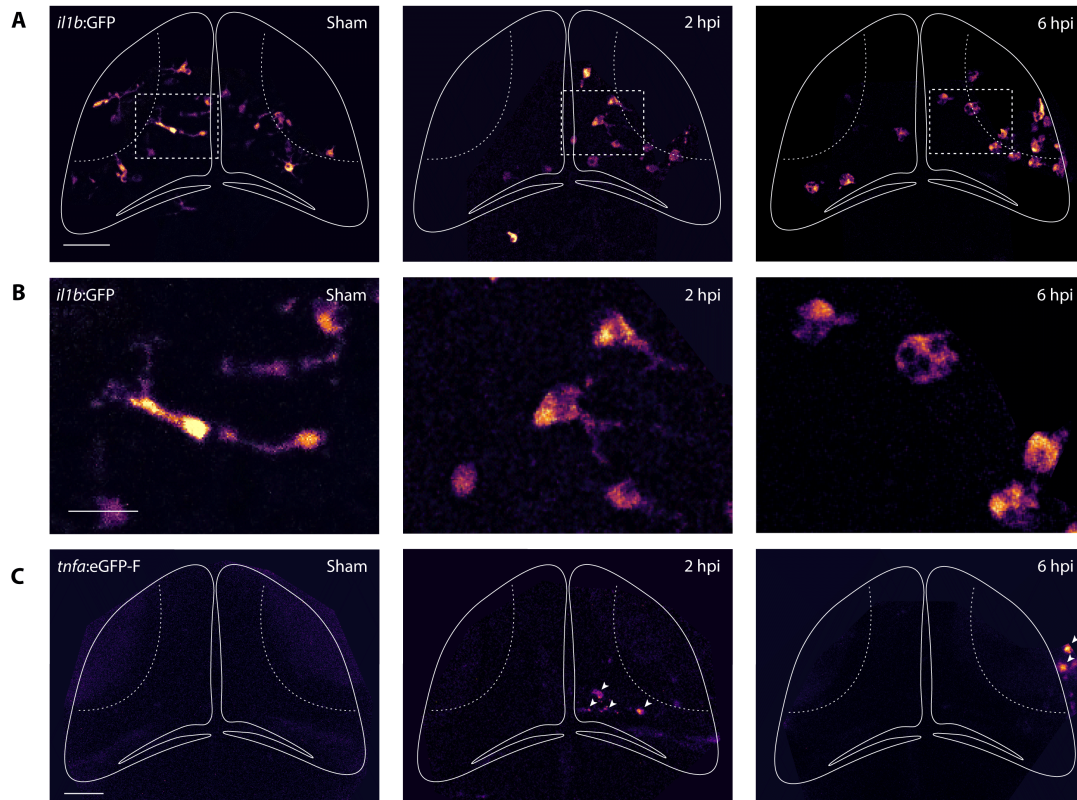


Figure 6.9: **Cells with microglia and macrophage morphology express *il1b* and *tnfa*.** (A) Images taken from *il1b:GFP* transgenic larvae either in control animals, or 2 or 6 hpi. (B) Close-ups of images in (A); location in tectum indicated by dashed boxes in (A). Notice the change of morphology of cells expressing *il1b* at 6 hpi (C) Representative images acquired using the *tnfa:eGFP-F* transgenic line.

6.5 Inhibition of pro-inflammatory cytokine Tnfa results in a reduction of secondary cell death

As I aimed to assess the role of microglia in secondary cell death, I made use of the CRISPR/Cas9 system to target *tnfa*, which I had shown to be present in cells with microglial morphology two hours after brain injury (Fig. 6.9 C). Targeting *tnfa* using a guide previously published by Tsarouchas et al. (2018), I detected a reduction in secondary cell death following brain injury at 6 hpi in *H2A:GFP* larvae (Fig. 6.10). Previous research in rodents had shown an ambiguous role for $\text{TNF}\alpha$ following brain injury - being neurotoxic or -protective depending on receptor subtype distribution (Bruce et al., 1996; Jara et al., 2007; Longhi et al., 2013; Talley et al., 1995). My data suggested that *Tnfa* serves a predominantly neurotoxic role following brain injury in larval zebrafish.

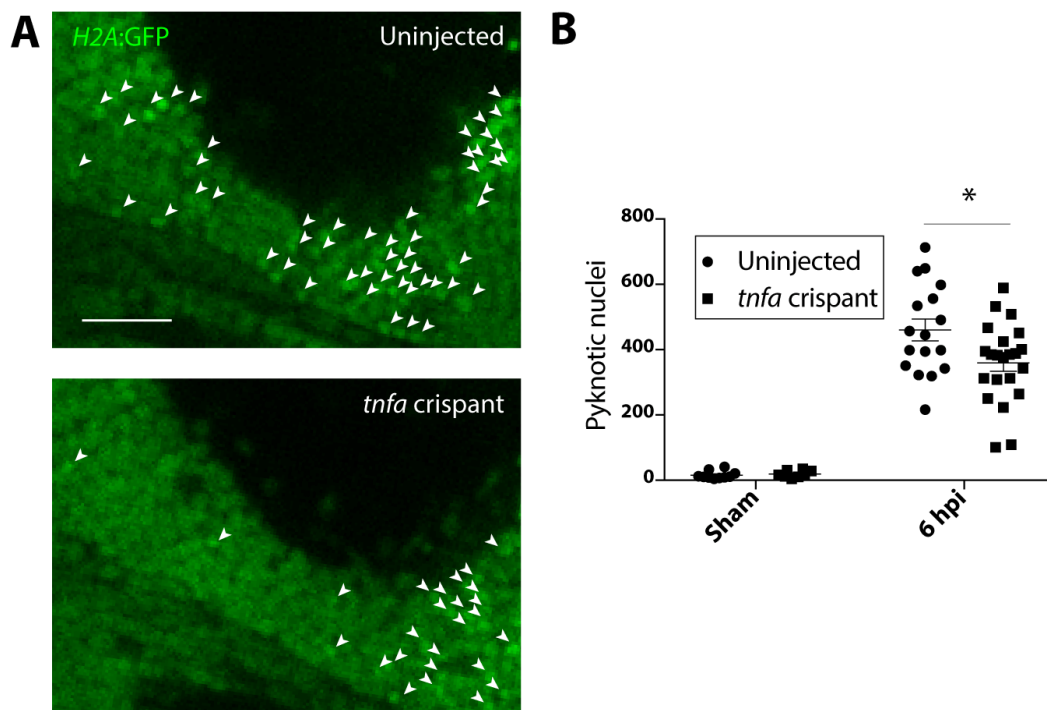


Figure 6.10: *tnfa* crisprants exhibit a reduction in secondary cell death following brain injury. (A) Representative close-up images of injury site in uninjected or *tnfa* crisprant transgenic *H2A:GFP* larvae at 6 hpi. Arrowheads point to pyknotic nuclei. Scale bar, 25 μm . (B) Quantification of pyknotic nuclei in uninjected or *tnfa* crisprant animals either uninjured (sham) or 6 hpi. *, $p \leq 0.05$ in Two-Way ANOVA; $n \geq 9$ per group.

6.6 Microglia/macrophages increase rate of phagocytosis following injury

In addition to production of cytokines and trophic factors, the ability to phagocytose particles, including pathogens or cellular debris, is a key function of microglia/macrophages. This is mediated by recognition of PAMPs and DAMPs. In previous experiments, I had observed phagocytosis of PI⁺ debris by mpeg1⁺ cells following injury (Fig. 6.1). Furthermore, double transgenic animals labelling microglia/macrophages and neurons (*mpeg1:GFP;NBT:dsRed*) revealed the presence of dead neurons inside mpeg1⁺ cells following injury (Fig. 6.11). As primary necrotic cell death can elicit secondary cell death via a variety of molecular mechanisms, for example by spillage of toxic intracellular factors, I hypothesised that phagocytosis could be beneficial in order to contain noxious intracellular substances released from necrotic cells. I therefore next aimed to quantify and perturb phagocytosis in order to draw conclusions on its effect following brain injury.

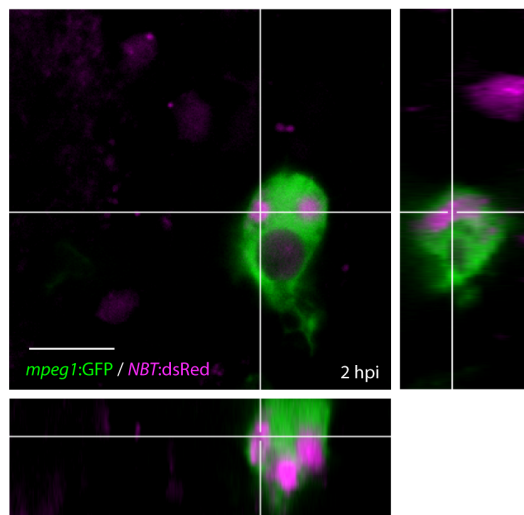


Figure 6.11: **Orthogonal view of neurons (magenta) in mpeg1⁺ cell (green) at 2 hours post injury.** Scale bar, 10 μ m

To investigate whether microglia increased their phagocytic activity following injury, I performed timelapse imaging for 48 min before an injury, and then for 48 min after injury (starting from 0.5 h post injury), acquiring a stack of the whole optic tectum every 6 min. I used the *mpeg1:GFP* transgenic line to visualise microglia/macrophages and bath application of PI to stain dead cells, and performed quantification using the 3D software IMARIS. Quantification of phagocytic events before and after injury revealed a significant increase of phagocytosis of PI⁺ cells following injury from no observed events before to 1.23 ± 0.4 per 48 min after injury (**, $p \leq 0.01$ in Mann-Whitney Test) (Fig. 6.12 A-C). However, due to the lack of PI⁺ cells in the optic tectum of sham animals at 4 days post fertilisation, this dataset was only minimally informative. Therefore, I also quantified

overall phagocytosis. To this end, I quantified engulfments of both PI⁺ and PI⁻ cells (most likely early apoptotic cells which are abundantly engulfed by microglia in 3 and 4 dpf zebrafish (Casano et al., 2016; Mazaheri et al., 2014)), which could occur either by cell rear movement (ball-chain formation followed by movement of the microglial cell towards the PI^{+/-} cargo with subsequent engulfment and visualisation of PI^{+/-} cell inside the microglial cell), or phagocytic branch retraction (formation of ball-chain around PI^{+/-} cell followed by retraction and visualisation of PI^{+/-} cell inside microglia) as previously described (Mazaheri et al., 2014) (Fig. 6.12 E). This data confirmed that overall phagocytosis was indeed increased at 0.5 hpi. Before injury, 0.61 ± 0.22 phagocytic events could be observed on average per *mpeg1*⁺ cell in the brain within 48 min. At 0.5 hours post injury, this was significantly increased to 2.21 ± 0.37 per 48 min (**, $p \leq 0.01$, $n = 8$ animals) (Fig. 6.12 D-F, Movies S6 and S7). Therefore, I demonstrated that in addition to changes in cell migration and displacement (Fig. 6.2), *mpeg1*⁺ cells also changed their phagocytic activity in response to injury.

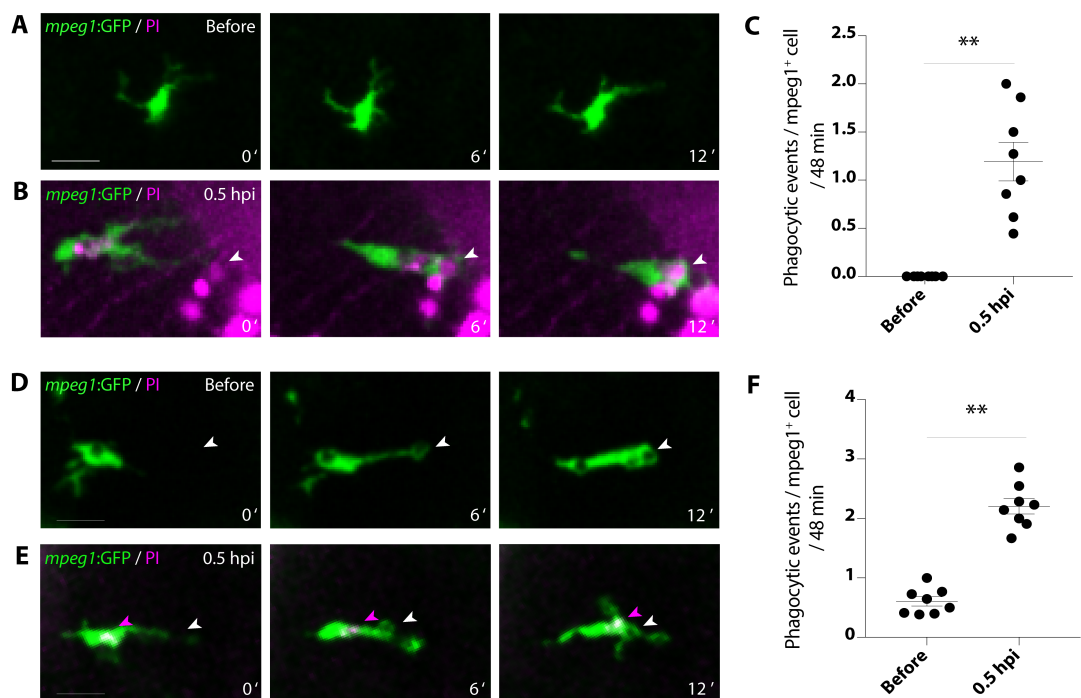


Figure 6.12: **Phagocytosis is significantly increased upon injury.** (A, B) Representative images of time-lapses of *mpeg1*:GFP animals stained with PI either before or 0.5 h after injury. Scale bar, 15 μ m. (C) Quantification of average phagocytic events of PI⁺ cells per *mpeg1*⁺ cell per 48 minutes. **, $p \leq 0.01$ in Mann-Whitney Test. $n \geq 8$ animals / group. (D, E) Representative images phagocytosis in *mpeg1*:GFP animals either before (D) or 0.5 h after injury (E). Representative *mpeg1*:GFP⁺ cell in (D) is engulfing PI⁻ cargo, while *mpeg1*:GFP⁺ cell in (E) has already engulfed PI⁺ cargo and is currently engulfing PI⁻ cargo. Scale bar, 15 μ m. (F) Quantification of average phagocytic events per *mpeg1*⁺ cell per 48 minutes. **, $p \leq 0.01$ in Mann-Whitney Test. $n = 8$ animals / group.

🎬 Figure corresponds to movies S6 (A, before) and S7 (B, 0.5 hpi).

To determine whether radial glia, which reportedly possess phagocytic capacity (Amaya et al., 2015; Nacher et al., 1999; Springer and Wilson, 1989), participate in phagocytosis following injury, I per-

formed timelapse imaging of *her4.3*:GFP larvae bathed in PI. In contrast to microglia/macrophages, *her4.3*⁺ positive radial glia appeared static following the injury and I did not observe any PI⁺ cells within radial glia or radial glia processes both in sham or injured animals. This, in addition to the fact that peripheral macrophages or neutrophils did not enter the brain following injury, suggested that microglia are the predominant phagocytes following brain injury in larval zebrafish.

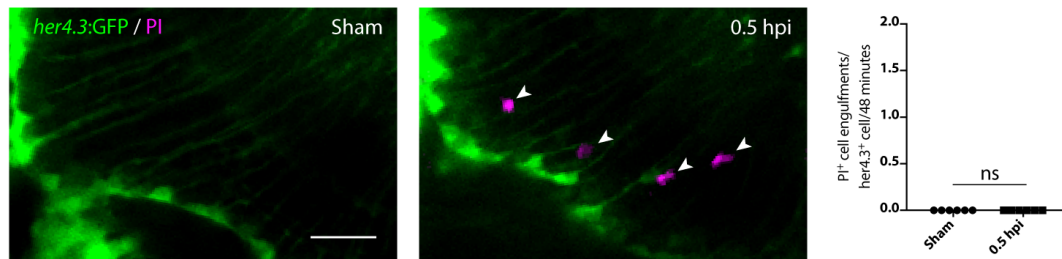


Figure 6.13: No internalised PI⁺ cells or debris can be seen in *her4.3*⁺ radial glia in sham or injured animals. Scale bar, 25 μ m. ns in Mann-Whitney test; n = 6 animals / group

6.7 Inhibition of phagocytosis leads to an increase of secondary cell death

As I hypothesised that rapid phagocytosis of dead cells in the injured tectum could prevent an exacerbation of secondary cell death, I expected inhibition of phagocytosis would lead to an elevated number of pyknotic nuclei at 6 hpi. To achieve an inhibition of phagocytosis, I employed two approaches; both involved interference with the phosphatidyl serine (PS) receptors to prevent microglial recognition of necrotic and apoptotic cells.

6.7.1 Pharmacological inhibition of phagocytosis via bath application of L-SOP

For a pharmacological, acute inhibition of phagocytosis, I treated injured and sham larvae with 1 μ M of *O*-Phospho-*L*-Serine, further referred to as L-SOP, with a pre-incubation of 1 h prior to injury to allow for sufficient uptake into the brain. L-SOP mimicks PS, which is a molecule exposed on necrotic (energy-independent) and apoptotic (energy-dependent) cells and is an important molecule recognised by microglial and macrophage receptors prior to phagocytosis (Bratton et al., 1997; Brouckaert et al., 2004; Krysko et al., 2004; Li et al., 2015; Segawa and Nagata, 2015). L-SOP saturates these receptors, therefore 'blinding' microglia to apoptotic cells, and has previously been shown to decrease the phagocytic uptake of apoptotic neurons by microglia in the zebrafish retina *in vivo* and rat cell culture *in vitro* (Bailey et al., 2010; Witting et al., 2000).

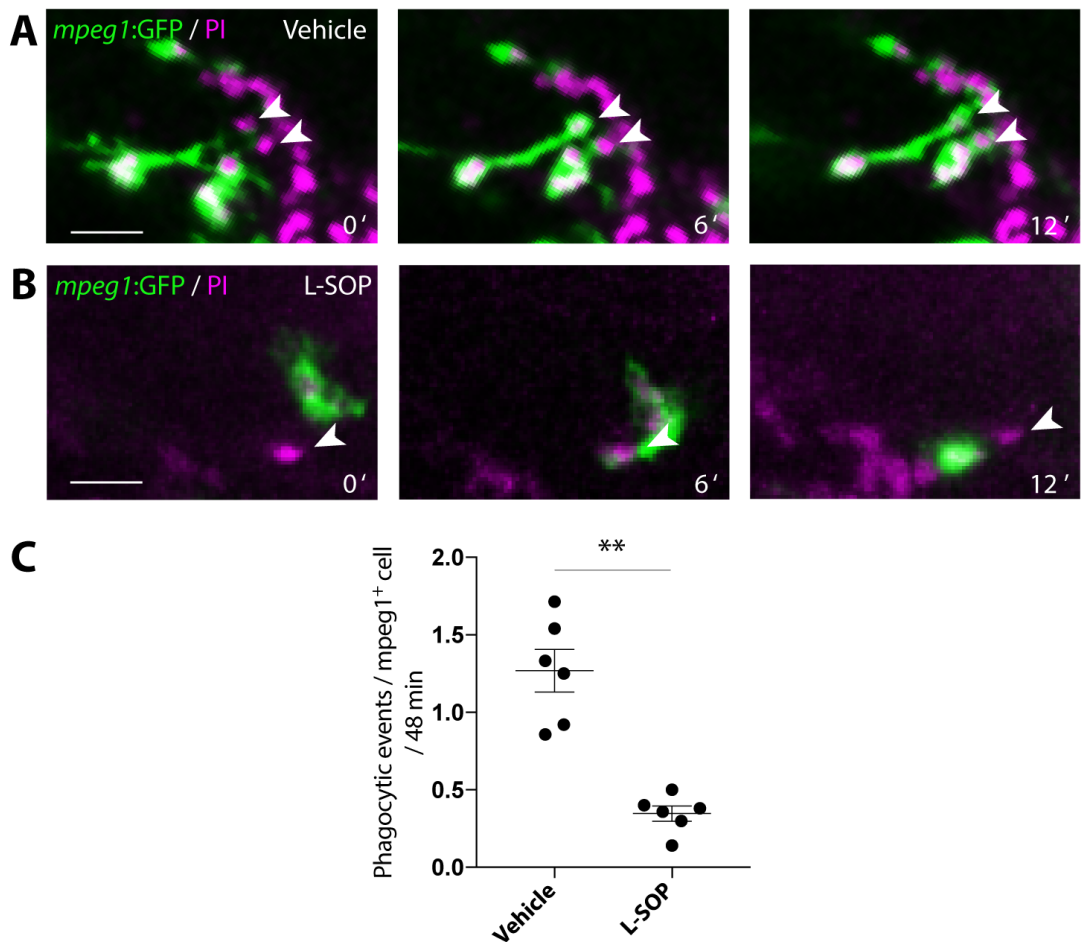


Figure 6.14: **Phagocytosis of PI⁺ cells is significantly decreased after treatment with L-SOP.** Representative images of timelapses of vehicle- (A) or L-SOP-treated (B) animals following injury. Scale bar, 15 μ m. (C) Quantification of average PI⁺ phagocytic events per *mpeg1*⁺ cell per 48 minutes. **, $p \leq 0.01$ in Student's *t*-Test. $n \geq 6$ animals / group.

■ Subfigure (B) corresponds to supplementary movie S8.

I treated animals with vehicle or L-SOP and quantified phagocytic events in a given time frame as previously. L-SOP treatment significantly decreased, but did not completely abolish, phagocytosis of PI⁺ cells between 0.5 hpi and 1.15 hpi (Fig. 6.14). Compared to an average of 1.23 ± 0.12 phagocytic events per *mpeg1*⁺ cell per 45 minutes in vehicle treated animals, L-SOP treated animals only displayed 0.35 ± 0.05 (**, $p \leq 0.01$ in Student's *t*-test), exhibiting a 72% reduction of phagocytic events.

To rule out that L-SOP affected microglial reactivity to the injury, I quantified recruitment of *mpeg1*⁺ cells to the lesion site in larvae treated either with vehicle or L-SOP. There was no significant difference of recruitment of *mpeg1*:GFP⁺ cells between the two groups (Fig. 6.15 A). Furthermore, as L-SOP has been shown to act as a group III metabotropic glutamate receptor agonist *in vitro* (Koulen et al., 1999), I wanted to assess whether L-SOP modified calcium dynamics

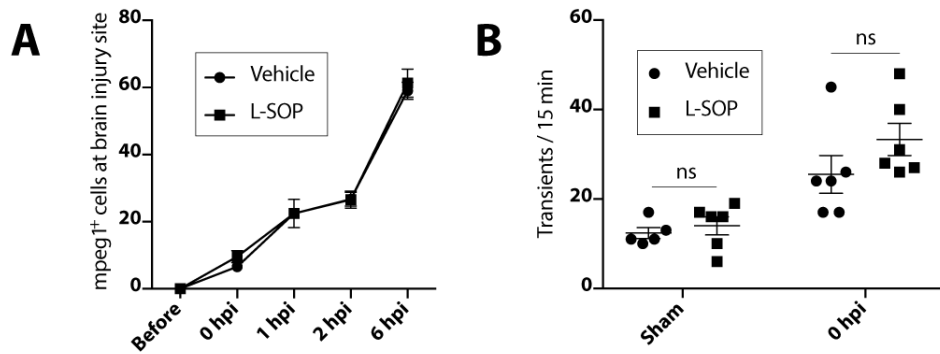


Figure 6.15: **Effect of L-SOP treatment on recruitment of mpeg1:GFP⁺ cells towards the site of brain injury (A), and effect on calcium transients in uninjured and injured β -actin:GCaMP6f larvae (B).** L-SOP had no significant effect on either of these two parameters. **(A)** ns for all timepoints in Two-Way ANOVA. **(B)** ns in Two-Way ANOVA.

in our model. I therefore quantified calcium transients in β -actin:GCaMP6f larvae treated with L-SOP or vehicle, which revealed that L-SOP did not significantly alter calcium dynamics in either sham or injured animals (Fig. 6.15 B).

To assess whether a reduction of phagocytosis affected secondary cell death, I treated *H2A:GFP* animals with L-SOP and quantified the number of pyknotic nuclei at 6 hpi. L-SOP treatment significantly increased the number of pyknotic nuclei at 6 hpi in injured, but not in sham animals (Fig. 6.16 A, C), which suggested that inhibition of phagocytosis did not result in increased cell death under baseline conditions. However, while this increase of pyknotic nuclei at 6 hpi was consistent with an overall neuroprotective effect of microglia, it could also be a direct result of reduced phagocytic clearance of dead cells resulting in accumulation of pyknotic nuclei over time. To exclude this possibility, I therefore performed timelapse imaging of *H2A:GFP* larvae between 4.5 and 5 hpi and quantified the number of newly appearing pyknotic nuclei, which provided me with a direct measure of the rate of secondary cell death. The number of newly appearing pyknotic nuclei - and therefore, the rate of secondary cell death -, was significantly increased in larvae treated with 1 μ M L-SOP compared to vehicle-treated larvae (Fig. 6.16 B, D), which suggested a neuroprotective role for phagocytosis following brain injury.

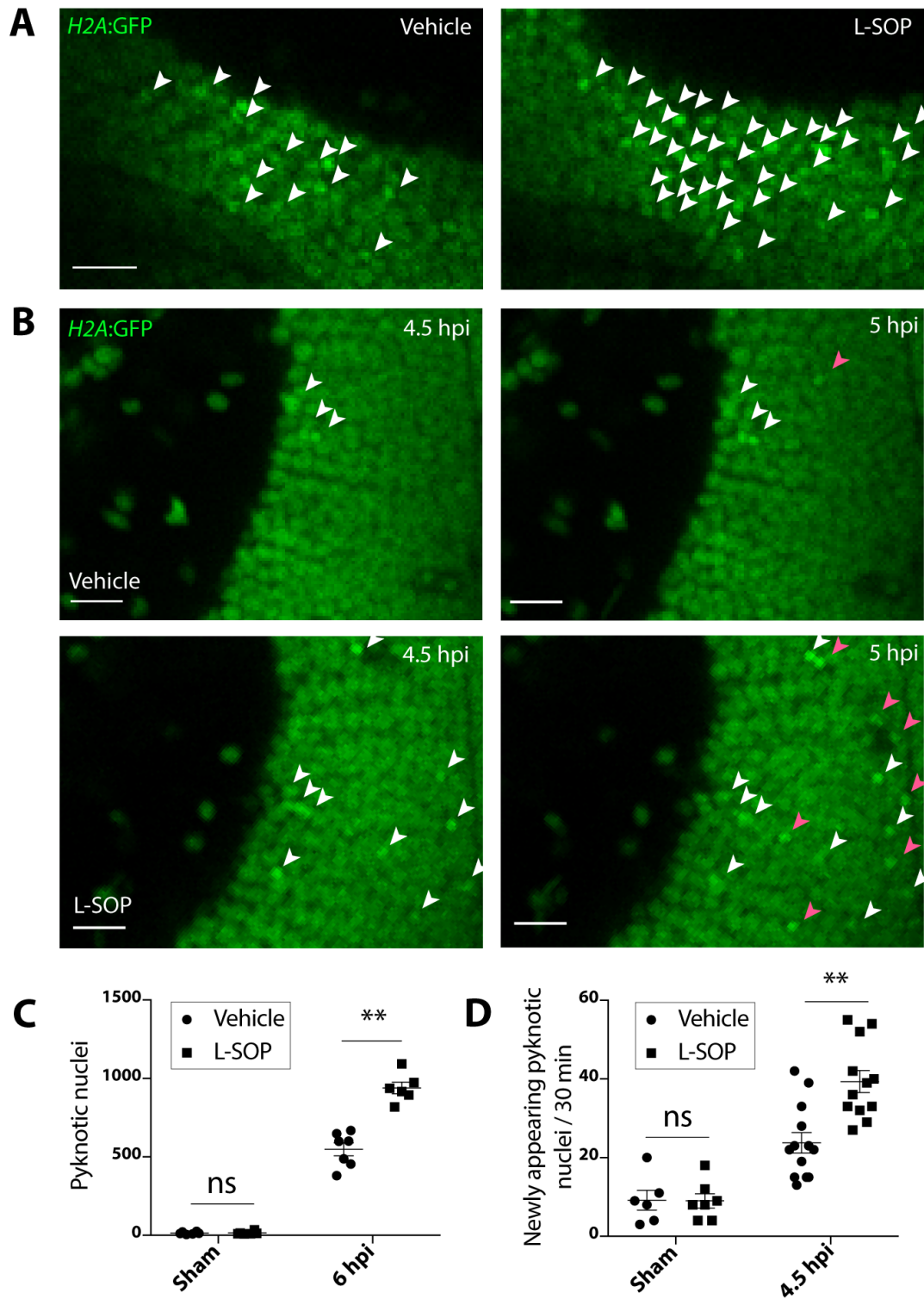


Figure 6.16: **Microglial phagocytosis limits secondary cell death.** (A) Representative images of vehicle- or L-SOP-treated animals at 6 hpi. Scale bar, 25 μ m. (B) Representative images of two timepoints of timelapse of vehicle- or L-SOP-treated animals between 4.5 and 5 hpi. Scale bar, 25 μ m. (C) Quantification of pyknotic nuclei in sham or injured animals treated with vehicle or L-SOP. **, $p \leq 0.01$ in Two-Way ANOVA. $n \geq 6$ animals / group. (D) Quantification of newly appearing pyknotic nuclei in sham or injured animals treated with vehicle or L-SOP. **, $p \leq 0.01$ in Two-Way ANOVA. $n \geq 6$ animals / group.

6.7.2 Genetic manipulation of phagocytosis using CRISPR/Cas9 targeted mutation of *adgrb1a/b*

To confirm my findings obtained by pharmacological inhibition of phagocytosis, I employed a second, genetic approach to disrupt PS recognition. Using CRISPR/Cas9-mediated gene editing, I targeted PS receptor BAI1 that has previously been shown to mediate engulfment of dead cells both in mammals (Park et al., 2007a) and zebrafish (Mazaheri et al., 2014). Zebrafish possess two paralogues of BAI1 (Harty et al., 2015), named *adgrb1a* and *adgrb1b*. Injection of guide RNAs with the Cas9 enzyme into one cell stage zebrafish embryos has been shown to efficiently generate mutations in a high number of cells and allows for study of gene function in the F0 generation, which we call crispants (Jao et al., 2013). To disrupt function of the two zebrafish BAI1 paralogues, I injected guide RNAs targeting exon 1 of *adgrb1a* and exon 4 of *adgrb1b* in one cell embryos, which indeed resulted in efficient disruption of these two genes as shown by loss of endonuclease restriction sites (Fig. 6.17 A). Importantly, disruption of these genes also resulted in a transcript level reduction of more than 50% for both genes (Fig. 6.17 B). Finally, we also confirmed mutation by sequencing of genomic DNA, which revealed a 54% mutation rate in *adgrb1a* (Fig. 6.18), and a 93% mutation rate in *adgrb1b* (Fig. 6.19).

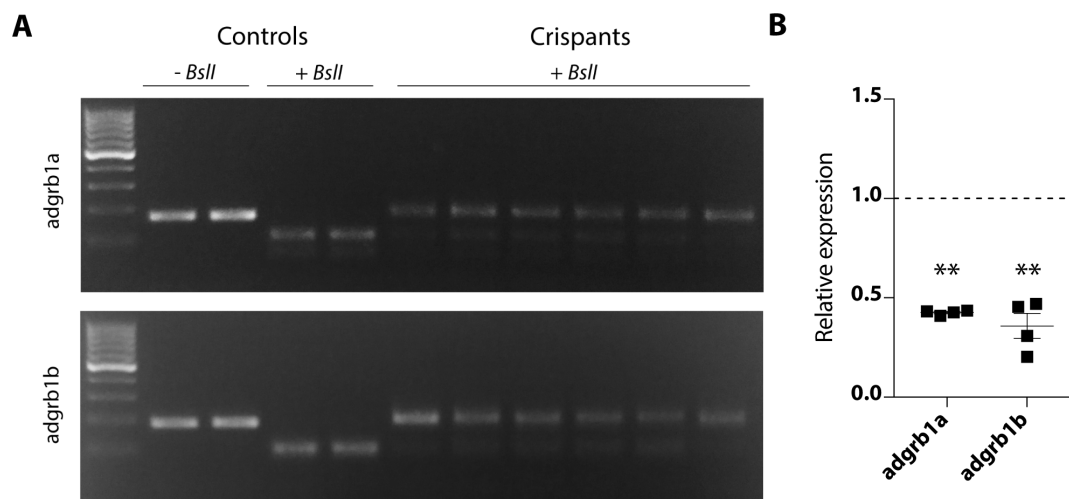


Figure 6.17: **CRISPR-guided mutation of *adgrb1a* and *adgrb1b* causes loss of endonuclease restriction site and reduction of transcript levels.** (A) Representative gel image following PCR product digestion with *BspI* in uninjected controls and crispants. (B) qRT-PCR analysis of relative expression of *adgrb1a* and *adgrb1b* transcript levels in whole larval bodies at 4 dpf. **, $p \leq 0.01$ in One-Way ANOVA compared to uninjected controls; 10 animals pooled per sample; $n = 4$.

adgrb1a

Mutations in 37 out of 68 sequenced alleles (54% mutation rate)

GTGACCCACGCAATGCTGTTGCTCCACAAGGGGGGGCTGCTGGATATATGCTTTAGTGCCCGACTGCCTG	Wild type	x31
GTGACCCACGCAATGCTGTTGCTCCACAAtaccacagaatttaaagtctacaatactctagccaag [...]	+341	(-2, +343)
[...] <u>gagtcgctctggagtaactggagtcagtttatgataagcgaccacaccatgctcgcaatgat [...]</u>	+114	(-125, +239)
GTGACCCACGCAATGCTGTTGCTCCACAAtataaaacatttggatataatGGGGCTGCTGGATATAT	+20	(-3, +23)
GTGACCCACGCAATGCTGTTGCTCCACAAtgatatatgcttttagtgcctgctgctggatataatGCTTTAG	+14	(-8, +22)
GTGACCCACGCAATGCTGTTGCTCCACAAtgctgttggcttgggggggctgctggatataatGCTTTAGT	+13	(-2, +15)
GTGACCCACGCAATGCTGTTGCTCCACAAGGGGGGcatatatacctgctggatataatGCTTTAGTGCCC	+9	(-1, +10)
GTGACCCACGCAATGCTGTTGCTCCACAAtgctccacaggggGCTGCTGGATATATGCTTTAGTGCCCGAC	+6	(-6, +12)
GTGACCCACGCAATGCTGTTGCTCCACAAtgctgggggggctgctggatataatGCTTTAGTGCCCGACT	+5	
GTGACCCACGCAATGCTGTTGCTCCACAAtgctggatataatgctgctggatataatGCTTTAGTGCCCGACTG	+3	(-7, +11)
GTGACCCACGCAATGCTGTTGCTCCACAAtgctgggctgctggatataatGCTTTAGTGCCCGACTGCTG	+3	(-5, +8)
GTGACCCACGCAATGCTGTTGCTCCACAAtgctgggctgctggatataatGCTTTAGTGCCCGACTGCTG	+3	(-3, +6)
GTGACCCACGCAATGCTGTTGCTCCACAAtgctgggctgctggatataatGCTTTAGTGCCCGACTGCTG	+1	(-8, +9)
GTGACCCACGCAATGCTGTTGCTCCACAAtgctgggctgctggatataatGCTTTAGTGCCCGACTGCTG	+1	(-5, +6)
GTGACCCACGCAATGCTGTTGCTCCACAAtgctgggctgctggatataatGCTTTAGTGCCCGACTGCTG	*2	x3
GTGACCCACGCAATGCTGTTGCTCCACAAtgctgggctgctggatataatGCTTTAGTGCCCGACTGCTG	*1	
GTGACCCACGCAATGCTGTTGCTCCACAAtatagctgctggatataatGCTTTAGTGCCCGACTGCTGCTG	-1	(-7, +6)
GTGACCCACGCAATGCTGTTGCTCCACAAtgctgggctgctggatataatGCTTTAGTGCCCGACTGCTG	-1	(-6, +5)
GTGACCCACGCAATGCTGTTGCTCCACAAtgctgggctgctggatataatGCTTTAGTGCCCGACTGCTG	-1	
GTGACCCACGCAATGCTGTTGCTCCACAAtatagctgctggatataatGCTTTAGTGCCCGACTGCTG	-2	(-2, +5)
GTGACCCACGCAATGCTGTTGCTCCACAAtgctgggctgctggatataatGCTTTAGTGCCCGACTGCTG	-2	
GTGACCCACGCAATGCTGTTGCTCCACAAtgctgggctgctggatataatGCTTTAGTGCCCGACTGCTG	-3	(-9, +6)
GTGACCCACGCAATGCTGTTGCTCCACAAtgctgggctgctggatataatGCTTTAGTGCCCGACTGCTG	-3	(-5, +2)
GTGACCCACGCAATGCTGTTGCTCCACAAtgctgggctgctggatataatGCTTTAGTGCCCGACTGCTG	-3	x2
GTGACCCACGCAATGCTGTTGCTCCACAAtatagctgctggatataatGCTTTAGTGCCCGACTGCTG	-4	(-10, +6)
GTGACCCACGCAATGCTGTTGCTCCACAAtgctgggctgctggatataatGCTTTAGTGCCCGACTGCTG	-4	(-5, +1)
GTGACCCACGCAATGCTGTTGCTCCACAAtgctgggctgctggatataatGCTTTAGTGCCCGACTGCTG	-5	(-13, +8)
GTGACCCACGCAATGCTGTTGCTCCACAAtgctgggctgctggatataatGCTTTAGTGCCCGACTGCTG	-5	(-10, +5)
GTGACCCACGCAATGCTGTTGCTCCACAAtgctgggctgctggatataatGCTTTAGTGCCCGACTGCTG	-5	(-6, +1)
GTGACCCACGCAATGCTGTTGCTCCACAAtgctgggctgctggatataatGCTTTAGTGCCCGACTGCTG	-9	
GTGACCCACGCAATGCTGTTGCTCCACAAtgctgggctgctggatataatGCTTTAGTGCCCGACTGCTG	-11	
GTGACCCACGCAATGCTGTTGCTCCACAAtgctgggctgctggatataatGCTTTAGTGCCCGACTGCTG	-15	
GTGACCCACGCAATGCTGTTGCTCCACAAtgctgggctgctggatataatGCTTTAGTGCCCGACTGCTG	-16	
GTGACCCACGCAATGCTGTTGCTCCACAAtgctgggctgctggatataatGCTTTAGTGCCCGACTGCTG	-18	
GTGACCCACGCAATGCTGTTGCTCCACAAtgctgggctgctggatataatGCTTTAGTGCCCGACTGCTG	-21	(-24, +3)

Figure 6.18: Mutations in *adgrb1a* transcripts revealed by sequencing. First line shows wild type sequence, with guide RNA target sequence underlined and highlighted protospacer adjacent motive (PAM) site. Insertions are highlighted with purple, while deletions are represented by -. Total number of inserted or deleted bases and frequency of each mutation shown next to each sequence.

adgrb1b

Mutations in 42 out of 45 sequenced alleles (93% mutation rate)

CGACTCAGAGAACC CGCGAGTGTAAACGGACCCCTACCGCGGCTCCGAGTGCAGAGGGGAATGGCTGGA	Wild type	x3
CGACTCAGAGAACC CGCGAGTGTAAACGGACCCCTaacctaacctaacctaacctaacctaacctaacct [...]	+88	(-3, +91)
CGACTCAGAGAACC CGCGAGTGTAAACGGACCCCTAggtggggaatggctggagCGGCGGCTCCGAGTGCAG	+15	(-2, +17)
CGACTCAGAGAACC CGCGAGTGTAAACGGACCCCTctgcentggTACGGCGGCTCCGAGTGCAGAGGGGAAT	+7	(-1, +8)
CGACTCAGAGAACC <u>cgcggggtgtaacggatcctcatteatc</u> CGGCGGCTCCGAGTGCAGAGGGGAATGCC	+4	(-24, +28)
CGACTCAGAGAACC CGCGAGTGTAAACGGACCCCTCATcatcCGGCGGCTCCGAGTGCAGAGGGGAATGCC	+4	(-1, +5)
CGACTCAGAGAACC CGCGAGTGTAAACGGACCCCTgagtgacagGCGCGGCTCCGAGTGCAGAGGGGAATGGCT	+3	(-7, +10)
CGACTCAGAGAACC CGCGAGTGTAAACGGACCCCTCATACGGCGGCTCCGAGTGCAGAGGGGAATGGCTGG	+1	x2
CGACTCAGAGAACC CGCGAGTGTAAACGGACCCCTCA-gTGGCGGCTCCGAGTGCAGAGGGGAATGGCTGGA	-1	(-3, +2)
CGACTCAGAGAACC CGCGAGTGTAAACGGACCCCTC--gcggaacccTACGGCGGCTCCGAGTGCAGAGGGGAATGGCTGGA	-2	(-11, +9)
CGACTCAGAGAACC CGCGAGTGTAAACGGACCCCTC--ACGGCGGCTCCGAGTGCAGAGGGGAATGGCTGGA	-2	
CGACTCAGAGAACC CGCGAGTGTAAACGG--gcccTACGGCGGCTCCGAGTGCAGAGGGGAATGGCTGGA	-3	(-7, +4)
CGACTCAGAGAACC CGCGAGTGTAAACGGACCC--TACGGCGGCTCCGAGTGCAGAGGGGAATGGCTGGA	-3	
CGACTCAGAGAACC CGCGAGTGTAAACGGACCCCTCA----gactCCGAGTGCAGAGGGGAATGGCTGGA	-6	(-8, +2)
CGACTCAGAGAACC CGCGAGTGTAAACGGACCCCTCA----atcatTCCGAGTGCAGAGGGGAATGGCTGGA	-4	(-9, +5)
CGACTCAGAGAACC CGCGAGTGTAAACGGACCCCT----CGGCGGCTCCGAGTGCAGAGGGGAATGGCTGGA	-4	x2
CGACTCAGAGAACC CGCGAGTGTAAACGGACCCga----GGTCCGAGTGCAGAGGGGAATGGCTGGA	-8	(-10, +2)
CGACTCAGAGAACC CGCGAGTGTAAACGGACCC----GGTCCGAGTGCAGAGGGGAATGGCTGGA	-10	
CGACTCAGAGAACC CGCGAGTGTAAAC--tagCGGCTCCGAGTGCAGAGGGGAATGGCTGGA	-11	(-13, +2)
CGACTCAGAGAACC CGCGAGTGTAAACGGACCC----TCGAGTGCAGAGGGGAATGGCTGGA	-12	x5
CGACTCAGAGAACC CGCGAGTGTAAACGGACCCCT----cgcggaCTCCGAGTGCAGAGGGGAATGGCTGGA	-13	(-19, +6)
CGACTCAGAGAACC CGCGAGTGTAAACGGACCCga----ACGGCGGCTCCGAGTGCAGAGGGGAATGGCTGGA	-13	
CGACTCAGAGAACC CGCGAGTGTAAACGGAC--CCGAGTGCAGAGGGGAATGGCTGGA	-15	
CGACTCAGAGAACC CG--agTACGGCGGCTCCGAGTGCAGAGGGGAATGGCTGGA	-17	(-19, +2)
CGA-----CTCCGAGTGCAGAGGGGAATGGCTGGA	-40	x2
C-----CTCCGAGTGCAGAGGGGAATGGCTGGA	-42	
[...]-----[...]	-98	(-135, +37)

Figure 6.19: Mutations in *adgrb1b* transcripts revealed by sequencing. First line shows wild type sequence, with guide RNA target sequence underlined and highlighted PAM site. Insertions are highlighted, with purple while deletions are represented by -. Total number of inserted or deleted bases and frequency of each mutation shown next to each sequence.

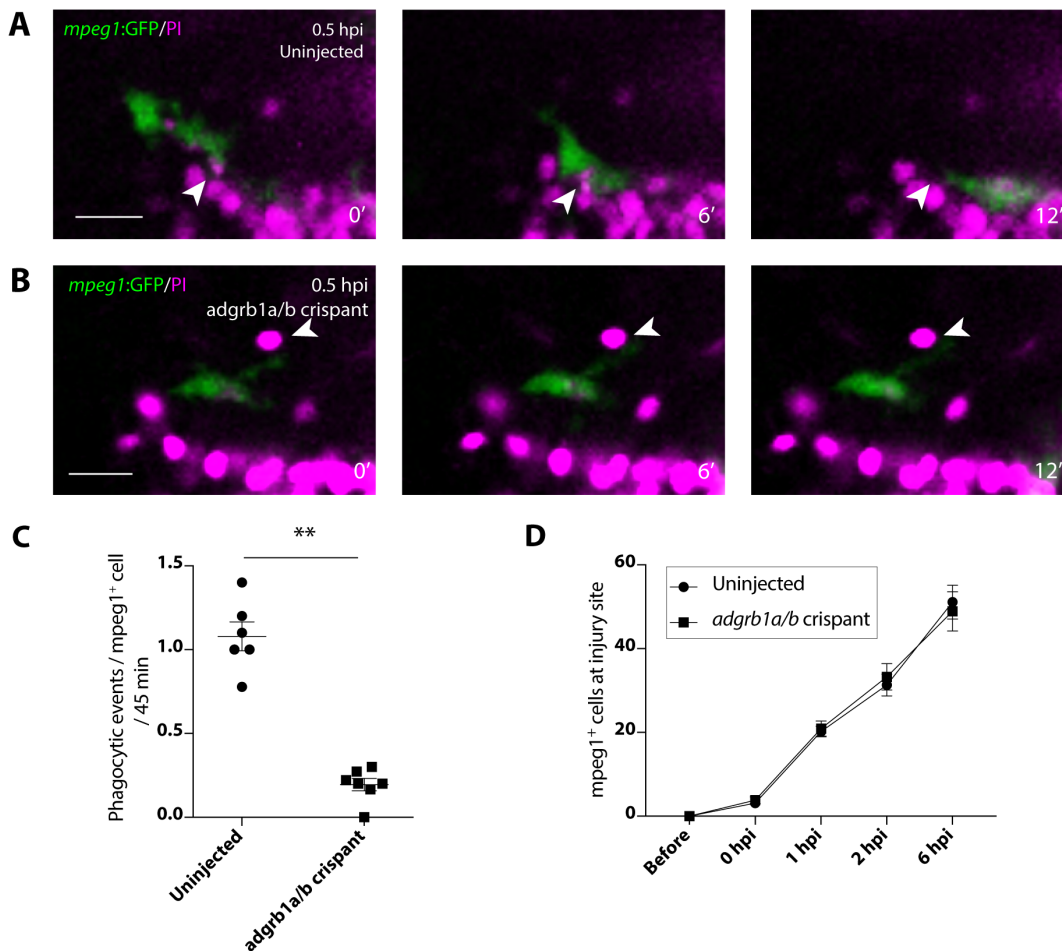


Figure 6.20: **Phagocytosis of PI⁺ cells is significantly decreased after CRISPR/Cas9 targeted mutation of zebrafish paralogues of PS receptor BAI1.** Representative images of timelapses of uninjected (**A**) or crisprant animals (**B**) following injury. Scale bar, 15 μ m. (**C**) Quantification of PI⁺ cells being engulfed per *mpeg1*⁺ cell in 48 minutes. **, $p \leq 0.01$ in Two-Way ANOVA. $n \geq 6$ animals / group. (**D**) Quantification of *mpeg1:GFP*⁺ cells at the site of brain injury before, 0, 1, 2, and 6 hpi. ns for all timepoints in Two-Way ANOVA. $n \geq 9$ animals / group.

■ Subfigure (B) corresponds to supplementary **movie S8**.

Similar to pharmacological manipulation of PS receptors, genetic mutation of *adgrb1a* and *adgrb1b* resulted in a significant decrease of phagocytosis of PI⁺ cells as observed by timelapse imaging of *mpeg1:GFP* transgenic larvae following injury bathed in PI (as above) (Fig. 6.20), while leaving microglial recruitment to the injury site intact (Fig. 6.20 D).

Importantly, genetic manipulation of *adgrb1a* and *adgrb1b* led to an increased number of pyknotic nuclei at 6 hpi (Fig. 6.21 A, C), and resulted in an increased rate of secondary cell death between 4.5 and 5 hpi as previously observed with L-SOP (Fig. 6.21 B, D). The fact that both pharmacological and genetic disruption of PS-mediated phagocytosis yielded similar results in terms of phagocytosis and cell death confirmed that these methods are useful to disrupt microglial phagocytic behaviour, and furthermore provided evidence that microglial phagocytosis exerts a net neuroprotective effect.

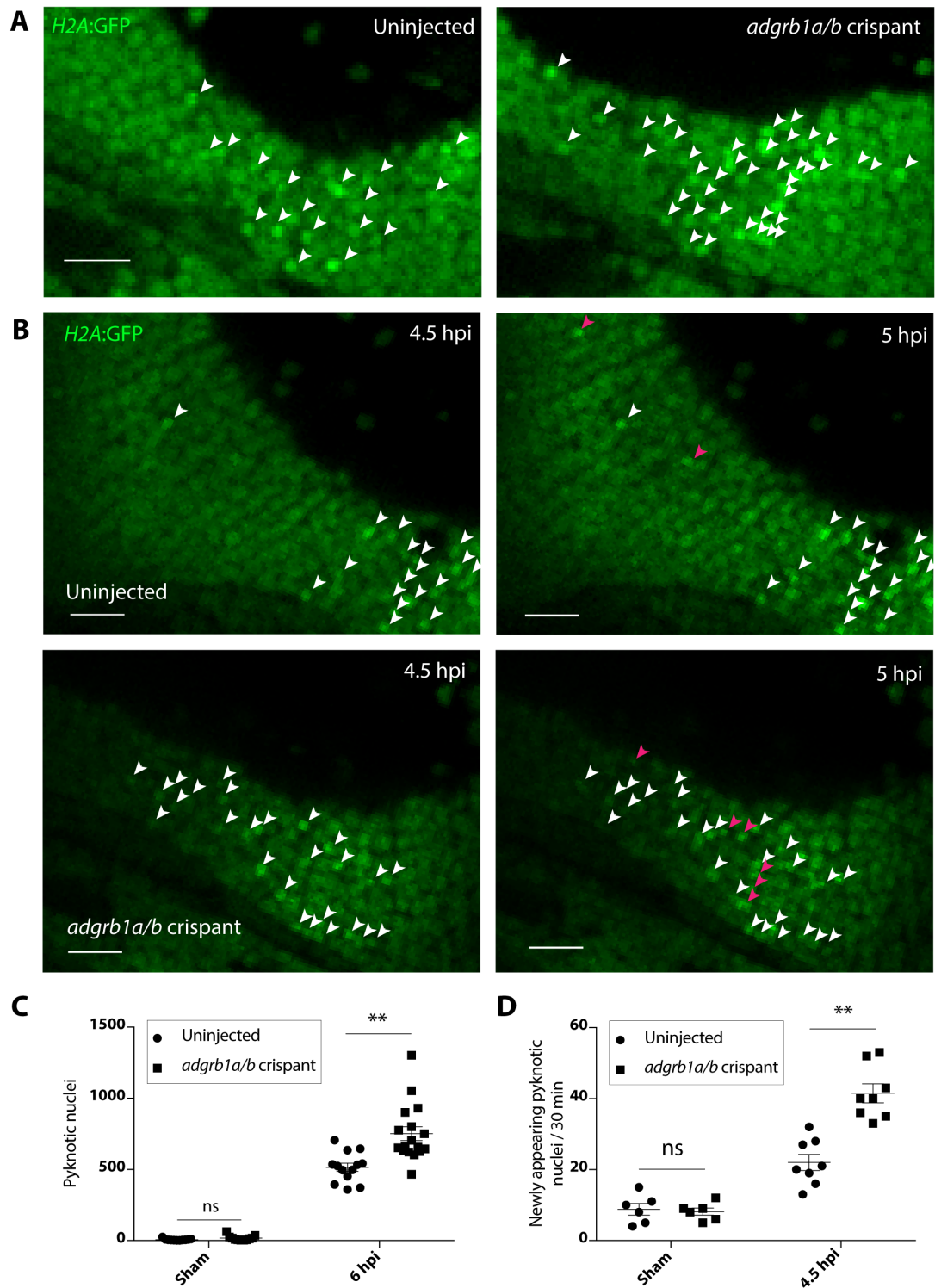


Figure 6.21: Inhibition of microglial phagocytosis through genetic manipulation of *adgrb1a* and *adgrb1b* significantly increases number of pyknotic nuclei at 6 hpi, and increases the rate of secondary cell death. (A) Representative images of uninjected or *adgrb1a/b* crisprant animals at 6 hpi. Scale bar, 25 μ m. (B) Representative images of two timepoints of timelapse of uninjected or *adgrb1a/b* crisprant animals between 4.5 and 5 hpi. Scale bar, 25 μ m. (C) Quantification of pyknotic nuclei in sham or injured uninjected or crisprant animals. **, $p \leq 0.01$ in Two-Way ANOVA. $n \geq 6$ animals / group. (D) Quantification of pyknotic nuclei in sham or injured uninjected or crisprant animals. **, $p \leq 0.01$ in Two-Way ANOVA. $n \geq 6$ animals / group.

6.8 Discussion

In this chapter, I presented my work on the role of microglia/macrophages in secondary cell death following brain injury, with particular focus on phagocytosis. My data shows that microglia react to the injury rapidly - the first microglia arrive at the site of injury within 5 min, and are the predominant phagocytic cell at the site of injury (Fig. 6.3). Microglia phagocytose PI⁺ cells and cellular debris (Fig. 6.12), and by inhibiting phagocytosis either via L-SOP or genetic mutation of phagocytosis receptor BAI1, I was able to demonstrate that phagocytosis can limit secondary cell death (Fig. 6.16, Fig. 6.21).

It was surprising to observe virtually no macrophages or neutrophils entering the brain following injury in wild type larvae. Recruitment of peripheral immune cells is commonly observed following mammalian TBI (Carlos et al., 1997; Clark et al., 1994; Foley et al., 2009; Hsieh et al., 2014; Roth et al., 2014). Even in another larval zebrafish CNS injury assay (spinal cord injury), neutrophils and macrophages arrive early and abundantly (Tsarouchas et al., 2018), while microglia only arrive at the site of injury at 24 to 48 hpi, although this is unsurprising as there are no or only very few resident microglia in the spinal cord in 4 dpf larval zebrafish (Tsarouchas et al., 2018). Using microglia, macrophage, and neutrophil markers (P2Y₁₂ expression and 4C4 immunoreactivity, *mpeg1*:GFP immune cell tracing, and myeloperoxidase expression, respectively) I detected that neither peripheral macrophages nor neutrophils were present in the brain following injury (Fig. 6.3, Fig. 6.7, Fig. 6.5). In *irf8*^{-/-} mutants, which lack microglia/macrophages and have an expanded neutrophil population, there is a significant neutrophil response to injury (Fig. 6.7). While both optic tectum and spinal cord are part of the CNS, a possible explanation for the different composition of immune cells observed at the injury site by Tsarouchas et al. (2018) and my data is the different (cellular) environment of the lesion site. Microglia are abundant in the optic tectum at 4 dpf, while they are not in the spinal cord at 3 dpf (Tsarouchas et al. (2018); Fig. 6.3). Although microglia are able to recruit neutrophils to sites of brain injury (Carlos et al., 1997), they have also been shown to be capable of reducing neutrophil infiltration following neuronal injury in mammalian brain slices (Neumann et al., 2008). Likewise, macrophages residing at the wound have been shown to repel approaching neutrophils following tail fin injury in zebrafish (Tauzin et al., 2014). Whether microglia participate in repulsion of peripheral macrophages and neutrophils, or whether there is a lack of chemoattractant factors for these cells following larval zebrafish brain injury remains to be determined.

6.8.1 Alterations in the whole head transcription levels of cytokines and trophic factors

Brain injury led to a rapid increase in transcript levels of both pro- and anti-inflammatory cytokines. As early as 1 h post injury, several cytokines and trophic factors - including *tnfa*, *il10*, and *bdnf* -

were significantly upregulated in wild type animals. Perhaps unsurprisingly, the lack of microglia in *irf8*^{-/-} mutants abolished the injury-induced changes in many cytokines following brain injury (Fig. 6.8); nonetheless, *tgfb1a* and *il4* were upregulated in *irf8*^{-/-} mutants, which suggested that microglia are not the main cellular source of these cytokines in response to injury.

Quantitative reverse-transcription PCR from whole heads revealed that *tnfa*, a typical pro-inflammatory cytokine, was rapidly upregulated following injury (Fig. 6.8). Using a transgenic reporter line revealed that *tnfa*:eGFP-F⁺ cells were initially detected in the brain (at 2 hpi); these cells were likely a subset of microglia (Fig. 6.9). Interestingly, at 6 hpi, mainly cells on the skin expressed GFP under the *tnfa* promoter. Based on my previous finding that immune cells do not commonly trespass following brain injury in larval zebrafish (Fig. 6.4), this suggests that different populations of microglia/macrophages induce *tnfa* expression at different time points following injury. TNF α has been reported to confer both neurotoxicity and neuroprotection in models of brain injury: deletion of TNF α in mice was shown to significantly improve behavioural recovery in a rodent model of brain injury (Berpohl et al., 2007), but genetic deletion of TNF receptors increased the lesion volume in another study (Bruce et al., 1996); furthermore, TNF α restricted cell death following oxidative stress elicited by NO (Turrin, 2006). A more recent study reported that different subtypes of TNF receptors can modulate the effect of TNF: deletion of the p55 TNF receptor resulted in attenuation of lesion volume and cognitive deficit, while deletion of p75 TNF receptor significantly worsened neuronal injury and cognitive outcome following experimental TBI in rodents (Longhi et al., 2013). This suggests that the effect of TNF α may depend on the temporal and cellular distribution of TNF receptors. Zebrafish possess TNF receptor homologues which carry out functions similar to mammalian TNF receptors (promote cell survival or induce apoptosis, amongst other functions) (Espin et al., 2013). In my injury assay, genetic mutation of *tnfa* resulted in a 30% reduction of pyknotic nuclei at 6 hpi (Fig. 6.10). Based on previous *in vivo* imaging data showing early induction of *tnfa* in cells with microglial morphology, this suggested that Tnfa from a microglial source may act neurotoxic although my manipulation was neither temporally nor spatially restricted, so this needs to be interpreted with caution. As there is no detailed cellular expression atlas of *tnfa* and its receptors during zebrafish development, I cannot speculate on the action of Tnfa on certain cell types. Furthermore, it is unclear whether Tnfa acts directly on neurons to promote neurotoxicity, or indirectly on microglia to promote a more neurotoxic or pro-inflammatory polarisation in zebrafish. To summarise, although my data provide a first overall insight on the role of Tnfa in secondary cell death in zebrafish, much needs to be done to investigate its specific role and to assess translatability to mammalian systems. Zebrafish microglia or neurons could react to Tnfa differently than their mammalian counterparts, for instance by differential receptor expression and downstream pathways. A more thorough understanding could be achieved by a detailed study of Tnf receptor expression in zebrafish using double colour *in situ* hybridisation for Tnf receptors and neuronal or

microglial markers, or by cell-type specific CRISPR/Cas9 knockout of Tnf or its respective receptors.

il1b is another pro-inflammatory cytokine commonly upregulated following experimental brain injury (Liu et al., 1993; Lu et al., 2005). Consistent with this, I found significant upregulation of *il1b* following injury to the larval zebrafish brain using qRT-PCR (Fig. 6.8), and detected *il1b* expression in cells with microglial morphology using the genetic fluorescent reporter line (*il1b*:GFP). IL-1 β is mainly thought to be released by activated microglia, however, it has previously been detected in development and may be a glial growth factor (Dziegielewska et al., 2000; Giulian et al., 1988). In the context of brain injury, *il1b* has been found to cause neuronal apoptosis (Holmin and Mathiesen, 2000; Lu et al., 2005). Wong et al. (2018) recently found that deletion of the IL-1 receptor IL-1R1 specifically on neurons or endothelial cells was able to reduce infarct size following ischaemic insult in mice, while global knockout of IL-1R1 had no effect on the overall infarct size. This suggested a neuroprotective effect of IL-1 receptor 1 mediated signalling on other cell types, such as microglia (Wong et al., 2018). The endogenous inhibitor of the IL-1 β signalling pathway, IL-1 receptor antagonist (IL-1ra), has furthermore been found to mitigate the neurotoxic effects of IL-1 β in experimental models of brain injury (Relton and Rothwell, 1992; Sun et al., 2017b; Toulmond and Rothwell, 1995), and higher serum levels are associated with better patient outcome (Hutchison et al., 2008). Interestingly, endogenous IL-1ra that could act neuroprotective against excitotoxic insults in glial-neuronal co-cultures was found to be produced by microglia, but not other glial cell types *in vitro* (Pinteaux et al., 2006). A recombinant human IL-1ra has qualified for safety and bioavailability in a phase II clinical trial for TBI (Helmy et al., 2014), but no phase III studies have been initiated yet.

Importantly, although wild type animals significantly upregulated several pro-inflammatory cytokines upon injury, I also detected increased expression of the anti-inflammatory cytokine *il10* and the trophic factors *bdnf* and *ngfb* (Fig. 6.8). IL-10 has been shown to confer neuroprotection in a multitude of CNS injury models: traumatic brain injury (Knobloch and Faden, 1998), spinal cord injury (Brewer et al., 1999), and focal stroke (Spera et al., 1998). It is predominantly produced by microglia, and can provide either direct neuroprotection via neuronal IL-10 receptors (Zhou et al., 2009b,a) or by indirect autocrine actions on microglia such as dampening an excessive inflammatory response that may exacerbate neuronal death (Cianciulli et al., 2015; Park et al., 2007b). Similarly, BDNF has been shown to exert neuroprotection (Chen et al., 2007; Wu et al., 2008), potentially due to enhancing microglial phagocytosis (Jiang et al., 2011), and there is evidence to suggest a neuroprotective role for NGF (Fantacci et al., 2013; Philips et al., 2001).

Intriguingly, I detected significantly increased expression of the anti-inflammatory factor *tgfb1* in *irf8*^{-/-} but not wild type animals. While microglia are thought to be the predominant source of *tgfb1a* (Lindholm et al., 1992), neurons have also been suggested to produce it in response to

neuronal injury (Yamashita et al., 1999). Therefore, injured neurons could be the cellular source of *tgfb1a* in *irf8*^{-/-} mutants. Data on TGF- β , the *tgfb1a* homologue in rodents and humans, following brain injury is conflicting - one study found that higher serum TGF- β levels correlated to a better patient outcome at 90 days following injury, suggesting a neuroprotective effect (Taylor et al., 2017), while another found antagonism of TGF- β signalling led to decreased apoptosis in a murine model of brain injury (Patel et al., 2017). The main action of TGF- β following brain injury is thought to be via microglial modulation (Taylor et al., 2017), but in *irf8*^{-/-} mutants these cells are absent. TGF- β is, however, also an effective neutrophil chemoattractant (Brandes et al., 1991; Fava et al., 1991; Reibman et al., 1991), which may explain the high numbers of neutrophils at the injury site in *irf8*^{-/-} mutants; microglia may therefore prevent neutrophil infiltration by suppression of *tgfb1a* expression. However, it is likely that several other factors may have contributed to neutrophil recruitment, such as reactive oxygen species (Niethammer et al., 2009).

This expression dataset - demonstrating increases in both pro- and anti-inflammatory cytokines as well as trophic factors - highlighted once more the complexity of molecular processes occurring following brain injury. However, I used whole head cDNA and so far only study candidate gene expression, which did not allow for discovery of novel, previously unknown genes involved in microglial function in response to injury. To investigate injury-induced changes in microglia in more detail, I therefore employed an RNA-sequencing approach from sorted *mpeg1*:GFP⁺ cells (see Chapter 7).

6.8.2 Microglial phagocytosis mediates neuroprotection

Microglia increased their phagocytic activity rapidly following injury, as observed by engulfment of PI⁺ or PI⁻ cells via cell rear movement or phagocytic branch retraction (Fig. 6.12). Coupling of microglial phagocytosis to cellular apoptosis has been quantified in other types of noxious brain injury, such as excitotoxicity in hippocampal slice cultures and LPS injection in the hippocampus (Abiega et al., 2016), but dynamic *in vivo* observations involving timelapse movies following injury and quantification of phagocytosis are so far sparse (Morsch et al., 2015).

Which factors may regulate microglial attraction and phagocytosis? As previously observed (Fig. 5.5, Sieger et al. (2012)), ATP is an important chemoattractant for microglia in zebrafish *in vivo*, which is in line with several other *in vitro* and *in vivo* studies in rodents (Abiega et al., 2016; Davalos et al., 2005; Nimmerjahn et al., 2005; Ohsawa et al., 2007). Microglia can furthermore be activated via ATP stimulation, with one example being TNF α expression two to three hours after exposure to high levels of ATP (Inoue et al., 1998); this was similar to what I observed *in vivo* (Fig. 6.9). However, exposure to high levels of ATP for extended periods of time (longer than 30 minutes), or neuronal hyperactivity as experienced during seizures, have been shown to impair microglial phagocytosis (Abiega et al., 2016; Fang et al., 2009). This is mediated, in part, by an

impairment to sense microgradients in ATP (Abiega et al., 2016). However, in my model I found that microglia were able to rapidly detect the injury site and increase their phagocytic capacity in response to the presence of PI⁺ cells (Fig. 6.1, Fig. 6.12). This suggested that zebrafish microglial phagocytosis may be resilient to harmful stimuli, and investigation of these cells could reveal novel strategies to enhance phagocytosis - and thereby neuroprotection - following TBI.

By employing a pharmacological inhibitor of phagocytosis and genetic manipulation of the PS receptor BAI1 (*adgrb1a/adgrb1b*), I discovered that phagocytosis of debris by microglia had a neuroprotective effect: the number of pyknotic nuclei was significantly increased with both treatments at 6 hpi (Fig. 6.16 A, C; Fig. 6.21 A, C). This effect extended beyond collection of apoptotic cells to decrease the number of apoptotic cells present at 6 hpi: when phagocytosis was inhibited, the rate at which new pyknotic cells appeared (i.e., secondary cell death occurred), was increased (Fig. 6.16 B, D; Fig. 6.21 B, D).

Neuroprotection via phagocytosis could occur through several mechanisms. It could be mediated via a direct effect of phagocytosis, such as containing toxic intracellular substances (Green et al., 2016; Wolf et al., 2017). One example of phagocytosis limiting secondary cell death is the Royal College of Surgeons (RCS) rat model of inherited retinal dystrophy (D'Cruz, 2000). Retinal degeneration was found to be caused by loss of MerTK, a phagocytosis receptor, on retinal pigment epithelium cells, whereby accumulation of primary cellular debris and spillage of intracellular factors lead to secondary retinal cell death. Cuenca et al. (2013) showed that neuronal cell loss in this model could be rescued via boosting phagocytosis. Microglia-mediated neuroprotection could also be caused by indirect effect, such as upregulation of anti-inflammatory or neuroprotective microglial transcripts following phagocytosis (Fadok et al., 1998; Wolf et al., 2017). Phagocytosis via PS recognition (as inhibited by both L-SOP and BAI1 receptor mutation) has been shown to cause a general anti-inflammatory profile and dampen inflammation, which is a mechanism often hijacked by cancer cells to decrease macrophage-mediated cell death, but also generally observed during efferocytosis, the removal of apoptotic cells (Birge et al., 2016; Fadok et al., 1998; Kim et al., 2004a). Similarly, phagocytosis of myelin has been shown to cause an anti-inflammatory microglial phenotype (Liu et al., 2006); TNF α , a pro-inflammatory cytokine, can increase phagocytosis of myelin, but inhibits this conversion to a protective phenotype (Kroner et al., 2014), adding further complexity to the interplay of cytokines and phagocytosis following injury.

Zebrafish microglia appear to be efficient phagocytes that can correctly target dying cells (Fig. 6.12). Here, my data show that rapid phagocytosis of cellular debris via a PS receptor-mediated mechanism is essential to prevent the exacerbation of secondary cell death following brain injury in larval zebrafish. Genes and pathways that render microglia in the zebrafish effective phagocytes in response to an injury, and thereby limit the occurrence of secondary cell death, could represent

attractive therapeutic targets for human TBI to improve the outcome of brain injuries and limit secondary cell death. These genes or pathways should ideally be specific to microglia and be targetable using small molecules that can easily penetrate the BBB for maximum therapeutic effect. However, more research will need to be carried out in order to identify such potential therapeutic targets and to investigate their role in mammalian microglia and the outcome of mammalian (and human) TBIs.

Chapter 7

Microglia/macrophage transcriptomic alterations in response to injury

7.1 Introduction

In vivo timelapse imaging had provided me with an insight into dynamic changes in microglial behaviour following injury, in particular migration and phagocytosis (Fig. 6.2, Fig. 6.12), and revealed a neuroprotective role for microglia via rapid phagocytosis of cellular debris (Fig. 6.16, Fig. 6.21). Candidate-driven analysis had revealed the upregulation of transcripts which had previously been shown to have pro- or anti-inflammatory or neurotrophic functions in response to injury (Fig. 6.8) (Basu et al., 2002; Chen et al., 2007; Cianciulli et al., 2015; Fantacci et al., 2013; Ferreira et al., 2014; Holmin and Mathiesen, 2000; Knobloch and Faden, 1998; Philips et al., 2001; Wu et al., 2008). However, I obtained this expression data from RNA extracted from whole larval heads following injury and it provided no information on the cellular source of transcripts. Furthermore, while there were some transgenic reporter lines to study the cellular sources of cytokines (*tnfa:eGFP-F* and *il-1 β :GFP*), this was not the case for all genes of interest. Finally, a candidate-driven approach did not allow for the unbiased identification of novel injury-induced transcripts that could potentially confer a neuroprotective function. Therefore, I aimed to assess transcriptomic alterations in microglia by performing RNA sequencing. With this dataset, I hoped to elucidate genes modulating microglial polarisation and behaviour (e.g., phagocytosis), as well as secreted factors with the potential to directly influence neuronal survival.

The work in this chapter was carried out in collaboration with the Queen's Medical Research Institute Flow Cytometry Facility and Edinburgh Genomics to perform fluorescence-activated cell sorting

(FACS), and bulk RNA sequencing, respectively. My qRT-PCR results from whole heads revealed that transcript levels change rapidly in response to injury, with changes in some transcript levels being detected as early as one to two hours post injury (Fig. 6.8). Furthermore, as an early microglial phagocytic response was crucial for conferring neuroprotection and limiting secondary cell death (Fig. 6.16, Fig. 6.21), I chose to extract RNA from sorted microglia at two hours post injury, allowing me to study early injury-induced changes in these cells that may confer later neuroprotection.

With the work in this chapter, I aimed to characterise injury-induced transcriptomic changes in microglia/macrophages by bulk RNA sequencing from sorted cells. I had so far shown a neuroprotective role for microglial phagocytosis; this could potentially be enhanced by understanding the pathways that elicit such a phagocytic and neuroprotective phenotype. Furthermore, RNA sequencing could identify whether microglia/macrophages produce any secreted molecules that might directly influence neuronal survival in response to injury. Therefore, RNA sequencing could elucidate transcripts that are directly or indirectly neuroprotective.

7.2 Sample preparation: cell yield, RNA quantity/quality and cDNA amplification results

To collect the microglial population of interest, I initially aimed to extract 4C4⁺ cells from larval heads as previously achieved by Mazzolini et al. (2018). Larvae were mounted, injured, released, and allowed to recover for 2 h. Following this, I decapitated larvae and subsequently followed the fluorescence-activated cell sorting (FACS) protocol published by Mazzolini et al. (2018). Briefly, the protocol entailed the generation of a single-cell suspension by mechanical homogenisation, removal of myelin using a 22% Percoll gradient, F_c block to prevent unspecific binding of antibodies to the F_c receptor, antibody staining, and resuspension of cells in a glucose-rich medium containing 2% normal goat serum to prevent formation of cell clusters (Mazzolini et al., 2018). All steps were carried out at 4 °C on ice to prevent (or minimise) changes in transcript levels during processing. Due to time constraints - the mounting, injuring, and releasing of larvae took roughly one hour per 100 animals -, I was only able to process a maximum of 400 larvae per day (a maximum of 200 larvae per group (sham or injury)). Conversely, Mazzolini et al. (2018) used a minimum of 600 larval heads per group. The percentage of retrieved 4C4⁺ cells was low (approximately 0.9% of live cells, Fig. 7.1). As a comparison, I repeated this experiment in *mpeg1*:GFP larvae, removing the steps of F_c blocking and antibody staining and instead sorting for the transgenically expressed GFP, which retrieved 2% of live cells from heads (Fig. 7.1 A). The low number of recovered 4C4⁺ cells resulted in a very low RNA yield compared to *mpeg1*:GFP⁺ cells (Table 7.1 B). Interestingly, the RNA yield for the two groups was not proportionate to cell yield. This could have been a result of

fluctuations in the presence of ambient RNAses during RNA extraction, or due to an increased loss of cells in the 4C4 group following pelleting after FACS (after which cell number is not assessed anymore) compared to the *mpeg1*:GFP group.

For bulk RNA sequencing, Edinburgh Genomics required a minimum input of 1.1 µg RNA. Even with the slightly higher cell and RNA yield following *mpeg1*:GFP⁺ sorting (Table 7.1), this was still two to three orders of magnitude larger than what I received following FACS-RNA extraction. Therefore, I was required to use a commercial kit for reverse transcription of the RNA and subsequent isothermal amplification of the cDNA. Based on the recommendation of Edinburgh Genomics, we purchased the NuGEN Ovation[®] RNA-Seq System V2. The minimum input for this system was 500 pg in 5 µL, equivalent to an RNA concentration of 100 pg/µL. My injury assay was not scalable and I could not pool more than 200 heads per treatment per experimental day; as the values for 4C4⁺ cells and subsequent RNA were below the minimum requirements even for the amplification kit, this approach was therefore not feasible for generating sufficient amounts of RNA/cDNA for bulk RNA sequencing. Therefore, I decided to proceed using the transgenic line *mpeg1*:GFP, which provided me with higher cell and RNA yields, but had the significant limitation that it was not specific to microglia and extracted both microglia and macrophages in the head region and would therefore make the biological validation following sequencing more complex. Furthermore, whole head imaging - including the ventral side - revealed that *mpeg1*:GFP transgenic larvae had about 150 *mpeg1*⁺ cells in the cardiac region, which were not present in 4C4 cells (Fig. 7.2). Based on this data, I carefully excluded the cardiac region during decapitation of larvae for future steps.

mpeg1:GFP⁺ cells were sorted directly into QIAGEN[®] RNAProtect Cell Reagent to prevent changes to the transcriptome following FACS, and were stored at 4 °C for a maximum of four days until RNA extraction using the QIAGEN[®] RNEasy Micro Kit. Samples were eluted in 14 µL of nuclease-free water, and RNA quantity and quality was analysed using the LabChip GX24 by Dr. Pamela Brown. Following RNA quantity and quality analysis, RNA was reverse transcribed and amplified for RNA sequencing using the NuGEN Ovation[®] RNA-Seq System V2. The minimum input for this amplification reaction were 500 pg (in 5 µL), which I exceeded (Table. 7.2). Quality and quantity of cDNA was then assessed by Edinburgh Genomics prior to library preparation. Gel bands of cDNA supplied to Edinburgh Genomics are shown in Fig. 7.3. A summary of all results prior to RNA sequencing is shown in Table 7.2.

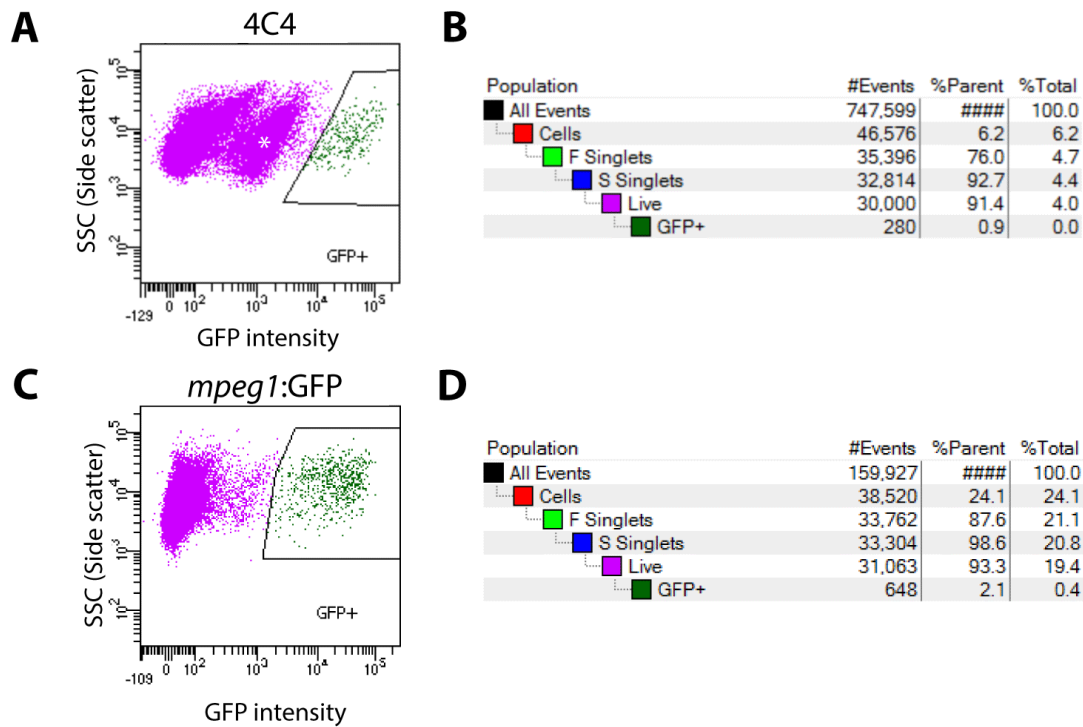


Figure 7.1: **Representative plots of side scatter (SSC) to GFP intensity from FACS reports sorting for 4C4 or *mpeg1:GFP*.** (A) SSC against GFP intensity for 4C4⁺ cell sorting. White asterisk indicates population of cells unstained by the secondary antibody (as determined by no secondary control). (B) Population report. Only 0.9% of live cells are GFP⁺. (C) SSC against GFP intensity for *mpeg1:GFP* sorting. (D) Population report. 2.1% of live cells are GFP⁺.

Table 7.1: **Cell and RNA yields using different markers for fluorescence activated cell sorting.** Values for antibody-dependent sorting of 4C4⁺ microglial cells, or sorting using the *mpeg1:GFP*) transgenic line. RNA amounts were determined on the the LabChip GX24.

Cell type	Cell yield	RNA concentration	Total RNA extracted (14 μ L)
Microglia (4C4 ⁺)	3 919	24 pg/ μ L	336 pg
Microglia/macrophages (<i>mpeg1:GFP</i> ⁺)	22 000	500 pg/ μ L	7 ng

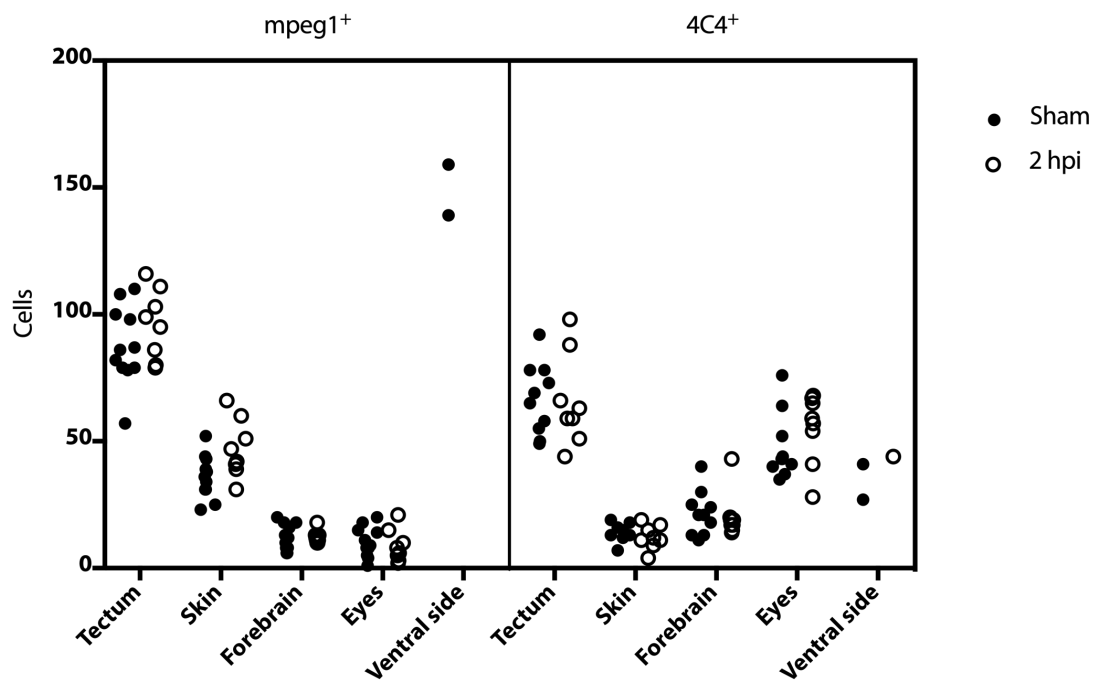


Figure 7.2: Quantification of *mpeg1*⁺ and 4C4⁺ cells in the whole larval head. Acquired from dorsal or ventral imaging of the whole head in *mpeg1*:GFP transgenic larvae and anti-4C4 immunostained larvae.

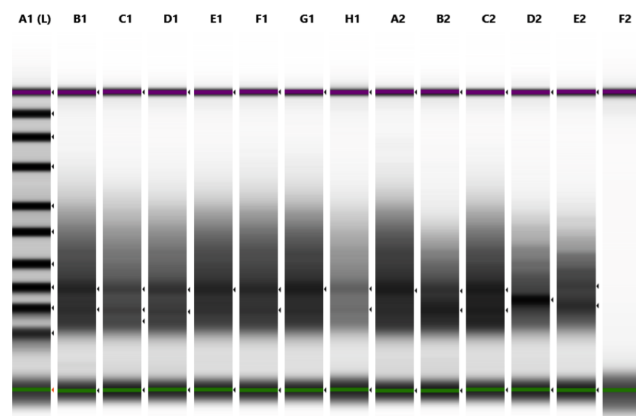


Figure 7.3: Quality control gel of cDNA following Amplification using NuGEN[®] Ovation RNA-Seq System V2. A1, Ladder. B1, Sham 1. C1, Sham 2. D1, Sham 3. E1, Sham 4. F1, Sham 5. G1, Sham 6. H1, 2 hpi 1. A2, 2 hpi 2. B2, 2 hpi 3. C2, 2 hpi 4. D2, 2 hpi 5. E2, 2 hpi 6. F2, Empty lane.

Table 7.2: **Cell yields, RNA quantity/quality and cDNA quantity.** Cell number obtained following FACS of *mpeg1*:GFP⁺ cells. RNA quantity and quality obtained following RNA extraction by analysis on the LabChip GX24. cDNA quantity obtained by analysis on the NanoDrop One following amplification reaction.

Sample	Heads	Cells	Cells/head	RNA quantity (ng/ μ L)	Total RNA extracted (ng)	RNA in amplification reaction (ng)	RIN	RNA/cell (pg)	cDNA output (ng/ μ L)
Sham 1	198	35,484	179	1.21	16.94	6.05	10	0.48	26.60
Sham 2	198	29,945	151	0.77	10.84	3.87	10	0.36	20.60
Sham 3	170	24,781	146	0.76	10.57	3.78	10	0.43	16.50
Sham 4	180	26,574	148	0.81	11.35	4.06	10	0.43	26.90
Sham 5	180	28,829	160	1.03	14.39	5.14	10	0.50	26.70
Sham 6	200	28,368	141	0.82	11.49	4.11	10	0.41	26.10
2 hpi 1	198	27,766	140	0.58	8.09	2.89	10	0.29	15.80
2 hpi 2	198	29,796	150	0.54	7.57	2.71	10	0.25	22.00
2 hpi 3	160	25,685	161	0.73	10.23	3.66	10	0.40	15.50
2 hpi 4	150	22,224	148	0.60	8.37	2.99	10	0.38	22.50
2 hpi 5	180	23,885	132	0.58	8.11	2.90	10	0.34	15.30
2 hpi 6	180	20,003	111	0.68	9.49	3.39	10	0.47	12.80
Average	183	26,945	147	0.76	10.62	3.79	10	0.34	20.60

7.3 RNA sequencing results and exploratory analysis

Illumina Sequencing Library was prepared by Edinburgh Genomics, and sequencing was performed using the Illumina NovaSeq System. Bioinformatics Analysis was carried out by Dr. Katie Emelianova at Edinburgh Genomics.

Following PCA analyses, three samples from 2 hpi sorted macrophages were excluded from further analysis due to high duplicate and low mapping rate, and low clustering with other samples from their group: 2 hpi 3, 5, and 6. Interestingly, these three samples also had different size distribution compared to the other samples on the quality control gel following cDNA amplification (Fig. 7.3; lanes B2, D2, and E2), but were not conspicuous in terms of RNA quality or quantity (Table 7.2). It is possible that mistakes were made during the amplification reaction, resulting in abnormal size distribution or a failure of representative cDNA amplification. The NuGEN Ovation[®] RNA-Seq V2 System is a highly sensitive amplification kit, and therefore even minor mistakes when carrying out the protocol could result in considerable changes of the outcome. For clarity of further analysis, sample 2 hpi 4 was from now on called 2 hpi 3.

For filtering the list differentially expressed genes received from Edinburgh Genomics, I employed the False Discovery Rate (FDR) rather than p values, as the unadjusted p value would yield a high number of false positives in my dataset of 32 000 detected genes. By empirical choice, I set the FDR to ≤ 0.05 , accepting a false discovery rate of 5%. With this approach, I obtained 225 significantly downregulated and 567 upregulated genes, which showed that injury elicited a transcriptional response in microglia/macrophages as early as 2 hpi.

To make sense of this gene list, and focus on the genes with the largest fold change, I further analysed genes with a logarithmic fold change of at least 1.2 (either up or down); this cut-off was chosen empirically and only included genes that more than duplicated or halved their expression in response to injury, although much smaller changes may still carry biological significance. After applying the fold change cut-off, the list contained 193 upregulated and 65 downregulated genes. Next, I created heatmaps for a visual representation of changes in transcripts (excerpts of these Figures shown in Fig. 7.4, Fig. 7.5).

As this list was still difficult to draw conclusions of, and to gain an insight into overall transcriptomic trends occurring in microglia/macrophages following injury, I decided to perform gene ontology (GO) enrichment analysis. This could potentially enable me to understand pathways that are enriched in response to injury. I used an online tool based on the PANTHER Classification system (Mi et al., 2013) to perform GO enrichment analysis (<https://www.panther.db>). For this preliminary analysis, I aimed to go ahead using only upregulated genes. To do so, I uploaded my list of upregulated

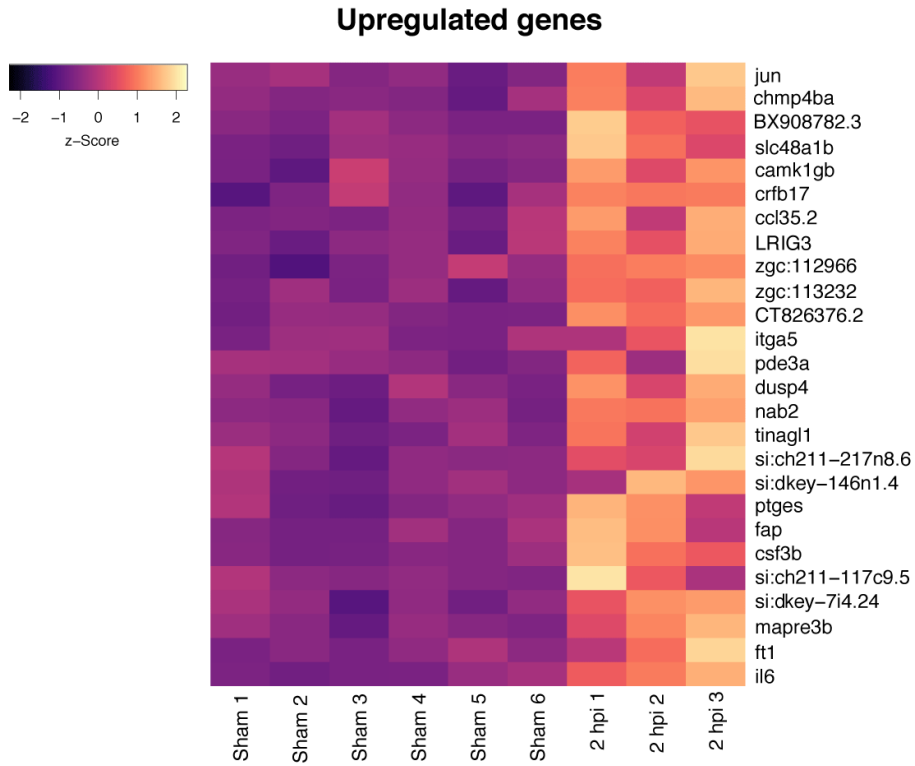


Figure 7.4: Excerpt of significantly upregulated genes and their respective expression in individual samples. $FDR \leq 0.05$, fold change ≥ 1.2 .

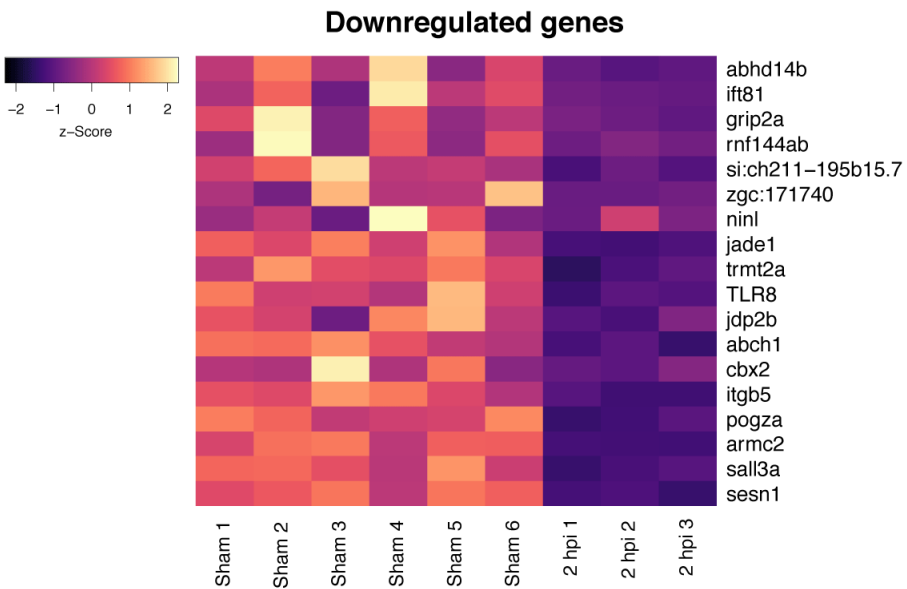


Figure 7.5: Excerpt of significantly downregulated genes and their respective expression in individual samples. $FDR \leq 0.05$, fold change ≤ 1.2 .

genes (Fold change ≥ 1.2 , FDR < 0.05 , as previously described), and compared it to a background gene list of all detected genes in the sequencing. Gene ontology enrichment revealed enrichment of several GO terms, some of the which were to be expected - such as cell migration and immune response -, but also some unexpected terms (Fig. 7.6, Table 7.3).

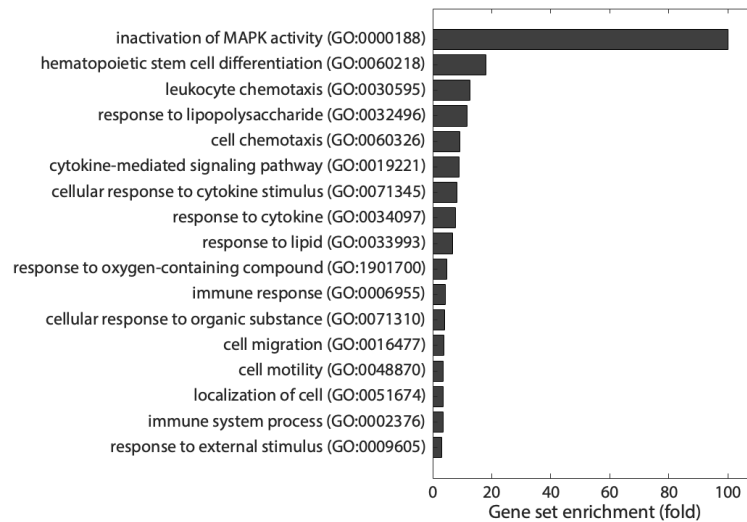


Figure 7.6: **Visual representation of enriched GO terms in list of upregulated genes from RNA sequencing dataset.** Genes were filtered by an FDR ≤ 0.05 , and a fold change of ≥ 1.2

Table 7.3: **Gene ontology analysis of upregulated genes in RNA sequencing dataset.** Analysis shows mapped genes in background, and how many of these are represented in the upregulated list. Fold enrichment is then performed based on expected values in a random dataset.

GO biological process	Background	Upregulated	Expected	Fold enrichment	FDR
inactivation of MAPK activity (GO:0000188)	4	3	0.3	> 100	1.10E-02
hematopoietic stem cell differentiation (GO:0060218)	38	5	0.28	17.97	4.16E-02
leukocyte chemotaxis (GO:0030595)	76	7	0.56	12.58	4.20E-03
response to lipopolysaccharide (GO:0032496)	58	5	0.42	11.78	3.26E-03
cell chemotaxis (GO:0060326)	119	8	0.87	9.18	6.01E-03
cytokine-mediated signaling pathway (GO:0019221)	107	7	0.78	8.94	1.08E-02
cellular response to cytokine stimulus (GO:0071345)	115	7	0.84	8.31	1.48E-02
response to cytokine (GO:0034097)	141	8	1.03	7.75	1.06E-02
response to lipid (GO:0033993)	144	7	1.05	6.64	3.44E-02
response to oxygen-containing compound (GO:1901700)	252	9	1.84	4.88	3.54E-02
immune response (GO:0006955)	387	12	2.83	4.24	1.67E-02
cellular response to organic substance (GO:0071310)	654	18	4.97	3.76	6.95E-03
cell migration (GO:0048870)	468	13	3.43	3.79	2.04E-02
cell motility (GO:0048870)	490	13	3.59	3.62	2.94E-02
localisation of cell (GO:0051674)	490	13	3.59	3.62	3.07E-02
immune system process (GO:0002376)	845	22	6.19	3.56	2.95E-03
response to external stimulus (GO:0009605)	731	16	5.35	2.99	3.50E-02

7.4 Comparison of RNA sequencing results to qRT-PCR results from whole heads

I then assessed whether qRT-PCR results presented in Fig. 6.8 were compatible with the RNA sequencing results. Although these samples were obtained from whole heads rather than sorted cells, the comparison of wild type animals and *irf8*^{-/-} mutants lacking microglia/macrophages allowed for preliminary estimation of microglia/macrophage expression changes following injury.

I queried expression of *il1b*, *tnfa*, *tnfb*, *il4*, *il10*, *tgfb1a*, *ngfb*, and *bdnf* in my RNA sequencing dataset. The results are presented in Fig. 7.7 and Table 7.4. *il1b*, *tnfb*, and *il10* were significantly upregulated in response to injury (although *il10* had a slightly higher FDR than 0.05) (Fig. 7.7, Table 7.4). This was in line with previous whole head qRT-PCR at 2 hpi, although *tnfb* upregulation was not significant at this point in whole heads (Fig. 6.8). *il4*, *tgfb1a*, *tnfa*, *ngfb* (Table 7.4), and *bdnf* expression were not significantly altered 2 hpi, and *bdnf* transcripts were only detected in a single sham sample (Fig. 7.7). For *tnfa*, *ngfb*, and *bdnf*, the RNA sequencing results from sorted microglia/macrophages were therefore different than previous qRT-PCR results from whole heads, which had revealed a significant upregulation of these genes at 2 hpi (Fig. 6.8).

Table 7.4: Counts per million (CPM) values for genes previously analysed using qRT-PCR from whole heads in wild type and *irf8*^{-/-} mutant animals. n.d. = not detected; n.a. = not applicable.

Gene name	Mean CPM sham	Mean CPM 2 hpi	Fold change (linear)	FDR
<i>il1b</i>	84.04	360.23	4.29	5.57E-10
<i>tnfb</i>	48.38	72.16	1.49	0.048
<i>il4</i>	5.30	5.64	1.06	0.966
<i>il10</i>	3.93	9.59	2.43	0.088
<i>tgfb1a</i>	13.75	12.89	0.94	0.942
<i>tnfa</i>	1.62	4.83	2.97	0.361
<i>ngfb</i>	0.29	0.05	0.22	0.618
<i>bdnf</i>	0.01	n.d.	n.a.	n.a.

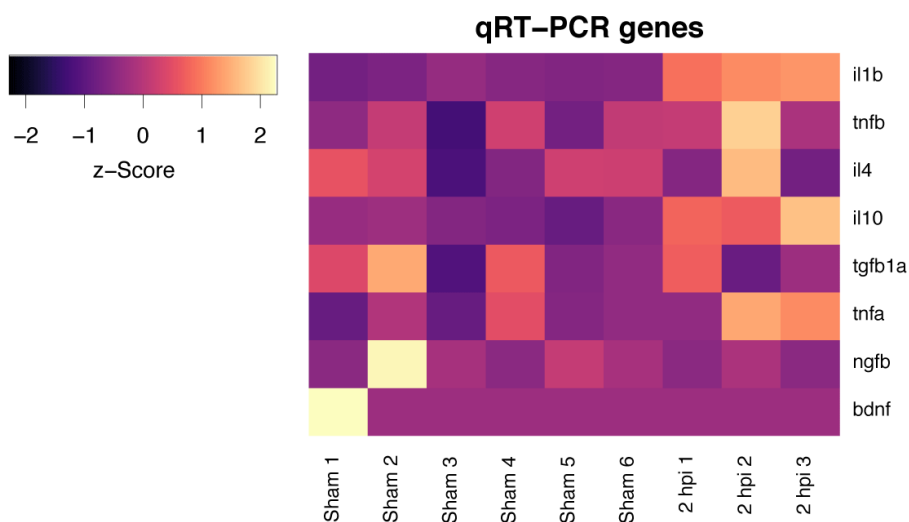


Figure 7.7: Expression of genes previously analysed in whole head qRT-PCR in RNA sequencing from sorted microglia/macrophages.

7.5 Selected findings of interest from RNA sequencing

In this section, I am presenting three groups of genes I found potentially interesting for conferring microglia(/macrophage)-mediated neuroprotection; either indirect, by regulation of microglia/macrophage polarisation (Chapter 7.5.1, Chapter 7.5.2), or direct, by action on neuronal survival (Chapter 7.5.2, Chapter 7.5.3). The results in this section were obtained shortly before compilation of this thesis, therefore any analysis is very preliminary and warrants further validation.

7.5.1 MAP kinase pathway inactivation (dusp gene upregulation)

Inactivation of MAP kinase was the most enriched GO term of significantly upregulated genes with a more than hundredfold enrichment (Fig. 7.6, Table 7.3), and I decided to analyse this pathway in more detail. I downloaded the gene list associated with this GO term using the online database AmiGO (Carbon et al. (2009); <http://amigo.geneontology.org/amigo>) and created heatmaps visualising the transcript levels of corresponding genes in my RNA sequencing dataset. Many of these genes (although not all more than by a fold change of 1.2; Fig. 7.8 A and Table 7.5), were upregulated in response to injury.

7.5.2 Cytokines and cytokine receptors

I also detected significant increases in the transcript levels of certain cytokines and cytokine receptors in microglia/macrophages (see Fig. 7.8 C and Table 7.6)

Table 7.5: Counts per million (CPM) values for *dusp* genes. Notice the FDR for *dusp6* and *dusp1* is > 0.05.

Gene name	Mean CPM sham	Mean CPM 2 hpi	Fold change	FDR
<i>dusp6</i>	241.91	310.67	1.28	0.090
<i>dusp1</i>	173.32	206.93	1.20	0.350
<i>dusp2</i>	54.90	155.22	2.83	6.39E-07
<i>dusp5</i>	31.08	79.88	2.57	4.21E-05
<i>dusp8a</i>	10.97	28.95	2.64	0.0130
<i>dusp4</i>	3.86	17.60	4.56	0.002

Table 7.6: Counts per million (CPM) values for cytokine and cytokine receptor genes.

Gene name	Mean CPM sham	Mean CPM 2 hpi	Fold change	FDR
<i>tnfrsf11a</i>	126.88	190.43	1.51	0.009
<i>il34</i>	64.62	98.03	1.52	0.033
<i>il6st (gp130)</i>	71.84	123.73	1.62	2.51E-05
<i>il1r2</i>	291.97	535.71	1.84	1.75E-05
<i>il13ra1</i>	13.48	25.37	1.88	0.040
<i>il4r.1</i>	43.54	84.00	1.97	0.001
<i>il10</i>	3.93	9.59	2.43	0.088
<i>il1b</i>	84.04	360.23	4.29	5.57E-10
<i>m17</i>	8.12	40.40	4.96	6.63E-06
<i>il6</i>	1.68	9.40	5.58	0.005
<i>il15l</i>	0.40	3.17	7.84	0.133
<i>tnfrsf9b</i>	6.13	51.42	8.40	1.13E-05
<i>tnfrsf18</i>	2.31	23.33	9.99	5.72E-05
<i>lta (tnfb)</i>	0.02	0.90	23.92	0.072

Table 7.7: Counts per million (CPM) values for genes encoding neurotrophic factors.

Gene name	Mean CPM sham	Mean CPM 2 hpi	Fold change	FDR
<i>hbegfb</i>	7.89	22.48	2.97	0.003
<i>manf</i>	39.85	66.02	1.66	0.046
<i>inhbaa</i>	20.79	42.29	2.03	0.009

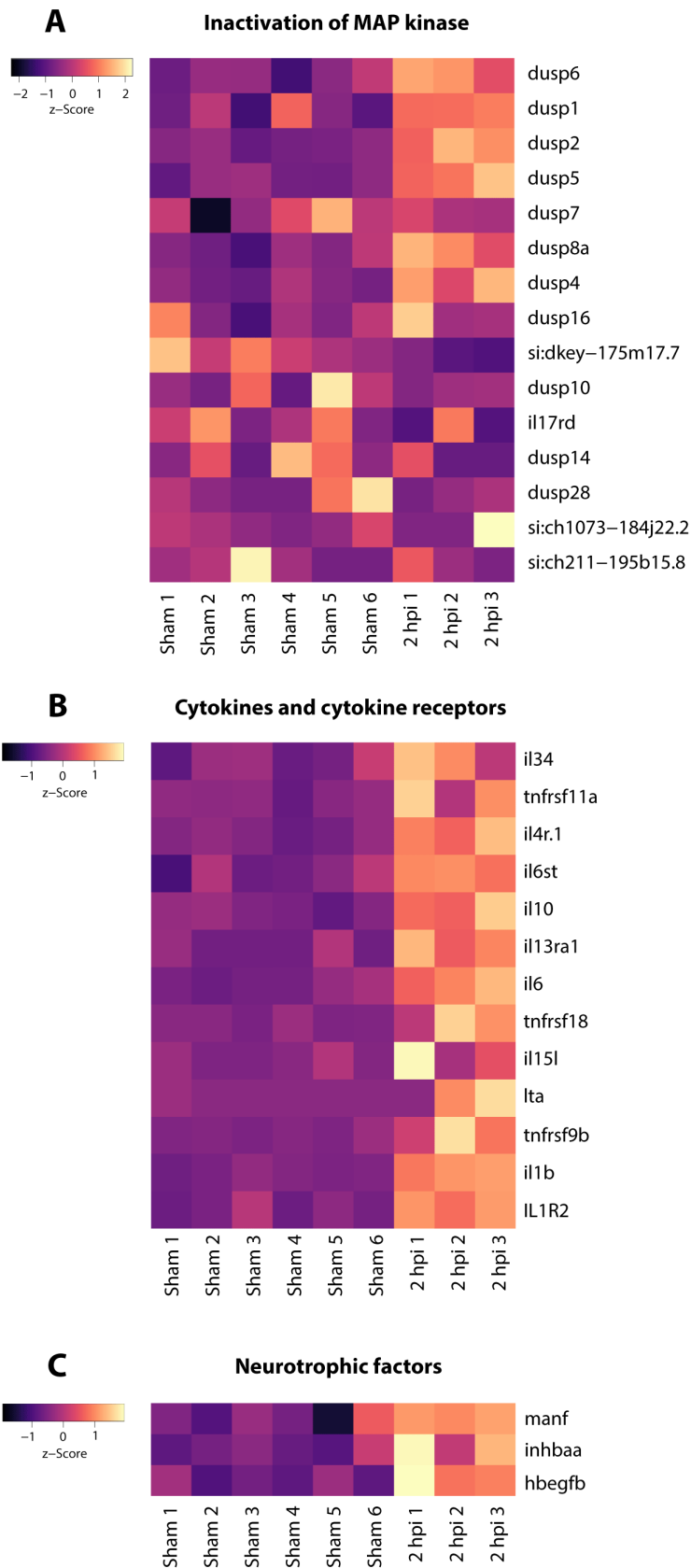


Figure 7.8: **Heatmaps of relative transcript levels of selected genes in RNA sequencing dataset, normalised per row (assigned z-Score).** (A) Relative transcript levels for genes in the GO term MAP kinase inactivation. (B) Relative transcript levels for cytokine and cytokine receptors that were upregulated in RNA sequencing dataset. (C) Relative transcript levels for genes implicated in neurotrophic functions.

7.5.3 Neurotrophic factors

I furthermore found three factors that may have neuroprotective functions upregulated in my RNA sequencing dataset of microglia/macrophages following injury (Fig. 7.8, Table 7.7), suggesting that microglia/macrophages are potentially directly conveying neuronal survival via release of these molecules following brain injury in larval zebrafish.

7.6 Discussion

In this chapter, I have described my most recent results obtained from bulk RNA sequencing of sorted *mpeg1*:GFP⁺ cells at 2 hour post injury. RNA sequencing confirmed previous results obtained from whole head qRT-PCR (Fig. 6.8, Fig. 7.7), while offering new insights and a large list of potentially interesting genes that could modulate neuronal survival directly or indirectly. Although I have focussed my current preliminary analysis on genes that have previously been implied in neuroprotection, further experimental studies will potentially allow for discovery of novel injury-induced genes conferring neuroprotection (see Chapter 7.6.6).

7.6.1 Comparison to whole head qRT-PCR

In my RNA sequencing results, I found *il1b* upregulation in response to injury, consistent with previous data comparing whole head RNA in wild type animals and *irf8*^{-/-} mutants (Fig. 6.8) and *in vivo* imaging (Fig. 6.9). Similarly, *il10* was upregulated in both experiments (Fig. 6.8, Fig. 7.7). Interestingly, *tnfa* showed a more heterogeneous picture and was only increased in two out of three injury samples (Fig. 7.7); this could be explained by the fact that *in vivo* imaging revealed only few cells - potentially microglia in the brain, but this has not been confirmed - express *tnfa* at 2 hpi (Fig. 6.9), and bulk RNA sequencing may have diluted out the effect, or did not include said population of *tnfa*-expressing cells. *tnfb* was significantly upregulated in the RNA sequencing dataset but not qRT-PCRs at 2 hpi, suggesting that expression is higher in microglia/macrophages than in other cells at this time.

Contrary to prior qRT-PCR results comparing wild types and microglia/macrophage-less *irf8*^{-/-} mutants (Fig. 6.8), neither *ngfb* nor *bdnf* were upregulated in the RNA sequencing dataset from *mpeg1*⁺ cells in response to injury (Fig. 7.7). This suggested that larval zebrafish microglia/macrophages induce the expression of these two genes in other cells, for example in radial glia or neurons which have previously been shown to be able to express these factors (Biane et al., 2014; Fulmer et al., 2014; Cacialli et al., 2018). Neuronal *bdnf* expression has previously been demonstrated in the injured adult zebrafish telencephalon, and has been linked to the regenerative success of the zebrafish brain (Cacialli et al., 2018); microglia could therefore indirectly promote neuronal survival following injury by enhancing expression of *bdnf* in these cells (Fig. 6.8). Indeed,

microglia have recently been shown to have a profound impact on the neuronal transcriptome under inflammatory conditions (Qiu et al., 2018), rendering this a plausible explanation.

As expected, *il4*, and *tgfb1a* were not significantly altered after 2 hpi (Fig. 6.8, Fig. 7.7). This result confirmed that these genes are not of microglia/macrophage origin following brain injury in larval zebrafish.

7.6.2 MAP kinase inactivation

I observed a significant enrichment in the upregulation of genes involved in the inactivation of MAP kinase (Fig. 7.8), in particular dual-specificity phosphatases (DUSPs). DUSPs dephosphorylate, and thereby inactivate, the p38 MAP kinase. This is of relevance to microglia/macrophage activation, as p38 MAP kinase is required for the production of several pro-inflammatory cytokines including $\text{TNF}\alpha$, which has been shown to mediate secondary cell death by several groups, including my own data (Fig. 6.10; Bachstetter et al. (2011); Bianchi et al. (1996); Cohen et al. (1996); Kim et al. (2004b)), and is a mediator of microglial inflammation (He et al., 2018). In rodent experimental models of brain injury, rapid and significant upregulation of p38 MAP kinase pathway is observed, and is linked to a pro-inflammatory immune response (Bachstetter et al., 2013). Although I found upregulation of a single MAP kinase in my RNA sequencing data set (*mapk6*, 1.95 linear fold change, $\text{FDR} = 3.01\text{E-}05$), I also detected increased expression of *dusp1*, *dusp2*, *dusp4*, *dusp5*, *dusp6*, and *dusp8a*. Many of these DUSPs are known to be upregulated upon stimulation with the anti-inflammatory IL-10 *in vitro* (Hammer et al., 2005), suggesting their participation in anti-inflammatory functions.

DUSPs are therefore thought of as proteins capable of putting a brake on excessive inflammation (Lang et al., 2006), and (alongside pharmacological approaches to inhibition of MAP kinase inactivation) have been implicated in neuroprotection (although not all studies investigated microglial involvement in this process). For example, the induction of *dusp1* or the mammalian protein product MAP kinase phosphatase 1 (MKP-1) have been shown to mediate the neuroprotective effects of endocannabinoid anandamide following excitotoxicity *in vivo* (Eljaschewitsch et al., 2006). Pharmacological inhibition of DUSP1 significantly increased the lesion size, and enhanced the inflammatory and apoptotic response in an experimental stroke model (Liu et al., 2014). Other DUSPs have also been shown to confer neuroprotection: induction of DUSP2 protected neurons from genotoxic stress (Morente et al., 2014); DUSP6 prevented glutamate excitotoxicity-induced cell death in hippocampal neurons *in vitro* (Huang et al., 2017); and DUSP8 mediated the neuroprotective effects of rosiglitazone following ischaemia in mice (Okami et al., 2013). Although the latter studies look at neurons directly rather than microglia-mediated neuroprotection, there appears to be a strong role for inhibition of MAP kinase for neuroprotection following brain injury in several cell types, however

this does not usually appear to occur at significant levels in rodent models unless modulated by pharmacological intervention (Bachstetter et al., 2013; Okami et al., 2013).

7.6.3 Cytokine & cytokine receptors

Based on a multitude of prior studies (reviewed by Ziebell and Morganti-Kossmann (2010)), and prior cytokine level studies in whole heads of larval zebrafish during the course of my own research (Fig. 6.8, Fig. 7.7, Chapter 7.6.1), it was unsurprising to observe an upregulation of several cytokines and cytokine receptors in my microglia/macrophage RNA sequencing dataset. Amongst these were *tnfrsf11a* (homologue of RANK; 1.51 fold increase), *il34* (1.52 fold increase), *il6st* (il6 signal transducer, or gp130; 1.62 fold increase), *il1r2* (decoy il1 receptor; 1.84 fold increase), *il13ra1* (1.88 fold upregulation), *il4r.1* (1.97 fold increase), *il1b* (4.29 fold increase), *m17* (LIF; 4.96 fold increase), *il6* (5.58 fold increase), *tnfrsf9b* (8.40 fold increase), *tnfrsf18* (9.99 fold increase). Also *il10*, *il15l*, and *lta* were significantly upregulated (2.43, 7.84, and 23.92 fold, respectively), although with an FDR > 0.05 (0.088 for *il10*, 0.133 for *il15l*, and 0.072 for *lta*). Increases of *tnfa* transcript levels were also detected (2.97 fold), although at a FDR of 0.36.

Traumatic brain injury in rodents is predominantly associated with the upregulation of pro-inflammatory cytokines in microglia/macrophages, which can result in a neuro-inflammatory or even neurotoxic role of these innate immune cells. However, there is increasing evidence that there are endogenous neuroprotective pathways activated by cytokines following injury (Morganti-Kossmann et al., 2018). In line with other transcripts mentioned so far which are thought to confer neuroprotection, many of the cytokine and cytokine receptor transcripts increased following zebrafish TBI are thought to be beneficial for neuronal survival.

One of the most prominent anti-inflammatory cytokines is IL-10, and I detected significant upregulation of *il10* transcript levels in response to injury, although the FDR was slightly above 0.05 (0.088). IL-10 has long been known to show pro-recovery properties in response to brain injuries. As early as 1998, it was discovered that intravenous treatment with IL-10 was able to significantly improve the neurological outcome of rodents and dampen pro-inflammatory cytokine production following experimental brain injury (Knobloch and Faden, 1998), and many studies demonstrating neuroprotective and anti-inflammatory properties followed in a variety of injury models (reviewed by Garcia et al. (2017)), although no clinical studies have so far tested a beneficial effect of IL-10 administration. This is perhaps due to the fact that IL-10 is used as a prognostic marker for brain injury, and higher levels are associated with a worse outcome, which may however stem more from a general immune dysregulation following CNS injury rather than a neurotoxic function of IL-10 (Rodney et al., 2018).

IL-34, the gene product of *il34*, is a powerful neuroprotective cytokine, conveying neuroprotection following a β -amyloid insult both by modulating microglial activation following CSF-1 receptor stimulation (Mizuno et al., 2011), and by direct action on neurons. There, it has been shown to promote neuronal survival (also via CSF-1 receptor stimulation) following excitotoxicity *in vivo* (Luo et al., 2013).

Another prominent cytokine featured in the RNA sequencing list of upregulated genes was *il1b*. My *in vivo* imaging in the previous chapter (Fig. 6.9), which revealed expression of IL-1 β in cells with microglia/macrophage-like morphology, validated these RNA sequencing results. As discussed previously, IL-1 β has typically been associated with conveying neurotoxic functions following acute CNS injuries (reviewed by (Murray et al., 2015)), although a recent study showed that IL-1 β may play different roles on endothelial cells, neurons, or glia: while deletion of neuronal or endothelial IL-1 receptor resulted in a reduced lesion size following ischaemia, global deletion of this receptor did in fact not cause any change in lesion size, which suggests that action of IL-1 β on glia may be neuroprotective while it may be neurotoxic via action on endothelial cells or neurons. Furthermore, I detected upregulation *il1r2*, which is the gene corresponding to a decoy receptor for IL-1 β . While it is structurally similar to IL-1 receptor 1, it lacks the intracellular signalling domain, and therefore actually dampens IL-1 β signalling (Peters et al., 2013). It can also be found intracellularly in microglia/macrophages, binding to and preventing release of pro-IL-1 (Zheng et al., 2013). Therefore, increased transcript levels of *il1r2* could prevent excessive IL-1 β signalling.

IL-4 receptor α (the mammalian homologue gene product of *il4r.1*, which I found upregulated in my RNA sequencing dataset) was previously reported to sway microglial activation to a neuroprotective phenotype. IL-4 itself is thereby usually of neuronal origin, as a stress-released molecule instructing microglia/macrophages to help: neurons in the penumbra (i.e., neurons who can potentially survive the insult) but not in the ischemic core expressed IL-4 in a rodent stroke model (Zhao et al., 2015). Increased neuronal IL-4 in turn leads to upregulation of the IL-4 receptor on microglia/macrophages (Zhao et al., 2015). Cerebral ischemia in IL-4^{-/-} mice resulted in a larger lesion area, increased neuronal loss in the acute phase (up to 5 days post injury), and increased sensorimotor and cognitive deficits compared to wild type animals (Liu et al., 2016); furthermore, microglia showed a more pro-inflammatory phenotype in these animals. Cerebral infusion of recombinant IL-4 was able to rescue behavioural deficits and macrophage polarisation in these animals. Similarly, systemic administration of IL-4 following spinal cord injury promoted cellular survival and behavioural improvements, as well as a decrease of pro-inflammatory markers as assessed by immunohistochemistry (Lima et al., 2017). Therefore IL-4 is thought to be a critical player in neuroprotection following CNS injury.

Another potentially neuroprotective receptor I found increased transcript levels of in response to injury was IL-13 receptor α 1 (*il13a1*). IL-13, the ligand of IL-13 receptor, is a neuroprotective

cytokine, although the exact mode of action is not known. It may act synergistically with IL-4 on neurons directly to stimulate survival (Mori et al., 2016), but can also mediate cell death of activated microglia by induction of cyclooxygenase 2, therefore potentially exerting an indirectly beneficial effect for neuronal survival following injury by dampening excessive inflammation (Yang et al., 2002, 2006).

In my RNA sequencing dataset, there was upregulation of several members of the TNF receptor superfamily (*tnfrsf*), including *tnfrsf11a*, *tnfrsf9b* and *tnfrsf18*. These can induce both pro- (*tnfrsf9b*, *tnfrsf18*) and anti-inflammatory (*tnfrsf11a*) activation patterns in microglia, so it would be interesting to further investigate whether they are co-expressed on the same cells, or distinct subsets. *Tnfrsf9b*, or its mammalian homologue protein product CD137-mediated signalling on microglia, has been shown to cause oligodendrocyte and neuronal apoptosis via downstream release of reactive oxygen species (Abdullah, 2016; Yeo et al., 2012), potentially contributing to a pro-inflammatory and pro-apoptotic environment following brain injuries. Similarly, the product of the mammalian homologue of *tnfrsf18*, GTR (glucocorticoid-induced TNF receptor), induced pro-inflammatory and neurotoxic microglial activation (Hwang et al., 2010), and genetic deletion of GTR or pharmacological inhibition via a GTR-Fc-fusion protein resulted in a significant reduction of apoptotic cell death following spinal cord injury (Nocentini et al., 2008). In contrast, *tnfrsf11a* or the protein of its mammalian homologue receptor activator of NF κ B (RANK), have been associated with an anti-inflammatory role, as inhibition of RANK following experimental ischemia in rodents resulted in an increased lesion volume (Shimamura et al., 2014), and recently a partial agonist has been shown to be therapeutically effective in reducing lesion size by dampening inflammation following ischemia in a pre-clinical study (Kurinami et al., 2016). This effect is in part associated with a decreased release of pro-inflammatory cytokines upon microglia/macrophage RANK activation (Maruyama et al., 2006).

I detected significant upregulation of several genes associated with the IL-6 pathway: *il6st* (gp130), *il6*, and *m17* (homologue of mammalian LIF). Although IL-6 can have pro- and anti-inflammatory functions (Scheller et al., 2011), this finding was exciting as in the context of neuronal injuries, these genes have been implicated in neuroprotection. IL-6-dependent neuroprotection is mediated by signal transducer (gp130) activation and STAT signalling in ischaemia (Jung et al., 2011; Loddick et al., 1998), and deficiency of IL-6 has been shown to worsen recovery from brain injury (Ley et al., 2011), therefore release of IL-6 by microglia/macrophages could improve neuronal survival following CNS injuries. Similarly, M17 (LIF) promoted neuronal survival following ischaemia in rats via direct action on neurons by gp130 and downstream STAT signalling (Suzuki et al., 2005), therefore providing a synergistic pathway to IL-6. LIF-dependent STAT3 activation has been shown to protect photoreceptors from light damage-induced cell death (Ueki et al., 2008). LIF also enhanced the expression of neurotrophic factors following CNS injury, and therefore increased

corticospinal axon growth (Blesch et al., 1999) and locomotor functional recovery following spinal cord injury (Zang and Cheema, 2003). Finally, LIF has been shown to act on neural progenitors: in the homeostatic adult mammalian brain, it reduces neurogenesis while it expands the progenitor pool by promoting neural stem cell renewal (Bauer and Patterson, 2006). Conversely, LIF is a key mediator of adult neurogenesis following injury in the olfactory bulb (Bauer et al., 2003). While there is abundant information on the role of IL-6/LIF/gp130 signalling directly in neurons, less is known about the (autocrine) function, particularly via gp130, on microglia/macrophages, although it has been suggested that IL-6 can induce the upregulation of SOCS3 and release of IL-10 upon LPS stimulation while reducing IL-1 β and TNF α production *in vitro* (Minogue et al., 2012).

Taken together, even based on only expression changes in cytokines and cytokine receptors, a complex picture of injury-induced transcriptomic changes emerges; both pro- and anti-inflammatory cytokines and cytokine receptors are increasingly transcribed upon injury, and a more thorough investigation on the effects on the outcome needs to be carried out to dissect the molecular functions of each (see Chapter 7.6.6).

7.6.4 Neurotrophic factors

In my RNA sequencing dataset, I observed significant upregulation of several genes previously implicated in neuroprotection.

manf is the gene encoding mesencephalic astrocyte-derived neurotrophic factor, and while the name suggests this is an astrocyte-specific factor, MANF is in fact highly evolutionarily conserved and found in both invertebrates and vertebrates (Lindholm and Saarma, 2010). Previous research *in vitro* showed that MANF is capable of rescuing neurons (Hellman et al., 2011) and neuroblastoma cells (SHSY-5Y cells) (Sun et al., 2017a) from apoptosis. *In vivo*, the role of MANF as a neuroprotective factor has primarily been studied in models of Parkinson's disease (Voutilainen et al., 2009), stroke (Mätlik et al., 2018; Xu et al., 2018b; Yang et al., 2014), spinal cord injury (Gao et al., 2018), and retinal injury (Neves et al., 2016), where overexpression or administration of recombinant MANF has been consistently found to improve neuronal survival and, where applicable, functional recovery (Gao et al., 2018; Mätlik et al., 2018; Xu et al., 2018b). MANF is thought to rescue from apoptosis by activation of Akt signalling (Gao et al., 2018; Xu et al., 2018b), and may also have neuroregenerative functions by enhancing neural progenitor differentiation and migration (Tseng et al., 2018). Interestingly, although many of the effects of MANF may be modulated via direct action on neurons, MANF has also been shown to be a potent modulator of microglial function. It was previously shown that MANF is upregulated in microglia following stroke and predominantly expressed in amoeboid cells (Shen et al., 2012). It increases the phagocytic activity of microglia (Mätlik et al., 2018), which I have shown can exert a neuroprotective function following

brain injury (Fig. 6.16, Fig. 6.21), and promotes tissue repair following retinal injury (Neves et al., 2016).

Heparin-binding epidermal growth factor (HB-EGF, the gene product of *hbegfb*) has previously been shown to be released from microglia (Opanashuk et al., 1999) and macrophages (Edwards et al., 2009) upon IL-4 stimulation. It may act in an autocrine manner to generate a pro-regenerative or regulatory polarisation of macrophages (and most likely microglia as well) (Wei and Besner, 2015; Zhao et al., 2016). Aside from its function on immune cells, HB-EGF has been reported to be a potent neurotrophic factor in the developing CNS (Kornblum et al., 1999), and its induction in regions of enhanced survival following cerebral ischaemia has led to the hypothesis that it could be a neuroprotective factor following injury (Kawahara et al., 1999). HB-EGF has subsequently been shown to directly decrease neuronal cell death following oxygen-glucose-deprivation (a model of ischaemia) (Zhou and Besner, 2010), and kainate-induced excitotoxicity *in vitro* (Opanashuk et al., 1999), potentially via activation of Akt signalling (Farkas and Kriegstein, 2002). This neuroprotective effect was also demonstrated *in vivo*, whereby intravitreal injection of recombinant HB-EGF improved retinal photoreceptor survival following light damage (Inoue et al., 2013), although the actions in this model were likely to be more complex than a direct action on neurons as the authors also found decreased levels of ROS compared to controls, pointing to an altered microglial polarisation following HB-EGF treatment.

Inhibin subunit β a (*inhbaa*, also called activin β a) is a subunit of the neurotrophic molecule activin. Similar to MANF and HB-EGF, activin may also exert an autocrine anti-inflammatory function on microglia (Sugama et al., 2007). Activin exerts a neurotrophic function on hippocampal neurons *in vitro* via a calcium-dependent mechanism (Iwahori et al., 1997), and exerts a powerful neuroprotective effect following a multitude of brain insults *in vivo*, including models of stroke (Buchthal et al., 2018; Wu et al., 1999) and Huntington's disease (Hughes et al., 1999).

7.6.5 Limitations of the current dataset

One of the major limitations concerning this dataset of injury-induced genes is that I was unable to specifically extract microglial cells using anti-4C4 cell antibody labelling as previously described by Mazzolini et al. because the cell and subsequent RNA yields were too low to provide me with sufficient material for bulk RNA sequencing (Fig. 7.1, Table 7.1). As microglia-specific cell sorting was not feasible under my conditions, I had to extract both microglia and macrophages using the *mpeg1*:GFP transgenic reporter line. Although I cut the heads prior to generation of the cell suspension to exclude *mpeg1*:GFP⁺ cells from the trunk and rest of the body in my RNA sequencing dataset, I still included macrophages on the skin, in the eye, and on/in the heart with this marker (Fig. 7.2), although I sought to exclude cardiac macrophages as much

as possible by taking care during decapitation. The 'contamination' of RNA from non-microglial *mpeg1*⁺ cells in the sequencing data could significantly alter the results and their interpretation. Further experiments based on my RNA sequencing therefore require thorough controls such as confirming expression of genes of interest in microglia using two-colour *in situ* hybridisation or immunohistochemistry using the gene of interest and a microglial transcript or epitope (e.g., *p2y12* or 4C4), although the distinction between microglia/macrophages may be achieved by localisation alone as my previous data has shown (Fig. 6.3).

Following injury, microglia in the brain and macrophages on the skin are likely functionally and transcriptionally distinct. This is emphasised by the fact that I detected microglia and macrophages in different locations - in the brain, and on the skin, respectively; while microglia may predominantly modulate brain repair and secondary cell death following this mechanical injury assay, macrophages may be involved in skin wound closure and epithelial repair. Therefore, reiterating the point above, transcripts that are upregulated in response to injury may not be necessarily brain repair-specific, but may be macrophage-derived and involved in repair of the skin.

Making matters more complex, CNS injury has been shown to result in differential activation of microglial subsets (Hsieh et al., 2014; Gertig and Hanisch, 2014). Recent advances in single cell RNA sequencing (scRNA-seq) make it feasible to study such subpopulations (Papalexi and Satija, 2018), and future scRNA-seq could potentially add more depth to injury-induced transcriptional changes in this larval zebrafish assay, i.e. which transcripts are co-expressed? Is there a subpopulation of microglia that is particularly associated with neuroprotective transcripts?

For the time being, however, the dataset offers a first insight into the transcriptional changes in the microglia/macrophage population induced by brain injury, and will provide a base for investigating the role of microglia/macrophages in the future.

7.6.6 Future outlook

The data presented in this chapter was obtained only recently, therefore further validation of the results is required to confirm transcriptional changes. For this purpose, we will perform qRT-PCR from sorted *mpeg1*:GFP⁺ cells against genes of interest to confirm differential expression. For the subsequent investigation of genes of interest, we will be able to utilise CRISPR/Cas9 to generate crispants as described in the previous chapter (Chapter 6.7.2). While these CRISPR/Cas9 mutations will not be cell-specific or temporally controlled at this first stage of investigation, they have the advantage of allowing us to rapidly investigate alterations in secondary cell death following gene mutation, for example by use of the *H2A*:GFP transgenic line. With CRISPR/Cas9, we are able to design and validate highly active guide RNAs, and following validation of guide efficiency

in vivo, which takes less than a week, phenotypic data (e.g. cell death at 6 hpi) can be obtained within one week, effectively allowing us to investigate up to 12 genes of interest within a time as little as three months. Additionally, some of the genes and pathways presented in this section also have known pharmacological inhibitors which we can employ in a temporally specific manner. Therefore, this larval zebrafish model will be a powerful tool to rapidly study genes of interest from my RNA sequencing results.

Depending on the outcome of initial studies, we can then assess the molecular mechanisms of how certain genes convey neuroprotection - or neurotoxicity - using other transgenic lines. For example, as this RNA sequencing experiment was carried out in microglia/macrophages, an obvious first choice of analysis would be the *mpeg1*:GFP transgenic line. Here, we can assess whether mutation in genes affects recruitment to the injury site or phagocytosis. Furthermore, we can investigate immune cell composition at the injury site using the *mpeg*:mCherry;*p2y12*:P2Y₁₂-GFP or *mpo*:GFP transgenic lines: does knockout of a certain gene allow peripheral macrophages or neutrophils to enter the brain? Additionally, we will be able to assess whether excitotoxicity will be altered by quantifying calcium transients in the *β-actin*:GCaMP6f transgenic line. We are also interested in oxidative stress, and will quantify the presence of hydrogen peroxide or nitric oxide using fluorescent probes (Lepiller et al., 2007) or genetically encoded ratiometric (Niethammer et al., 2009) or fluorescence resonance electron transfer (FRET) sensors (Xu et al., 2018a), and can assess whether these are altered following genetic mutation of genes of interest.

As a reverse approach, we will be able to study overexpression of genes of interest. This can be achieved in a cell- and temporally-specific manner by using the previously described tetON system (Knopf et al., 2010), which allows for tissue-specific conditional gene expression in zebrafish by crossing cell-type specific tetActivator lines with gene-specific tetResponder lines. A multitude of tetActivator lines are available within the Edinburgh zebrafish community, and we will be able to easily generate tetResponder lines using molecular cloning with the Tol2 system (Kwan et al., 2007) and injection of this construct using Tol2 transposase into one cell stage zebrafish embryos. Gene expression will then only occur in tissues of interest under control of doxycyclin. Using this system, we will be able to assess cell-type specific overexpression of genes of interest on cell death in the context of neuronal injury.

To summarise, the injury model described in this thesis in combination with CRISPR/Cas9 will provide an ideal platform for rapid assessment of consequences of genetic mutation of genes of interest.

Chapter 8

Discussion

8.1 A simple, new zebrafish assay to investigate secondary cell death

In this thesis, I have described my work on the establishment and characterisation of a new larval zebrafish model of mechanical brain injury that allows for real-time *in vivo* visualisation of cell death dynamics and repair mechanisms. In comparison to rodent models, where *in vivo* visualisation of cell death and microglial injury reactions is much more challenging, the larval zebrafish is ideally suited for this type of analysis.

Using a simple mechanical injury assay (Fig. 4.1, Fig. 4.2), I was able to elicit immediate cell death, as labelled by PI staining. Employing PI but also several other markers of cell death, such as phosphatidyl serine exposure (Fig. 4.6 A), nuclear condensation (Fig. 4.4), and Caspase-3 (Fig. 4.6 C), allowed me to observe the occurrence of cell death dynamics following injury. With the exception of Caspase-3 activation, which I detected via immunostaining, I could assess all of the other markers by live imaging as we had transgenic fluorescent reporter lines. For further analyses of the effects of drugs and other manipulations, I chose to primarily focus on nuclear condensation, as the background level of positive cells with this markers was very low and therefore provided me with a high signal to noise ratio. This is explained by the fact that PS exposure and Caspase-3 occur during early apoptosis (Balasubramanian and Schroit, 2003; Porter and Jänicke, 1999; Segawa and Nagata, 2015; Wyllie, 1997), while nuclear pyknosis is a late step of apoptosis (Oberhammer et al., 1994; Toné et al., 2007). The relatively high baseline levels of PS⁺ and Caspase-3⁺ cells are likely the result of developmental apoptosis to control for a surplus of generated neurons (reviewed by Dekkers et al. (2013) and Nijhawan et al. (2000)). However, these cells are generally rapidly removed by microglia before they reach later stages of apoptosis, explaining a low baseline of pyknotic nuclei under normal conditions.

To my knowledge, this is the first (larval) zebrafish assay assessing neuronal cell death dynamics, in particular whether cells die through primary or secondary cell death, following CNS injury. Although some previous studies investigating adult zebrafish CNS trauma, either in brain stab lesion or spinal cord transection assessed cell death, they predominantly focussed on regenerative neurogenesis or axon regrowth, respectively (Baumgart et al., 2012; Becker et al., 1997; Kishimoto et al., 2012; Kroehne et al., 2011; März et al., 2011). In the larval zebrafish, reports have shown increased numbers of cell death following CNS trauma, but not addressed whether this was primary or secondary cell death (Ohnmacht et al., 2016). Primary cell death is defined as cell death directly related to the physical disruption of tissue and cell membranes, while secondary cell death is related to delayed and indirect neurotoxic biochemical pathways elicited by the injury (Bayly et al., 2006; Stoica and Faden, 2010). This distinction is important as secondary cell death can potentially be prevented via pharmacological intervention whereas primary cell death cannot.

Here, I described that mechanical injury of the larval zebrafish induced two waves of cell death (Fig. 4.2, Fig. 4.4). Immediately upon injury of the brain, I observed accumulation of PI⁺ cells at and around the injury site (Fig. 4.2). Due to the rapid appearance and large diameter, PI⁺ were likely to have died from accidental necrosis. Starting from 1 hpi, I observed progressive accumulation of pyknotic nuclei (Fig. 4.4), which likely corresponds to secondary cell death. The numbers of Caspase-3⁺ and phosphatidylserine⁺ cells also peaked at 6 hpi (Fig. 4.6). In contrast to that, PI⁺ cells decreased rapidly between zero to one hour post injury (Fig. 4.2).

I was able to significantly decrease the number of pyknotic nuclei at 6 hpi by treatment with NMDA receptor inhibitors (Fig. 5.10), but not the number of PI⁺ cells at 0 hpi, suggesting that the occurrence of pyknotic nuclei was at least in part the result of a progressive dysfunction of the glutamatergic system, and therefore constituted secondary cell death. An increase of glutamate significantly increased the appearance of pyknotic nuclei (Fig. 5.11).

I also aimed to investigate the type of cell death. Zebrafish lack the main enzyme regulating necroptosis (MLKL) (Czabotar and Murphy, 2015), therefore I mainly aimed to distinguish between necrotic and apoptotic cell death. Caspase-3 is a key enzyme in apoptosis (Wyllie, 1997), whereas other markers (PI uptake, exposure of phosphatidylserine, and nuclear condensation) can occur both in necrotic or apoptotic cells (Fink and Cookson, 2005). Given the temporal and spatial dynamics I detected these markers at, in combination with the fact that I could detect numbers of Caspase-3⁺ cells significantly higher than baseline at 6 hpi but not 0 hpi (Fig. 4.6 C-D), suggested that cells immediately following injury had died through necrosis, and cells at 6 hpi died through apoptosis. In combination with tracing of individual neurons that were either structurally damaged directly by mechanical injury or not (Fig. 4.7), this data showed that neurons can die through

primary necrotic or secondary apoptotic cell death. In mammals, neurons can die both through necrosis and apoptosis after brain injury (Stoica and Faden, 2010). My experiments show that the same occurs in larval zebrafish in response to injury (Fig. 4.2, Fig. 4.4). However, in contrast to mammals, where both necrotic and apoptotic persist for days to weeks following an injury (Clark et al., 1999; Cortez et al., 1989; Sato et al., 2001; Williams et al., 2001; Zhou et al., 2012), larval zebrafish are able to remove necrotic cells within two to four hours (Fig. 4.2), and apoptotic cells within one day (Fig. 4.2). As clearance of debris is a crucial step for successful wound repair in the CNS (Neumann et al., 2009), this may in part explain the enhanced reparative and regenerative success of zebrafish following CNS injury.

Maas et al. (2017) reported a lack of success in phase III clinical trials for TBI. While a lot has been learned about the molecular mechanisms underlying secondary cell death following experimental TBI in rodents (Maas et al., 2017), the repeated failure of clinical trials raises the possibility that there are additional mechanisms driving secondary cell death which are still poorly understood. Despite advances in 2-photon imaging, *in vivo* timelapse imaging to investigate dynamics of cell death and the immune system still remains difficult in rodent models. Therefore, I proposed the use of the larval zebrafish for mechanistic investigations into secondary cell death. The strength of the larval zebrafish lies in the ease of genetic and pharmacological inhibition in combination with real-time *in vivo* imaging tools, allowing for rapid elucidation of molecular mechanisms and visualisation of dynamic cellular processes following injury. In combination with the large number of animals that can be processed per experiment, this renders the larval zebrafish a powerful platform to investigate mechanisms underlying secondary cell death following brain injury *in vivo*.

8.2 Conserved pathophysiology between rodent TBI and zebrafish mechanical brain injury

An important aspect of any disease model is how well it replicates the original pathology. Glutamate excitotoxicity is one of the main and central pathologies around TBI (Lipton and Rosenberg, 1994; Olney, 1969). Here, I show that this pathophysiological process is conserved in zebrafish. Following injury, there is a consistent increase of calcium transients in neurons (Fig. 5.8, Fig. 5.2). Combining *in vivo* calcium timelapse imaging with quantification of pyknotic nuclei in the same animals, I found a spatial correlation between regions with high calcium transients and a high density of pyknotic nuclei (Fig. 5.9).

Inhibition of glutamate signalling via NMDA receptor inhibitors resulted in the significant reduction of calcium transients down to baseline levels for up to 6 hpi (Fig. 5.10). The same NMDA receptor treatment also significantly decreased the number of pyknotic nuclei at 6 hpi (Fig. 5.10) but not

PI⁺ cells at 0 hpi, therefore specifically targeting secondary cell death. Conversely, application of *L*-glutamate as used by McCutcheon et al. (2016) resulted in a significant increase of pyknotic nuclei in injured animals at 6 hpi (Fig. 5.11), but did not cause cell death in uninjured animals. This is in contrast to what McCutcheon et al. reported, as treatment with *L*-glutamate caused cell death; however, the authors exposed zebrafish larvae to glutamate for 48 h before they saw an effect in intact animals. The relatively short exposure time to *L*-glutamate in my experiment (6 h) is therefore a likely explanation for the lack of a neurotoxic effect.

Similar to secondary cell death following CNS trauma, zebrafish excitotoxicity and cell death have been addressed in very few zebrafish studies. McCutcheon et al. (2016) developed an excitotoxic model of brain injury by placing zebrafish larvae in a bath application of *L*-glutamate for 24 h. Skaggs et al. (2014) induced an excitotoxic brain injury to mimic Huntington's disease or stroke by injection of quinolonic acid in the adult zebrafish brain. Sheets (2017) induced excitotoxic hair cell loss by exposure to kainate or NMDA. While the above studies show that excitotoxicity is capable of inducing cell death in the zebrafish, they elicit excitotoxicity by a pharmacological treatment. As far as I know, the research carried out in my thesis is therefore first to induce and describe excitotoxicity in zebrafish following mechanical brain injury.

8.3 Early calcium signalling: friend or foe?

In addition to sustained calcium signalling following injury, I also observed immediate calcium waves and described the underlying signalling pathways. While an early neuronal calcium wave was elicited by glutamate, potentially released from damaged and dying neurons, a radial glial wave was elicited specifically by ATP. Previous research in larval zebrafish had shown that calcium waves in the first few seconds following injury can recruit microglia to a site of brain injury (Sieger et al., 2012). In other organisms and tissues, calcium waves have been demonstrated to aid wound repair. Herrgen et al. (2014) show that rapid calcium waves in the *Xenopus laevis* optic tectum can induce an actin-dependent expulsion of dead cells following injury to prevent further cell death. In the larval zebrafish, fin regeneration depends on an immediate epithelial calcium signalling (Yoo et al., 2012). In *Drosophila melanogaster* embryos, a rapid calcium wave indirectly recruits immune cells by activating the NADPH oxidase DUOX and thereby establishing a H₂O₂ gradient which in turn attracts immune cells (Razzell et al., 2013). I did not address whether H₂O₂ could play a role in the recruitment of immune cells in my brain injury assay, however Sieger et al. (2012) demonstrated that H₂O₂ is not required for microglial recruitment following brain injury in the 3 dpf larval zebrafish. Therefore, based on my results and previous studies, it seems most likely that the first microglia are recruited directly by calcium or ATP (Fig. 5.5, Sieger et al. (2012)).

Unfortunately, due to a lack of tools to inhibit calcium signalling with high temporal and spatial

control and minimal toxic adverse effects, I was unable to further investigate the role of immediate calcium waves following injury. It would have been particularly interesting to investigate two distinct questions concerning early calcium signalling:

- *What is the effect of early neuronal calcium waves on secondary cell death?*

Justet et al. (2016) describe a calcium wave in a bovine epithelial cell culture model of scratch injury capable of inhibiting excessive apoptosis during epithelial wound healing. These waves were similar to what I observed following brain injury *in vivo* (Fig. 5.1), as they developed within under five seconds of injury, originated from the injury site and subsequently spread throughout the rest of the tissue in an ATP-dependent manner. In rodent models of brain injury, neuronal calcium waves following injury are not described so far, which may however be due to technical constraints hampering *in vivo* imaging within minutes following brain injury. It would have been interesting to specifically ablate the early neuronal calcium wave following injury while not affecting any other mode of signalling, including persistent excitotoxic calcium activity; however, I was unable to do this as even following ventricular injection instead of bath application, the effect of NMDA receptor inhibitors MK801+AP5 lasted for at least 60 min (although n numbers in this experiment were small; Fig. 5.5), which was not temporally specific enough to only ablate injury-induced neuronal calcium signalling.

- *Do radial glial calcium waves affect proliferation behaviour?*

Weissman et al. (2004) showed that ATP-dependent calcium waves in neural progenitors can induce proliferation *in vitro*. I was therefore interested in whether the early ATP-dependent radial glial calcium wave could also induce proliferation in progenitors. However, with the tools at hand I was unable to do this - treatment with ATP inhibitors had an effect on recruitment of microglia (Fig. 5.5), and these cells have previously been shown to regulate injury-induced proliferation in the zebrafish brain (Kyritsis et al., 2012).

8.4 A critical role for microglial phagocytosis of debris in neuroprotection

An important finding of my thesis is that rapid microglial phagocytosis of debris following brain injury exerts a neuroprotective role (Fig. 6.16, Fig. 6.21). Tight coupling of apoptosis and phagocytosis has previously been shown to be a key function of microglia in health; disruption of this coupling has been shown to occur in mouse hippocampi following excitotoxic seizure-like lesions *in vitro* and *in vivo* (Abiega et al., 2016). This is in part attributed due to excessive amounts of ATP, which can destroy danger signal gradients and therefore 'blind' microglia.

My data show that rapid phagocytosis of debris is crucial for limiting secondary cell death, as the rate of appearance of pyknotic nuclei was significantly increased by pharmacological and genetic

inhibition of phagocytosis by targeting PS receptors (Fig. 6.16, Fig. 6.21). This result is in line with the previous finding that microglial clearance of neuronal debris protected neurons in microglia-neuronal co-culture (Noda et al., 2011). There is also evidence for a neuroprotective role of microglial phagocytosis following ischaemia *in vivo*: Kawabori et al. (2015) show that deletion of microglial receptor TREM2 results in an attenuation of phagocytic activity and an exacerbation of lesion volume following ischaemic stroke. In contrast to a neuroprotective role for microglial phagocytosis, some studies report a detrimental role: Neher et al. (2011) argue that microglial phagocytosis can be a *cause* rather than consequence of cell death. Production of peroxynitrite by activated microglia caused transient exposure of phosphatidyl serine and other *eat-me* signals in microglia-neuron co-culture, resulting in phagocytosis of stressed-but-viable neurons through activated microglia (Neher et al., 2011). Nomura et al. (2017) show that phagocytosis of live neurons (called phagoptosis) is facilitated by microglial release of adaptor proteins milk fat globulin-EGF factor 8 protein (MFG-E8) and galectin-3 (Gal-3) (Nomura et al., 2017). Following microglial activation, for example by lipopolysaccharide (LPS) or cerebral ischaemia, MFG-E8 and Gal-3 are transiently upregulated *in vitro* and *in vivo* (Neher et al., 2013; Nomura et al., 2017), bind to stressed cells (more so than dead cells), and opsonise them for microglial Mer tyrosine kinase (MerTK) recognition and phagocytosis (Nomura et al., 2017).

How can the contrasting findings in studies investigating the role of microglial phagocytosis be explained? The inflammatory environment and polarisation may play a key role. Neher et al. (2011) and Nomura et al. (2017) observed phagocytosis of live neurons by LPS-stimulated, pro-inflammatory microglia. Conversely, TREM2 is associated with suppression of inflammation in microglia. In addition to exacerbating ischaemic tissue damage upon deletion (Kawabori et al., 2015), TREM2 overexpression has been shown to provide neuroprotection, rescue spatial cognitive defects in a mouse model of tau pathology, and promote an anti-inflammatory polarisation of microglia characterised by upregulation of Arg1, IL-10, and IL-4 (Jiang et al., 2016). Interestingly, microglial LPS stimulation has been shown to result in a downregulation of TREM2 (Owens et al., 2017). The underlying microglial polarisation may therefore dictate whether phagocytosis is beneficial or detrimental. In my larval zebrafish model of brain injury, I describe a net beneficial effect of microglial phagocytosis. Interestingly, in contrast to prior mammalian findings my Neher et al. (2011) and Nomura et al. (2017), my RNA sequencing dataset reveals that the larval zebrafish does not upregulate the homologues of alectin-3, MFG-E8 or MerTK in response to injury, suggesting that these molecules may only play a minor role in the response to injury; conversely, the phagocytosis receptor BAI1 encoded by the gene *adgrb1b* was upregulated nearly four-fold (with a FDR of 0.07). Zebrafish lack a TREM2 homologue, therefore I could not study the contribution of this receptor to microglial phagocytosis and secondary cell death in larval zebrafish.

8.5 Conclusion & future outlook

With the work described in this thesis, I proposed the larval zebrafish as a new model organism to investigate secondary cell death after mechanical brain injury. I aimed to set up a simple method for the induction mechanical brain injury, and found that I was able to elicit both primary and secondary neuronal cell death in response to brain injury in larval zebrafish (Fig. 4.2, Fig. 4.4, Fig. 4.7) as had previously been observed in rodent models and human patients in response to injury. Due to the larval zebrafish's amenity for *in vivo* imaging, this allowed for imaging-based investigation of the mechanisms underlying secondary neuronal cell death.

Investigating the role of the immune system in response to injury, I have identified a neuroprotective role for rapid microglial phagocytosis of debris; failure to engulf debris as a result of pharmacological or genetic interference with phosphatidyl serine receptors resulted in a significantly enhanced rate of secondary cell death (Fig. 6.16, Fig. 6.21). I have furthermore investigated changes in immune messengers and neurotrophic factors in response to injury (Fig. 6.8), and most recently performed an RNA sequencing experiment from sorted microglia/macrophages (Chapter 7). The results obtained from RNA sequencing of microglia/macrophages will provide a useful starting point for the identification of neuroprotective transcripts following validation.

With the key advantages of an amenability to *in vivo* timelapse imaging and readily available fluorescent reporter lines, as well as the emergence of rapid CRISPR/Cas9-mediated genome editing (Jao et al., 2013) and high-throughput automated screening technologies for larval zebrafish (Pardo-Martin et al., 2010), this model will provide a powerful platform for the future investigation of cellular and molecular reactions to brain injury.

Bibliography

Abdullah NSB, 2016. *Role of CD137-CD137L interaction in microglia-mediated immune response*. Ph.D. thesis, National University of Singapore.

Abiega O, Beccari S, Diaz-Aparicio I, Nadjar A, Layé S, Leyrolle Q, Gómez-Nicola D, Domercq M, Pérez-Samartín A, Sánchez-Zafra V, Paris I, Valero J, Savage JC, Hui CW, Tremblay MÈ, Deudero JJP, Brewster AL, Anderson AE, Zaldumbide L, Galbarriatu L, Marinas A, dM Vivanco M, Matute C, Maletic-Savatic M, Encinas JM, and Sierra A, 2016. Neuronal Hyperactivity Disturbs ATP Microgradients, Impairs Microglial Motility, and Reduces Phagocytic Receptor Expression Triggering Apoptosis/Microglial Phagocytosis Uncoupling. *PLoS Biology*, 14(5). doi:10.1371/journal.pbio.1002466.

Adams SM, de Rivero Vaccari JC, and Corriveau RA, 2004. Pronounced Cell Death in the Absence of NMDA Receptors in the Developing Somatosensory Thalamus. *Journal of Neuroscience*, 24(42):9441–9450. doi:10.1523/JNEUROSCI.3290-04.2004.

Adelson PD, 2009. Hypothermia following Pediatric Traumatic Brain Injury. *Journal of Neurotrauma*, 26(3):429. doi:10.1089/NEU.2008.0571.

Adelson PD, Wisniewski SR, Beca J, Brown SD, Bell M, Muizelaar JP, Okada P, Beers SR, Balasubramani GK, and Hirtz D, 2013. Comparison of hypothermia and normothermia after severe traumatic brain injury in children (Cool Kids): A phase 3, randomised controlled trial. *The Lancet Neurology*, 12(6):546–553. doi:10.1016/S1474-4422(13)70077-2.

Adinolfi E, Pizzirani C, Idzko M, Panther E, Norgauer J, Di Virgilio F, and Ferrari D, 2005. P2X(7) receptor: Death or life? *Purinergic Signalling*, 1(3):219–27. doi:10.1007/s11302-005-6322-x.

Adolf B, Chapouton P, Lam CS, Topp S, Tannhäuser B, Strähle U, Götz M, and Bally-Cuif L, 2006. Conserved and acquired features of adult neurogenesis in the zebrafish telencephalon. *Developmental Biology*, 295(1):278–293.

Aguzzi A, Barres BA, and Bennett ML, 2013. Microglia: Scapegoat, Saboteur, or Something Else? *Science*, 339(6116):156–161. doi:10.1126/science.1227901.

- Albalawi F, Lu W, Beckel JM, Lim JC, McCaughey SA, and Mitchell CH**, 2017. The P2X7 Receptor Primes IL-1 β and the NLRP3 Inflammasome in Astrocytes Exposed to Mechanical Strain. *Frontiers in Cellular Neuroscience*, 11:227. doi:10.3389/fncel.2017.00227.
- Allen C, Thornton P, Denes A, McColl BW, Pierozynski A, Monestier M, Pinteaux E, Rothwell NJ, and Allan SM**, 2012. Neutrophil cerebrovascular transmigration triggers rapid neurotoxicity through release of proteases associated with decondensed DNA. *Journal of Immunology*, 189(1):381–92. doi:10.4049/jimmunol.1200409.
- Allen NJ and Lyons DA**, 2018. Glia as architects of central nervous system formation and function. *Science*, 362(6411):181–185. doi:10.1126/SCIENCE.AAT0473.
- Amaya DA, Wegner M, Stolt CC, Chehrehasa F, Ekberg JA, and St John JA**, 2015. Radial glia phagocytose axonal debris from degenerating overextending axons in the developing olfactory bulb. *Journal of Comparative Neurology*, 523(2):183–196. doi:10.1002/cne.23665.
- Annegers JF, Hauser WA, Coan SP, and Rocca WA**, 1998. A Population-Based Study of Seizures after Traumatic Brain Injuries. *New England Journal of Medicine*, 338(1):20–24. doi:10.1056/NEJM199801013380104.
- Anthonymuthu TS, Kenny EM, and Bayr H**, 2016. Therapies targeting lipid peroxidation in traumatic brain injury. *Brain Research*, 1640(Pt A):57–76. doi:10.1016/j.brainres.2016.02.006.
- Antunes M, Pereira T, Cordeiro JV, Almeida L, and Jacinto A**, 2013. Coordinated waves of actomyosin flow and apical cell constriction immediately after wounding. *Journal of Cell Biology*, 202(2):365–379.
- Aoyama N, Katayama Y, Kawamata T, Maeda T, Mori T, Yamamoto T, Kikuchi T, and Uwahodo Y**, 2002. Effects of antioxidant, OPC-14117, on secondary cellular damage and behavioral deficits following cortical contusion in the rat. *Brain Research*, 934(2):117–124. doi:10.1016/S0006-8993(02)02366-1.
- Arvidsson A, Collin T, Kirik D, Kokaia Z, and Lindvall O**, 2002. Neuronal replacement from endogenous precursors in the adult brain after stroke. *Nature Medicine*, 8(9):963–970.
- Askew K, Li K, Olmos-Alonso A, Garcia-Moreno F, Liang Y, Richardson P, Tipton T, Chapman MA, Riecken K, Beccari S, Sierra A, Molnár Z, Cragg MS, Garaschuk O, Perry VH, and Gomez-Nicola D**, 2017. Coupled Proliferation and Apoptosis Maintain the Rapid Turnover of Microglia in the Adult Brain. *Cell Reports*, 18(2):391–405. doi:10.1016/j.celrep.2016.12.041.
- Aurora AB, Porrello ER, Tan W, Mahmoud AI, Hill JA, Bassel-Duby R, Sadek HA, and Olson EN**, 2014. Macrophages are required for neonatal heart regeneration. *Journal of Clinical Investigation*, 124(3):1382–1392. doi:10.1172/JCI72181.

- Bachstetter AD, Rowe RK, Kaneko M, Goulding D, Lifshitz J, and Van Eldik LJ**, 2013. The p38 MAPK Regulates Microglial Responsiveness to Diffuse Traumatic Brain Injury. *Journal of Neuroscience*, 33(14):6143–6153. doi:10.1523/JNEUROSCI.5399-12.2013.
- Bachstetter AD, Xing B, de Almeida L, Dimayuga ER, Watterson DM, and Van Eldik LJ**, 2011. Microglial p38 α MAPK is a key regulator of proinflammatory cytokine up-regulation induced by toll-like receptor (TLR) ligands or beta-amyloid (A β). *Journal of Neuroinflammation*, 8(1):79. doi:10.1186/1742-2094-8-79.
- Bader MF, Taupenot L, Ulrich G, Aunis D, and Ciesielski-Treska J**, 1994. Bacterial endotoxin induces [Ca²⁺]_i transients and changes the organization of actin in microglia. *Glia*, 11(4):336–344. doi:10.1002/glia.440110406.
- Bailey TJ, Fossum SL, Fimbel SM, Montgomery JE, and Hyde DR**, 2010. The inhibitor of phagocytosis, O-phospho-L-serine, suppresses Müller glia proliferation and cone cell regeneration in the light-damaged zebrafish retina. *Experimental Eye Research*, 91(5):601–612. doi:10.1016/j.exer.2010.07.017.
- Balasubramanian K and Schroit AJ**, 2003. Aminophospholipid Asymmetry: A Matter of Life and Death. *Annual Review of Physiology*, 65(1):701–734. doi:10.1146/annurev.physiol.65.092101.142459.
- Barnes DE, Kaup A, Kirby KA, Byers AL, Diaz-Arrastia R, and Yaffe K**, 2014. Traumatic brain injury and risk of dementia in older veterans. *Neurology*, 83(4):312–319. doi:10.1212/WNL.0000000000000616.
- Barouch R and Schwartz M**, 2002. Autoreactive T cells induce neurotrophin production by immune and neural cells in injured rat optic nerve: implications for protective autoimmunity. *FASEB journal*, 16(10):1304–1306. doi:10.1096/fj.01-0467fje.
- Barry D and McDermott K**, 2005. Differentiation of radial glia from radial precursor cells and transformation into astrocytes in the developing rat spinal cord. *Glia*, 50(3):187–197. doi:10.1002/glia.20166.
- Basu A, Krady JK, O'Malley M, Styren SD, DeKosky ST, and Levison SW**, 2002. The type 1 interleukin-1 receptor is essential for the efficient activation of microglia and the induction of multiple proinflammatory mediators in response to brain injury. *Journal of Neuroscience*, 22(14):6071–82. doi:20026616.
- Bauer S and Patterson PH**, 2006. Leukemia Inhibitory Factor Promotes Neural Stem Cell Self-Renewal in the Adult Brain. *Journal of Neuroscience*, 26(46):12089–12099. doi:10.1523/JNEUROSCI.3047-06.2006.

- Bauer S, Rasika S, Han J, Mauduit C, Raccurt M, Morel G, Jourdan F, Benahmed M, Moyse E, and Patterson PH**, 2003. Leukemia inhibitory factor is a key signal for injury-induced neurogenesis in the adult mouse olfactory epithelium. *Journal of Neuroscience*, 23(5):1792–803.
- Baumgart EV, Barbosa JS, Bally-cuif L, Götz M, and Ninkovic J**, 2012. Stab wound injury of the zebrafish telencephalon: A model for comparative analysis of reactive gliosis. *Glia*, 60(3):343–357.
- Bayir H, Kagan VE, Borisenko GG, Tyurina YY, Janesko KL, Vagni VA, Billiar TR, Williams DL, and Kochanek PM**, 2005. Enhanced Oxidative Stress in iNOS-Deficient Mice after Traumatic Brain Injury: Support for a Neuroprotective Role of iNOS. *Journal of Cerebral Blood Flow & Metabolism*, 25(6):673–684. doi:10.1038/sj.jcbfm.9600068.
- Bayly PV, Dikranian KT, Black EE, Young C, Qin YQ, Labruyere J, and Olney JW**, 2006. Spatiotemporal evolution of apoptotic neurodegeneration following traumatic injury to the developing rat brain. *Brain Research*, 1107(1):70–81. doi:10.1016/j.brainres.2006.05.102.
- Bayr H, Kagan VE, Clark RSB, Janesko-Feldman K, Rafikov R, Huang Z, Zhang X, Vagni V, Billiar TR, and Kochanek PM**, 2006. Neuronal NOS-mediated nitration and inactivation of manganese superoxide dismutase in brain after experimental and human brain injury. *Journal of Neurochemistry*, 101(1):168–181. doi:10.1111/j.1471-4159.2006.04353.x.
- Becker CG and Becker T**, 2008. Adult zebrafish as a model for successful central nervous system regeneration. *Restorative Neurology and Neuroscience*, 26:71–80.
- Becker CG, Lieberoth BC, Morellini F, Feldner J, Becker T, and Schachner M**, 2004. L1.1 Is Involved in Spinal Cord Regeneration in Adult Zebrafish. *Journal of Neuroscience*, 24(36):7837–7842. doi:10.1523/JNEUROSCI.2420-04.2004.
- Becker T, Wullmann MF, Becker CG, Bernhardt RR, and Schachner M**, 1997. Axonal regrowth after spinal cord transection in adult zebrafish. *Journal of Comparative Neurology*, 377(4):577–595.
- Beer R, Franz G, Srinivasan A, Hayes RL, Pike BR, Newcomb JK, Zhao X, Schmutzhard E, Poewe W, and Kampfl A**, 2000. Temporal profile and cell subtype distribution of activated caspase-3 following experimental traumatic brain injury. *Journal of Neurochemistry*, 75(3):1264–73.
- Belanger HG, Kretzmer T, Vanderploeg RD, and French LM**, 2010. Symptom complaints following combat-related traumatic brain injury: Relationship to traumatic brain injury severity and posttraumatic stress disorder. *Journal of the International Neuropsychological Society*, 16(1):194–199. doi:10.1017/S1355617709990841.

- Bennett ML, Bennett FC, Liddel SA, Ajami B, Zamanian JL, Fernhoff NB, Mulinyawe SB, Bohlen CJ, Adil A, Tucker A, Weissman IL, Chang EF, Li G, Grant GA, Hayden Gephart MG, and Barres BA**, 2016. New tools for studying microglia in the mouse and human CNS. *Proceedings of the National Academy of Sciences*, 113(12):E1738–E1746. doi: 10.1073/pnas.1525528113.
- Berpohl D, You Z, Lo EH, Kim HH, and Whalen MJ**, 2007. TNF Alpha and Fas Mediate Tissue Damage and Functional Outcome after Traumatic Brain Injury in Mice. *Journal of Cerebral Blood Flow & Metabolism*, 27(11):1806–1818. doi:10.1038/sj.jcbfm.9600487.
- Berridge MJ, Bootman MD, and Roderick HL**, 2003. Calcium signalling: dynamics, homeostasis and remodelling. *Nature Reviews Molecular Cell Biology*, 4(7):517–529. doi:10.1038/nrm1155.
- Bianchi M, Bloom O, Raabe T, Cohen PS, Chesney J, Sherry B, Schmidtayerova H, Calandra T, Zhang X, Bukrinsky M, Ulrich P, Cerami A, and Tracey KJ**, 1996. Suppression of proinflammatory cytokines in monocytes by a tetravalent guanylylhydrazone. *Journal of Experimental Medicine*, 183(3):927–36.
- Biane J, Conner JM, and Tuszynski MH**, 2014. Nerve growth factor is primarily produced by GABAergic neurons of the adult rat cortex. *Frontiers in Cellular Neuroscience*, 8:220. doi: 10.3389/fncel.2014.00220.
- Birge RB, Boeltz S, Kumar S, Carlson J, Wanderley J, Calianese D, Barcinski M, Brekken RA, Huang X, Hutchins JT, Freimark B, Empig C, Mercer J, Schroit AJ, Schett G, and Herrmann M**, 2016. Phosphatidylserine is a global immunosuppressive signal in efferocytosis, infectious disease, and cancer. *Cell Death and Differentiation*, 23(6):962–978. doi: 10.1038/cdd.2016.11.
- Blesch A, Uy HS, Grill RJ, Cheng JG, Patterson PH, and Tuszynski MH**, 1999. Leukemia inhibitory factor augments neurotrophin expression and corticospinal axon growth after adult CNS injury. *Journal of Neuroscience*, 19(9):3556–66.
- Bohlen CJ, Bennett FC, Tucker AF, Collins HY, Mulinyawe SB, and Barres BA**, 2017. Diverse Requirements for Microglial Survival, Specification, and Function Revealed by Defined-Medium Cultures. *Neuron*, 94(4):759–773.e8. doi:10.1016/j.neuron.2017.04.043.
- Bombardier CH, Fann JR, Temkin NR, Esselman PC, Barber J, and Dikmen SS**, 2010. Rates of Major Depressive Disorder and Clinical Outcomes Following Traumatic Brain Injury. *Journal of the American Medical Association*, 303(19):1938–1945. doi:10.1001/jama.2010.599.
- Boniakowski AE, Kimball AS, Joshi A, Schaller M, Davis FM, DenDekker A, Obi AT, Moore BB, Kunkel SL, and Gallagher KA**, 2018. Murine macrophage chemokine receptor CCR2 plays

- a crucial role in macrophage recruitment and regulated inflammation in wound healing. *European Journal of Immunology*, 48(9):1445–1455. doi:10.1002/eji.201747400.
- Boraschi D, Bossù P, Ruggiero P, Tagliabue A, Bertini R, Macchia G, Gasbarro C, Pellegrini L, Melillo G, Ulisse E, Visconti U, Bizzarri C, Del Grosso E, Mackay AR, Frascotti G, Frigerio F, Grifantini R, and Grandi G**, 1995. Mapping of receptor binding sites on IL-1 beta by reconstruction of IL-1ra-like domains. *Journal of Immunology*, 155(10):4719–25.
- Böttcher C, Schlickeiser S, Sneebroeck MAM, Kunkel D, Knop A, Paza E, Fidzinski P, Kraus L, Snijders GJL, Kahn RS, Schulz AR, Mei HE, Hol EM, Siegmund B, Glaben R, Spruth EJ, de Witte LD, and Priller J**, 2019. Human microglia regional heterogeneity and phenotypes determined by multiplexed single-cell mass cytometry. *Nature Neuroscience*, 22(1):78–90. doi:10.1038/s41593-018-0290-2.
- Bournazou I, Pound JD, Duffin R, Bournazos S, Melville LA, Brown SB, Rossi AG, and Gregory CD**, 2009. Apoptotic human cells inhibit migration of granulocytes via release of lactoferrin. *Journal of Clinical Investigation*, 119(1):20–32. doi:10.1172/JCI36226.
- Braakman R, Schouten HJA, Blaauw-van Dishoeck M, and Minderhoud JM**, 1983. Megadose steroids in severe head injury. *Journal of Neurosurgery*, 58(3):326–330. doi:10.3171/jns.1983.58.3.0326.
- Braet K, Aspeslagh S, Vandamme W, Willecke K, Martin PEM, Evans WH, and Leybaert L**, 2003. Pharmacological sensitivity of ATP release triggered by photoliberation of inositol-1,4,5-trisphosphate and zero extracellular calcium in brain endothelial cells. *Journal of Cellular Physiology*, 197(2):205–213. doi:10.1002/jcp.10365.
- Bramlett HM and Dietrich WD**, 2001. Neuropathological Protection after Traumatic Brain Injury in Intact Female Rats Versus Males or Ovariectomized Females. *Journal of Neurotrauma*, 18(9):891–900. doi:10.1089/089771501750451811.
- Bramlett HM, Green EJ, Dietrich WD, Busto R, Globus MYT, and Ginsberg MD**, 1995. Posttraumatic Brain Hypothermia Provides Protection from Sensorimotor and Cognitive Behavioral Deficits. *Journal of Neurotrauma*, 12(3):290–306. doi:10.1089/neu.1995.12.289.
- Brandes ME, Mai UE, Ohura K, and Wahl SM**, 1991. Type I transforming growth factor-beta receptors on neutrophils mediate chemotaxis to transforming growth factor-beta. *Journal of Immunology*, 147(5):1600–6.
- Bratton DL, Fadok VA, Richter DA, Kailey JM, Guthrie LA, and Henson PM**, 1997. Appearance of phosphatidylserine on apoptotic cells requires calcium-mediated nonspecific flip-flop and is enhanced by loss of the aminophospholipid translocase. *Journal of Biological Chemistry*, 272(42):26159–26165. doi:10.1074/jbc.272.42.26159.

- Brennan FH, Hall JC, Guan Z, and Popovich PG**, 2018. Microglia limit lesion expansion and promote functional recovery after spinal cord injury in mice. *bioRxiv*, page 410258. doi: 10.1101/410258.
- Brewer KL, Bethea JR, and Yeziarski RP**, 1999. Neuroprotective Effects of Interleukin-10 Following Excitotoxic Spinal Cord Injury. *Experimental Neurology*, 159(2):484–493. doi: 10.1006/exnr.1999.7173.
- Brinkmann V, Reichard U, Goosmann C, Fauler B, Uhlemann Y, Weiss DS, Weinrauch Y, and Zychlinsky A**, 2004. Neutrophil Extracellular Traps Kill Bacteria. *Science*, 303(5663):1532–1535. doi:10.1126/science.1092385.
- Brouckaert G, Kalai M, Krysko DV, Saelens X, Vercammen D, Ndlovu MN, Ndlovu M, Haegeman G, D'Herde K, and Vandenabeele P**, 2004. Phagocytosis of necrotic cells by macrophages is phosphatidylserine dependent and does not induce inflammatory cytokine production. *Molecular Biology of the Cell*, 15(3):1089–100. doi:10.1091/mbc.e03-09-0668.
- Bruce AJ, Boling W, Kindy MS, Peschon J, Kraemer PJ, Carpenter MK, Holtsberg FW, and Mattson MP**, 1996. Altered neuronal and microglial responses to excitotoxic and ischemic brain injury in mice lacking TNF receptors. *Nature Medicine*, 2(7):788–794. doi:10.1038/nm0796-788.
- Bryan CJ**, 2013. Multiple traumatic brain injury and concussive symptoms among deployed military personnel. *Brain Injury*, 27(12):1333–1337. doi:10.3109/02699052.2013.823651.
- Buchthal B, Weiss U, and Bading H**, 2018. Post-injury Nose-to-Brain Delivery of Activin A and SerpinB2 Reduces Brain Damage in a Mouse Stroke Model. *Molecular Therapy*, 26(10):2357–2365. doi:10.1016/J.YMTHE.2018.07.018.
- Butovsky O, Jedrychowski MP, Moore CS, Cialic R, Lanser AJ, Gabriely G, Koeglsperger T, Dake B, Wu PM, Doykan CE, Fanek Z, Liu L, Chen Z, Rothstein JD, Ransohoff RM, Gygi SP, Antel JP, and Weiner HL**, 2014. Identification of a unique TGF- β dependent molecular and functional signature in microglia. *Nature Neuroscience*, 17(1):131–143. doi:10.1038/nn.3599.
- Butovsky O, Ziv Y, Schwartz A, Landa G, Talpalar AE, Pluchino S, Martino G, and Schwartz M**, 2006. Microglia activated by IL-4 or IFN- γ differentially induce neurogenesis and oligodendrogenesis from adult stem/progenitor cells. *Molecular and Cellular Neuroscience*, 31(1):149–160. doi:10.1016/j.mcn.2005.10.006.
- Bye N, Habgood MD, Callaway JK, Malakooti N, Potter A, Kossmann T, and Morganti-Kossmann MC**, 2007. Transient neuroprotection by minocycline following traumatic brain injury is associated with attenuated microglial activation but no changes in cell apoptosis or neutrophil infiltration. *Experimental Neurology*, 204(1):220–233. doi:10.1016/J.EXPNEUROL.2006.10.013.

- Cacialli P, D'angelo L, Kah O, Coumaillau P, Gueguen MM, Pellegrini E, and Lucini C**, 2018. Neuronal expression of brain derived neurotrophic factor in the injured telencephalon of adult zebrafish. *Journal of Comparative Neurology*, 526(4):569–582. doi:10.1002/cne.24352.
- Calabrese V, Mancuso C, Calvani M, Rizzarelli E, Butterfield DA, and Stella AMG**, 2007. Nitric oxide in the central nervous system: neuroprotection versus neurotoxicity. *Nature Reviews Neuroscience*, 8:766–775. doi:10.1038/nrn2214.
- Cameron HA and McKay RD**, 2001. Adult neurogenesis produces a large pool of new granule cells in the dentate gyrus. *Journal of Comparative Neurology*, 435(4):406–17.
- Cancelliere C, Kristman VL, Cassidy JD, Hincapié CA, Côté P, Boyle E, Carroll LJ, Stålnacke BM, Nygren-de Boussard C, and Borg J**, 2014. Systematic Review of Return to Work After Mild Traumatic Brain Injury: Results of the International Collaboration on Mild Traumatic Brain Injury Prognosis. *Archives of Physical Medicine and Rehabilitation*, 95(3):S201–S209. doi:10.1016/j.apmr.2013.10.010.
- Cao X, Li LP, Qin XH, Li SJ, Zhang M, Wang Q, Hu HH, Fang YY, Gao YB, Li XW, Sun LR, Xiong WC, Gao TM, and Zhu XH**, 2013. Astrocytic Adenosine 5-Triphosphate Release Regulates the Proliferation of Neural Stem Cells in the Adult Hippocampus. *Stem Cells*, 31(8):1633–1643. doi:10.1002/stem.1408.
- Carbon S, Ireland A, Mungall CJ, Shu S, Marshall B, Lewis S, Lomax J, Mungall C, Hitz B, Balakrishnan R, Dolan M, Wood V, Hong E, and Gaudet P**, 2009. AmiGO: Online access to ontology and annotation data. *Bioinformatics*, 25(2):288–289. doi:10.1093/bioinformatics/btn615.
- Cardona AE, Pioro EP, Sasse ME, Kostenko V, Cardona SM, Dijkstra IM, Huang D, Kidd G, Dombrowski S, Dutta R, Lee JC, Cook DN, Jung S, Lira SA, Littman DR, and Ransohoff RM**, 2006. Control of microglial neurotoxicity by the fractalkine receptor. *Nature Neuroscience*, 9(7):917–924. doi:10.1038/nn1715.
- Carlos TM, Clark RSB, Franicola-Higgins D, Schiding JK, and Kochanek PM**, 1997. Expression of endothelial adhesion molecules and recruitment of neutrophils after traumatic brain injury in rats. *Journal of Leukocyte Biology*, 61(3):279–285. doi:10.1002/jlb.61.3.279.
- Casano AM, Albert M, and Peri F**, 2016. Developmental Apoptosis Mediates Entry and Positioning of Microglia in the Zebrafish Brain Report Developmental Apoptosis Mediates Entry and Positioning of Microglia in the Zebrafish Brain. *Cell Reports*, 16(4):897–906. doi:10.1016/j.celrep.2016.06.033.
- Castriotta RJ, Wilde MC, Lai JM, Atanasov S, Masel BE, and Kuna ST**, 2007. Prevalence and consequences of sleep disorders in traumatic brain injury. *Journal of clinical sleep medicine : JCSM : official publication of the American Academy of Sleep Medicine*, 3(4):349–56.

- Center for Disease Control and Prevention (CDC) and National Center for Injury Prevention and Control**, 2003. Report to Congress on Mild Traumatic Brain Injury in the United States: Steps to Prevent a Serious Public Health Problem. Technical report, Centers for Disease Control and Prevention, Atlanta, GA.
- Centers for Disease Control and Prevention (CDC)**, 2011. Nonfatal Traumatic Brain Injuries Related to Sports and Recreation Activities Among Persons Aged <19 Years. *Morbidity and Mortality Weekly Report*, 60(39):1337–1342.
- Cernak I, Savic VJ, Kotur J, Prokic V, Veljovic M, and Grbovic D**, 2000. Characterization of Plasma Magnesium Concentration and Oxidative Stress Following Graded Traumatic Brain Injury in Humans. *Journal of Neurotrauma*, 17(1):53–68. doi:10.1089/neu.2000.17.53.
- Chamak B, Morandi V, and Mallat M**, 1994. Brain macrophages stimulate neurite growth and regeneration by secreting thrombospondin. *Journal of Neuroscience Research*, 38(2):221–233. doi:10.1002/jnr.490380213.
- Chan P, Epstein C, Li Y, Huang T, Carlson E, Kinouchi H, Yang G, Kamii H, Mikawa S, Kondo T, Copin JC, Chen SF, Chan T, Gafni J, Gobbel G, and Reola E**, 1995. Transgenic Mice and Knockout Mutants in the Study of Oxidative Stress in Brain Injury. *Journal of Neurotrauma*, 12(5):815–824. doi:10.1089/neu.1995.12.815.
- Chao CC, Hu S, Molitor TW, Shaskan EG, and Peterson PK**, 1992. Activated microglia mediate neuronal cell injury via a nitric oxide mechanism. *Journal of Immunology*, 149(8):2736–41.
- Chapman PF, Atkins CM, Allen MT, Haley JE, and Steinmetz JE**, 1992. Inhibition of nitric oxide synthesis impairs two different forms of learning. *Neuroreport*, 3(7):567–70.
- Charlton SJ, Brown CA, Weisman GA, Turner JT, Erb L, and Boarder MR**, 1996. PPADS and suramin as antagonists at cloned P2Y- and P2U-purinoceptors. *British Journal of Pharmacology*, 118(3):704–710. doi:10.1111/j.1476-5381.1996.tb15457.x.
- Chen H, Richard M, Sandler DP, Umbach DM, and Kamel F**, 2007. Head Injury and Amyotrophic Lateral Sclerosis. *American Journal of Epidemiology*, 166(7):810–816. doi:10.1093/aje/kwm153.
- Chen TW, Wardill TJ, Sun Y, Pulver SR, Renninger SL, Baohan A, Schreiter ER, Kerr RA, Orger MB, Jayaraman V, Looger LL, Svoboda K, and Kim DS**, 2013. Ultra-sensitive fluorescent proteins for imaging neuronal activity. *Nature*, 499(7458):295–300. doi:10.1038/nature12354.

- Chesnut RM, Marshall LF, Klauber MR, Blunt BA, Baldwin N, Eisenberg HM, Jane JA, Marmarou A, and Foulkes MA**, 1993. The role of secondary brain injury in determining outcome from severe head injury. *Journal of Trauma*, 34(2):216–22.
- Chifflet S, Justet C, Hernández JA, Nin V, Escande C, and Benech JC**, 2012. Early and late calcium waves during wound healing in corneal endothelial cells. *Wound Repair and Regeneration*, 20(1):28–37. doi:10.1111/j.1524-475X.2011.00749.x.
- Chiu I, Morimoto E, Goodarzi H, Liao J, O’Keeffe S, Phatnani H, Muratet M, Carroll M, Levy S, Tavazoie S, Myers R, and Maniatis T**, 2013. A Neurodegeneration-Specific Gene-Expression Signature of Acutely Isolated Microglia from an Amyotrophic Lateral Sclerosis Mouse Model. *Cell Reports*, 4(2):385–401. doi:10.1016/j.celrep.2013.06.018.
- Choi BY, Jang BG, Kim JH, Lee BE, Sohn M, Song HK, and Suh SW**, 2012. Prevention of traumatic brain injury-induced neuronal death by inhibition of NADPH oxidase activation. *Brain Research*, 1481:49–58. doi:10.1016/j.brainres.2012.08.032.
- Choi DW**, 1985. Glutamate neurotoxicity in cortical cell culture is calcium dependent. *Neuroscience Letters*, 58(3):293–297. doi:10.1016/0304-3940(85)90069-2.
- Choi DW**, 1988. Glutamate neurotoxicity and diseases of the nervous system. *Neuron*, 1(8):623–634. doi:10.1007/BF00523090.
- Choi YB, Tanneti L, Le DA, Ortiz J, Bai G, Chen HSV, and Lipton SA**, 2000. Molecular basis of NMDA receptor-coupled ion channel modulation by S-nitrosylation. *Nature Neuroscience*, 3(1):15–21. doi:10.1038/71090.
- Chong ZZ, Li F, and Maiese K**, 2005. Oxidative stress in the brain: Novel cellular targets that govern survival during neurodegenerative disease. *Progress in Neurobiology*, 75(3):207–246. doi:10.1016/j.pneurobio.2005.02.004.
- Christensen J, Pedersen MG, Pedersen CB, Sidenius P, Olsen J, and Vestergaard M**, 2009. Long-term risk of epilepsy after traumatic brain injury in children and young adults: a population-based cohort study. *The Lancet*, 373(9669):1105–1110. doi:10.1016/S0140-6736(09)60214-2.
- Cianciulli A, Dragone T, Calvello R, Porro C, Trotta T, Lofrumento DD, and Panaro MA**, 2015. IL-10 plays a pivotal role in anti-inflammatory effects of resveratrol in activated microglia cells. *International Immunopharmacology*, 24(2):369–376. doi:10.1016/j.intimp.2014.12.035.
- Clark AG, Miller AL, Vaughan E, Yu HYE, Penkert R, and Bement WM**, 2009. Integration of Single and Multicellular Wound Responses. *Current Biology*, 19(16):1389–1395. doi:10.1016/j.cub.2009.06.044.

- Clark RB, Kochanek PM, Chen M, Watkins SC, Marion DW, Chen J, Hamilton RL, Loeffert JE, and Graham SH**, 1999. Increases in Bcl-2 and cleavage of caspase-1 and caspase-3 in human brain after head injury. *FASEB Journal*, 13(8):813–821.
- Clark RS, Kochanek PM, Watkins SC, Chen M, Dixon CE, Seidberg NA, Melick J, Loeffert JE, Nathaniel PD, Jin KL, and Graham SH**, 2000. Caspase-3 mediated neuronal death after traumatic brain injury in rats. *Journal of neurochemistry*, 74(2):740–53.
- Clark RSB, Kochanek PM, Marion DW, Schiding JK, White M, Palmer AM, and DeKosky ST**, 1996. Mild Posttraumatic Hypothermia Reduces Mortality after Severe Controlled Cortical Impact in Rats. *Journal of Cerebral Blood Flow & Metabolism*, 16(2):253–261. doi:10.1097/00004647-199603000-00010.
- Clark RSB, Schiding JK, Kaczorowski SL, Marion DW, and Kochanek PM**, 1994. Neutrophil Accumulation After Traumatic Brain Injury in Rats: Comparison of Weight Drop and Controlled Cortical Impact Models. *Journal of Neurotrauma*, 11(5):499–506. doi:10.1089/neu.1994.11.499.
- Claude J, Linnartz-Gerlach B, Kudin AP, Kunz WS, and Neumann H**, 2013. Microglial CD33-Related Siglec-E Inhibits Neurotoxicity by Preventing the Phagocytosis-Associated Oxidative Burst. *Journal of Neuroscience*, 33(46):18270–18276. doi:10.1523/JNEUROSCI.2211-13.2013.
- Clausen F, Hånell A, Björk M, Hillered L, Mir AK, Gram H, and Marklund N**, 2009. Neutralization of interleukin-1 β modifies the inflammatory response and improves histological and cognitive outcome following traumatic brain injury in mice. *European Journal of Neuroscience*, 30(3):385–396. doi:10.1111/j.1460-9568.2009.06820.x.
- Clements JD, Lester RA, Tong G, Jahr CE, and Westbrook GL**, 1992. The time course of glutamate in the synaptic cleft. *Science*, 258(5087):1498–501.
- Clifton GL, Allen S, Barrodale P, Plenger P, Berry J, Koch S, Fletcher J, Hayes RL, and Choi SG**, 1993. A Phase II Study of Moderate Hypothermia in Severe Brain Injury. *Journal of Neurotrauma*, 10(3):263–271. doi:10.1089/neu.1993.10.263.
- Clifton GL, Jiang JY, Lyeth BG, Jenkins LW, Hamm RJ, and Hayes RL**, 1991. Marked protection by moderate hypothermia after experimental traumatic brain injury. *Journal of Cerebral Blood Flow and Metabolism*, 11(1):114–121. doi:10.1038/jcbfm.1991.13.
- Clifton GL, Miller ER, Choi SC, Levin HS, McCauley S, Smith KR, Muizelaar JP, Wagner FC, Marion DW, Luerssen TG, Chesnut RM, and Schwartz M**, 2001. Lack of Effect of Induction of Hypothermia after Acute Brain Injury. *New England Journal of Medicine*, 344(8):556–563. doi:10.1056/NEJM200102223440803.

- Clifton GL, Valadka A, Zygun D, Coffey CS, Drever P, Fourwinds S, Janis LS, Wilde E, Taylor P, Harshman K, Conley A, Puccio A, Levin HS, McCauley SR, Bucholz RD, Smith KR, Schmidt JH, Scott JN, Yonas H, and Okonkwo DO**, 2011. Very early hypothermia induction in patients with severe brain injury (the National Acute Brain Injury Study: Hypothermia II): a randomised trial. *The Lancet Neurology*, 10(2):131–139. doi:10.1016/S1474-4422(10)70300-8.
- Cohen PS, Nakshatri H, Dennis J, Caragine T, Bianchi M, Cerami A, and Tracey KJ**, 1996. CNI-1493 inhibits monocyte/macrophage tumor necrosis factor by suppression of translation efficiency. *Proceedings of the National Academy of Sciences of the United States of America*, 93(9):3967–71. doi:10.1073/PNAS.93.9.3967.
- Colonna M and Butovsky O**, 2017. Microglia Function in the Central Nervous System During Health and Neurodegeneration. *Annual Review of Immunology*, 35(1):441–468. doi:10.1146/annurev-immunol-051116-052358.
- Colwell AS, Longaker MT, and Lorenz HP**, 2003. Fetal wound healing. *Frontiers in Bioscience*, 8:s1240–8.
- Connolly GP**, 1995. Differentiation by pyridoxal 5phosphate, PPADS and IsoPPADS between responses mediated by UTP and those evoked by α,β methyleneATP on rat sympathetic ganglia. *British Journal of Pharmacology*, 114(3):727–731. doi:10.1111/j.1476-5381.1995.tb17199.x.
- Conti AC, Raghupathi R, Trojanowski JQ, and McIntosh TK**, 1998. Experimental brain injury induces regionally distinct apoptosis during the acute and delayed post-traumatic period. *Journal of Neuroscience*, 18(15):5663–72.
- Cooper DJ, Rosenfeld JV, Murray L, Arabi YM, Davies AR, D'Urso P, Kossmann T, Ponsford J, Seppelt I, Reilly P, and Wolfe R**, 2011. Decompressive Craniectomy in Diffuse Traumatic Brain Injury. *New England Journal of Medicine*, 364(16):1493–1502. doi:10.1056/NEJMoa1102077.
- Cooper PR, Hagler H, Clark WK, and Barnett P**, 1979. Enhancement of experimental cerebral edema after decompressive craniectomy: implications for the management of severe head injuries. *Neurosurgery*, 4(4):296–300.
- Cooper SR, Emond MR, Duy PQ, Liebau BG, Wolman MA, and Jontes JD**, 2015. Protocadherins control the modular assembly of neuronal columns in the zebrafish optic tectum. *Journal of Cell Biology*, 211(4):807–814.
- Corbo CP, Othman NA, Gutkin MC, Alonso ADC, and Fulop ZL**, 2012. Use of different morphological techniques to analyze the cellular composition of the adult zebrafish optic tectum. *Microscopy Research and Technique*, 75(3):325–333. doi:10.1002/jemt.21061.

- Cordeiro JV and Jacinto A**, 2013. The role of transcription-independent damage signals in the initiation of epithelial wound healing. *Nature Reviews Molecular Cell Biology*, 14(4):249–62.
- Corps KN, Roth TL, and McGavern DB**, 2015. Inflammation and neuroprotection in traumatic brain injury. *Journal of the American Medical Association neurology*, 72(3):355–62. doi:10.1001/jamaneurol.2014.3558.
- Corr DT and Hart DA**, 2013. Biomechanics of Scar Tissue and Uninjured Skin. *Advances in Wound Care*, 2(2):37–43. doi:10.1089/wound.2011.0321.
- Cortez SC, McIntosh TK, and Noble LJ**, 1989. Experimental fluid percussion brain injury: vascular disruption and neuronal and glial alterations. *Brain Research*, 482(2):271–282. doi:10.1016/0006-8993(89)91190-6.
- Crane PK, Gibbons LE, Dams-O'Connor K, Trittschuh E, Leverenz JB, Keene CD, Sonnen J, Montine TJ, Bennett DA, Leurgans S, Schneider JA, and Larson EB**, 2016. Association of Traumatic Brain Injury With Late-Life Neurodegenerative Conditions and Neuropathologic Findings. *Journal of the American Medical Association Neurology*, 73(9):1062. doi:10.1001/jamaneurol.2016.1948.
- Cuenca N, Fernández-Sánchez L, McGill TJ, Lu B, Wang S, Lund R, Huhn S, and Capela A**, 2013. Phagocytosis of photoreceptor outer segments by transplanted human neural stem cells as a neuroprotective mechanism in retinal degeneration. *Investigative Ophthalmology and Visual Science*, 54(10):6745–6756. doi:10.1167/iovs.13-12860.
- Cunningham CL, Martinez-Cerdeno V, and Noctor SC**, 2013. Microglia Regulate the Number of Neural Precursor Cells in the Developing Cerebral Cortex. *Journal of Neuroscience*, 33(10):4216–4233. doi:10.1523/JNEUROSCI.3441-12.2013.
- Curvello V, Pastor P, Hekierski H, and Armstead WM**, 2018. Inhaled Nitric Oxide Protects Cerebral Autoregulation and Reduces Hippocampal Necrosis After Traumatic Brain Injury Through Inhibition of ET-1, ERK MAPK and IL-6 Upregulation in Pigs. *Neurocritical Care*, pages 1–11. doi:10.1007/s12028-018-0638-1.
- Czabotar PE and Murphy JM**, 2015. A tale of two domains - a structural perspective of the pseudokinase, MLKL. *FEBS Journal*, 282(22):4268–4278. doi:10.1111/febs.13504.
- Das A, Sinha M, Datta S, Abas M, Chaffee S, Sen CK, and Roy S**, 2015. Monocyte and Macrophage Plasticity in Tissue Repair and Regeneration. *The American Journal of Pathology*, 185(10):2596–2606. doi:10.1016/j.ajpath.2015.06.001.
- Dash PK, Mach SA, and Moore AN**, 2001. Enhanced neurogenesis in the rodent hippocampus following traumatic brain injury. *Journal of Neuroscience Research*, 63(4):313–319.

- Davalos D, Grutzendler J, Yang G, Kim JV, Zuo Y, Jung S, Littman DR, Dustin ML, and Gan WB**, 2005. ATP mediates rapid microglial response to local brain injury in vivo. *Nature Neuroscience*, 8(6):752–758. doi:10.1038/nn1472.
- Davis SM, Albers GW, Diener HC, Lees KR, and Norris J**, 1997. Termination of Acute Stroke Studies Involving Selfotel Treatment. *The Lancet*, 349(9044):32. doi:10.1016/S0140-6736(05)62166-6.
- Davis SM, Lees KR, Albers GW, Diener HC, Markabi S, Karlsson G, and Norris J**, 2000. Selfotel in acute ischemic stroke : possible neurotoxic effects of an NMDA antagonist. *Stroke*, 31(2):347–54.
- Dawson VL, Dawson TM, London ED, Brecht DS, and Snyder SH**, 1991. Nitric oxide mediates glutamate neurotoxicity in primary cortical cultures. *Proceedings of the National Academy of Sciences of the United States of America*, 88(14):6368–71. doi:10.1073/PNAS.88.14.6368.
- D’Cruz PM**, 2000. Mutation of the receptor tyrosine kinase gene *Mertk* in the retinal dystrophic RCS rat. *Human Molecular Genetics*, 9(4):645–651. doi:10.1093/hmg/9.4.645.
- de Couto G, Liu W, Tseliou E, Sun B, Makkar N, Kanazawa H, Arditi M, and Marbán E**, 2015. Macrophages mediate cardioprotective cellular postconditioning in acute myocardial infarction. *Journal of Clinical Investigation*, 125(8):3147–3162. doi:10.1172/JCI81321.
- Dearden NM, Gibson JS, McDowall DG, Gibson RM, and Cameron MM**, 1986. Effect of high-dose dexamethasone on outcome from severe head injury. *Journal of Neurosurgery*, 64(1):81–88. doi:10.3171/jns.1986.64.1.0081.
- Dekkers MP, Nikolettou V, and Barde YA**, 2013. Death of developing neurons: New insights and implications for connectivity. *Journal of Cell Biology*, 203(3):385–393. doi:10.1083/jcb.201306136.
- DeWitt DS, Smith TG, Deyo DJ, Miller KR, Uchida T, and Prough DS**, 1997. L-Arginine and Superoxide Dismutase Prevent or Reverse Cerebral Hypoperfusion after Fluid-Perfusion Traumatic Brain Injury. *Journal of Neurotrauma*, 14(4):223–233. doi:10.1089/neu.1997.14.223.
- Dietrich WD, Alonso O, Busto R, Globus MY, and Ginsberg MD**, 1994a. Post-traumatic brain hypothermia reduces histopathological damage following concussive brain injury in the rat. *Acta Neuropathologica*, 87(3):250–258. doi:10.1007/BF00296740.
- Dietrich WD, Alonso O, and Halley M**, 1994b. Early Microvascular and Neuronal Consequences of Traumatic Brain Injury: A Light and Electron Microscopic Study in Rats. *Journal of Neurotrauma*, 11(3):289–301. doi:10.1089/neu.1994.11.289.

- Dimlich RV, Tornheim PA, Kindel RM, Hall ED, Braugler JM, and McCall JM**, 1990. Effects of a 21-aminosteroid (U-74006F) on cerebral metabolites and edema after severe experimental head trauma. *Advances in Neurology*, 52:365–75.
- Dixon C, Markgraf C, Angileri F, Pike B, Wolfson E, Newcomb J, Bismar M, Blanco A, Clifton G, and Hayes RL**, 1998. Protective Effects of Moderate Hypothermia on Behavioral Deficits But Not Necrotic Cavitation Following Cortical Impact Injury in the Rat. *Journal of Neurotrauma*, 15(2):95–103. doi:10.1089/neu.1998.15.95.
- Djebaili M, Guo Q, Pettus EH, Hoffman SW, and Stein DG**, 2005. The Neurosteroids Progesterone and Allopregnanolone Reduce Cell Death, Gliosis, and Functional Deficits after Traumatic Brain Injury in Rats. *Journal of Neurotrauma*, 22(1):106–118. doi:10.1089/neu.2005.22.106.
- Dobin A, Davis CA, Schlesinger F, Drenkow J, Zaleski C, Jha S, Batut P, Chaisson M, and Gingeras TR**, 2013. STAR: ultrafast universal RNA-seq aligner. *Bioinformatics*, 29(1):15–21. doi:https://doi.org/10.1093/bioinformatics/bts635.
- Don EK, Formella I, Badrock AP, Hall TE, Morsch M, Hortle E, Hogan A, Chow S, Gwee SS, Stoddart JJ, Nicholson G, Chung R, and Cole NJ**, 2017. A Tol2 Gateway-Compatible Toolbox for the Study of the Nervous System and Neurodegenerative Disease. *Zebrafish*, 14(1):69–72. doi:10.1089/zeb.2016.1321.
- Du L, Bayir H, Lai Y, Zhang X, Kochanek PM, Watkins SC, Graham SH, and Clark RSB**, 2004. Innate gender-based proclivity in response to cytotoxicity and programmed cell death pathway. *Journal of Biological Chemistry*, 279(37):38563–70. doi:10.1074/jbc.M405461200.
- Duffield JS, Forbes SJ, Constandinou CM, Clay S, Partolina M, Vuthoori S, Wu S, Lang R, and Iredale JP**, 2005. Selective depletion of macrophages reveals distinct, opposing roles during liver injury and repair. *Journal of Clinical Investigation*, 115(1):56–65. doi:10.1172/JCI22675.
- Dziegielewska KM, Møller JE, Potter AM, Ek J, Lane MA, and Saunders NR**, 2000. Acute-phase cytokines IL-1beta and TNF-alpha in brain development. *Cell and Tissue Research*, 299(3):335–45.
- Edelmann K, Glashauser L, Sprungala S, Hesi B, Fritschle M, Ninkovic J, Godinho L, and Chapouton P**, 2013. Increased radial glia quiescence, decreased reactivation upon injury and unaltered neuroblast behavior underlie decreased neurogenesis in the aging zebrafish telencephalon. *Journal of Comparative Neurology*, 521(13):3099–3115. doi:10.1002/cne.23347.
- Edwards JP, Zhang X, and Mosser DM**, 2009. The Expression of Heparin-Binding Epidermal Growth Factor-Like Growth Factor by Regulatory Macrophages. *Journal of Immunology*, 182(4):1929–1939. doi:10.4049/jimmunol.0802703.

- Edwards P, Arango M, Balica L, Cottingham R, El-Sayed H, Farrell B, Fernandes J, Gogichaisvili T, Golden N, Hartzenberg B, Husain M, Ulloa MI, Jerbi Z, Khamis H, Komolafe E, Laloë V, Lomas G, Ludwig S, Mazairac G, Muñoz Sánchez MdIA, Nasi L, Ollidashi F, Plunkett P, Roberts I, Sandercock P, Shakur H, Soler C, Stocker R, Svoboda P, Trenkler S, Venkataramana NK, Wasserberg J, Yates D, Yutthakasemsunt S, and trial collaborators C**, 2005. Final results of MRC CRASH, a randomised placebo-controlled trial of intravenous corticosteroid in adults with head injury outcomes at 6 months. *The Lancet*, 365(9475):1957–1959. doi:10.1016/S0140-6736(05)66552-X.
- Eichhoff G, Brawek B, and Garaschuk O**, 2011. Microglial calcium signal acts as a rapid sensor of single neuron damage in vivo. *Biochimica et Biophysica Acta - Molecular Cell Research*, 1813(5):1014–1024. doi:10.1016/j.bbamcr.2010.10.018.
- Eilers PHC and Goeman JJ**, 2004. Enhancing scatterplots with smoothed densities. *Bioinformatics*, 20(5):623–628. doi:10.1093/bioinformatics/btg454.
- Ekdahl CT, Claassen JH, Bonde S, Kokaia Z, and Lindvall O**, 2003. Inflammation is detrimental for neurogenesis in adult brain. *Proceedings of the National Academy of Sciences of the United States of America*, 100(23):13632–13637.
- Eljaschewitsch E, Witting A, Mawrin C, Lee T, Schmidt PM, Wolf S, Hoertnagl H, Raine CS, Schneider-Stock R, Nitsch R, and Ullrich O**, 2006. The Endocannabinoid Anandamide Protects Neurons during CNS Inflammation by Induction of MKP-1 in Microglial Cells. *Neuron*, 49(1):67–79. doi:10.1016/j.neuron.2005.11.027.
- Ellett F, Pase L, Hayman JW, Andrianopoulos A, and Lieschke GJ**, 2011. mpeg1 promoter transgenes direct macrophage-lineage expression in zebrafish. *Blood*, 117(4):e49–56.
- Elliott MR, Chekeni FB, Tramont PC, Lazarowski ER, Kadl A, Walk SF, Park D, Woodson RI, Ostankovich M, Sharma P, Lysiak JJ, Harden TK, Leitinger N, and Ravichandran KS**, 2009. Nucleotides released by apoptotic cells act as a find-me signal to promote phagocytic clearance. *Nature*, 461(7261):282–286. doi:10.1038/nature08296.
- Elliott MR and Ravichandran KS**, 2010. Clearance of apoptotic cells: implications in health and disease. *Journal of Cell Biology*, 189(7):1059–1070. doi:10.1083/jcb.201004096.
- Esmann L, Idel C, Sarkar A, Hellberg L, Behnen M, Möller S, van Zandbergen G, Klinger M, Köhl J, Bussmeyer U, Solbach W, and Laskay T**, 2010. Phagocytosis of Apoptotic Cells by Neutrophil Granulocytes: Diminished Proinflammatory Neutrophil Functions in the Presence of Apoptotic Cells. *Journal of Immunology*, 184(1):391–400. doi:10.4049/jimmunol.0900564.
- Espin R, Roca FJ, Candel S, Sepulcre MP, Gonzalez-Rosa JM, Alcaraz-Perez F, Meseguer J, Cayuela ML, Mercader N, and Mulero V**, 2013. TNF receptors regulate vascular homeostasis

- in zebrafish through a caspase-8, caspase-2 and P53 apoptotic program that bypasses caspase-3. *Disease Models & Mechanisms*, 6(2):383–396. doi:10.1242/dmm.010249.
- Fabian RH, Dewitt DS, and Kent TA**, 1998. The 21-aminosteroid U-74389G reduces cerebral superoxide anion concentration following fluid percussion injury of the brain. *Journal of Neurotrauma*, 15(6):433–40. doi:10.1089/neu.1998.15.433.
- Faden AI, Demediuk P, Panter SS, and Vink R**, 1989. The role of excitatory amino acids and NMDA receptors in traumatic brain injury. *Science*, 244(4906):798–800. doi:10.1126/science.2567056.
- Faden AI, Wu J, Stoica BA, and Loane DJ**, 2016. Progressive inflammation-mediated neurodegeneration after traumatic brain or spinal cord injury. *British Journal of Pharmacology*, 173(4):681–691. doi:10.1111/bph.13179.
- Fadok VA, Bratton DL, Konowal A, Freed PW, Westcott JY, and Henson PM**, 1998. Macrophages that have ingested apoptotic cells in vitro inhibit proinflammatory cytokine production through autocrine/paracrine mechanisms involving TGF-beta, PGE2, and PAF. *Journal of Clinical Investigation*, 101(4):890–898. doi:10.1172/JCI1112.
- Fan L, Young PR, Barone FC, Feuerstein GZ, Smith DH, and McIntosh TK**, 1995. Experimental brain injury induces expression of interleukin-1 β mRNA in the rat brain. *Molecular Brain Research*, 30(1):125–130. doi:10.1016/0169-328X(94)00287-O.
- Fang KM, Yang CS, Sun SH, and Tzeng SF**, 2009. Microglial phagocytosis attenuated by short-term exposure to exogenous ATP through P2X ₇ receptor action. *Journal of Neurochemistry*, 111(5):1225–1237. doi:10.1111/j.1471-4159.2009.06409.x.
- Fantacci C, Capozzi D, Ferrara P, and Chiaretti A**, 2013. Neuroprotective role of nerve growth factor in hypoxic-ischemic brain injury. *Brain Sciences*, 3(3):1013–22. doi:10.3390/brainsci3031013.
- Farkas LM and Kriegstein K**, 2002. Heparin-binding epidermal growth factor-like growth factor (HB-EGF) regulates survival of midbrain dopaminergic neurons. *Journal of Neural Transmission*, 109(3):267–277. doi:10.1007/s007020200022.
- Faul M and Coronado V**, 2015. Epidemiology of traumatic brain injury. *Handbook of Clinical Neurology*, 127:3–13. doi:10.1016/B978-0-444-52892-6.00001-5.
- Faul M, Xu L, Wald MM, Coronado V, and Dellinger AM**, 2010. Traumatic brain injury in the United States: national estimates of prevalence and incidence, 2002-2006. *Injury Prevention*, 16(Supplement 1):A268–A268. doi:10.1136/ip.2010.029215.951.

- Faulkner JR, Herrmann JE, Woo MJ, Tansey KE, Doan NB, and Sofroniew MV**, 2004. Reactive Astrocytes Protect Tissue and Preserve Function after Spinal Cord Injury. *Journal of Neuroscience*, 24(9):2143–2155.
- Fava RA, Olsen NJ, Postlethwaite AE, Broadley KN, Davidson JM, Nanney LB, Lucas C, and Townes AS**, 1991. Transforming growth factor beta 1 (TGF-beta 1) induced neutrophil recruitment to synovial tissues: implications for TGF-beta-driven synovial inflammation and hyperplasia. *Journal of Experimental Medicine*, 173(5):1121–32.
- Fee D, Crumbaugh A, Jacques T, Herdrich B, Sewell D, Auerbach D, Piaskowski S, Hart MN, Sandor M, and Fabry Z**, 2003. Activated/effector CD4+T cells exacerbate acute damage in the central nervous system following traumatic injury. *Journal of Neuroimmunology*, 136(1-2):54–66. doi:10.1016/S0165-5728(03)00008-0.
- Ferreira R, Lively S, and Schlichter LC**, 2014. IL-4 type 1 receptor signaling up-regulates KCNN4 expression, and increases the KCa3.1 current and its contribution to migration of alternative-activated microglia. *Frontiers in Cellular Neuroscience*, 8:183. doi:10.3389/fncel.2014.00183.
- Festjens N, Vanden Berghe T, and Vandenabeele P**, 2006. Necrosis, a well-orchestrated form of cell demise: Signalling cascades, important mediators and concomitant immune response. *Biochimica et Biophysica Acta - Bioenergetics*, 1757(9-10):1371–1387. doi:10.1016/j.bbabi.2006.06.014.
- Festoff BW, Ameenuddin S, Arnold PM, Wong A, Santacruz KS, and Citron BA**, 2006. Minocycline neuroprotects, reduces microgliosis, and inhibits caspase protease expression early after spinal cord injury. *Journal of Neurochemistry*, 97(5):1314–1326. doi:10.1111/j.1471-4159.2006.03799.x.
- Figaji AA, Fieggen AG, and Peter JC**, 2003. Early decompressive craniotomy in children with severe traumatic brain injury. *Child's Nervous System*, 19(9):666–673. doi:10.1007/s00381-003-0804-3.
- Fineberg NA, Haddad PM, Carpenter L, Gannon B, Sharpe R, Young AH, Joyce E, Rowe J, Wellsted D, Nutt DJ, and Sahakian BJ**, 2013. The size, burden and cost of disorders of the brain in the UK. *Journal of Psychopharmacology*, 27(9):761–70.
- Fink SL and Cookson BT**, 2005. Apoptosis, Pyroptosis, and Necrosis: Mechanistic Description of Dead and Dying Eukaryotic Cells. *Infection and Immunity*, 73(4):1907–1916. doi:10.1128/IAI.73.4.1907-1916.2005.
- Fischer R, Maier O, Siegemund M, Wajant H, Scheurich P, and Pfizenmaier K**, 2011. A TNF Receptor 2 Selective Agonist Rescues Human Neurons from Oxidative Stress-Induced Cell Death. *PLoS ONE*, 6(11):e27621. doi:10.1371/journal.pone.0027621.

- Fitch MT, Doller C, Combs CK, Landreth GE, and Silver J**, 1999. Cellular and molecular mechanisms of glial scarring and progressive cavitation: in vivo and in vitro analysis of inflammation-induced secondary injury after CNS trauma. *Journal of Neuroscience*, 19(19):8182–98.
- Fleminger S, Oliver DL, Lovestone S, Rabe-Hesketh S, and Giora A**, 2003. Head injury as a risk factor for Alzheimer's disease: the evidence 10 years on; a partial replication. *Journal of Neurology, Neurosurgery, and Psychiatry*, 74(7):857–62. doi:10.1136/JNNP.74.7.857.
- Foley LM, Hitchens TK, Ho C, Janesko-Feldman KL, Melick JA, Bayr H, and Kochanek PM**, 2009. Magnetic Resonance Imaging Assessment of Macrophage Accumulation in Mouse Brain after Experimental Traumatic Brain Injury. *Journal of Neurotrauma*, 26(9):1509–1519. doi:10.1089/neu.2008.0747.
- Forrest D, Yuzaki M, Soares HD, Ng L, Luk DC, Sheng M, Stewart CL, Morgan JI, Connor JA, and Curran T**, 1994. Targeted disruption of NMDA receptor 1 gene abolishes NMDA response and results in neonatal death. *Neuron*, 13(2):325–38.
- Fosque BF, Sun Y, Dana H, Yang CT, Ohyama T, Tadross MR, Patel R, Zlatic M, Kim DS, Ahrens MB, Jayaraman V, Looger LL, and Schreier ER**, 2015. Neural circuits. Labeling of active neural circuits in vivo with designed calcium integrators. *Science*, 347(6223):755–760. doi:10.1126/science.1260922.
- Frantz S, Hofmann U, Fraccarollo D, Schäfer A, Kranepuhl S, Hagedorn I, Nieswandt B, Nahrendorf M, Wagner H, Bayer B, Pachel C, Schön MP, Kneitz S, Bobinger T, Weidemann F, Ertl G, and Bauersachs J**, 2013. Monocytes/macrophages prevent healing defects and left ventricular thrombus formation after myocardial infarction. *FASEB Journal*, 27(3):871–881. doi:10.1096/fj.12-214049.
- Fricker M, Neher JJ, Zhao JW, Théry C, Tolkovski AM, and Brown GC**, 2012a. MFG-E8 mediates primary phagocytosis of viable neurons during neuroinflammation. *Journal of Neuroscience*, 32(8):2657–2666. doi:10.1523/JNEUROSCI.4837-11.2012.
- Fricker M, Oliva-Martín MJ, and Brown GC**, 2012b. Primary phagocytosis of viable neurons by microglia activated with LPS or A β is dependent on calreticulin/LRP phagocytic signalling. *Journal of Neuroinflammation*, 9(1):697. doi:10.1186/1742-2094-9-196.
- Frugier T, Morganti-Kossmann MC, O'Reilly D, and McLean CA**, 2010. In situ detection of inflammatory mediators in post mortem human brain tissue after traumatic injury. *Journal of Neurotrauma*, (3):497–507. doi:10.1089/neu.2009.1120.
- Fulmer CG, VonDran MW, Stillman AA, Huang Y, Hempstead BL, and Dreyfus CF**, 2014. Astrocyte-Derived BDNF Supports Myelin Protein Synthesis after Cuprizone-Induced Demyelination. *Journal of Neuroscience*, 34(24):8186–8196. doi:10.1523/JNEUROSCI.4267-13.2014.

- Gaab MR, Trost HA, Alcantara A, Karimi-Nejad A, Moskopp D, Schultheiss R, Bock WJ, Piek J, Klinge H, and Scheil F**, 1994. "Ultrahigh" dexamethasone in acute brain injury. Results from a prospective randomized double-blind multicenter trial (GUDHIS). German Ultrahigh Dexamethasone Head Injury Study Group.
- Gahm C, Holmin S, and Mathiesen T**, 2000. Temporal profiles and cellular sources of three nitric oxide synthase isoforms in the brain after experimental contusion. *Neurosurgery*, 46(1):169–77.
- Gampe K, Stefani J, Hammer K, Brendel P, Pötzsch A, Enikolopov G, Enyoji K, Acker-Palmer A, Robson SC, and Zimmermann H**, 2015. NTPDase2 and purinergic signaling control progenitor cell proliferation in neurogenic niches of the adult mouse brain. *Stem Cells*, 33(1):253–64. doi:10.1002/stem.1846.
- Gao L, Xu W, Fan S, Li T, Zhao T, Ying G, Zheng J, Li J, Zhang Z, Yan F, Zhu Y, and Chen G**, 2018. MANF attenuates neuronal apoptosis and promotes behavioral recovery via Akt/MDM-2/p53 pathway after traumatic spinal cord injury in rats. *BioFactors*, 44(4):369–386. doi:10.1002/biof.1433.
- Garcia JM, Stillings SA, Leclerc JL, Phillips H, Edwards NJ, Robicsek SA, Hoh BL, Blackburn S, and Doré S**, 2017. Role of Interleukin-10 in Acute Brain Injuries. *Frontiers in Neurology*, 8:244. doi:10.3389/fneur.2017.00244.
- Gardner RC, Burke JF, Nettiksimmons J, Goldman S, Tanner CM, and Yaffe K**, 2015. Traumatic brain injury in later life increases risk for Parkinson disease. *Annals of Neurology*, 77(6):987–995. doi:10.1002/ana.24396.
- Gardner RC, Burke JF, Nettiksimmons J, Kaup A, Barnes DE, and Yaffe K**, 2014. Dementia Risk After Traumatic Brain Injury vs Nonbrain Trauma. *Journal of the American Medical Association Neurology*, 71(12):1490. doi:10.1001/jamaneurol.2014.2668.
- Gardner RC and Yaffe K**, 2015. Epidemiology of mild traumatic brain injury and neurodegenerative disease. *Molecular and Cellular Neuroscience*, 66(PB):75–80. doi:10.1016/j.mcn.2015.03.001.
- Garthwaite J, Garthwaite G, Palmer RM, and Moncada S**, 1989. NMDA receptor activation induces nitric oxide synthesis from arginine in rat brain slices. *European Journal of Pharmacology*, 172(4-5):413–6.
- Gemberling M, Bailey TJ, Hyde DR, and Poss KD**, 2013. The zebrafish as a model for complex tissue regeneration. *Trends in Genetics*, 29(11):611–620. doi:10.1016/j.tig.2013.07.003.
- Gentleman S, Leclercq P, Moyes L, Graham D, Smith C, Griffin W, and Nicoll J**, 2004. Long-term intracerebral inflammatory response after traumatic brain injury. *Forensic Science International*, 146(2-3):97–104. doi:10.1016/j.forsciint.2004.06.027.

- Gerber YN, Saint-Martin GP, Bringuier CM, Bartolami S, Goze-Bac C, Noristani HN, and Perrin FE**, 2018. CSF1R Inhibition Reduces Microglia Proliferation, Promotes Tissue Preservation and Improves Motor Recovery After Spinal Cord Injury. *Frontiers in Cellular Neuroscience*, 12:368. doi:10.3389/fncel.2018.00368.
- Gertig U and Hanisch UK**, 2014. Microglial diversity by responses and responders. *Frontiers in Cellular Neuroscience*, 8(April):1–9. doi:10.3389/fncel.2014.00101.
- Ginhoux F, Greter M, Leboeuf M, Nandi S, See P, Gokhan S, Mehler MF, Conway SJ, Ng LG, Stanley ER, Samokhvalov IM, and Merad M**, 2010. Fate Mapping Analysis Reveals That Adult Microglia Derive from Primitive Macrophages. *Science*, 330(6005):841–845. doi:10.1126/science.1194637.
- Girouard H, Wang G, Gallo EF, Anrather J, Zhou P, Pickel VM, and Iadecola C**, 2009. NMDA receptor activation increases free radical production through nitric oxide and NOX2. *Journal of Neuroscience*, 29(8):2545–52. doi:10.1523/JNEUROSCI.0133-09.2009.
- Giulian D and Baker J**, 1986. Characterization of Ameboid Mammalian Brain Microglia Isolated from Developing. *Journal of Neuroscience*, 6(August):2163–2178. doi:https://doi.org/10.1523/JNEUROSCI.06-08-02163.1986.
- Giulian D, Young DG, Woodward J, Brown DC, and Lachman LB**, 1988. Interleukin-1 is an astroglial growth factor in the developing brain. *Journal of Neuroscience*, 8(2):709–714. doi:10.1071/MF08146.
- Globus MYT, Alonso O, Dietrich WD, Busto R, and Ginsberg MD**, 1995. Glutamate release and free radical production following brain injury: effects of posttraumatic hypothermia. *Journal of Neurochemistry*, 65(4):1704–1711. doi:10.1046/j.1471-4159.1995.65041704.x.
- Godwin JW, Debuque R, Salimova E, and Rosenthal NA**, 2017. Heart regeneration in the salamander relies on macrophage-mediated control of fibroblast activation and the extracellular landscape. *npj Regenerative Medicine*, 2(1):22. doi:10.1038/s41536-017-0027-y.
- Godwin JW, Pinto AR, and Rosenthal NA**, 2013. Macrophages are required for adult salamander limb regeneration. *Proceedings of the National Academy of Sciences of the United States of America*, 110(23):9415–20. doi:10.1073/pnas.1300290110.
- Goldshmit Y, Sztal TE, Jusuf PR, Hall TE, Nguyen-Chi M, and Currie PD**, 2012. Fgf-Dependent Glial Cell Bridges Facilitate Spinal Cord Regeneration in Zebrafish. *Journal of Neuroscience*, 32(22):7477–7492. doi:10.1523/JNEUROSCI.0758-12.2012.
- Goldstein FC, Caveney AF, Hertzberg VS, Silbergleit R, Yeatts SD, Palesch YY, Levin HS, and Wright DW**, 2017. Very Early Administration of Progesterone Does Not Improve Neuropsy-

- chological Outcomes in Subjects with Moderate to Severe Traumatic Brain Injury. *Journal of Neurotrauma*, 34(1):115–120. doi:10.1089/neu.2015.4313.
- Golstein P and Kroemer G**, 2007. Cell death by necrosis: towards a molecular definition. *Trends in Biochemical Sciences*, 32(1):37–43. doi:10.1016/j.tibs.2006.11.001.
- Gould E, Cameron HA, and McEwen BS**, 1994. Blockade of NMDA receptors increases cell death and birth in the developing rat dentate gyrus. *Journal of Comparative Neurology*, 340(4):551–565. doi:10.1002/cne.903400408.
- Grabert K, Michael T, Karavolos MH, Clohisey S, Baillie JK, Stevens MP, Freeman TC, Summers KM, and McColl BW**, 2016. Microglial brain regiondependent diversity and selective regional sensitivities to aging. *Nature Neuroscience*, 19(3):504–516. doi:10.1038/nn.4222.
- Graham DI, Ford I, Adams JH, Doyle D, Teasdale GM, Lawrence AE, and McLellan DR**, 1989. Ischaemic brain damage is still common in fatal non-missile head injury. *Journal of Neurology Neurosurgery and Psychiatry*, 52(3):346–350. doi:10.1136/jnnp.52.3.346.
- Grandel H, Kaslin J, Ganz J, Wenzel I, and Brand M**, 2006. Neural stem cells and neurogenesis in the adult zebrafish brain: Origin, proliferation dynamics, migration and cell fate. *Developmental Biology*, 295(1):263–277. doi:10.1016/J.YDBIO.2006.03.040.
- Green DR, Oguin TH, and Martinez J**, 2016. The clearance of dying cells: Table for two. *Cell Death and Differentiation*, 23(6):915–926. doi:10.1038/cdd.2015.172.
- Greenhalgh AD and David S**, 2014. Differences in the phagocytic response of microglia and peripheral macrophages after spinal cord injury and its effects on cell death. *Journal of Neuroscience*, 34(18):6316–22. doi:10.1523/JNEUROSCI.4912-13.2014.
- Grumme T, Baethmann A, Kolodziejczyk D, Krimmer J, Fischer M, von Eisenhart Rothe B, Pelka R, Bennefeld H, Pöllauer E, and Kostron H**, 1995. Treatment of patients with severe head injury by triamcinolone: a prospective, controlled multicenter clinical trial of 396 cases. *Research in Experimental Medicine*, 195(4):217–29.
- Gude DR, Alvarez SE, Paugh SW, Mitra P, Yu J, Griffiths R, Barbour SE, Milstien S, and Spiegel S**, 2008. Apoptosis induces expression of sphingosine kinase 1 to release sphingosine-1-phosphate as a "come-and-get-me" signal. *FASEB journal*, 22(8):2629–38. doi:10.1096/fj.08-107169.
- Guinamard R, Simard C, and Del Negro C**, 2013. Flufenamic acid as an ion channel modulator. *Pharmacology & Therapeutics*, 138(2):272–284. doi:10.1016/j.pharmthera.2013.01.012.
- Gurtner GC, Werner S, Barrandon Y, and Longaker MT**, 2008. Wound repair and regeneration. *Nature*, 453(7193):314–321. doi:10.1038/nature07039.

- Gyoneva S, Kim D, Katsumoto A, Kokiko-Cochran ON, Lamb BT, and Ransohoff RM,** 2015. Ccr2 deletion dissociates cavity size and tau pathology after mild traumatic brain injury. *Journal of Neuroinflammation*, 12(1):228. doi:10.1186/s12974-015-0443-0.
- Hall ED, Andrus PK, and Yonkers PA,** 1993. Brain hydroxyl radical generation in acute experimental head injury. *Journal of Neurochemistry*, 60(2):588–94. doi:10.1111/j.1471-4159.1993.tb03189.x.
- Hall ED, Detloff MR, Johnson K, and Kupina NC,** 2004. Peroxynitrite-Mediated Protein Nitration and Lipid Peroxidation in a Mouse Model of Traumatic Brain Injury. *Journal of Neurotrauma*, 21(1):9–20. doi:10.1089/089771504772695904.
- Hall ED, McCall JM, and Means ED,** 1994. Therapeutic potential of the lazaroids (21-aminosteroids) in acute central nervous system trauma, ischemia and subarachnoid hemorrhage. *Advances in Pharmacology*, 28:221–68.
- Hall ED, Vaishnav RA, and Mustafa AG,** 2010. Antioxidant therapies for traumatic brain injury. *Neurotherapeutics*, 7(1):51–61. doi:10.1016/j.nurt.2009.10.021.
- Hall ED, Yonkers PA, McCall JM, and Braughler JM,** 1988. Effects of the 21-aminosteroid U74006F on experimental head injury in mice. *Journal of Neurosurgery*, 68(3):456–461. doi:10.3171/jns.1988.68.3.0456.
- Hamm RJ, Temple MD, Pike BR, and Ellis EF,** 1996. The effect of postinjury administration of polyethylene glycol-conjugated superoxide dismutase (pegorgotein, Dismutec) or lidocaine on behavioral function following fluid-percussion brain injury in rats. *Journal of Neurotrauma*, 13(6):325–332. doi:10.1089/neu.1996.13.325.
- Hammer M, Mages J, Dietrich H, Schmitz F, Striebel F, Murray P, Wagner H, and Lang R,** 2005. Control of dual-specificity phosphatase-1 expression in activated macrophages by IL-10. *European Journal of Immunology*, 35(10):2991–3001. doi:10.1002/eji.200526192.
- Harders A, Kakarieka A, and Braakman R,** 1996. Traumatic subarachnoid hemorrhage and its treatment with nimodipine. German tSAH Study Group. *Journal of Neurosurgery*, 85(1):82–89. doi:10.3171/jns.1996.85.1.0082.
- Hardingham GE, Fukunaga Y, and Bading H,** 2002. Extrasynaptic NMDARs oppose synaptic NMDARs by triggering CREB shut-off and cell death pathways. *Nature Neuroscience*, 5(5):405–414. doi:10.1038/nn835.
- Harks EG, de Roos AD, Peters PH, de Haan LH, Brouwer A, Ypey DL, van Zoelen EJ, and Theuvenet AP,** 2001. Fenamates: a novel class of reversible gap junction blockers. *Journal of Pharmacology and Experimental Therapeutics*, 298(3):1033–41.

- Harty BL, Krishnan A, Sanchez NE, Schiöth HB, and Monk KR**, 2015. Defining the gene repertoire and spatiotemporal expression profiles of adhesion G protein-coupled receptors in zebrafish. *BMC Genomics*, 16(1):62. doi:10.1186/s12864-015-1296-8.
- Hasegawa T, Hall CJ, Crosier PS, Abe G, Kawakami K, Kudo A, and Kawakami A**, 2017. Transient inflammatory response mediated by interleukin-1 β is required for proper regeneration in zebrafish fin fold. *eLife*, 6. doi:10.7554/eLife.22716.
- Hawthorne G, Gruen RL, and Kaye AH**, 2009. Traumatic Brain Injury and Long-Term Quality of Life: Findings from an Australian Study. *Journal of Neurotrauma*, 26(10):1623–1633. doi:10.1089/neu.2008.0735.
- Haynes SE, Hollopeter G, Yang G, Kurpius D, Dailey ME, Gan WB, and Julius D**, 2006. The P2Y₁₂ receptor regulates microglial activation by extracellular nucleotides. *Nature Neuroscience*, 9(12):1512–1519. doi:10.1038/nn1805.
- He J, Evans CO, Hoffman SW, Oyesiku N, and Stein DG**, 2004. Progesterone and allopregnanolone reduce inflammatory cytokines after traumatic brain injury. *Experimental Neurology*, 189(2):404–412. doi:10.1016/j.expneurol.2004.06.008.
- He Y, She H, Zhang T, Xu H, Cheng L, Yepes M, Zhao Y, and Mao Z**, 2018. p38 MAPK inhibits autophagy and promotes microglial inflammatory responses by phosphorylating ULK1. *Journal of Cell Biology*, 217(1):315–328. doi:10.1083/jcb.201701049.
- Hellman M, Arumäe U, Yu Ly, Lindholm P, Peränen J, Saarma M, and Permi P**, 2011. Mesencephalic astrocyte-derived neurotrophic factor (MANF) has a unique mechanism to rescue apoptotic neurons. *Journal of Biological Chemistry*, 286(4):2675–80. doi:10.1074/jbc.M110.146738.
- Helmy A, Guilfoyle MR, Carpenter KL, Pickard JD, Menon DK, and Hutchinson PJ**, 2014. Recombinant Human Interleukin-1 Receptor Antagonist in Severe Traumatic Brain Injury: A Phase II Randomized Control Trial. *Journal of Cerebral Blood Flow & Metabolism*, 34(5):845–851. doi:10.1038/jcbfm.2014.23.
- Heneka MT and Feinstein DL**, 2001. Expression and function of inducible nitric oxide synthase in neurons. *Journal of Neuroimmunology*, 114(1-2):8–18. doi:10.1016/S0165-5728(01)00246-6.
- Henson PM**, 2005. Dampening inflammation. *Nature Immunology*, 6(12):1179–1181. doi:10.1038/ni1205-1179.
- Herculano-Houzel S and Lent R**, 2005. Isotropic Fractionator: A Simple, Rapid Method for the Quantification of Total Cell and Neuron Numbers in the Brain. *Journal of Neuroscience*, 25(10):2518–2521.

- Herrgen L, Voss OP, and Akerman CJ**, 2014. Calcium-Dependent Neuroepithelial Contractions Expel Damaged Cells from the Developing Brain. *Developmental Cell*, 31(5):599–613. doi: 10.1016/j.devcel.2014.10.012.
- Hicks R, Soares H, Smith D, and McIntosh T**, 1996. Temporal and spatial characterization of neuronal injury following lateral fluid-percussion brain injury in the rat. *Acta Neuropathologica*, 91(3):236–246. doi:10.1007/s004010050421.
- Hiebert JB, Shen Q, Thimmesch AR, and Pierce JD**, 2015. Traumatic Brain Injury and Mitochondrial Dysfunction. *American Journal of the Medical Sciences*, 350(2):132–138. doi: 10.1097/MAJ.0000000000000506.
- Hochreiter-Hufford A and Ravichandran KS**, 2013. Clearing the Dead: Apoptotic Cell Sensing, Recognition, Engulfment, and Digestion. *Cold Spring Harbor Perspectives in Biology*, 5:1–a008748. doi:10.1101/cshperspect.a008748.
- Hoek RM, Ruuls SR, Murphy CA, Wright GJ, Goddard R, Zurawski SM, Blom B, Homola ME, Streit WJ, Brown MH, Barclay AN, and Sedgwick JD**, 2000. Down-regulation of the macrophage lineage through interaction with OX2 (CD200). *Science*, 290(5497):1768–71. doi:10.1126/SCIENCE.290.5497.1768.
- Hoepfner DJ, Hengartner MO, and Schnabel R**, 2001. Engulfment genes cooperate with ced-3 to promote cell death in *Caenorhabditis elegans*. *Nature*, 412(6843):202–206. doi: 10.1038/35084103.
- Holmin S and Mathiesen T**, 2000. Intracerebral administration of interleukin-1 β and induction of inflammation, apoptosis, and vasogenic edema. *Journal of Neurosurgery*, 92(1):108–120. doi: 10.3171/jns.2000.92.1.0108.
- Holmin S, Söderlund J, Biberfeld P, and Mathiesen T**, 1998. Intracerebral inflammation after human brain contusion. *Neurosurgery*, 42(2):291–299. doi:10.1097/00006123-199802000-00047.
- Honda S, Sasaki Y, Ohsawa K, Imai Y, Nakamura Y, Inoue K, and Kohsaka S**, 2001. Extracellular ATP or ADP induce chemotaxis of cultured microglia through Gi/o-coupled P2Y receptors. *Journal of Neuroscience*, 21(6):1975–82. doi:10.1523/JNEUROSCI.21-06-01975.2001.
- Honeybul S and Ho KM**, 2011. Long-Term Complications of Decompressive Craniectomy for Head Injury. *Journal of Neurotrauma*, 28(6):929–935. doi:10.1089/neu.2010.1612.
- Hootman JM, Dick R, and Agel J**, 2007. Epidemiology of collegiate injuries for 15 sports: Summary and recommendations for injury prevention initiatives. *Journal of Athletic Training*, 42(2):311–319. doi:10.1111/j.1600-0838.2006.00528.x.

- Horn KP, Busch SA, Hawthorne AL, van Rooijen N, and Silver J**, 2008. Another Barrier to Regeneration in the CNS: Activated Macrophages Induce Extensive Retraction of Dystrophic Axons through Direct Physical Interactions. *Journal of Neuroscience*, 28(38):9330–9341. doi:10.1523/JNEUROSCI.2488-08.2008.
- Howe K, Clark MD, Torroja CF, Torrance J, Berthelot C, Muffato M, Collins JE, Humphray S, et al.**, 2013. The zebrafish reference genome sequence and its relationship to the human genome. *Nature*, 496(7446):498–503.
- Hsieh CL, Kim CC, Ryba BE, Niemi EC, Bando JK, Locksley RM, Liu J, Nakamura MC, and Seaman WE**, 2013. Traumatic brain injury induces macrophage subsets in the brain. *European Journal of Immunology*, 43(8):2010–2022. doi:10.1002/eji.201243084.
- Hsieh CL, Niemi EC, Wang SH, Lee CC, Bingham D, Zhang J, Cozen ML, Charo I, Huang EJ, Liu J, and Nakamura MC**, 2014. CCR2 Deficiency Impairs Macrophage Infiltration and Improves Cognitive Function after Traumatic Brain Injury. *Journal of Neurotrauma*, 31(20):1677–1688. doi:10.1089/neu.2013.3252.
- Huang X, Liao W, Huang Y, Jiang M, Chen J, Wang M, Lin H, Guan S, and Liu J**, 2017. Neuroprotective effect of dual specificity phosphatase 6 against glutamate-induced cytotoxicity in mouse hippocampal neurons. *Biomedicine & Pharmacotherapy*, 91:385–392. doi:10.1016/j.biopha.2017.04.096.
- Huang Z, Huang PL, Ma J, Meng W, Ayata C, Fishman MC, and Moskowitz MA**, 1996. Enlarged Infarcts in Endothelial Nitric Oxide Synthase Knockout Mice are Attenuated by Nitro-L-Arginine. *Journal of Cerebral Blood Flow & Metabolism*, 16(5):981–987. doi:10.1097/00004647-199609000-00023.
- Hughes PE, Alexi T, Williams CE, Clark RG, and Gluckman PD**, 1999. Administration of recombinant human activin-A has powerful neurotrophic effects on select striatal phenotypes in the quinolinic acid lesion model of Huntington's disease. *Neuroscience*, 92(1):197–209. doi:10.1016/S0306-4522(98)00724-6.
- Hui SP, Dutta A, and Ghosh S**, 2010. Cellular response after crush injury in adult zebrafish spinal cord. *Developmental Dynamics*, 239(11):2962–2979. doi:10.1002/dvdy.22438.
- Hutchinson PJ, Koliass AG, Timofeev IS, Corteen EA, Czosnyka M, Timothy J, Anderson I, Bulters DO, Belli A, Eynon CA, Wadley J, Mendelow AD, Mitchell PM, Wilson MH, Critchley G, Sahuquillo J, Unterberg A, Servadei F, Teasdale GM, Pickard JD, Menon DK, Murray GD, and Kirkpatrick PJ**, 2016. Trial of Decompressive Craniectomy for Traumatic Intracranial Hypertension. *New England Journal of Medicine*, 375(12):1119–1130. doi:10.1056/NEJMoa1605215.

- Hutchinson PJ, O'Connell MT, Rothwell NJ, Hopkins SJ, Nortje J, Carpenter KL, Timofeev I, Al-Rawi PG, Menon DK, and Pickard JD**, 2007. Inflammation in Human Brain Injury: Intracerebral Concentrations of IL-1 α , IL-1 β , and Their Endogenous Inhibitor IL-1ra. *Journal of Neurotrauma*, 24(10):1545–1557. doi:10.1089/neu.2007.0295.
- Hutchison JS, Ward RE, Lacroix J, Hébert PC, Barnes MA, Bohn DJ, Dirks PB, Doucette S, Fergusson D, Gottesman R, Joffe AR, Kirpalani HM, Meyer PG, Morris KP, Moher D, Singh RN, and Skippen PW**, 2008. Hypothermia Therapy after Traumatic Brain Injury in Children. *New England Journal of Medicine*, 358(23):2447–2456. doi:10.1056/NEJMoa0706930.
- Hwang H, Lee S, Lee WH, Lee HJ, and Suk K**, 2010. Stimulation of glucocorticoid-induced tumor necrosis factor receptor family-related protein ligand (GITRL) induces inflammatory activation of microglia in culture. *Journal of Neuroscience Research*, 88(10):2188–2196. doi:10.1002/jnr.22378.
- Ibrahim S, Hu W, Wang X, Gao X, He C, and Chen J**, 2016. Traumatic Brain Injury Causes Aberrant Migration of Adult-Born Neurons in the Hippocampus. *Scientific Reports*, 6(21793):1–12.
- Ikonomidou C, Bosch F, Miksa M, Bittigau P, Vöckler J, Dikranian K, Tenkova TI, Stefovská V, Turski L, and Olney JW**, 1999. Blockade of NMDA receptors and apoptotic neurodegeneration in the developing brain. *Science*, 283(5398):70–4.
- Ikonomidou C, Stefovská V, and Turski L**, 2000. Neuronal death enhanced by N-methyl-D-aspartate antagonists. *Proceedings of the National Academy of Sciences*, 97(23):12885–12890. doi:10.1073/pnas.220412197.
- Ikonomidou C and Turski L**, 2002. Why did NMDA receptor antagonists fail clinical trials for stroke and traumatic brain injury? *The Lancet Neurology*, 1(6):383–386. doi:10.1016/S1474-4422(02)00164-3.
- Ilie G, Boak A, Adlaf EM, Asbridge M, and Cusimano MD**, 2013. Prevalence and correlates of traumatic brain injuries among adolescents. *Journal of the American Medical Association*, 309(24):2550–2552. doi:10.1001/jama.2013.6750.
- Inoue K, Nakajima K, Morimoto T, Kikuchi Y, Koizumi S, Illes P, and Kohsaka S**, 1998. ATP stimulation of Ca(2+)-dependent plasminogen release from cultured microglia. *British Journal of Pharmacology*, 40:156–163.
- Inoue Y, Tsuruma K, Nakanishi T, Oyagi A, Ohno Y, Otsuka T, Shimazawa M, and Hara H**, 2013. Role of heparin-binding epidermal growth factor-like growth factor in light-induced photoreceptor degeneration in mouse retina. *Investigative Ophthalmology and Visual Science*, 54(6):3815–3829. doi:10.1167/iovs.12-11236.

- Ishii T, Sato K, Kakumoto T, Miura S, Touhara K, Takeuchi S, and Nakata T**, 2015. Light generation of intracellular Ca²⁺ signals by a genetically encoded protein BACCS. *Nature Communications*, 6(May):8021. doi:10.1038/ncomms9021.
- Iwahori Y, Saito H, Torii K, and Nishiyama N**, 1997. Activin exerts a neurotrophic effect on cultured hippocampal neurons. *Brain Research*, 760(1-2):52–58. doi:10.1016/S0006-8993(97)00275-8.
- Izumi Y, Clifford DB, and Zorumski CF**, 1992. Inhibition of long-term potentiation by NMDA-mediated nitric oxide release. *Science*, 257(5074):1273–1277.
- Jafari S, Etmnan M, Aminzadeh F, and Samii A**, 2013. Head injury and risk of Parkinson disease: A systematic review and meta-analysis. *Movement Disorders*, 28(9):1222–1229. doi:10.1002/mds.25458.
- Jaffrey SR, Erdjument-Bromage H, Ferris CD, Tempst P, and Snyder SH**, 2001. Protein S-nitrosylation: a physiological signal for neuronal nitric oxide. *Nature Cell Biology*, 3(2):193–197. doi:10.1038/35055104.
- James G and Butt AM**, 2002. P2Y and P2X purinoceptor mediated Ca²⁺ signalling in glial cell pathology in the central nervous system. *European Journal of Pharmacology*, 447(2-3):247–260. doi:10.1016/S0014-2999(02)01756-9.
- Jao LE, Wentz SR, and Chen W**, 2013. Efficient multiplex biallelic zebrafish genome editing using a CRISPR nuclease system. *Proceedings of the National Academy of Sciences*, 110(34):13904–13909. doi:10.1073/pnas.1308335110.
- Jara JH, Singh BB, Floden AM, and Combs CK**, 2007. Tumor necrosis factor alpha stimulates NMDA receptor activity in mouse cortical neurons resulting in ERK-dependent death. *Journal of Neurochemistry*, 100(5):1407–1420. doi:10.1111/j.1471-4159.2006.04330.x.
- Jeong HK, Ji K, Min K, and Joe EH**, 2013. Brain Inflammation and Microglia: Facts and Misconceptions. *Experimental Neurobiology*, 22(2):59. doi:10.5607/en.2013.22.2.59.
- Jeong HK, Ji Km, Kim B, Kim J, Jou I, and Joe Eh**, 2010a. Inflammatory Responses Are Not Sufficient to Cause Delayed Neuronal Death in ATP-Induced Acute Brain Injury. *PLoS ONE*, 5(10):e13756. doi:10.1371/journal.pone.0013756.
- Jeong HK, Jou I, and Joe Eh**, 2010b. Systemic LPS administration induces brain inflammation but not dopaminergic neuronal death in the substantia nigra. *Experimental and Molecular Medicine*, 42(12):823. doi:10.3858/emm.2010.42.12.085.
- Jiang T, Zhang YD, Chen Q, Gao Q, Zhu XC, Zhou JS, Shi JQ, Lu H, Tan L, and Yu JT**, 2016. TREM2 modifies microglial phenotype and provides neuroprotection in P301S tau transgenic mice. *Neuropharmacology*, 105:196–206. doi:10.1016/j.neuropharm.2016.01.028.

- Jiang Y, Wei N, Lu T, Zhu J, Xu G, and Liu X**, 2011. Intranasal brain-derived neurotrophic factor protects brain from ischemic insult via modulating local inflammation in rats. *Neuroscience*, 172:398–405. doi:10.1016/j.neuroscience.2010.10.054.
- Johansen T, Krabbe C, Schmidt SI, Serrano AM, and Meyer M**, 2017. Comparative Analysis of Spontaneous and Stimulus-Evoked Calcium Transients in Proliferating and Differentiating Human Midbrain-Derived Stem Cells. *Stem Cells International*, 2017:1–14. doi:10.1155/2017/9605432.
- Johnson WD and Griswold DP**, 2017. Traumatic brain injury: a global challenge. *The Lancet Neurology*, 16(12):949–950. doi:10.1016/S1474-4422(17)30362-9.
- Jorge RE, Robinson RG, Moser D, Tateno A, Crespo-Facorro B, and Arndt S**, 2004. Major Depression Following Traumatic Brain Injury. *Archives of General Psychiatry*, 61:42–50. doi:10.1001/archpsyc.61.1.42.ABSTRACT.
- Jung JE, Kim GS, and Chan PH**, 2011. Neuroprotection by interleukin-6 is mediated by signal transducer and activator of transcription 3 and antioxidative signaling in ischemic stroke. *Stroke*, 42(12):3574–9. doi:10.1161/STROKEAHA.111.626648.
- Justet C, Hernandez JA, Torriglia A, and Chifflet S**, 2016. Fast calcium wave inhibits excessive apoptosis during epithelial wound healing. *Cell and Tissue Research*, 365:343–356. doi:10.1007/s00441-016-2388-8.
- Kalkonde YV, Jawaid A, Qureshi SU, Shirani P, Wheaton M, Pinto-Patarroyo GP, and Schulz PE**, 2012. Medical and environmental risk factors associated with frontotemporal dementia: A case-control study in a veteran population. *Alzheimer's & Dementia*, 8(3):204–210. doi:10.1016/j.jalz.2011.03.011.
- Kamm K, VanderKolk W, Lawrence C, Jonker M, and Davis AT**, 2006. The Effect of Traumatic Brain Injury Upon the Concentration and Expression of Interleukin-1 β and Interleukin-10 in the Rat. *Journal of Trauma*, 60(1):152–157. doi:10.1097/01.ta.0000196345.81169.a1.
- Kanemaru K, Kubota J, Sekiya H, Hirose K, Okubo Y, and Iino M**, 2013. Calcium-dependent N-cadherin up-regulation mediates reactive astrogliosis and neuroprotection after brain injury. *Proceedings of the National Academy of Sciences*, 110(28):11612–11617. doi:10.1073/pnas.1300378110.
- Katayama Y, Becker DP, Tamura T, and Hovda DA**, 1990. Massive increases in extracellular potassium and the indiscriminate release of glutamate following concussive brain injury. *Journal of Neurosurgery*, 73(6):889–900. doi:10.3171/jns.1990.73.6.0889.
- Kawabori M, Kacimi R, Kauppinen T, Calosing C, Kim JY, Hsieh CL, Nakamura MC, and Yenari MA**, 2015. Triggering Receptor Expressed on Myeloid Cells 2 (TREM2) Deficiency

- Attenuates Phagocytic Activities of Microglia and Exacerbates Ischemic Damage in Experimental Stroke. *Journal of Neuroscience*, 35(8):3384–3396. doi:10.1523/JNEUROSCI.2620-14.2015.
- Kawahara N, Mishima K, Higashiyama S, Taniguchi N, Tamura A, and Kirino T**, 1999. The Gene for Heparin-Binding Epidermal Growth Factor-Like Growth Factor is Stress-Inducible: Its Role in Cerebral Ischemia. *Journal of Cerebral Blood Flow & Metabolism*, 19(3):307–320. doi:10.1097/00004647-199903000-00009.
- Kawamata T, Katayama Y, Hovda DA, Yoshino A, and Becker DP**, 1992. Administration of Excitatory Amino Acid Antagonists via Microdialysis Attenuates the Increase in Glucose Utilization Seen following Concussive Brain Injury. *Journal of Cerebral Blood Flow & Metabolism*, 12(1):12–24. doi:10.1038/jcbfm.1992.3.
- Keane RW, Kraydieh S, Lotocki G, Alonso OF, Aldana P, and Dietrich WD**, 2001. Apoptotic and Antiapoptotic Mechanisms after Traumatic Brain Injury. *Journal of Cerebral Blood Flow & Metabolism*, 21(10):1189–1198. doi:10.1097/00004647-200110000-00007.
- Keller JN, Kindy MS, Holtsberg FW, Clair DKS, Yen Hc, Germeyer A, Steiner SM, Brucekeller AJ, Hutchins JB, and Mattson MP**, 1998. Apoptosis and Reduces Ischemic Brain Injury: Suppression of Peroxynitrite Production, Lipid Peroxidation, and Mitochondrial Dysfunction. *Journal of Neuroscience*, 18(2):687–697. doi:10.1523/JNEUROSCI.18-02-00687.1998.
- Kenne E, Erlandsson A, Lindbom L, Hillered L, and Clausen F**, 2012. Neutrophil depletion reduces edema formation and tissue loss following traumatic brain injury in mice. *Journal of Neuroinflammation*, 9(1):512. doi:10.1186/1742-2094-9-17.
- Kielian T, Mayes P, and Kielian M**, 2002. Characterization of microglial responses to Staphylococcus aureus: effects on cytokine, costimulatory molecule, and Toll-like receptor expression. *Journal of Neuroimmunology*, 130(1-2):86–99. doi:10.1016/S0165-5728(02)00216-3.
- Kim CC, Nakamura MC, and Hsieh CL**, 2016. Brain trauma elicits non-canonical macrophage activation states. *Journal of Neuroinflammation*, 13(1):117. doi:10.1186/s12974-016-0581-z.
- Kim DH, Sun Y, Yun S, Kim B, Hwang CN, Nelson B, and Lee SH**, 2004a. Mechanical property characterization of the zebrafish embryo chorion. In *Annual International Conference of the IEEE Engineering in Medicine and Biological Society*, pages 5061–4.
- Kim S, Elkon KB, and Ma X**, 2004b. Transcriptional Suppression of Interleukin-12 Gene Expression following Phagocytosis of Apoptotic Cells. *Immunity*, 21(5):643–653. doi:10.1016/j.immuni.2004.09.009.
- Kinoshita K, Chatzipanteli K, Vitarbo E, Truettner JS, Alonso OF, Dietrich WD, Selman WR, Lee SM, and Kelly DF**, 2002. Interleukin-1 β messenger ribonucleic acid and protein levels

- after fluid-percussion brain injury in rats: Importance of injury severity and brain temperature. *Neurosurgery*, 51(1):195–203. doi:10.1097/00006123-200207000-00027.
- Kishimoto N, Shimizu K, and Sawamoto K**, 2012. Neuronal regeneration in a zebrafish model of adult brain injury. *Disease Models & Mechanisms*, 5(2):200–209. doi:10.1242/dmm.007336.
- Kizil C, Dudczig S, Kyritsis N, Machate A, Blaesche J, Kroehne V, and Brand M**, 2012. The chemokine receptor *cxcr5* regulates the regenerative neurogenesis response in the adult zebrafish brain. *Neural Development*, 7(1):27. doi:10.1186/1749-8104-7-27.
- Klepeis VE, Cornell-Bell A, and Trinkaus-Randall V**, 2001. Growth factors but not gap junctions play a role in injury-induced Ca²⁺ waves in epithelial cells. *Journal of Cell Science*, 114(23):4185–4195.
- Knoblach SM and Faden AI**, 1998. Interleukin-10 Improves Outcome and Alters Proinflammatory Cytokine Expression after Experimental Traumatic Brain Injury. *Experimental Neurology*, 153(1):143–151. doi:10.1006/EXNR.1998.6877.
- Knoblach SM, Fan L, and Faden AI**, 1999. Early neuronal expression of tumor necrosis factor- α after experimental brain injury contributes to neurological impairment. *Journal of Neuroimmunology*, 95(1-2):115–125. doi:10.1016/S0165-5728(98)00273-2.
- Knoblach SM, Nikolaeva M, Huang X, Fan L, Krajewski S, Reed JC, and Faden AI**, 2002. Multiple Caspases Are Activated after Traumatic Brain Injury: Evidence for Involvement in Functional Outcome. *Journal of Neurotrauma*, 19(10):1155–1170. doi:10.1089/08977150260337967.
- Knopf F, Schnabel K, Haase C, Pfeifer K, Anastassiadis K, and Weidinger G**, 2010. Dually inducible TetON systems for tissue-specific conditional gene expression in zebrafish. *Proceedings of the National Academy of Sciences of the United States of America*, 107(46):19933–8. doi:10.1073/pnas.1007799107.
- Kocher T**, 1901. Hirnerschütterung, Hirndruck und chirurgische Eingriffe bei Hirnkrankheiten. Technical report, Alfred Holder, Wien, AT.
- Kohman RA and Rhodes JS**, 2013. Neurogenesis, inflammation and behavior. *Brain, Behavior, and Immunity*, 27(1):22–32. doi:10.1016/j.bbi.2012.09.003.
- Koizumi S, Shigemoto-Mogami Y, Nasu-Tada K, Shinozaki Y, Ohsawa K, Tsuda M, Joshi BV, Jacobson KA, Kohsaka S, and Inoue K**, 2007. UDP acting at P2Y₆ receptors is a mediator of microglial phagocytosis. *Nature*, 446(7139):1091–1095. doi:10.1038/nature05704.
- Kontos HA and Wei EP**, 1986. Superoxide production in experimental brain injury. *Journal of Neurosurgery*, 64(5):803–807. doi:10.3171/jns.1986.64.5.0803.

- Kornblum HI, Zurcher SD, Werb Z, Derynck R, and Seroogy KB**, 1999. Multiple trophic actions of heparin-binding epidermal growth factor (HB-EGF) in the central nervous system. *European Journal of Neuroscience*, 11(9):3236–3246. doi:10.1046/j.1460-9568.1999.00744.x.
- Kotwal GJ, Sarojini H, and Chien S**, 2015. Pivotal role of ATP in macrophages fast tracking wound repair and regeneration. *Wound Repair and Regeneration*, 23(5):724–727. doi:10.1111/wrr.12323.
- Koulen P, Kuhn R, Wässle H, and Brandstätter JH**, 1999. Modulation of the intracellular calcium concentration in photoreceptor terminals by a presynaptic metabotropic glutamate receptor. *Proceedings of the National Academy of Sciences of the United States of America*, 96(17):9909–14.
- Kraft A, Jubal ER, von Laer R, Döring C, Rocha A, Grebbin M, Zenke M, Kettenmann H, Stroh A, and Momma S**, 2017. Astrocytic Calcium Waves Signal Brain Injury to Neural Stem and Progenitor Cells. *Stem Cell Reports*, 8(3):701–714. doi:10.1016/j.stemcr.2017.01.009.
- Kreutzer JS, Seel RT, and Gourley E**, 2001. The prevalence and symptom rates of depression after traumatic brain injury: a comprehensive examination. *Brain Injury*, 15(7):563–576. doi:10.1080/02699050010009108.
- Kriegstein A and Alvarez-Buylla A**, 2009. The Glial Nature of Embryonic and Adult Neural Stem Cells. *Annual Review of Neuroscience*, 32(1):149–184. doi:10.1146/annurev.neuro.051508.135600.
- Kroehne V, Freudenreich D, Hans S, Kaslin J, and Brand M**, 2011. Regeneration of the adult zebrafish brain from neurogenic radial glia-type progenitors. *Development*, 138(22):4831–4841. doi:10.1242/dev.072587.
- Kroemer G, Galluzzi L, Vandenabeele P, Abrams J, Alnemri ES, Baehrecke EH, Blagosklonny MV, El-Deiry WS, Golstein P, Green DR, Hengartner M, Knight RA, Kumar S, Lipton SA, Malorni W, Nuñez G, Peter ME, Tschopp J, Yuan J, Piacentini M, Zhivotovsky B, and Melino G**, 2009. Classification of cell death: recommendations of the Nomenclature Committee on Cell Death 2009. *Cell Death & Differentiation*, 16(1):3–11. doi:10.1038/cdd.2008.150.
- Kroner A, Greenhalgh A, Zarruk J, PassosdosSantos R, Gaestel M, and David S**, 2014. TNF and Increased Intracellular Iron Alter Macrophage Polarization to a Detrimental M1 Phenotype in the Injured Spinal Cord. *Neuron*, 83(5):1098–1116. doi:10.1016/J.NEURON.2014.07.027.
- Krysko O, de Ridder L, and Cornelissen M**, 2004. Phosphatidylserine exposure during early primary necrosis (oncosis) in JB6 cells as evidenced by immunogold labeling technique. *Apoptosis*, 9(4):495–500. doi:10.1023/B:APPT.0000031452.75162.75.

- Kulick MB and von Kügelgen I**, 2002. P2Y-receptors mediating an inhibition of the evoked entry of calcium through N-type calcium channels at neuronal processes. *Journal of Pharmacology and Experimental Therapeutics*, 303(2):520–6. doi:10.1124/jpet.102.037960.
- Kumar A, Stoica BA, Sabirzhanov B, Burns MP, Faden AI, and Loane DJ**, 2013. Traumatic brain injury in aged animals increases lesion size and chronically alters microglial/macrophage classical and alternative activation states. *Neurobiology of Aging*, 34(5):1397–1411. doi: 10.1016/j.neurobiolaging.2012.11.013.
- Kurinami H, Shimamura M, Nakagami H, Shimizu H, Koriyama H, Kawano T, Wakayama K, Mochizuki H, Rakugi H, and Morishita R**, 2016. A Novel Therapeutic Peptide as a Partial Agonist of RANKL in Ischemic Stroke. *Scientific Reports*, 6(1):38062. doi:10.1038/srep38062.
- Kwan KM, Fujimoto E, Grabher C, Mangum BD, Hardy ME, Campbell DS, Parant JM, Yost HJ, Kanki JP, and Chien CB**, 2007. The Tol2kit: A multisite gateway-based construction kit for Tol2 transposon transgenesis constructs. *Developmental Dynamics*, 236(11):3088–3099. doi:10.1002/dvdy.21343.
- Kyritsis N, Kizil C, Zocher S, Kroehne V, Kaslin J, Freudenreich D, Iltzsch A, and Brand M**, 2012. Acute Inflammation Initiates the Regenerative Response in the Adult Zebrafish Brain. *Science*, 338. doi:10.1126/science.1228773.
- Lai SL, Marín-Juez R, Moura PL, Kuenne C, Lai JKH, Tseke AT, Guenther S, Looso M, and Stainier DY**, 2017. Reciprocal analyses in zebrafish and medaka reveal that harnessing the immune response promotes cardiac regeneration. *eLife*, 6:1–20. doi:10.7554/eLife.25605.
- Lalancette-Hebert M, Gowing G, Simard A, Weng YC, and Kriz J**, 2007. Selective Ablation of Proliferating Microglial Cells Exacerbates Ischemic Injury in the Brain. *Journal of Neuroscience*, 27(10):2596–2605. doi:10.1523/JNEUROSCI.5360-06.2007.
- Lampron A, Larochelle A, Laflamme N, Préfontaine P, Plante MM, Sánchez MG, Yong VW, Stys PK, Tremblay MÈ, and Rivest S**, 2015. Inefficient clearance of myelin debris by microglia impairs remyelinating processes. *Journal of Experimental Medicine*, 212(4):481–495. doi:10.1084/jem.20141656.
- Lang R, Hammer M, and Mages J**, 2006. DUSP meet immunology: dual specificity MAPK phosphatases in control of the inflammatory response. *Journal of Immunology*, 177(11):7497–504.
- Langlois JA and Sattin RW**, 2005. Traumatic brain injury in the United States: research and programs of the Centers for Disease Control and Prevention (CDC). *Journal of Head Trauma Rehabilitation*, 20(3):187–8.

- Lauber K, Bohn E, Kröber SM, Xiao Yj, Blumenthal SG, Lindemann RK, Marini P, Wiedig C, Zobywalski A, Baksh S, Xu Y, Autenrieth IB, Schulze-Osthoff K, Belka C, Stuhler G, and Wesselborg S**, 2003. Apoptotic cells induce migration of phagocytes via caspase-3-mediated release of a lipid attraction signal. *Cell*, 113(6):717–30.
- Lavine KJ, Epelman S, Uchida K, Weber KJ, Nichols CG, Schilling JD, Ornitz DM, Randolph GJ, and Mann DL**, 2014. Distinct macrophage lineages contribute to disparate patterns of cardiac recovery and remodeling in the neonatal and adult heart. *Proceedings of the National Academy of Sciences*, 111(45):16029–16034. doi:10.1073/pnas.1406508111.
- Lee S, Park JY, Lee WH, Kim H, Park HC, Mori K, and Suk K**, 2009. Lipocalin-2 Is an Autocrine Mediator of Reactive Astrocytosis. *Journal of Neuroscience*, 29(1):234–249. doi:10.1523/JNEUROSCI.5273-08.2009.
- Lee YK, Hou SW, Lee CC, Hsu CY, Huang YS, and Su YC**, 2013. Increased Risk of Dementia in Patients with Mild Traumatic Brain Injury: A Nationwide Cohort Study. *PLoS ONE*, 8(5):e62422. doi:10.1371/journal.pone.0062422.
- Leist M, Volbracht C, Kühnle S, Fava E, Ferrando-May E, and Nicotera P**, 1997. Caspase-mediated apoptosis in neuronal excitotoxicity triggered by nitric oxide. *Molecular Medicine*, 3(11):750–64.
- Lenzlinger PM, Morganti-Kossmann MC, Laurer HL, and McIntosh TK**, 2001. The duality of the inflammatory response to traumatic brain injury. *Molecular Neurobiology*, 24(1-3):169–81.
- Lepiller S, Laurens V, Bouchot A, Herbomel P, Solary E, and Chluba J**, 2007. Imaging of nitric oxide in a living vertebrate using a diaminofluorescein probe. *Free Radical Biology and Medicine*, 43(4):619–627. doi:10.1016/j.freeradbiomed.2007.05.025.
- Ley EJ, Clond MA, Singer MB, Shouhed D, and Salim A**, 2011. IL6 Deficiency Affects Function After Traumatic Brain Injury. *Journal of Surgical Research*, 170(2):253–256. doi:10.1016/j.jss.2011.03.006.
- Li MS and David S**, 1996. Topical glucocorticoids modulate the lesion interface after cerebral cortical stab wounds in adult rats. *Glia*, 18(4):306–318. doi:10.1002/(SICI)1098-1136(199612)18:4<306::AID-GLIA5j3.0.CO;2-V.
- Li T, Pang S, Yu Y, Wu X, Guo J, and Zhang S**, 2013. Proliferation of parenchymal microglia is the main source of microgliosis after ischaemic stroke. *Brain*, 136(12):3578–3588. doi:10.1093/brain/awt287.
- Li Z, Venegas V, Nagaoka Y, Morino E, Raghavan P, Audhya A, Nakanishi Y, and Zhou Z**, 2015. Necrotic Cells Actively Attract Phagocytes through the Collaborative Action of Two Distinct PS-Exposure Mechanisms. *PLoS Genetics*, 11(6):e1005285. doi:10.1371/journal.pgen.1005285.

- Liang D, Bhatta S, Gerzanich V, and Simard JM**, 2007. Cytotoxic edema: mechanisms of pathological cell swelling. *Neurosurgical Focus*, 22(5):1–9. doi:10.3171/foc.2007.22.5.3.
- Liao Y, Liu P, Guo F, Zhang ZY, and Zhang Z**, 2013. Oxidative Burst of Circulating Neutrophils Following Traumatic Brain Injury in Human. *PLoS ONE*, 8(7):e68963. doi: 10.1371/journal.pone.0068963.
- Liao Y, Smyth GK, and Shi W**, 2014. featurecounts: an efficient general purpose program for assigning sequence reads to genomic features. *Bioinformatics*, 30:923–930. doi: <http://doi.org/10.1093/bioinformatics/btt656>.
- Lima R, Monteiro S, Lopes JP, Barradas P, Vasconcelos NL, Gomes ED, Assunção-Silva RC, Teixeira FG, Morais M, Sousa N, Salgado AJ, and Silva NA**, 2017. Systemic Interleukin-4 Administration after Spinal Cord Injury Modulates Inflammation and Promotes Neuroprotection. *Pharmaceuticals*, 10(4). doi:10.3390/ph10040083.
- Lin SL, Li B, Rao S, Yeo EJ, Hudson TE, Nowlin BT, Pei H, Chen L, Zheng JJ, Carroll TJ, Pollard JW, McMahon AP, Lang RA, and Duffield JS**, 2010. Macrophage Wnt7b is critical for kidney repair and regeneration. *Proceedings of the National Academy of Sciences of the United States of America*, 107(9):4194–9. doi:10.1073/pnas.0912228107.
- Lincoln AE, Caswell SV, Almquist JL, Dunn RE, Norris JB, and Hinton RY**, 2011. Trends in concussion incidence in high school sports: A prospective 11-year study. *American Journal of Sports Medicine*, 39(5):958–963. doi:10.1177/0363546510392326.
- Lindholm D, Castren E, Kiefer R, Zafra F, and Thoenen H**, 1992. Transforming growth factor- β 1 in the rat brain: Increase after injury and inhibition of astrocyte proliferation. *Journal of Cell Biology*, 117(2):395–400. doi:10.1083/jcb.117.2.395.
- Lindholm P and Saarma M**, 2010. Novel CDFN/MANF family of neurotrophic factors. *Developmental Neurobiology*, 70(5):360–371. doi:10.1002/dneu.20760.
- Liou AK, Clark RS, Henshall DC, Yin XM, and Chen J**, 2003. To die or not to die for neurons in ischemia, traumatic brain injury and epilepsy: a review on the stress-activated signaling pathways and apoptotic pathways. *Progress in Neurobiology*, 69(2):103–142. doi:10.1016/S0301-0082(03)00005-4.
- Lipton SA and Rosenberg PA**, 1994. Excitatory amino acids as a final common pathway for neurologic disorders. *The New England Journal of Medicine*, 330(9):613–622. doi: 10.1056/NEJM199403033300907.
- Liu L, Doran S, Xu Y, Manwani B, Ritzel R, Benashski S, McCullough L, and Li J**, 2014. Inhibition of mitogen-activated protein kinase phosphatase-1 (MKP-1) increases experimental stroke injury. *Experimental Neurology*, 261:404–411. doi:10.1016/j.expneurol.2014.05.009.

- Liu T, McDonnell PC, Young PR, White RF, Siren AL, Hallenbeck JM, Barone FC, and Feurestein GZ**, 1993. Interleukin-1 beta mRNA expression in ischemic rat cortex. *Stroke*, 24(11):1746–51.
- Liu X, Hashimoto-Torii K, Torii M, Ding C, and Rakic P**, 2010. Gap Junctions/Hemichannels Modulate Interkinetic Nuclear Migration in the Forebrain Precursors. *Journal of Neuroscience*, 30(12):4197–4209. doi:10.1523/JNEUROSCI.4187-09.2010.
- Liu X, Liu J, Zhao S, Zhang H, Cai W, Cai M, Ji X, Leak RK, Gao Y, Chen J, and Hu X**, 2016. Interleukin-4 Is Essential for Microglia/Macrophage M2 Polarization and Long-Term Recovery After Cerebral Ischemia. *Stroke*, 47(2):498–504. doi:10.1161/STROKEAHA.115.012079.
- Liu Y, Hao W, Letiembre M, Walter S, Kulanga M, Neumann H, and Fassbender K**, 2006. Suppression of microglial inflammatory activity by myelin phagocytosis: role of p47-PHOX-mediated generation of reactive oxygen species. *Journal of Neuroscience*, 26(50):12904–13. doi:10.1523/JNEUROSCI.2531-06.2006.
- Loane DJ and Kumar A**, 2016. Microglia in the TBI brain: The good, the bad, and the dysregulated. *Experimental Neurology*, 275(0 3):316–327. doi:10.1016/j.expneurol.2015.08.018.
- Loane DJ, Kumar A, Stoica BA, Cabatbat R, and Faden AI**, 2014. Progressive Neurodegeneration After Experimental Brain Trauma. *Journal of Neuropathology & Experimental Neurology*, 73(1):14–29. doi:10.1097/NEN.0000000000000021.
- Locatelli G, Theodorou D, Kendirli A, Jordão MJC, Staszewski O, Phulphagar K, Cantuti-Castelvetri L, Dagkalis A, Bessis A, Simons M, Meissner F, Prinz M, and Kerschensteiner M**, 2018. Mononuclear phagocytes locally specify and adapt their phenotype in a multiple sclerosis model. *Nature Neuroscience*, 21(9):1196–1208. doi:10.1038/s41593-018-0212-3.
- Loddick SA, Turnbull AV, and Rothwell NJ**, 1998. Cerebral Interleukin-6 is Neuroprotective during Permanent Focal Cerebral Ischemia in the Rat. *Journal of Cerebral Blood Flow & Metabolism*, 18(2):176–179. doi:10.1097/00004647-199802000-00008.
- Loddick SA, Wong ML, Bongiorno PB, Gold PW, Licinio J, and Rothwell NJ**, 1997. Endogenous Interleukin-1 Receptor Antagonist is Neuroprotective. *Biochemical and Biophysical Research Communications*, 234(1):211–215. doi:10.1006/bbrc.1997.6436.
- Lois C and Alvarez-Buylla A**, 1993. Proliferating subventricular zone cells in the adult mammalian forebrain can differentiate into neurons and glia. *Proceedings of the National Academy of Sciences of the United States of America*, 90(5):2074–7.
- Longhi L, Perego C, Ortolano F, Aresi S, Fumagalli S, Zanier ER, Stocchetti N, and De Simoni MG**, 2013. Tumor Necrosis Factor in Traumatic Brain Injury: Effects of Genetic Deletion

- of p55 or p75 Receptor. *Journal of Cerebral Blood Flow & Metabolism*, 33(8):1182–1189. doi: 10.1038/jcbfm.2013.65.
- Lou J, Lenke LG, Ludwig FJ, and O'Brien MF**, 1998. Apoptosis as a mechanism of neuronal cell death following acute experimental spinal cord injury. *Spinal Cord*, 36(10):683–90.
- Love NR, Chen Y, Ishibashi S, Kritsiligkou P, Lea R, Koh Y, Gallop JL, Dorey K, and Amaya E**, 2013. Amputation-induced reactive oxygen species are required for successful *Xenopus* tadpole tail regeneration. *Nature Cell Biology*, 15(2):222–228. doi:10.1038/ncb2659.
- Lu KT, Wang YW, Yang JT, Yang YL, and Chen HI**, 2005. Effect of Interleukin-1 on Traumatic Brain Injury-Induced Damage to Hippocampal Neurons. *Journal of Neurotrauma*, 22(8):885–895. doi:10.1089/neu.2005.22.885.
- Luo J, Elwood F, Britschgi M, Villeda S, Zhang H, Ding Z, Zhu L, Alabsi H, Getachew R, Narasimhan R, Wabl R, Fainberg N, James ML, Wong G, Relton J, Gambhir SS, Pollard JW, and Wyss-Coray T**, 2013. Colony-stimulating factor 1 receptor (CSF1R) signaling in injured neurons facilitates protection and survival. *Journal of Experimental Medicine*, 210(1):157–72. doi: 10.1084/jem.20120412.
- Lyons DA, Guy AT, and Clarke JDW**, 2003. Monitoring neural progenitor fate through multiple rounds of division in an intact vertebrate brain. *Development*, 130(15):3427–36.
- Maas AI, Murray G, Henney H, Kassem N, Legrand V, Mangelus M, Muizelaar JP, Stocchetti N, Knoller N, and Pharmos TBI investigators**, 2006. Efficacy and safety of dexamethasone in severe traumatic brain injury: results of a phase III randomised, placebo-controlled, clinical trial. *The Lancet Neurology*, 5(1):38–45. doi:10.1016/S1474-4422(05)70253-2.
- Maas AIR, Menon DK, Adelson PD, Andelic N, Bell MJ, Belli A, Bragge P, Brazinova A, et al.**, 2017. Traumatic brain injury: integrated approaches to improve prevention, clinical care, and research. *The Lancet Neurology*, 16(12):987–1048. doi:10.1016/S1474-4422(17)30371-X.
- Maas AIR, Roozenbeek B, and Manley GT**, 2010. Clinical Trials in Traumatic Brain Injury: Past Experience and Current Developments. *Neurotherapeutics*, 7(1):115–126. doi: 10.1016/j.nurt.2009.10.022.
- Maas AIR, Stocchetti N, and Bullock R**, 2008. Moderate and severe traumatic brain injury in adults. *The Lancet Neurology*, 7:728–41.
- Mahler J and Driever W**, 2007. Expression of the zebrafish intermediate neurofilament Nestin in the developing nervous system and in neural proliferation zones at postembryonic stages. *BMC Developmental Biology*, 7(1):89. doi:10.1186/1471-213X-7-89.

- Maiese K**, 2002. Organic brain disease. In VS Ramachandran, editor, *Encyclopedia of the Human Brain*, pages 509–526. Elsevier Science, 1st edition edition.
- Manley GT, Fujimura M, Ma T, Noshita N, Filiz F, Bollen AW, Chan P, and Verkman AS**, 2000. Aquaporin-4 deletion in mice reduces brain edema after acute water intoxication and ischemic stroke. *Nature Medicine*, 6(2):159–163. doi:10.1038/72256.
- Mantovani A, Sica A, Sozzani S, Allavena P, Vecchi A, and Locati M**, 2004. The chemokine system in diverse forms of macrophage activation and polarization. *Trends in Immunology*, 25(12):677–686. doi:10.1016/J.IT.2004.09.015.
- Marion DW, Obrist WD, Earlier PM, Penrod LE, and Darby JM**, 1993. The use of moderate therapeutic hypothermia for patients with severe head injuries: a preliminary report. *Journal of Neurosurgery*, 79(3):354–362. doi:10.3171/jns.1993.79.3.0354.
- Marion DW, Penrod LE, Kelsey SF, Obrist WD, Kochanek PM, Palmer AM, Wisniewski SR, and DeKosky ST**, 1997. Treatment of Traumatic Brain Injury with Moderate Hypothermia. *New England Journal of Medicine*, 336(8):540–546. doi:10.1056/NEJM199702203360803.
- Markgraf CG, Clifton GL, and Moody MR**, 2001. Treatment window for hypothermia in brain injury. *Journal of Neurosurgery*, 95(6):979–983. doi:10.3171/jns.2001.95.6.0979.
- Marshall LF, Maas AIR, Marshall SB, Bricolo A, Fearnside M, Iannotti F, Klauber MR, Lagarrigue J, Lobato R, Persson L, Pickard JD, Piek J, Servadei F, Wellis GN, Morris GF, Means ED, and Musch B**, 1998. A multicenter trial on the efficacy of using tirilazad mesylate in cases of head injury. *Journal of Neurosurgery*, 89(4):519–525. doi:10.3171/jns.1998.89.4.0519.
- Martin M**, 2011. Cutadapt removes adapter sequences from high-throughput sequencing reads. *EMBnet journal*, 17. doi:https://doi.org/10.14806/ej.17.1.200.
- Martinez FO and Gordon S**, 2014. The M1 and M2 paradigm of macrophage activation: time for reassessment. *F1000Prime Reports*, 6:1–13. doi:10.12703/P6-13.
- Martland HS**, 1928. Punch drunk. *Journal of the American Medical Association*, 91(15):1103. doi:10.1001/jama.1928.02700150029009.
- Maruyama K, Takada Y, Ray N, Kishimoto Y, Penninger JM, Yasuda H, and Matsuo K**, 2006. Receptor Activator of NF- B Ligand and Osteoprotegerin Regulate Proinflammatory Cytokine Production in Mice. *Journal of Immunology*, 177(6):3799–3805. doi:10.4049/jimmunol.177.6.3799.
- März M, Schmidt R, Rastegar S, and Strähle U**, 2011. Regenerative response following stab injury in the adult zebrafish telencephalon. *Developmental Dynamics*, 240(9):2221–2231. doi:10.1002/dvdy.22710.

- Masel BE and DeWitt DS**, 2010. Traumatic Brain Injury: A Disease Process, Not an Event. *Journal of Neurotrauma*, 27(8):1529–1540. doi:10.1089/neu.2010.1358.
- Masel BE, Scheibel RS, Kimbark T, and Kuna ST**, 2001. Excessive daytime sleepiness in adults with brain injuries. *Archives of Physical Medicine and Rehabilitation*, 82(11):1526–1532. doi:10.1053/apmr.2001.26093.
- Mätlik K, Anttila JE, Kuan-Yin T, Smolander OP, Pakarinen E, Lehtonen L, Abo-Ramadan U, Lindholm P, Zheng C, Harvey B, Arumäe U, Lindahl M, and Airavaara M**, 2018. Post-stroke delivery of MANF promotes functional recovery in rats. *Science Advances*, 4(5):eaap8957. doi:10.1126/sciadv.aap8957.
- Mauritz W, Wilbacher I, Majdan M, Leitgeb J, Janciak I, Brazinova A, and Rusnak M**, 2008. Epidemiology, treatment and outcome of patients after severe traumatic brain injury in European regions with different economic status. *European Journal of Public Health*, 18(6):575–580. doi:10.1093/eurpub/ckn079.
- Mazaheri F, Breus O, Durdu S, Haas P, Wittbrodt J, Gilmour D, and Peri F**, 2014. Distinct roles for BAI1 and TIM-4 in the engulfment of dying neurons by microglia. *Nature Communications*, 5(May):1–11.
- Mazzolini J, Chia K, and Sieger D**, 2018. Isolation and RNA Extraction of Neurons, Macrophages and Microglia from Larval Zebrafish Brains. *Journal of Visualized Experiments*, (134):e57431–e57431. doi:10.3791/57431.
- McCutcheon V, Park E, Liu E, Wang Y, Wen XY, and Baker AJ**, 2016. A Model of Excitotoxic Brain Injury in Larval Zebrafish: Potential Application for High-Throughput Drug Evaluation to Treat Traumatic Brain Injury. *Zebrafish*, 13(3):161–169. doi:10.1089/zeb.2015.1188.
- McIntosh TK, Thomas M, Smith D, and Banbury M**, 1992. The Novel 21-Aminosteroid U74006F Attenuates Cerebral Edema and Improves Survival after Brain Injury in the Rat. *Journal of Neurotrauma*, 9(1):33–46. doi:10.1089/neu.1992.9.33.
- McLean A, Dikmen S, Temkin N, Wyler AR, and Gale JL**, 1984. Psychosocial functioning at 1 month after head injury. *Neurosurgery*, 14(4):393–9.
- Meier P, Finch A, and Evan G**, 2000. Apoptosis in development. *Nature*, 407(6805):796–801. doi:10.1038/35037734.
- Menon DK, Schwab K, Wright DW, Maas AI, and Demographics and Clinical Assessment Working Group of the International and Interagency Initiative toward Common Data Elements for Research on Traumatic Brain Injury and Psychological Health**, 2010. Position Statement: Definition of Traumatic Brain Injury. *Archives of Physical Medicine and Rehabilitation*, 91(11):1637–1640. doi:10.1016/j.apmr.2010.05.017.

- Mésenge C, Margail I, Verrecchia C, Allix M, Boulu RG, and Plotkine M**, 1998. Protective effect of melatonin in a model of traumatic brain injury in mice. *Journal of Pineal Research*, 25(1):41–46. doi:10.1111/j.1600-079X.1998.tb00384.x.
- Metchnikoff E**, 1905. *Immunity in Infective Diseases*. Cambridge University Press, New York.
- Mi H, Muruganujan A, Casagrande JT, and Thomas PD**, 2013. Large-scale gene function analysis with the PANTHER classification system. *Nature Protocols*, 8(8):1551–1566. doi:10.1038/nprot.2013.092.
- Mikawa S, Kinouchi H, Kamii H, Gobbel GT, Chen SF, Carlson E, Epstein CJ, and Chan PH**, 1996. Attenuation of acute and chronic damage following traumatic brain injury in copper, zincsuperoxide dismutase transgenic mice. *Journal of Neurosurgery*, 85(5):885–891. doi:10.3171/jns.1996.85.5.0885.
- Mildner A, Huang H, Radke J, Stenzel W, and Priller J**, 2017. P2Y ₁₂ receptor is expressed on human microglia under physiological conditions throughout development and is sensitive to neuroinflammatory diseases. *Glia*, 65(2):375–387. doi:10.1002/glia.23097.
- Mills CD, Kincaid K, Alt JM, Heilman MJ, and Hill AM**, 2000. M-1/M-2 macrophages and the Th1/Th2 paradigm. *Journal of immunology (Baltimore, Md. : 1950)*, 164(12):6166–73.
- Min KJ, Jeong HK, Kim B, Hwang DH, Shin HY, Nguyen AT, Kim Jh, Jou I, Kim BG, and Joe Eh**, 2012. Spatial and temporal correlation in progressive degeneration of neurons and astrocytes in contusion-induced spinal cord injury. *Journal of Neuroinflammation*, 9(1):627. doi:10.1186/1742-2094-9-100.
- Minakami R and Sumimotoa H**, 2006. Phagocytosis-Coupled Activation of the Superoxide-Producing Phagocyte Oxidase, a Member of the NADPH Oxidase (Nox) Family. *International Journal of Hematology*, 84(3):193–198. doi:10.1532/IJH97.06133.
- Miñambres E, Ballesteros MA, Mayorga M, Marin MJ, Muñoz P, Figols J, and López-Hoyos M**, 2008. Cerebral Apoptosis in Severe Traumatic Brain Injury Patients: An In Vitro, In Vivo, and Postmortem Study. *Journal of Neurotrauma*, 25(6):581–591. doi:10.1089/neu.2007.0398.
- Ming GI and Song H**, 2005. Adult Neurogenesis in the Mammalian Central Nervous System. *Annual Review of Neuroscience*, 28:223–50.
- Minns MS, Teicher G, Rich CB, and Trinkaus-Randall V**, 2016. Purinoreceptor P2X7 regulation of Ca²⁺ mobilization and cytoskeletal rearrangement is required for corneal reepithelialization after injury. *American Journal of Pathology*, 186(2):285–296. doi:10.1016/j.ajpath.2015.10.006.
- Minogue AM, Barrett JP, and Lynch MA**, 2012. LPS-induced release of IL-6 from glia modulates production of IL-1 β in a JAK2-dependent manner. *Journal of Neuroinflammation*, 9(1):629. doi:10.1186/1742-2094-9-126.

- Mizuno T, Doi Y, Mizoguchi H, Jin S, Noda M, Sonobe Y, Takeuchi H, and Suzumura A**, 2011. Interleukin-34 selectively enhances the neuroprotective effects of microglia to attenuate oligomeric amyloid- β neurotoxicity. *American Journal of Pathology*, 179(4):2016–27. doi: 10.1016/j.ajpath.2011.06.011.
- Moalem G, Gdalyahu A, Shani Y, Otten U, Lazarovici P, Cohen IR, and Schwartz M**, 2000. Production of Neurotrophins by Activated T Cells: Implications for Neuroprotective Autoimmunity. *Journal of Autoimmunity*, 15(3):331–345. doi:10.1006/jaut.2000.0441.
- Moalem G, Leibowitz Amit R, Yoles E, Mor F, Cohen IR, and Schwartz M**, 1999. Autoimmune T cells protect neurons from secondary degeneration after central nervous system axotomy. *Nature Medicine*, 5(1):49–55. doi:10.1038/4734.
- Moeendarbary E, Weber IP, Sheridan GK, Koser DE, Soleman S, Haenzi B, Bradbury EJ, Fawcett J, and Franze K**, 2017. The soft mechanical signature of glial scars in the central nervous system. *Nature Communications*, 8:14787. doi:10.1038/ncomms14787.
- Monif M, Reid CA, Powell KL, Smart ML, and Williams DA**, 2009. The P2X7 Receptor Drives Microglial Activation and Proliferation: A Trophic Role for P2X7R Pore. *Journal of Neuroscience*, 29(12):3781–3791. doi:10.1523/JNEUROSCI.5512-08.2009.
- Monje ML, Toda H, and Palmer TD**, 2003. Inflammatory Blockade Restores Adult Hippocampal Neurogenesis. *Science*, 302(5651):1760–1765.
- Monti B and Contestabile A**, 2000. Blockade of the NMDA receptor increases developmental apoptotic elimination of granule neurons and activates caspases in the rat cerebellum. *European Journal of Neuroscience*, 12(9):3117–23.
- Morente V, Pérez-Sen R, Ortega F, Huerta-Cepas J, Delicado EG, and Miras-Portugal MT**, 2014. Neuroprotection elicited by P2Y13 receptors against genotoxic stress by inducing DUSP2 expression and MAPK signaling recovery. *Biochimica et Biophysica Acta - Molecular Cell Research*, 1843(9):1886–1898. doi:10.1016/j.bbamcr.2014.05.004.
- Morganti JM, Jopson TD, Liu S, Riparip LK, Guandique CK, Gupta N, Ferguson AR, and Rosi S**, 2015. CCR2 Antagonism Alters Brain Macrophage Polarization and Ameliorates Cognitive Dysfunction Induced by Traumatic Brain Injury. *Journal of Neuroscience*, 35(2):748–760. doi: 10.1523/JNEUROSCI.2405-14.2015.
- Morganti JM, Riparip LK, and Rosi S**, 2016. Call Off the Dog(ma): M1/M2 Polarization Is Concurrent following Traumatic Brain Injury. *PLoS ONE*, 11(1):e0148001. doi: 10.1371/journal.pone.0148001.

- Morganti-Kossmann MC, Rancan M, Stahel PF, and Kossmann T**, 2002. Inflammatory response in acute traumatic brain injury: a double-edged sword. *Current Opinion in Critical Care*, 8(2):101–105. doi:10.1097/00075198-199512000-00016.
- Morganti-Kossmann MC, Semple BD, Hellewell SC, Bye N, and Ziebell JM**, 2018. The complexity of neuroinflammation consequent to traumatic brain injury: from research evidence to potential treatments. *Acta Neuropathologica*, pages 1–25. doi:10.1007/s00401-018-1944-6.
- Mori S, Maher P, and Conti B**, 2016. Neuroimmunology of the Interleukins 13 and 4. *Brain Sciences*, 6(2). doi:10.3390/brainsci6020018.
- Morikawa E, Mori H, Kiyama Y, Mishina M, Asano T, and Kirino T**, 1998. Attenuation of focal ischemic brain injury in mice deficient in the epsilon1 (NR2A) subunit of NMDA receptor. *Journal of Neuroscience*, 18(23):9727–32. doi:10.1523/JNEUROSCI.18-23-09727.1998.
- Morris GF, Bullock R, Marshall SB, Marmarou A, Maas A, and Marshall LF**, 1999. Failure of the competitive N-methyl-d-aspartate antagonist Selfotel (CGS 19755) in the treatment of severe head injury: results of two Phase III clinical trials. *Journal of Neurosurgery*, 91(5):737–743. doi:10.3171/jns.1999.91.5.0737.
- Morsch M, Radford R, Lee A, Don EK, Badrock AP, Hall TE, Cole NJ, and Chung R**, 2015. In vivo characterization of microglial engulfment of dying neurons in the zebrafish spinal cord. *Frontiers in Cellular Neuroscience*, 9:1–11. doi:10.3389/fncel.2015.00321.
- Mortimer JA, Van Duijn CM, Chandra V, Fratiglioni L, Graves AB, Heyman A, Jorm AF, Kokmen E, Kondo K, Rocca WA, Shalat SL, and Soininen H**, 1991. Head Trauma as a Risk Factor for Alzheimer's Disease: A Collaborative Re-Analysis of Case-Control Studies. *International Journal of Epidemiology*, 20:S28–S35. doi:10.1093/ije/20.Supplement_2.S28.
- Mosmann TR, Cherwinski H, Bond MW, Giedlin MA, and Coffman RL**, 1986. Two types of murine helper T cell clone. I. Definition according to profiles of lymphokine activities and secreted proteins. *Journal of immunology (Baltimore, Md. : 1950)*, 136(7):2348–57.
- Mosser DM and Edwards JP**, 2008. Exploring the full spectrum of macrophage activation. *Nature Reviews Immunology*, 8(12):958–969. doi:10.1038/nri2448.Exploring.
- Muizelaar JP, Marmarou A, Young HF, Choi SC, Wolf A, Schneider RL, and Kontos HA**, 1993. Improving the outcome of severe head injury with the oxygen radical scavenger polyethylene glycol-conjugated superoxide dismutase: a Phase II trial. *Journal of Neurosurgery*, 78(3):375–382. doi:10.3171/jns.1993.78.3.0375.
- Mukhin A, Ivanova S, Allen J, and Faden A**, 1998. Mechanical injury to neuronal/glial cultures in microplates: Role of NMDA receptors and pH in secondary neuronal cell death. *Journal*

of *Neuroscience Research*, 51(6):748–758. doi:10.1002/(SICI)1097-4547(19980315)51:6;748::AID-JNR8j3.0.CO;2-B.

Münch E, Horn P, Schürer L, Piepgras A, Paul T, and Schmiedek P, 2000. Management of Severe Traumatic Brain Injury by Decompressive Craniectomy. *Neurosurgery*, 47(2):315–323. doi:10.1097/00006123-200008000-00009.

Murray KN, Parry-Jones AR, and Allan SM, 2015. Interleukin-1 and acute brain injury. *Frontiers in Cellular Neuroscience*, 9:18. doi:10.3389/fncel.2015.00018.

Nacher J, Ramírez C, Palop JJ, Molowny A, Luis de la Iglesia JA, and López-García C, 1999. Radial glia and cell debris removal during lesion-regeneration of the lizard medial cortex. *Histology and Histopathology*, 14(1):89–101. doi:10.14670/HH-14.89.

Nagamoto-Combs K, McNeal DW, Morecraft RJ, and Combs CK, 2007. Prolonged Microgliosis in the Rhesus Monkey Central Nervous System after Traumatic Brain Injury. *Journal of Neurotrauma*, 24(11):1719–1742. doi:10.1089/neu.2007.0377.

Nathoo N, Narotam PK, Agrawal DK, Connolly CA, van Dellen JR, Barnett GH, and Chetty R, 2004. Influence of apoptosis on neurological outcome following traumatic cerebral contusion. *Journal of Neurosurgery*, 101(2):233–240. doi:10.3171/jns.2004.101.2.0233.

Neher JJ, Emmrich JV, Fricker M, Mander PK, They C, and Brown GC, 2013. Phagocytosis executes delayed neuronal death after focal brain ischemia. *Proceedings of the National Academy of Sciences*, 110(43):E4098–E4107. doi:10.1073/pnas.1308679110.

Neher JJ, Neniskyte U, Zhao JW, Bal-Price A, Tolkovski AM, and Brown GC, 2011. Inhibition of microglial phagocytosis is sufficient to prevent inflammatory neuronal death. *Journal of Immunology*, 186(8):4973–4983. doi:10.4049/jimmunol.1003600.

Neumann H, Kotter MR, and Franklin RJ, 2009. Debris clearance by microglia: An essential link between degeneration and regeneration. *Brain*, 132(2):288–295. doi:10.1093/brain/awn109.

Neumann J, Sauerzweig S, Ronicke R, Gunzer F, Dinkel K, Ullrich O, Gunzer M, and Reymann KG, 2008. Microglia Cells Protect Neurons by Direct Engulfment of Invading Neutrophil Granulocytes: A New Mechanism of CNS Immune Privilege. *Journal of Neuroscience*, 28(23):5965–5975. doi:10.1523/JNEUROSCI.0060-08.2008.

Neve LD, Savage AA, Koke JR, and García DM, 2012. Activating transcription factor 3 and reactive astrocytes following optic nerve injury in zebrafish. *Comparative Biochemistry and Physiology - C Toxicology and Pharmacology*, 155(2):213–218. doi:10.1016/j.cbpc.2011.08.006.

Neves J, Zhu J, Sousa-Victor P, Konjikusic M, Riley R, Chew S, Qi Y, Jasper H, and Lamba DA, 2016. Immune modulation by MANF promotes tissue repair and regenerative success in the retina. *Science*, 353(6294):aaf3646. doi:10.1126/science.aaf3646.

- Nguyen HX, O'Barr TJ, and Anderson AJ**, 2007. Polymorphonuclear leukocytes promote neurotoxicity through release of matrix metalloproteinases, reactive oxygen species, and TNF- α . *Journal of Neurochemistry*, 102(3):900–912. doi:10.1111/j.1471-4159.2007.04643.x.
- Nguyen-Chi M, Laplace-Builhé B, Travnickova J, Luz-Crawford P, Tejedor G, Lutfalla G, Kissa K, Jorgensen C, and Djouad F**, 2017. TNF signaling and macrophages govern fin regeneration in zebrafish larvae. *Cell Death and Disease*, 8(8):e2979. doi:10.1038/cddis.2017.374.
- Nguyen-Chi M, Laplace-Builhé B, Travnickova J, Luz-Crawford P, Tejedor G, Phan QT, Duroux-Richard I, Levraud JP, Kissa K, Lutfalla G, Jorgensen C, and Djouad F**, 2015. Identification of polarized macrophage subsets in zebrafish. *eLife*, 4:e07288. doi:10.7554/eLife.07288.
- Nicholls J and Saunders N**, 1996. Regeneration of immature mammalian spinal cord after injury. *Trends in Neurosciences*, 19(6):229–234.
- Niethammer P, Grabher C, Look AT, and Mitchison TJ**, 2009. A tissue-scale gradient of hydrogen peroxide mediates rapid wound detection in zebrafish. *Nature*, 459(7249):996–9. doi:10.1038/nature08119.
- Nijhawan D, Honarpour N, and Wang X**, 2000. Apoptosis in Neural Development and Disease. *Annual Review of Neuroscience*, 23(1):73–87. doi:10.1146/annurev.neuro.23.1.73.
- Nimmerjahn A, Kirchhoff F, and Helmchen F**, 2005. Resting microglial cells are highly dynamic surveillants of brain parenchyma in vivo. *Science*, 308(5726):1314–8. doi:10.1126/science.1110647.
- Nocentini G, Cuzzocrea S, Genovese T, Bianchini R, Mazzon E, Ronchetti S, Esposito E, Rosanna DP, Bramanti P, and Riccardi C**, 2008. Glucocorticoid-Induced Tumor Necrosis Factor Receptor-Related (GTR)-Fc Fusion Protein Inhibits GTR Triggering and Protects from the Inflammatory Response after Spinal Cord Injury. *Molecular Pharmacology*, 73(6):1610–1621. doi:10.1124/mol.107.044354.
- Noctor SC, Flint AC, Weissman TA, Dammerman RS, and Kriegstein AR**, 2001. Neurons derived from radial glial cells establish radial units in neocortex. *Nature*, 409(6821):714–720.
- Noda M, Doi Y, Liang J, Kawanokuchi J, Sonobe Y, Takeuchi H, Mizuno T, and Suzumura A**, 2011. Fractalkine Attenuates Excito-neurotoxicity via Microglial Clearance of Damaged Neurons and Antioxidant Enzyme Heme Oxygenase-1 Expression. *Journal of Biological Chemistry*, 286(3):2308–2319. doi:10.1074/jbc.M110.169839.
- Nomura K, Vilalta A, Allendorf DH, Hornik TC, and Brown GC**, 2017. Activated Microglia Desialylate and Phagocytose Cells via Neuraminidase, Galectin-3, and Mer Tyrosine Kinase. *Journal of Immunology*, 198(12):4792–4801. doi:10.4049/jimmunol.1502532.

- Nonaka M, Chen XH, Pierce JE, Leoni MJ, McIntosh TK, Wolf JA, and Smith DH**, 1999. Prolonged Activation of NF- κ B Following Traumatic Brain Injury in Rats. *Journal of Neurotrauma*, 16(11):1023–1034. doi:10.1089/neu.1999.16.1023.
- Nordström P, Michaëlsson K, Gustafson Y, and Nordström A**, 2014. Traumatic brain injury and young onset dementia: A nationwide cohort study. *Annals of Neurology*, 75(3):374–381. doi:10.1002/ana.24101.
- Novoa B and Figueras A**, 2012. Zebrafish: Model for the study of inflammation and the innate immune response to infectious diseases. *Advances in Experimental Medicine and Biology*, 946:253–275. doi:10.1007/978-1-4614-0106-3_15.
- Numminen HJ**, 2011. The incidence of traumatic brain injury in an adult population - how to classify mild cases? *European Journal of Neurology*, 18(3):460–464. doi:10.1111/j.1468-1331.2010.03179.x.
- Oberhammer FA, Hochegger K, Fröschl G, Tiefenbacher R, and Pavelka M**, 1994. Chromatin condensation during apoptosis is accompanied by degradation of lamin A+B, without enhanced activation of cdc2 kinase. *Journal of Cell Biology*, 126(4):827–37.
- Oehmichen M, Walter T, Meissner C, and Friedrich HJ**, 2003. Time Course of Cortical Hemorrhages after Closed Traumatic Brain Injury: Statistical Analysis of Posttraumatic Histomorphological Alterations. *Journal of Neurotrauma*, 20(1):87–103. doi:10.1089/08977150360517218.
- Ogryzko NV, Lewis A, Wilson HL, Meijer AH, Renshaw SA, and Elks PM**, 2018. Hif-1 α induced expression of Il-1 β protects against mycobacterial infection in zebrafish. *bioRxiv*. doi:10.1101/306506.
- Ohnmacht J, Yang YJ, Maurer GW, Barreiro-Iglesias A, Tsarouchas TM, Wehner D, Sieger D, Becker CG, and Becker T**, 2016. Spinal motor neurons are regenerated after mechanical lesion and genetic ablation in larval zebrafish. *Development*, 143:1464–1474. doi:10.1242/dev.129155.
- Ohsawa K, Irino Y, Nakamura Y, Akazawa C, Inoue K, and Kohsaka S**, 2007. Involvement of P2X4 and P2Y12 Receptors in ATP-Induced Microglial Chemotaxis. *Glia*, 55(14):1416–1425. doi:10.1002/glia.20489.
- Okami N, Narasimhan P, Yoshioka H, Sakata H, Kim GS, Jung JE, Maier CM, and Chan PH**, 2013. Prevention of JNK phosphorylation as a mechanism for rosiglitazone in neuroprotection after transient cerebral ischemia: activation of dual specificity phosphatase. *Journal of Cerebral Blood Flow and Metabolism*, 33(1):106–14. doi:10.1038/jcbfm.2012.138.
- Olney JW**, 1969. Brain lesions, obesity, and other disturbances in mice treated with monosodium glutamate. *Science*, 164(3880):719–21.

- Opanashuk LA, Mark RJ, Porter J, Damm D, Mattson MP, and Seroogy KB**, 1999. Heparin-Binding Epidermal Growth Factor-Like Growth Factor in Hippocampus: Modulation of Expression by Seizures and Anti-Excitotoxic Action. *Journal of Neuroscience*, 19(1):133–146. doi:10.1523/JNEUROSCI.19-01-00133.1999.
- Orihara Y, Ikematsu K, Tsuda R, and Nakasono I**, 2001. Induction of nitric oxide synthase by traumatic brain injury. *Forensic Science International*, 123(2-3):142–9.
- Osnato M and Giliberti V**, 1927. Postconcussion neurosis - traumatic encephalitis. *Archives of Neurology & Psychiatry*, 18(2):181. doi:10.1001/archneurpsyc.1927.02210020025002.
- Owens DF and Kriegstein AR**, 1998. Patterns of Intracellular Calcium Fluctuation in Precursor Cells of the Neocortical Ventricular Zone. *Journal of Neuroscience*, 18(14):5374–5388. doi:10.1523/JNEUROSCI.18-14-05374.1998.
- Owens R, Grabert K, Davies CL, Alfieri A, Antel JP, Healy LM, and McColl BW**, 2017. Divergent Neuroinflammatory Regulation of Microglial TREM Expression and Involvement of NF- κ B. *Frontiers in Cellular Neuroscience*, 11:56. doi:10.3389/fncel.2017.00056.
- Paolicelli RC, Bolasco G, Pagani F, Maggi L, Scianni M, Panzanelli P, Giustetto M, Ferreira TA, Guiducci E, Dumas L, Ragozzino D, and Gross CT**, 2011. Synaptic Pruning by Microglia Is Necessary for Normal Brain Development. *Science*, 333(6048):1456–1458. doi:10.1126/science.1202529.
- Papalexi E and Satija R**, 2018. Single-cell RNA sequencing to explore immune cell heterogeneity. *Nature Reviews Immunology*, 18(1):35–45. doi:10.1038/nri.2017.76.
- Pardo-Martin C, Chang TY, Koo BK, Gilleland CL, Wasserman SC, and Yanik MF**, 2010. High-throughput in vivo vertebrate screening. *Nature Methods*, 7(8):634–636. doi:10.1038/nmeth.1481.
- Park D, Tosello-Trampont AC, Elliott MR, Lu M, Haney LB, Ma Z, Klibanov AL, Mandell JW, and Ravichandran KS**, 2007a. BAI1 is an engulfment receptor for apoptotic cells upstream of the ELMO/Dock180/Rac module. *Nature*, 450(7168):430–434. doi:10.1038/nature06329.
- Park E, Bell JD, and Baker AJ**, 2008. Traumatic brain injury: Can the consequences be stopped? *Canadian Medical Association Journal*, 178(9):1163–1170. doi:10.1503/cmaj.080282.
- Park KW, Lee HG, Jin BK, and Lee YB**, 2007b. Interleukin-10 endogenously expressed in microglia prevents lipopolysaccharide-induced neurodegeneration in the rat cerebral cortex in vivo. *Experimental & Molecular Medicine*, 39(6):812–819. doi:10.1038/emm.2007.88.
- Patel RK, Prasad N, Kuwar R, Haldar D, and Abdul-Muneer P**, 2017. Transforming growth factor-beta 1 signaling regulates neuroinflammation and apoptosis in mild traumatic brain injury. *Brain, Behavior, and Immunity*, 64:244–258. doi:10.1016/j.bbi.2017.04.012.

- Pauls S, Geldmacher-Voss B, and Campos-Ortega JA**, 2001. A zebrafish histone variant H2A.F/Z and a transgenic H2A.F/Z:GFP fusion protein for in vivo studies of embryonic development. *Development Genes and Evolution*, 211(12):603–610.
- Pearson RA, Dale N, Laudet E, and Mobbs P**, 2005. ATP Released via Gap Junction Hemichannels from the Pigment Epithelium Regulates Neural Retinal Progenitor Proliferation. *Neuron*, 46(5):731–744. doi:10.1016/J.NEURON.2005.04.024.
- Peeters W, van den Brande R, Polinder S, Brazinova A, Steyerberg EW, Lingsma HF, and Maas AI**, 2015. Epidemiology of traumatic brain injury in Europe. *Acta Neurochirurgica*, 157(10):1683–1696. doi:10.1007/s00701-015-2512-7.
- Perez-Pinzon MA, Yenari MA, Sun GH, Kunis DM, and Steinberg GK**, 1997. SNX-111, a novel, presynaptic N-type calcium channel antagonist, is neuroprotective against focal cerebral ischemia in rabbits. *Journal of the Neurological Sciences*, 153(1):25–31.
- Peri F and Nüsslein-Volhard C**, 2008. Live Imaging of Neuronal Degradation by Microglia Reveals a Role for v0-ATPase a1 in Phagosomal Fusion In Vivo. *Cell*, 133(5):916–927.
- Perry VH, Brown MC, and Gordon S**, 1987. The macrophage response to central and peripheral nerve injury. A possible role for macrophages in regeneration. *Journal of Experimental Medicine*, 165(4):1218–23.
- Peter C, Wesselborg S, Herrmann M, and Lauber K**, 2010. Dangerous attraction: Phagocyte recruitment and danger signals of apoptotic and necrotic cells. *Apoptosis*, 15(9):1007–1028. doi: 10.1007/s10495-010-0472-1.
- Peters VA, Joesting JJ, and Freund GG**, 2013. IL-1 receptor 2 (IL-1R2) and its role in immune regulation. *Brain, Behavior, and Immunity*, 32:1–8. doi:10.1016/j.bbi.2012.11.006.
- Petrie TA, Strand NS, Yang CT, Rabinowitz JS, and Moon RT**, 2015. Macrophages modulate adult zebrafish tail fin regeneration. *Development*, 142(2):406–406. doi:10.1242/dev.120642.
- Pettus EH, Wright DW, Stein DG, and Hoffman SW**, 2005. Progesterone treatment inhibits the inflammatory agents that accompany traumatic brain injury. *Brain Research*, 1049(1):112–119. doi:10.1016/J.BRAINRES.2005.05.004.
- Pfaffl MW**, 2001. A new mathematical model for relative quantification in real-time RT-PCR. *Nucleic Acids Research*, 29(9):e45.
- Philips MF, Mattiasson G, Wieloch T, Björklund A, Johansson BB, Tomasevic G, Martínez-Serrano A, Lenzlinger PM, Sinson G, Grady MS, and McIntosh TK**, 2001. Neuroprotective and behavioral efficacy of nerve growth factor-transfected hippocampal progenitor cell transplants after experimental traumatic brain injury. *Journal of Neurosurgery*, 94(5):765–774. doi: 10.3171/jns.2001.94.5.0765.

- Pinteaux E, Rothwell NJ, and Boutin H**, 2006. Neuroprotective actions of endogenous interleukin-1 receptor antagonist (IL-1ra) are mediated by glia. *Glia*, 53(5):551–556. doi:10.1002/glia.20308.
- Pohl D, Bittigau P, Ishimaru MJ, Stadthaus D, Hubner C, Olney JW, Turski L, and Ikonomidou C**, 1999. N- Methyl-D-aspartate antagonists and apoptotic cell death triggered by head trauma in developing rat brain. *Proceedings of the National Academy of Sciences*, 96:2508–2513. doi: 10.1073/pnas.96.5.2508.
- Poleo G, Brown CW, Laforest L, and Akimenko MA**, 2001. Cell proliferation and movement during early fin regeneration in zebrafish. *Developmental Dynamics*, 221(4):380–390. doi: 10.1002/dvdy.1152.
- Pompucci A, De Bonis P, Pettorini B, Petrella G, Di Chirico A, and Anile C**, 2007. Decompressive Craniectomy for Traumatic Brain Injury: Patient Age and Outcome. *Journal of Neurotrauma*, 24(7):1182–1188. doi:10.1089/neu.2006.0244.
- Ponsford J, Cameron P, Fitzgerald M, Grant M, and Mikocka-Walus A**, 2011. Long-Term Outcomes after Uncomplicated Mild Traumatic Brain Injury: A Comparison with Trauma Controls. *Journal of Neurotrauma*, 28(6):937–946. doi:10.1089/neu.2010.1516.
- Pont-Lezica L, Beumer W, Colasse S, Drexhage H, Versnel M, and Bessis A**, 2014. Microglia shape corpus callosum axon tract fasciculation: functional impact of prenatal inflammation. *European Journal of Neuroscience*, 39(10):1551–1557. doi:10.1111/ejn.12508.
- Porter AG and Jänicke RU**, 1999. Emerging roles of caspase-3 in apoptosis. *Cell Death & Differentiation*, 6(2):99–104. doi:10.1038/sj.cdd.4400476.
- Pozner A, Xu B, Palumbos S, Gee JM, Tvrđik P, and Capecchi MR**, 2015. Intracellular calcium dynamics in cortical microglia responding to focal laser injury in the PC::G5-tdT reporter mouse. *Frontiers in Molecular Neuroscience*, 8:1–10. doi:10.3389/fnmol.2015.00012.
- Prewitt CM, Niesman IR, Kane CJ, and Houlé JD**, 1997. Activated Macrophage/Microglial Cells Can Promote the Regeneration of Sensory Axons into the Injured Spinal Cord. *Experimental Neurology*, 148(2):433–443. doi:10.1006/exnr.1997.6694.
- Prinz M, Priller J, Sisodia S, and Neuroscience RR**, 2011. Heterogeneity of CNS myeloid cells and their roles in neurodegeneration. *Nature Neuroscience*, 14:1227–1235. doi:10.1038/nn.2923.
- Pyo H, Jou I, Jung S, Hong S, and Joe EH**, 1998. Mitogen-activated protein kinases activated by lipopolysaccharide and beta-amyloid in cultured rat microglia. *Neuroreport*, 9(5):871–4.
- Qin L, Liu Y, Wang T, Wei SJ, Block ML, Wilson B, Liu B, and Hong JS**, 2004. NADPH Oxidase Mediates Lipopolysaccharide-induced Neurotoxicity and Proinflammatory Gene Expression in Activated Microglia. *Journal of Biological Chemistry*, 279(2):1415–1421. doi:10.1074/jbc.M307657200.

- Qiu J, Dando O, Baxter PS, Hasel P, Heron S, Simpson TI, and Hardingham GE**, 2018. Mixed-species RNA-seq for elucidation of non-cell-autonomous control of gene transcription. *Nature Protocols*, 13(10):2176–2199. doi:10.1038/s41596-018-0029-2.
- Rabinowitz AR and Levin HS**, 2014. Cognitive Sequelae of Traumatic Brain Injury. *Psychiatric Clinics of North America*, 37(1):1–11. doi:10.1016/j.psc.2013.11.004.
- Radi R, Rodriguez M, Castro L, and Telleri R**, 1994. Inhibition of Mitochondrial Electron Transport by Peroxynitrite. *Archives of Biochemistry and Biophysics*, 308(1):89–95. doi:10.1006/abbi.1994.1013.
- Ramlackhansingh AF, Brooks DJ, Greenwood RJ, Bose SK, Turkheimer FE, Kinnunen KM, Gentleman S, Heckemann RA, Gunanayagam K, Gelosa G, and Sharp DJ**, 2011. Inflammation after trauma: Microglial activation and traumatic brain injury. *Annals of Neurology*, 70:374–383. doi:10.1002/ana.22455.
- Randall RD and Thayer SA**, 1992. Glutamate-induced calcium transient triggers delayed calcium overload and neurotoxicity in rat hippocampal neurons. *Journal of Neuroscience*, 12(5):1882–95. doi:10.1523/JNEUROSCI.12-05-01882.1992.
- Ransohoff RM**, 2016a. A polarizing question: Do M1 and M2 microglia exist? *Nature Neuroscience*, 19(8):987–991. doi:10.1038/nn.4338.
- Ransohoff RM**, 2016b. How neuroinflammation contributes to neurodegeneration. *Science*, 353(6301):777–783. doi:10.1126/science.aag2590.
- Rao VL, Dogan A, Todd KG, Bowen KK, and Dempsey RJ**, 2001. Neuroprotection by memantine, a non-competitive NMDA receptor antagonist after traumatic brain injury in rats. *Brain Research*, 911(1):96–100.
- Ravichandran KS**, 2010. Find-me and eat-me signals in apoptotic cell clearance: progress and conundrums. *Journal of Experimental Medicine*, 207(9):1807–1817. doi:10.1084/jem.20101157.
- Ravichandran KS**, 2011. Beginnings of a Good Apoptotic Meal: The Find-Me and Eat-Me Signaling Pathways. *Immunity*, 35(4):445–455.
- Ravin R, Blank PS, Busse B, Ravin N, Vira S, Bezrukov L, Waters H, Guerrero-Cazares H, Quinones-Hinojosa A, Lee PR, Fields RD, Bezrukov SM, and Zimmerberg J**, 2016. Blast shockwaves propagate Ca²⁺ activity via purinergic astrocyte networks in human central nervous system cells. *Scientific Reports*, 6:25713. doi:10.1038/srep25713.
- Razzell W, Evans IR, Martin P, and Wood W**, 2013. Calcium flashes orchestrate the wound inflammatory response through duox activation and hydrogen peroxide release. *Current Biology*, 23(5):424–429.

- Reibman J, Meixler S, Lee TC, Gold LI, Cronstein BN, Haines KA, Kolasinski SL, and Weissmann G**, 1991. Transforming growth factor beta 1, a potent chemoattractant for human neutrophils, bypasses classic signal-transduction pathways. *Proceedings of the National Academy of Sciences of the United States of America*, 88(15):6805–9.
- Reilly P, Graham D, Hume Adams J, and Jennett B**, 1975. Patients with head injury who talk and die. *The Lancet*, 306(7931):375–377. doi:10.1016/S0140-6736(75)92893-7.
- Reimer MM, Sorensen I, Kuscha V, Frank RE, Liu C, Becker CG, and Becker T**, 2008. Motor Neuron Regeneration in Adult Zebrafish. *Journal of Neuroscience*, 28(34):8510–8516. doi:10.1523/JNEUROSCI.1189-08.2008.
- Relton JK and Rothwell NJ**, 1992. Interleukin-1 receptor antagonist inhibits ischaemic and excitotoxic neuronal damage in the rat. *Brain Research Bulletin*, 29(2):243–6.
- Renshaw SA, Loynes CA, Trushell DMI, Elworthy S, Inghard PW, and Whyte MK**, 2006. A transgenic zebrafish model of neutrophilic inflammation. *Blood*, 108:3976–3978.
- Resende RR, Adhikari A, da Costa JL, Lorençon E, Ladeira MS, Guatimosim S, Kihara AH, and Ladeira LO**, 2010a. Influence of spontaneous calcium events on cell-cycle progression in embryonal carcinoma and adult stem cells. *Biochimica et Biophysica Acta - Molecular Cell Research*, 1803(2):246–260. doi:10.1016/j.bbamcr.2009.11.008.
- Resende RR, da Costa JL, Kihara AH, Adhikari A, and Lorençon E**, 2010b. Intracellular Ca²⁺ Regulation During Neuronal Differentiation of Murine Embryonal Carcinoma and Mesenchymal Stem Cells. *Stem Cells and Development*, 19(3):379–394. doi:10.1089/scd.2008.0289.
- Rice AC, Khaldi A, Harvey HB, Salman NJ, White F, Fillmore H, and Bullock MR**, 2003. Proliferation and neuronal differentiation of mitotically active cells following traumatic brain injury. *Experimental Neurology*, 183(2):406–417.
- Richardson R, Slanchev K, Kraus C, Knyphausen P, Eming S, and Hammerschmidt M**, 2013. Adult Zebrafish as a Model System for Cutaneous Wound-Healing Research. *Journal of Investigative Dermatology*, 133(6):1655–1665. doi:10.1038/jid.2013.16.
- Rimel RW, Giordani B, Barth JT, and Jane JA**, 1982. Moderate head injury: completing the clinical spectrum of brain trauma. *Neurosurgery*, 11(3):344–51.
- Rink A, Fung KM, Trojanowski JQ, Lee VM, Neugebauer E, and McIntosh TK**, 1995. Evidence of apoptotic cell death after experimental traumatic brain injury in the rat. *The American Journal of Pathology*, 147(6):1575–83.
- Robinson MD, McCarthy DJ, and Smyth GK**, 2010. edgeR: a bioconductor package for differential expression analysis of digital gene expression data. *Bioinformatics*, 26:139–140. doi:10.1093/bioinformatics/btp616.

- Robinson MD and Oshlack A**, 2010. A scaling normalization method for differential expression analysis of RNA-seq data. *Genome Biology*, 11(R25). doi:10.1186/gb-2010-11-3-r25.
- Rodney T, Osier N, and Gill J**, 2018. Pro- and anti-inflammatory biomarkers and traumatic brain injury outcomes: A review. *Cytokine*, 110:248–256. doi:10.1016/j.cyto.2018.01.012.
- Rogove AD and Tsirka SE**, 1998. Neurotoxic responses by microglia elicited by excitotoxic injury in the mouse hippocampus. *Current Biology*, 8(1):19–25. doi:10.1016/S0960-9822(98)70016-8.
- Roof RL, Duvdevani R, Braswell L, and Stein DG**, 1994. Progesterone Facilitates Cognitive Recovery and Reduces Secondary Neuronal Loss Caused by Cortical Contusion Injury in Male Rats. *Experimental Neurology*, 129(1):64–69. doi:10.1006/exnr.1994.1147.
- Roof RL, Duvdevani R, Heyburn JW, and Stein DG**, 1996. Progesterone Rapidly Decreases Brain Edema: Treatment Delayed up to 24 Hours Is Still Effective. *Experimental Neurology*, 138(2):246–251. doi:10.1006/exnr.1996.0063.
- Roof RL, Duvdevani R, and Stein DG**, 1992. Progesterone treatment attenuates brain edema following contusion injury in male and female rats. *Restorative Neurology and Neuroscience*, 4(6):425–7. doi:10.3233/RNN-1992-4608.
- Roof RL, Duvdevani R, and Stein DG**, 1993. Gender influences outcome of brain injury: progesterone plays a protective role. *Brain Research*, 607(1-2):333–336. doi:10.1016/0006-8993(93)91526-X.
- Rozenbeek B, Maas AIR, and Menon DK**, 2013. Changing patterns in the epidemiology of traumatic brain injury. *Nature Reviews Neurology*, 9(4):231–236. doi:10.1038/nrneurol.2013.22.
- Rosso SM, Landweer EJ, Houterman M, Donker Kaat L, van Duijn CM, and van Swieten JC**, 2003. Medical and environmental risk factors for sporadic frontotemporal dementia: a retrospective case-control study. *Journal of Neurology, Neurosurgery, and Psychiatry*, 74(11):1574–6.
- Roth TL, Nayak D, Atanasijevic T, Koretsky AP, Latour LL, and McGavern DB**, 2014. Transcranial amelioration of inflammation and cell death after brain injury. *Nature*, 505(7482):223–8. doi:10.1038/nature12808.
- Rothman SM and Olney JW**, 1986. Glutamate and the pathophysiology of hypoxic-ischemic brain damage. *Annals of Neurology*, 19(2):105–111. doi:10.1002/ana.410190202.
- Rubin LL and Staddon JM**, 1999. The cell biology of the blood-brain barrier. *Annual Review of Neuroscience*, 22(1):11–28. doi:10.1146/annurev.neuro.22.1.11.
- Rutland-Brown W, Langlois JA, Thomas KE, and Xi YL**, 2003. *Journal of Head Trauma Rehabilitation*, (6):544–8.

- Saatman KE, Duhaime AC, Bullock R, Maas AI, Valadka A, and Manley GT**, 2008. Classification of Traumatic Brain Injury for Targeted Therapies. *Journal of Neurotrauma*, 25(7):719–738. doi:10.1089/neu.2008.0586.
- Sammak PJ, Hinman LE, Tran PO, Sjaastad MD, and Machen TE**, 1997. How do injured cells communicate with the surviving cell monolayer? *Journal of Cell Science*, 110(4):465–475.
- Sánchez-Iranzo H, Galardi-Castilla M, Sanz-Morejón A, González-Rosa JM, Costa R, Ernst A, Sainz de Aja J, Langa X, and Mercader N**, 2018. Transient fibrosis resolves via fibroblast inactivation in the regenerating zebrafish heart. *Proceedings of the National Academy of Sciences of the United States of America*, 115(16):4188–4193. doi:10.1073/pnas.1716713115.
- Sato M, Chang E, Igarashi T, and Noble LJ**, 2001. Neuronal injury and loss after traumatic brain injury: Time course and regional variability. *Brain Research*, 917(1):45–54. doi:10.1016/S0006-8993(01)02905-5.
- Sato T, Takahoko M, and Okamoto H**, 2006. HuC:Kaede, a useful tool to label neural morphologies in networks in vivo. *Genesis*, 44(3):136–142. doi:10.1002/gene.20196.
- Sattler R, Xiong Z, Lu WY, Hafner M, MacDonald JF, and Tymianski M**, 1999. Specific coupling of NMDA receptor activation to nitric oxide neurotoxicity by PSD-95 protein. *Science*, 284(5421):1845–1848. doi:10.1126/science.284.5421.1845.
- Scaffidi P, Misteli T, and Bianchi ME**, 2002. Release of chromatin protein HMGB1 by necrotic cells triggers inflammation. *Nature*, 418(6894):191–195. doi:10.1038/nature00858.
- Schafer D, Lehrman E, Kautzman A, Koyama R, Mardinly A, Yamasaki R, Ransohoff R, Greenberg M, Barres B, and Stevens B**, 2012. Microglia Sculpt Postnatal Neural Circuits in an Activity and Complement-Dependent Manner. *Neuron*, 74(4):691–705. doi:10.1016/j.neuron.2012.03.026.
- Scheller J, Chalaris A, Schmidt-Arras D, and Rose-John S**, 2011. The pro- and anti-inflammatory properties of the cytokine interleukin-6. *Biochimica et Biophysica Acta - Molecular Cell Research*, 1813(5):878–888. doi:10.1016/J.BBAMCR.2011.01.034.
- Schilling M, Besselmann M, Müller M, Strecker JK, Ringelstein EB, and Kiefer R**, 2005. Predominant phagocytic activity of resident microglia over hematogenous macrophages following transient focal cerebral ischemia: An investigation using green fluorescent protein transgenic bone marrow chimeric mice. *Experimental Neurology*, 196(2):290–297. doi:10.1016/j.expneurol.2005.08.004.
- Schinder AF, Olson EC, Spitzer NC, and Montal M**, 1996. Mitochondrial dysfunction is a primary event in glutamate neurotoxicity. *Journal of Neuroscience*, 16(19):6125–33. doi:10.1523/JNEUROSCI.16-19-06125.1996.

- Schulz JB, Matthews RT, Jenkins BG, Ferrante RJ, Siwek D, Henshaw DR, Cipolloni PB, Mecocci P, Kowall NW, and Rosen BR**, 1995. Blockade of neuronal nitric oxide synthase protects against excitotoxicity in vivo. *Journal of Neuroscience*, 15(12):8419–29. doi: 10.1523/JNEUROSCI.15-12-08419.1995.
- Schuman EM and Madison DV**, 1991. A requirement for the intercellular messenger nitric oxide in long-term potentiation. *Science*, 254(5037):1503–6.
- Scott EK and Baier H**, 2009. The cellular architecture of the larval zebrafish tectum, as revealed by gal4 enhancer trap lines. *Frontiers in Neural Circuits*, 3(13):1–14.
- Scott G, Zetterberg H, Jolly A, Cole JH, De Simoni S, Jenkins PO, Feeney C, Owen DR, Lingford-Hughes A, Howes O, Patel MC, Goldstone AP, Gunn RN, Blennow K, Matthews PM, and Sharp DJ**, 2018. Minocycline reduces chronic microglial activation after brain trauma but increases neurodegeneration. *Brain*, 141(2):459–471. doi:10.1093/brain/awx339.
- Segawa K and Nagata S**, 2015. An Apoptotic Eat Me' Signal: Phosphatidylserine Exposure. *Trends in Cell Biology*, 25(11):639–650. doi:10.1016/j.tcb.2015.08.003.
- Segawa M, Fukada Si, Yamamoto Y, Yahagi H, Kanematsu M, Sato M, Ito T, Uezumi A, Hayashi S, Miyagoe-Suzuki Y, Takeda S, Tsujikawa K, and Yamamoto H**, 2008. Suppression of macrophage functions impairs skeletal muscle regeneration with severe fibrosis. *Experimental Cell Research*, 314(17):3232–3244. doi:10.1016/J.YEXCR.2008.08.008.
- Seifman MA, Adamides AA, Nguyen PN, Vallance SA, Cooper DJ, Kossmann T, Rosenfeld JV, and Morganti-Kossmann MC**, 2008. Endogenous Melatonin Increases in Cerebrospinal Fluid of Patients after Severe Traumatic Brain Injury and Correlates with Oxidative Stress and Metabolic Disarray. *Journal of Cerebral Blood Flow & Metabolism*, 28(4):684–696. doi:10.1038/sj.jcbfm.9600603.
- Selassie AW, Zaloshnja E, Langlois JA, Miller T, Jones P, and Steiner C**, 2008. Incidence of long-term disability following traumatic brain injury hospitalization, United States, 2003. *Journal of Head Trauma Rehabilitation*, 23(2):123–31. doi:10.1097/01.HTR.0000314531.30401.39.
- Semple BD, Bye N, Rancan M, Ziebell JM, and Morganti-Kossmann MC**, 2010. Role of CCL2 (MCP-1) in Traumatic Brain Injury (TBI): Evidence from Severe TBI Patients and CCL2/ Mice. *Journal of Cerebral Blood Flow & Metabolism*, 30(4):769–782. doi:10.1038/jcbfm.2009.262.
- Semple BD, O'Brien TJ, Gimlin K, Wright DK, Kim SE, Casillas-Espinosa PM, Webster KM, Petrou S, and Noble-Haeusslein LJ**, 2017. Interleukin-1 Receptor in Seizure Susceptibility after Traumatic Injury to the Pediatric Brain. *Journal of Neuroscience*, 37(33):7864–7877. doi: 10.1523/JNEUROSCI.0982-17.2017.

- Shabir S and Southgate J**, 2008. Calcium signalling in wound-responsive normal human urothelial cell monolayers. *Cell Calcium*, 44(5):453–464.
- Shear DA, Galani R, Hoffman SW, and Stein DG**, 2002. Progesterone Protects against Necrotic Damage and Behavioural Abnormalities Caused by Traumatic Brain Injury. *Experimental Neurology*, 178(1):59–67. doi:10.1006/exnr.2002.8020.
- Shechter R and Schwartz M**, 2013. CNS sterile injury: Just another wound healing? *Trends in Molecular Medicine*, 19(3):135–143. doi:10.1016/j.molmed.2012.11.007.
- Sheets L**, 2017. Excessive activation of ionotropic glutamate receptors induces apoptotic hair-cell death independent of afferent and efferent innervation. *Scientific Reports*, 7(1):41102. doi:10.1038/srep41102.
- Shen Y, Sun A, Wang Y, Cha D, Wang H, Wang F, Feng L, Fang S, and Shen Y**, 2012. Upregulation of mesencephalic astrocyte-derived neurotrophic factor in glial cells is associated with ischemia-induced glial activation. *Journal of Neuroinflammation*, 9:254. doi:10.1186/1742-2094-9-254.
- Shiau CE, Kaufman Z, Meireles AM, and Talbot WS**, 2015. Differential Requirement for irf8 in Formation of Embryonic and Adult Macrophages in Zebrafish. *PLoS ONE*, 10(1):e0117513.
- Shibuki K and Okada D**, 1991. Endogenous nitric oxide release required for long-term synaptic depression in the cerebellum. *Nature*, 349(6307):326–328. doi:10.1038/349326a0.
- Shimamura M, Nakagami H, Osako MK, Kurinami H, Koriyama H, Zhengda P, Tomioka H, Tenma A, Wakayama K, and Morishita R**, 2014. OPG/RANKL/RANK axis is a critical inflammatory signaling system in ischemic brain in mice. *Proceedings of the National Academy of Sciences*, 111(22):8191–8196. doi:10.1073/pnas.1400544111.
- Shimizu Y, Ueda Y, and Ohshima T**, 2018. Wnt signaling regulates proliferation and differentiation of radial glia in regenerative processes after stab injury in the optic tectum of adult zebrafish. *Glia*, 66(7):1382–1394. doi:10.1002/glia.23311.
- Shohami E, Novikov M, Bass R, Yamin A, and Gallily R**, 1994. Closed Head Injury Triggers Early Production of TNF α and IL-6 by Brain Tissue. *Journal of Cerebral Blood Flow & Metabolism*, 14(4):615–619. doi:10.1038/jcbfm.1994.76.
- Sieger D, Moritz C, Ziegenhals T, Prykhodzij S, and Peri F**, 2012. Long-Range Ca²⁺ Waves Transmit Brain-Damage Signals to Microglia. *Developmental Cell*, 22(6):1138–1148.
- Sierra A, Abiega O, Shahraz A, and Neumann H**, 2013. Janus-faced microglia: beneficial and detrimental consequences of microglial phagocytosis. *Frontiers in Cellular Neuroscience*, 7:6. doi:10.3389/fncel.2013.00006.

- Sierra A, Encinas JM, Deudero JJ, Chancey JH, Enikolopov G, Overstreet-Wadiche LS, Tsirka SE, and Maletic-Savatic M**, 2010. Microglia Shape Adult Hippocampal Neurogenesis through Apoptosis-Coupled Phagocytosis. *Cell Stem Cell*, 7(4):483–495. doi:10.1016/j.stem.2010.08.014.
- Silver J and Miller JH**, 2004. Regeneration beyond the glial scar. *Nature Reviews Neuroscience*, 5(2):146–156. doi:10.1038/nrn1326.
- Silver JM, Kramer R, Greenwald S, and Weissman M**, 2001. The association between head injuries and psychiatric disorders: findings from the New Haven NIMH Epidemiologic Catchment Area Study. *Brain Injury*, 15(11):935–945. doi:10.1080/02699050110065295.
- Simkin J, Gawriluk TR, Gensel JC, and Seifert AW**, 2017. Macrophages are necessary for epimorphic regeneration in African spiny mice. *eLife*, 6. doi:10.7554/eLife.24623.
- Simon RP, Swan JH, Griffiths T, and Meldrum BS**, 1984. Blockade of N-methyl-D-aspartate receptors may protect against ischemic damage in the brain. *Science*, 226(4676):850–2.
- Sinz EH, Kochanek PM, Dixon CE, Clark RS, Carcillo JA, Schiding JK, Chen M, Wisniewski SR, Carlos TM, Williams D, DeKosky ST, Watkins SC, Marion DW, and Billiar TR**, 1999. Inducible nitric oxide synthase is an endogenous neuroprotectant after traumatic brain injury in rats and mice. *Journal of Clinical Investigation*, 104(5):647–656. doi:10.1172/JCI6670.
- Skaggs K, Goldman D, and Parent JM**, 2014. Excitotoxic brain injury in adult zebrafish stimulates neurogenesis and long-distance neuronal integration. *Glia*, 62(12):2061–2079. doi:10.1002/glia.22726.
- Skolnick BE, Maas AI, Narayan RK, van der Hoop RG, MacAllister T, Ward JD, Nelson NR, and Stocchetti N**, 2014. A Clinical Trial of Progesterone for Severe Traumatic Brain Injury. *New England Journal of Medicine*, 371(26):2467–2476. doi:10.1056/NEJMoa1411090.
- Smith FM, Raghupathi R, MacKinnon MA, McIntosh TK, Saatman KE, Meaney DF, and Graham DI**, 2000. TUNEL-positive staining of surface contusions after fatal head injury in man. *Acta Neuropathologica*, 100(5):537–545. doi:10.1007/s004010000222.
- Smith SL, Andrus PK, Zhang JR, and Hall ED**, 1994. Direct Measurement of Hydroxyl Radicals, Lipid Peroxidation, and BloodBrain Barrier Disruption Following Unilateral Cortical Impact Head Injury in the Rat. *Journal of Neurotrauma*, 11(4):393–404. doi:10.1089/neu.1994.11.393.
- Soares HD, Hicks RR, Smith D, and McIntosh TK**, 1995. Inflammatory leukocytic recruitment and diffuse neuronal degeneration are separate pathological processes resulting from traumatic brain injury. *Journal of Neuroscience*, 15(12):8223–33. doi:10.1523/JNEUROSCI.15-12-08223.1995.
- Somasundaram A, Shum AK, McBride HJ, Kessler JA, Feske S, Miller RJ, and Prakriya M**, 2014. Store-Operated CRAC Channels Regulate Gene Expression and Proliferation in Neural Progenitor Cells. *Journal of Neuroscience*, 34(27):9107–9123. doi:10.1523/JNEUROSCI.0263-14.2014.

- Spera PA, Ellison JA, Feuerstein GZ, and Barone FC**, 1998. IL-10 reduces rat brain injury following focal stroke. *Neuroscience Letters*, 251(3):189–92.
- Springer AD and Wilson BR**, 1989. Light microscopic study of degenerating cobalt-filled optic axons in goldfish: Role of microglia and radial glia in debris removal. *Journal of Comparative Neurology*, 282(1):119–132. doi:10.1002/cne.902820109.
- Squarzoni P, Oller G, Hoeffel G, Pont-Lezica L, Rostaing P, Low D, Bessis A, Ginhoux F, and Garel S**, 2014. Microglia Modulate Wiring of the Embryonic Forebrain. *Cell Reports*, 8(5):1271–1279. doi:10.1016/j.celrep.2014.07.042.
- Srinivas M and Spray DC**, 2003. Closure of Gap Junction Channels by Arylamino benzoates. *Molecular Pharmacology*, 63(6):1389–1397. doi:10.1124/mol.63.6.1389.
- Stahel PF, Shohami E, Younis FM, Kariya K, Otto VI, Lenzlinger PM, Grosjean MB, Eugster HP, Trentz O, Kossmann T, and Morganti-Kossmann MC**, 2000. Experimental Closed Head Injury: Analysis of Neurological Outcome, Blood-Brain Barrier Dysfunction, Intracranial Neutrophil Infiltration, and Neuronal Cell Death in Mice Deficient in Genes for Pro-Inflammatory Cytokines. *Journal of Cerebral Blood Flow & Metabolism*, 20(2):369–380. doi:10.1097/00004647-200002000-00019.
- Stanisstreet M**, 1982. Calcium and wound healing in *Xenopus* early embryos. *Journal of Embryology and Experimental Morphology*, 67:195–205.
- Steinberg TH, Newman AS, Swanson JA, and Silverstein SC**, 1987. ATP₄- permeabilizes the plasma membrane of mouse macrophages to fluorescent dyes. *Journal of Biological Chemistry*, 262(18):8884–8888. doi:10.1007/s11128-018-1873-2.
- Stevens B, Allen NJ, Vazquez LE, Howell GR, Christopherson KS, Nouri N, Micheva KD, Mehalow AK, Huberman AD, Stafford B, Sher A, Litke A, Lambris JD, Smith SJ, John SW, and Barres BA**, 2007. The Classical Complement Cascade Mediates CNS Synapse Elimination. *Cell*, 131(6):1164–1178. doi:10.1016/j.cell.2007.10.036.
- Stoica BA and Faden AI**, 2010. Cell Death Mechanisms and Modulation in Traumatic Brain Injury. *Neurotherapeutics*, 7(1):3–12. doi:10.1016/j.nurt.2009.10.023.
- Stout CE, Costantin JL, Naus CCG, and Charles AC**, 2002. Intercellular Calcium Signaling in Astrocytes via ATP Release through Connexin Hemichannels. *Journal of Biological Chemistry*, 277(12):10482–10488. doi:10.1074/jbc.M109902200.
- Stover JF, Belli A, Boret H, Bulters D, Sahuquillo J, Schmutzhard E, Zavala E, Ungerstedt U, Schinzel R, Tegtmeier F, and NOSTRA Investigators**, 2014. Nitric Oxide Synthase Inhibition with the Antipterin VAS203 Improves Outcome in Moderate and Severe Traumatic Brain Injury: A

- Placebo-Controlled Randomized Phase IIa Trial (NOSTRA). *Journal of Neurotrauma*, 31(19):1599–1606. doi:10.1089/neu.2014.3344.
- Streisinger G, Walker C, Dower N, Knauber D, and Singer F**, 1981. Production of clones of homozygous diploid zebra fish (*Brachydanio rerio*). *Nature*, 291(5813):293–296. doi: 10.1038/291293a0.
- Stroncek JD and Reichert WM**, 2008. *Overview of Wound Healing in Different Tissue Types*. CRC Press/Taylor & Francis.
- Sugama S, Takenouchi T, Kitani H, Fujita M, and Hashimoto M**, 2007. Activin as an anti-inflammatory cytokine produced by microglia. *Journal of Neuroimmunology*, 192(1-2):31–39. doi: 10.1016/j.jneuroim.2007.08.016.
- Sullivan PG, Thompson MB, and Scheff SW**, 1999. Cyclosporin A Attenuates Acute Mitochondrial Dysfunction Following Traumatic Brain Injury. *Experimental Neurology*, 160(1):226–234. doi: 10.1006/exnr.1999.7197.
- Sun D, Colello RJ, Daugherty WP, Kwon TH, McGinn MJ, Harvey HB, and Bullock MR**, 2005. Cell proliferation and neuronal differentiation in the dentate gyrus in juvenile and adult rats following traumatic brain injury. *Journal of Neurotrauma*, 22(1):95–105.
- Sun D, McGinn MJ, Zhou Z, Harvey HB, Bullock MR, and Colello RJ**, 2007. Anatomical integration of newly generated dentate granule neurons following traumatic brain injury in adult rats and its association to cognitive recovery. *Experimental Neurology*, 204(1):264–272.
- Sun H, Jiang M, Fu X, Cai Q, Zhang J, Yin Y, Guo J, Yu L, Jiang Y, Liu Y, Feng L, Nie Z, Fang J, and Jin L**, 2017a. Mesencephalic astrocyte-derived neurotrophic factor reduces cell apoptosis via upregulating HSP70 in SHSY-5Y cells. *Translational Neurodegeneration*, 6(1):12. doi:10.1186/s40035-017-0082-8.
- Sun M, Brady RD, Wright DK, Kim HA, Zhang SR, Sobey CG, Johnstone MR, O'Brien TJ, Semple BD, McDonald SJ, and Shultz SR**, 2017b. Treatment with an interleukin-1 receptor antagonist mitigates neuroinflammation and brain damage after polytrauma. *Brain, Behavior, and Immunity*, 66:359–371. doi:10.1016/j.bbi.2017.08.005.
- Suplat D, Krzemiński P, Pomorski P, and Barańska J**, 2007. P2Y1 and P2Y12 receptor cross-talk in calcium signalling: Evidence from nonstarved and long-term serum-deprived glioma C6 cells. *Purinergic Signalling*, 3(3):221–230. doi:10.1007/s11302-007-9051-5.
- Susin SA, Lorenzo HK, Zamzami N, Marzo I, Snow BE, Brothers GM, Mangion J, Jacotot E, Costantini P, Loeffler M, Larochette N, Goodlett DR, Aebersold R, Siderovski DP, Penninger JM, and Kroemer G**, 1999. Molecular characterization of mitochondrial apoptosis-inducing factor. *Nature*, 397(6718):441–446. doi:10.1038/17135.

- Sutton RL, Lescaudron L, and Stein DG**, 1993. Unilateral cortical contusion injury in the rat: vascular disruption and temporal development of cortical necrosis. *Journal of Neurotrauma*, 10(2):135–149. doi:10.1089/neu.1993.10.135.
- Suzuki S, Yamashita T, Tanaka K, Hattori H, Sawamoto K, Okano H, and Suzuki N**, 2005. Activation of cytokine signaling through leukemia inhibitory factor receptor (LIFR)/gp130 attenuates ischemic brain injury in rats. *Journal of Cerebral Blood Flow and Metabolism*, 25(6):685–693. doi:10.1038/sj.jcbfm.9600061.
- Szalay G, Martinecz B, Lénárt N, Környei Z, Orsolits B, Judák L, Császár E, Fekete R, West BL, Katona G, Rózsa B, and Dénes Á**, 2016. Microglia protect against brain injury and their selective elimination dysregulates neuronal network activity after stroke. *Nature Communications*, 7:11499. doi:10.1038/ncomms11499.
- Tagliaferri F, Compagnone C, Korsic M, Servadei F, and Kraus J**, 2006. A systematic review of brain injury epidemiology in Europe. *Acta Neurochirurgica*, 148(3):255–268. doi:10.1007/s00701-005-0651-y.
- Takada H, Furuya K, and Sokabe M**, 2014. Mechanosensitive ATP release from hemichannels and Ca²⁺ influx through TRPC6 accelerate wound closure in keratinocytes. *Journal of Cell Science*, 127(19):4159–4171. doi:10.1242/jcs.147314.
- Talley AK, Dewhurst S, Perry SW, Dollard SC, Gummuluru S, Fine SM, New D, Epstein LG, Gendelman HE, and Gelbard HA**, 1995. Tumor necrosis factor alpha-induced apoptosis in human neuronal cells: protection by the antioxidant N-acetylcysteine and the genes bcl-2 and crmA. *Molecular and Cellular Biology*, 15(5):2359–66. doi:10.1128/MCB.15.5.2359.
- Talman V and Ruskoaho H**, 2016. Cardiac fibrosis in myocardial infarction from repair and remodeling to regeneration. *Cell and Tissue Research*, 365(3):563–581. doi:10.1007/s00441-016-2431-9.
- Tang Z, Gan Y, Liu Q, Yin JX, Liu Q, Shi J, and Shi FD**, 2014. CX3CR1 deficiency suppresses activation and neurotoxicity of microglia/macrophage in experimental ischemic stroke. *Journal of Neuroinflammation*, 11(1):26. doi:10.1186/1742-2094-11-26.
- Taşç A, Okay Ö, Gezici AR, Ergün R, and Ergüngör F**, 2003. Prognostic value of interleukin-1 beta levels after acute brain injury. *Neurological Research*, 25(8):871–874. doi:10.1179/016164103771953998.
- Tashiro A, Sandler VM, Toni N, Zhao C, and Gage FH**, 2006. NMDA-receptor-mediated, cell-specific integration of new neurons in adult dentate gyrus. *Nature*, 442(7105):929–933. doi:10.1038/nature05028.

- Tauzin S, Starnes TW, Becker FB, ying Lam P, and Huttenlocher A**, 2014. Redox and Src family kinase signaling control leukocyte wound attraction and neutrophil reverse migration. *Journal of Cell Biology*, 207(5):589–598. doi:10.1083/jcb.201408090.
- Taylor A, Butt W, Rosenfeld J, Shann F, Ditchfield M, Lewis E, Klug G, Wallace D, Henning R, and Tibballs J**, 2001. A randomized trial of very early decompressive craniectomy in children with traumatic brain injury and sustained intracranial hypertension. *Child's Nervous System*, 17(3):154–162. doi:10.1007/s003810000410.
- Taylor RA, Chang CF, Goods BA, Hammond MD, Mac Grory B, Ai Y, Steinschneider AF, Renfroe SC, Askenase MH, McCullough LD, Kasner SE, Mullen MT, Hafler DA, Love JC, and Sansing LH**, 2017. TGF- β 1 modulates microglial phenotype and promotes recovery after intracerebral hemorrhage. *Journal of Clinical Investigation*, 127(1):280–292. doi:10.1172/JCI88647.
- Teasdale G and Jennett B**, 1974. Assessment of comae and impaired consciousness. A Practical Scale. *The Lancet*, 304(7872):81–84. doi:10.1016/S0140-6736(74)91639-0.
- Temkin NR, Anderson GD, Winn HR, Ellenbogen RG, Britz GW, Schuster J, Lucas T, Newell DW, Mansfield PN, Machamer JE, Barber J, and Dikmen SS**, 2007. Magnesium sulfate for neuroprotection after traumatic brain injury: a randomised controlled trial. *The Lancet Neurology*, 6(1):29–38. doi:10.1016/S1474-4422(06)70630-5.
- Thurman DJ**, 2016. The epidemiology of traumatic brain injury in children and youths: A review of research since 1990. *Journal of Child Neurology*, 31(1):20–27. doi:10.1177/0883073814544363.
- Tikka TM and Koistinaho JE**, 2001. Minocycline Provides Neuroprotection Against N-Methyl-D-aspartate Neurotoxicity by Inhibiting Microglia. *Journal of Immunology*, 166(12):7527–7533. doi:10.4049/jimmunol.166.12.7527.
- Toné S, Sugimoto K, Tanda K, Suda T, Uehira K, Kanouchi H, Samejima K, Minatogawa Y, and Earnshaw WC**, 2007. Three distinct stages of apoptotic nuclear condensation revealed by time-lapse imaging, biochemical and electron microscopy analysis of cell-free apoptosis. *Experimental Cell Research*, 313(16):3635–3644. doi:10.1016/j.yexcr.2007.06.018.
- Toulmond S and Rothwell NJ**, 1995. Interleukin-1 receptor antagonist inhibits neuronal damage caused by fluid percussion injury in the rat. *Brain Research*, 671(2):261–6.
- Tovell VE and Sanderson J**, 2008. Distinct P2Y Receptor Subtypes Regulate Calcium Signaling in Human Retinal Pigment Epithelial Cells. *Investigative Ophthalmology & Visual Science*, 49(1):350. doi:10.1167/jovs.07-1040.
- Tramontana MG, Cowan RL, Zald D, Prokop JW, and Guillamondegui O**, 2014. Traumatic brain injury-related attention deficits: Treatment outcomes with lisdexamfetamine dimesylate (Vyvanse). *Brain Injury*, 28(11):1461–1472. doi:10.3109/02699052.2014.930179.

- Tsarouchas TM, Wehner D, Cavone L, Munir T, Keatinge M, Lambertus M, Underhill A, Barrett T, Kassapis E, Ogryzko N, Feng Y, van Ham TJ, Becker T, and Becker CG**, 2018. Dynamic control of proinflammatory cytokines $IL-1\beta$ and $Tnf-\alpha$ by macrophages in zebrafish spinal cord regeneration. *Nature Communications*, 9(1):4670. doi:10.1038/s41467-018-07036-w.
- Tseng KY, Anttila JE, Khodosevich K, Tuominen RK, Lindahl M, Domanskyi A, and Airavaara M**, 2018. MANF Promotes Differentiation and Migration of Neural Progenitor Cells with Potential Neural Regenerative Effects in Stroke. *Molecular Therapy*, 26(1):238–255. doi:10.1016/j.ymthe.2017.09.019.
- Turrin NP**, 2006. Tumor Necrosis Factor But Not Interleukin 1 Mediates Neuroprotection in Response to Acute Nitric Oxide Excitotoxicity. *Journal of Neuroscience*, 26(1):143–151. doi:10.1523/JNEUROSCI.4032-05.2006.
- Ueki Y, Wang J, Chollangi S, and Ash JD**, 2008. STAT3 activation in photoreceptors by leukemia inhibitory factor is associated with protection from light damage. *Journal of Neurochemistry*, 105(3):784–796. doi:10.1111/j.1471-4159.2007.05180.x.
- Ueno M, Fujita Y, Tanaka T, Nakamura Y, Kikuta J, Ishii M, and Yamashita T**, 2013. Layer V cortical neurons require microglial support for survival during postnatal development. *Nature Neuroscience*, 16(5):543–551. doi:10.1038/nn.3358.
- Unterberg A, Stover J, Kress B, and Kiening K**, 2004. Edema and brain trauma. *Neuroscience*, 129(4):1019–1027. doi:10.1016/j.neuroscience.2004.06.046.
- Urrea C, Castellanos DA, Sagen J, Tsoulfas P, Bramlett HM, and Dietrich WD**, 2007. Widespread cellular proliferation and focal neurogenesis after traumatic brain injury in the rat. *Restorative Neurology and Neuroscience*, 25:65–76.
- van Amerongen MJ, Harmsen MC, van Rooijen N, Petersen AH, and van Luyn MJ**, 2007. Macrophage Depletion Impairs Wound Healing and Increases Left Ventricular Remodeling after Myocardial Injury in Mice. *The American Journal of Pathology*, 170(3):818–829. doi:10.2353/ajpath.2007.060547.
- Vargas ME, Yamagishi Y, Tessier-Lavigne M, and Sagasti A**, 2015. Live Imaging of Calcium Dynamics during Axon Degeneration Reveals Two Functionally Distinct Phases of Calcium Influx. *Journal of Neuroscience*, 35(45):15026–38. doi:10.1523/JNEUROSCI.2484-15.2015.
- Vergouwen MD, Vermeulen M, and Roos YB**, 2006. Effect of nimodipine on outcome in patients with traumatic subarachnoid haemorrhage: a systematic review. *The Lancet Neurology*, 5(12):1029–1032. doi:10.1016/S1474-4422(06)70582-8.

- Veroni C, Gabriele L, Canini I, Castiello L, Coccia E, Remoli ME, Columba-Cabezas S, Aricò E, Aloisi F, and Agresti C**, 2010. Activation of TNF receptor 2 in microglia promotes induction of anti-inflammatory pathways. *Molecular and Cellular Neuroscience*, 45(3):234–244. doi:10.1016/j.mcn.2010.06.014.
- Vincent AM and Maiese K**, 1999. Nitric Oxide Induction of Neuronal Endonuclease Activity in Programmed Cell Death. *Experimental Cell Research*, 246(2):290–300. doi:10.1006/EXCR.1998.4282.
- Virginio C, MacKenzie A, Rassendren FA, North RA, and Surprenant A**, 1999. Pore dilation of neuronal P2X receptor channels. *Nature Neuroscience*, 2(4):315–321. doi:10.1038/7225.
- Voigt T**, 1989. Development of glial cells in the cerebral wall of ferrets: Direct tracing of their transformation from radial glia into astrocytes. *Journal of Comparative Neurology*, 289(1):74–88. doi:10.1002/cne.902890106.
- Voll RE, Herrmann M, Roth EA, Stach C, Kalden JR, and Girkontaite I**, 1997. Immunosuppressive effects of apoptotic cells. *Nature*, 390:350–351. doi:10.1038/37022.
- Voutilainen MH, Back S, Porsti E, Toppinen L, Lindgren L, Lindholm P, Peranen J, Saarma M, and Tuominen RK**, 2009. Mesencephalic Astrocyte-Derived Neurotrophic Factor Is Neurorestorative in Rat Model of Parkinson's Disease. *Journal of Neuroscience*, 29(30):9651–9659. doi:10.1523/JNEUROSCI.0833-09.2009.
- Wada K, Chatzipanteli K, Kraydieh S, Busto R, and Dietrich WD**, 1998. Inducible Nitric Oxide Synthase Expression after Traumatic Brain Injury and Neuroprotection with Aminoguanidine Treatment in Rats. *Neurosurgery*, 43(6):1427–1436. doi:10.1097/00006123-199812000-00096.
- Walton EM, Cronan MR, Beerman RW, and Tobin DM**, 2015. The macrophage-specific promoter mfp4 allows live, long-term analysis of macrophage behavior during mycobacterial infection in zebrafish. *PLoS ONE*, 10(10):e0138949. doi:10.1371/journal.pone.0138949.
- Wang N, Liang H, and Zen K**, 2014. Molecular Mechanisms That Influence the Macrophage M1âM2 Polarization Balance. *Frontiers in Immunology*, 5:614. doi:10.3389/fimmu.2014.00614.
- Weckbach S, Neher M, Losacco JT, Bolden AL, Kulik L, Flierl MA, Bell SE, Holers VM, and Stahel PF**, 2012. Challenging the Role of Adaptive Immunity in Neurotrauma: Rag1 / Mice Lacking Mature B and T Cells Do Not Show Neuroprotection after Closed Head Injury. *Journal of Neurotrauma*, 29(6):1233–1242. doi:10.1089/neu.2011.2169.
- Wehner D, Tsarouchas TM, Michael A, Haase C, Weidinger G, Reimer MM, Becker T, and Becker CG**, 2017. Wnt signaling controls pro-regenerative Collagen XII in functional spinal cord regeneration in zebrafish. *Nature Communications*, 8(1):126. doi:10.1038/s41467-017-00143-0.

- Wei J and Besner GE**, 2015. M1 to M2 macrophage polarization in heparin-binding epidermal growth factor-like growth factor therapy for necrotizing enterocolitis. *Journal of Surgical Research*, 197(1):126–138. doi:10.1016/j.jss.2015.03.023.
- Weiner MW, Crane PK, Montine TJ, Bennett DA, and Veitch DP**, 2017. Traumatic brain injury may not increase the risk of Alzheimer disease. *Neurology*, 89(18):1923–1925. doi:10.1212/WNL.0000000000004608.
- Weissman TA, Riquelme PA, Ivic L, Flint AC, and Kriegstein AR**, 2004. Calcium waves propagate through radial glial cells and modulate proliferation in the developing neocortex. *Neuron*, 43(5):647–61.
- Werner C and Engelhard K**, 2007. Pathophysiology of traumatic brain injury. *British Journal of Anaesthesia*, 99(1):4–9.
- Westerfield M**, 2007. *The Zebrafish Book: A Guide for the Laboratory Use of Zebrafish (Danio rerio)*. University of Oregon Press, Eugene, Oregon.
- Wie MB, Koh JY, Won MH, Lee JC, Shin TK, Moon CJ, Ha HJ, Park SM, and Kim HC**, 2001. BAPTA/AM, an intracellular calcium chelator, induces delayed necrosis by lipoygenase-mediated free radicals in mouse cortical cultures. *Progress in Neuro-Psychopharmacology and Biological Psychiatry*, 25(8):1641–1659. doi:10.1016/S0278-5846(01)00202-0.
- Wilde MC, Castriotta RJ, Lai JM, Atanasov S, Masel BE, and Kuna ST**, 2007. Cognitive Impairment in Patients With Traumatic Brain Injury and Obstructive Sleep Apnea. *Archives of Physical Medicine and Rehabilitation*, 88(10):1284–1288. doi:10.1016/j.apmr.2007.07.012.
- Willenborg S, Lucas T, van Loo G, Knipper JA, Krieg T, Haase I, Brachvogel B, Hamerschmidt M, Nagy A, Ferrara N, Pasparakis M, and Eming SA**, 2012. CCR2 recruits an inflammatory macrophage subpopulation critical for angiogenesis in tissue repair. *Blood*, 120(3):613–25. doi:10.1182/blood-2012-01-403386.
- Williams RF, Magnotti LJ, Croce MA, Hargraves BB, Fischer PE, Schroepfel TJ, Zarzaur BL, Muhlbauer M, Timmons SD, and Fabian TC**, 2009. Impact of Decompressive Craniectomy on Functional Outcome After Severe Traumatic Brain Injury. *Journal of Trauma*, 66(6):1570–1576. doi:10.1097/TA.0b013e3181a594c4.
- Williams RW**, 2000. Mapping Genes that Modulate Mouse Brain Development: A Quantitative Genetic Approach. In AF Goffinet and P Rakic, editors, *Mouse Brain Development*, pages 21–49. Springer Berlin Heidelberg.
- Williams S, Raghupathi R, MacKinnon MA, McIntosh TK, Saatman KE, and Graham DI**, 2001. In situ DNA fragmentation occurs in white matter up to 12 months after head injury in man. *Acta Neuropathologica*, 102(6):581–590. doi:10.1007/s004010100410.

- Wilms H, Rosenstiel P, Sievers J, Deuschl G, Zecca L, and Lucius R**, 2003. Activation of microglia by human neuromelanin is NF-kappaB dependent and involves p38 mitogen-activated protein kinase: implications for Parkinson's disease. *FASEB Journal*, 17(3):500–502. doi:10.1096/fj.02-0314fje.
- Winter CD, Pringle AK, Clough GF, and Church MK**, 2004. Raised parenchymal interleukin-6 levels correlate with improved outcome after traumatic brain injury. *Brain*, 127(2):315–320. doi:10.1093/brain/awh039.
- Wirenfeldt M, Babcock AA, Ladeby R, Lambertsen KL, Dagnaes-Hansen F, Leslie RGQ, Owens T, and Finsen B**, 2005. Reactive microgliosis engages distinct responses by microglial subpopulations after minor central nervous system injury. *Journal of Neuroscience Research*, 82(4):507–514. doi:10.1002/jnr.20659.
- Witting A, Müller P, Herrmann A, Kettenmann H, and Nolte C**, 2000. Phagocytic clearance of apoptotic neurons by microglia/brain macrophages in vitro: Involvement of lectin-, integrin-, and phosphatidylserine-mediated recognition. *Journal of Neurochemistry*, 75(3):1060–1070. doi:10.1046/j.1471-4159.2000.0751060.x.
- Wolf SA, Boddeke H, and Kettenmann H**, 2017. Microglia in Physiology and Disease. *Annual Review of Physiology*, 79(1):619–643. doi:10.1146/annurev-physiol-022516-034406.
- Wong R, Lénárt N, Hill L, Toms L, Coutts G, Martinecz B, Császár E, Nyiri G, Papaemmanouil A, Waisman A, Müller W, Schwaninger M, Rothwell N, Francis S, Pinteaux E, Denés A, and Allan SM**, 2018. Interleukin-1 mediates ischaemic brain injury via distinct actions on endothelial cells and cholinergic neurons. *Brain, Behavior, and Immunity*. doi:10.1016/j.bbi.2018.11.012.
- Wright DW, Kellermann AL, Hertzberg VS, Clark PL, Frankel M, Goldstein FC, Salomone JP, Dent LL, Harris OA, Ander DS, Lowery DW, Patel MM, Denson DD, Gordon AB, Wald MM, Gupta S, Hoffman SW, and Stein DG**, 2007. ProTECT: A Randomized Clinical Trial of Progesterone for Acute Traumatic Brain Injury. *Annals of Emergency Medicine*, 49(4):391–402. doi:j.annemergmed.2006.07.932.
- Wright DW, Yeatts SD, Silbergleit R, Palesch YY, Hertzberg VS, Frankel M, Goldstein FC, Caveney AF, Howlett-Smith H, Bengelink EM, Manley GT, Merck LH, Janis LS, Barsan WG, and NETT Investigators**, 2014. Very Early Administration of Progesterone for Acute Traumatic Brain Injury. *New England Journal of Medicine*, 371(26):2457–2466. doi:10.1056/NEJMoa1404304.
- Wu DD, Lai M, Hughes PE, Sirimanne E, Gluckman PD, and Williams CE**, 1999. Expression of the activin axis and neuronal rescue effects of recombinant activin A following hypoxic-ischemic brain injury in the infant rat. *Brain Research*, 835(2):369–378. doi:10.1016/S0006-8993(99)01638-8.

- Wu H, Lu D, Jiang H, Xiong Y, Qu C, Li B, Mahmood A, Zhou D, and Chopp M**, 2008. Simvastatin-Mediated Upregulation of VEGF and BDNF, Activation of the PI3K/Akt Pathway, and Increase of Neurogenesis Are Associated with Therapeutic Improvement after Traumatic Brain Injury. *Journal of Neurotrauma*, 25(2):130–139. doi:10.1089/neu.2007.0369.
- Wullimann MF and Knipp S**, 2000. Proliferation pattern changes in the zebrafish brain from embryonic through early postembryonic stages. *Anatomy and Embryology*, 202(5):385–400. doi:10.1007/s004290000115.
- Wyllie AH**, 1997. Apoptosis: an overview. *British Medical Bulletin*, 53(3):451–65.
- Wynn TA, Vannella KM, and Diseases I**, 2016. Macrophages in tissue repair, regeneration, and fibrosis. *Immunity*, 44(3):450–462. doi:10.1016/j.immuni.2016.02.015.
- Xiao G, Wei J, Yan W, Wang W, and Lu Z**, 2008. Improved outcomes from the administration of progesterone for patients with acute severe traumatic brain injury: a randomized controlled trial. *Critical Care*, 12(2):R61. doi:10.1186/cc6887.
- Xiong Y, Shie FS, Zhang J, Lee CP, and Ho YS**, 2005. Prevention of mitochondrial dysfunction in post-traumatic mouse brain by superoxide dismutase. *Journal of Neurochemistry*, 95(3):732–744. doi:10.1111/j.1471-4159.2005.03412.x.
- Xu J, Wang T, Wu Y, Jin W, and Wen Z**, 2016. Microglia Colonization of Developing Zebrafish Midbrain Is Promoted by Apoptotic Neuron and Lysophosphatidylcholine. *Developmental Cell*, 38:214–222. doi:10.1016/j.devcel.2016.06.018.
- Xu K, He L, Yang X, Yang Y, and Lin W**, 2018a. A ratiometric fluorescent hydrogen peroxide chemosensor manipulated by an ICT-activated FRET mechanism and its bioimaging application in living cells and zebrafish. *The Analyst*, 143(15):3555–3559. doi:10.1039/C8AN00842F.
- Xu S and Chisholm AD**, 2011. A $G\alpha_q$ - $Ca(2+)$ signaling pathway promotes actin-mediated epidermal wound closure in *C. elegans*. *Current Biology*, 21(23):1960–7.
- Xu W, Gao L, Li T, Zheng J, Shao A, and Zhang J**, 2018b. Mesencephalic Astrocyte-Derived Neurotrophic Factor (MANF) Protects Against Neuronal Apoptosis via Activation of Akt/MDM2/p53 Signaling Pathway in a Rat Model of Intracerebral Hemorrhage. *Frontiers in Molecular Neuroscience*, 11:176. doi:10.3389/fnmol.2018.00176.
- Yakovlev AG, Knoblach SM, Fan L, Fox GB, Goodnight R, and Faden AI**, 1997. Activation of CPP32-like caspases contributes to neuronal apoptosis and neurological dysfunction after traumatic brain injury. *Journal of Neuroscience*, 17(19):7415–24.
- Yamaguchi Y and Miura M**, 2015. Programmed Cell Death in Neurodevelopment. *Developmental Cell*, 32(4):478–490. doi:10.1016/j.devcel.2015.01.019.

- Yamakami I and Mcintosh TK**, 1991. Alterations in Regional Cerebral Blood Flow Following Brain Injury in the Rat. *Journal of Cerebral Blood Flow & Metabolism*, 11:655–660.
- Yamamoto T, Maruyama W, Kato Y, Yi H, Shamoto-Nagai M, Tanaka M, Sato Y, and Naoi M**, 2002. Selective nitration of mitochondrial complex I by peroxynitrite: Involvement in mitochondria dysfunction and cell death of dopaminergic SH-SY5Y cells. *Journal of Neural Transmission*, 109(1):1–13. doi:10.1007/s702-002-8232-1.
- Yamasaki R, Lu H, Butovsky O, Ohno N, Rietsch AM, Cialic R, Wu PM, Doykan CE, Lin J, Coteleur AC, Kidd G, Zorlu MM, Sun N, Hu W, Liu L, Lee JC, Taylor SE, Uehlein L, Dixon D, Gu J, Floruta CM, Zhu M, Charo IF, Weiner HL, and Ransohoff RM**, 2014. Differential roles of microglia and monocytes in the inflamed central nervous system. *Journal of Experimental Medicine*, 211(8):1533–1549. doi:10.1084/jem.20132477.
- Yamashita K, Gerken U, Vogel P, Hossmann KA, and Wiessner C**, 1999. Biphasic expression of TGF- β 1 mRNA in the rat brain following permanent occlusion of the middle cerebral artery. *Brain Research*, 836(1-2):139–145. doi:10.1016/S0006-8993(99)01626-1.
- Yan Z, Li S, Liang Z, Tomić M, and Stojilkovic SS**, 2008. The P2X 7 Receptor Channel Pore Dilates under Physiological Ion Conditions. *Journal of General Physiology*, 132(5):563–573. doi:10.1085/jgp.200810059.
- Yang MS, Ji KA, Jeon SB, Jin BK, Kim SU, Jou I, and Joe E**, 2006. Interleukin-13 enhances cyclooxygenase-2 expression in activated rat brain microglia: implications for death of activated microglia. *Journal of immunology*, 177(2):1323–9. doi:10.4049/JIMMUNOL.177.2.1323.
- Yang MS, Park EJ, Sohn S, Kwon HJ, Shin WH, Pyo HK, Jin B, Choi KS, Jou I, and Joe EH**, 2002. Interleukin-13 and -4 induce death of activated microglia. *Glia*, 38(4):273–280. doi:10.1002/glia.10057.
- Yang W, Shen Y, Chen Y, Chen L, Wang L, Wang H, Xu S, Fang S, Fu Y, Yu Y, and Shen Y**, 2014. Mesencephalic astrocyte-derived neurotrophic factor prevents neuron loss via inhibiting ischemia-induced apoptosis. *Journal of the Neurological Sciences*, 344(1-2):129–138. doi:10.1016/j.jns.2014.06.042.
- Yeo SY, Kim M, Kim HS, Huh TL, and Chitnis AB**, 2007. Fluorescent protein expression driven by her4 regulatory elements reveals the spatiotemporal pattern of Notch signaling in the nervous system of zebrafish embryos. *Developmental Biology*, 301(2):555–567. doi:10.1016/J.YDBIO.2006.10.020.
- Yeo YA, Martínez Gómez JM, Croxford JL, Gasser S, Ling EA, and Schwarz H**, 2012. CD137 ligand activated microglia induces oligodendrocyte apoptosis via reactive oxygen species. *Journal of Neuroinflammation*, 9:173. doi:10.1186/1742-2094-9-173.

- Yin J, Xu K, Zhang J, Kumar A, and Yu FSX**, 2007. Wound-induced ATP release and EGF receptor activation in epithelial cells. *Journal of Cell Science*, 120(5):815–825. doi:10.1242/jcs.03389.
- Yin Y, Cui Q, Li Y, Irwin N, Fischer D, Harvey AR, and Benowitz LI**, 2003. Macrophage-derived factors stimulate optic nerve regeneration. *Journal of Neuroscience*, 23(6):2284–93. doi:10.1523/JNEUROSCI.23-06-02284.2003.
- Yin Y, Henzl MT, Lorber B, Nakazawa T, Thomas TT, Jiang F, Langer R, and Benowitz LI**, 2006. Oncomodulin is a macrophage-derived signal for axon regeneration in retinal ganglion cells. *Nature Neuroscience*, 9(6):843–852. doi:10.1038/nn1701.
- Yoo SK, Freisinger CM, LeBert DC, and Huttenlocher A**, 2012. Early redox, Src family kinase, and calcium signaling integrate wound responses and tissue regeneration in zebrafish. *Journal of Cell Biology*, 199(2):225–234. doi:10.1083/jcb.201203154.
- Yoshino A, Hovda DA, Kawamata T, Katayama Y, and Becker DP**, 1991. Dynamic changes in local cerebral glucose utilization following cerebral conclusion in rats: evidence of a hyper- and subsequent hypometabolic state. *Brain Research*, 561(1):106–19.
- Young B, Runge JW, Waxman KS, Harrington T, Wilberger J, Muizelaar JP, Boddy A, and Kupiec JW**, 1996. Effects of pegorgotein on neurologic outcome of patients with severe head injury: A multicenter, randomized controlled trial. *Journal of the American Medical Association*, 276(7):538–543. doi:10.1001/jama.276.7.538.
- Young W**, 1992. Role of calcium in central nervous system injuries. *Journal of Neurotrauma*, 9 Suppl 1:S9–25.
- Yrjänheikki J, Keinänen R, Pellikka M, Hökfelt T, and Koistinaho J**, 1998. Tetracyclines inhibit microglial activation and are neuroprotective in global brain ischemia. *Proceedings of the National Academy of Sciences*, 95(26):15769–15774. doi:10.1073/PNAS.95.26.15769.
- Zang DW and Cheema SS**, 2003. Leukemia Inhibitory Factor Promotes Recovery of Locomotor Function following Spinal Cord Injury in the Mouse. *Journal of Neurotrauma*, 20(11):1215–1222. doi:10.1089/089771503770802880.
- Zhang D, Xue Q, Chen J, Dong Y, Hou L, Jiang Y, and Wang J**, 2017. Decompressive craniectomy in the management of intracranial hypertension after traumatic brain injury: a systematic review and meta-analysis. *Scientific Reports*, 7(1):8800. doi:10.1038/s41598-017-08959-y.
- Zhang J, Malik A, Choi H, Ko R, Dissing-Olesen L, and MacVicar B**, 2014. Microglial CR3 Activation Triggers Long-Term Synaptic Depression in the Hippocampus via NADPH Oxidase. *Neuron*, 82(1):195–207. doi:10.1016/j.neuron.2014.01.043.

- Zhang QG, Laird MD, Han D, Nguyen K, Scott E, Dong Y, Dhandapani KM, and Brann DW**, 2012. Critical Role of NADPH Oxidase in Neuronal Oxidative Damage and Microglia Activation following Traumatic Brain Injury. *PLoS ONE*, 7(4):e34504. doi:10.1371/journal.pone.0034504.
- Zhang-Hooks Y, Agarwal A, Mishina M, and Bergles D**, 2016. NMDA Receptors Enhance Spontaneous Activity and Promote Neuronal Survival in the Developing Cochlea. *Neuron*, 89(2):337–350. doi:10.1016/j.neuron.2015.12.016.
- Zhao G, Liu L, Peek RM, Hao X, Polk DB, Li H, and Yan F**, 2016. Activation of epidermal growth factor receptor in macrophages mediates feedback inhibition of M2 polarization and gastrointestinal tumor cell growth. *Journal of Biological Chemistry*, 291:20462–20472. doi:10.1074/jbc.M116.750182.
- Zhao X, Wang H, Sun G, Zhang J, Edwards NJ, and Aronowski J**, 2015. Neuronal Interleukin-4 as a Modulator of Microglial Pathways and Ischemic Brain Damage. *Journal of Neuroscience*, 35(32):11281–11291. doi:10.1523/JNEUROSCI.1685-15.2015.
- Zheng Y, Humphry M, Maguire JJ, Bennett MR, and Clarke MCH**, 2013. Intracellular interleukin-1 receptor 2 binding prevents cleavage and activity of interleukin-1 α , controlling necrosis-induced sterile inflammation. *Immunity*, 38(2):285–95. doi:10.1016/j.immuni.2013.01.008.
- Zhou H, Chen L, Gao X, Luo B, and Chen J**, 2012. Moderate traumatic brain injury triggers rapid necrotic death of immature neurons in the hippocampus. *Journal of Neuropathology and Experimental Neurology*, 71(4):348–359. doi:10.1097/NEN.0b013e31824ea078.
- Zhou H, Lapointe BM, Clark SR, Zbytniuk L, and Kubes P**, 2006. A Requirement for Microglial TLR4 in Leukocyte Recruitment into Brain in Response to Lipopolysaccharide. *Journal of Immunology*, 177(11):8103–8110. doi:10.4049/JIMMUNOL.177.11.8103.
- Zhou Y and Besner GE**, 2010. Heparin-binding epidermal growth factor-like growth factor is a potent neurotrophic factor for PC12 cells. *Neuro-Signals*, 18(3):141–51. doi:10.1159/000319823.
- Zhou Z, Peng X, Insolera R, Fink DJ, and Mata M**, 2009a. IL-10 promotes neuronal survival following spinal cord injury. *Experimental Neurology*, 220(1):183–190. doi:10.1016/j.expneurol.2009.08.018.
- Zhou Z, Peng X, Insolera R, Fink DJ, and Mata M**, 2009b. Interleukin-10 provides direct trophic support to neurons. *Journal of Neurochemistry*, 110(5):1617–1627. doi:10.1111/j.1471-4159.2009.06263.x.
- Ziebell JM and Morganti-Kossmann MC**, 2010. Involvement of pro- and anti-inflammatory cytokines and chemokines in the pathophysiology of traumatic brain injury. *Neurotherapeutics*, 7(1):22–30. doi:10.1016/j.nurt.2009.10.016.

- Zupanc GKH**, 2006. Neurogenesis and neuronal regeneration in the adult fish brain. *Journal of Comparative Physiology*, 192(6):649–670.
- Zupanc GKH and Horschke I**, 1995. Proliferation zones in the brain of adult gymnotiform fish: A quantitative mapping study. *Journal of Comparative Neurology*, 353(2):213–233.
- Zupanc GKH, Kompass KS, Horschke I, Ott R, and Schwarz H**, 1998. Apoptosis after Injuries in the Cerebellum of Adult Teleost Fish. *Experimental Neurology*, 152(2):221–230.